



Universidad de Cantabria

**Escuela Técnica Superior de Ingenieros Industriales y de
Telecomunicación**

Departamento de Ingeniería Química y Química Inorgánica

“Ultrapurificación de peróxido de hidrógeno”

“Ultrapurification of hydrogen peroxide”

Memoria de Tesis Doctoral presentada para optar al título de
Doctor por la Universidad de Cantabria

Programa de Doctorado en Ingeniería Química y de Procesos
(BOE núm. 36, de 10 de febrero de 2010. RUCT: 5311209)
con Mención hacia la Excelencia
(BOE núm. 253, de 20 de Octubre de 2011. Referencia: MEE2011-0031)

Ricardo Abejón Elías

Directores de Tesis:

Prof. Dr. Ángel Irabien Gulías
Dra. Aurora Garea Vázquez

Santander, Noviembre 2012

La Tesis Doctoral se presenta como un resumen de trabajos previamente publicados en revistas científicas de carácter internacional incluidas en el *Journal of Citation Reports-Science Edition (JCR)*, cumpliendo con la normativa existente en la Universidad de Cantabria y en el Departamento de Ingeniería Química y Química Inorgánica referente a la elaboración de Tesis Doctorales por compendio de artículos. Durante la elaboración de la Tesis Doctoral se ha realizado una estancia predoctoral de tres meses (de Marzo a Junio de 2012) en el Centro de Investigación y Desarrollo del Grupo Solvay del Campus NOH Solvay de Bruselas (Bélgica) bajo la supervisión del Dr. Paul Deschrijver.

A continuación se listan las publicaciones que forman parte de la presente Tesis:

Compendio de artículos publicados/aceptados:

1. Abejón, R.; Garea, A.; Irabien, A. *Ultrapurification of hydrogen peroxide solution from ionic metals impurities to semiconductor grade by reverse osmosis*. Separation and Purification Technology, 76:44-51 (2010).
2. Abejón, R.; Garea, A.; Irabien, A. *Analysis, modelling and simulation of hydrogen peroxide ultrapurification by multistage reverse osmosis*. Chemical Engineering Research and Design, 90:442-452 (2012).
3. Abejón, R.; Garea, A.; Irabien, A. *Integrated countercurrent reverse osmosis cascades for hydrogen peroxide ultrapurification*. Computers and Chemical Engineering, 41:67-76 (2012).
4. Abejón, R.; Garea, A.; Irabien, A. *Optimum design of reverse osmosis systems for hydrogen peroxide ultrapurification*. AIChE Journal, 58:3718-3730 (2012).

Este trabajo ha sido financiado por el Ministerio de Educación y el Ministerio de Ciencia e Innovación de España a través de los proyectos CTM2006-00317 "*Sostenibilidad de la Producción: Intensificación e integración de procesos en la industria química y transformadora*" y CTQ2010-16608 "*Ultrapurificación de productos químicos basada en tecnología de membranas para alcanzar calidad grado electrónico*".

Durante la ejecución del presente trabajo, su autor, Ricardo Abejón Elías, ha disfrutado de la ayuda Predoctoral de Formación de Personal Investigador del Ministerio de Ciencia e Innovación con referencia BES-2008-003622 concedida por Resolución de 22 de febrero de 2008 de la Secretaría de Estado de Universidades e Investigación (BOE de 27 de febrero de 2008).

Nuestro más sincero agradecimiento hacia dichas instituciones.

Agradecimientos

En primer lugar tengo que expresar mi más sincero agradecimiento a los directores de esta Tesis, el Prof. Dr. Ángel Irabien y la Dra. Aurora Garea, ya que sin su esfuerzo a lo largo de estos años no hubiera sido posible la materialización de esta Tesis Doctoral. Muchas gracias por toda la paciencia, comprensión y dedicación brindadas en este tiempo y en especial por el apoyo recibido en los momentos más difíciles.

I would like to thank Dr. Paul Deschrijver, Dr. Pierre Dournel, Dr. Pierre Miquel and Ing. Frederique Desmedt from the R&D Team in H₂O₂ – Solvay Essential Chemicals the opportunity they gave me to complete a short research stay under their supervision. I am very grateful to all the rest of colleagues who I had the opportunity to work in Brussels with because they made me feel part of the team. Thank you very much for your patience!

I acknowledge the license of the artwork titled "Wassertropfen" (created by Sven Hoppe) which has been used to illustrate the cover of this Thesis. Thank you very much Sven.

Tengo que agradecer a los profesores del Departamento de Ingeniería Química y Química Inorgánica de la Universidad de Cantabria la formación recibida en los últimos años y que ha dado como fruto mi incorporación al mundo de la investigación.

Gracias a todo el Personal de Administración y Servicios del Departamento de Ingeniería Química y Química Inorgánica de la Universidad de Cantabria por facilitarme el trabajo gracias a la ayuda recibida en las labores técnicas y de gestión.

Quiero acordarme del resto de compañeros del Departamento de Ingeniería Química y Química Inorgánica de la Universidad de Cantabria, en especial de todos aquellos con los que he compartido laboratorio y despacho y agradecerles este gran ambiente de trabajo.

Y mi agradecimiento más especial para mis amigos porque han sido capaces de aguantarme durante todo este proceso y mi familia, especialmente a mis padres y hermana, porque si soy algo en la vida es gracias a ellos. Mención aparte merece Ainhoa porque seguramente ella ha sido la que ha tenido que sufrirme en los peores ratos pero espero haberlo podido compensar con los buenos momentos que hemos compartido. Si no ha sido así, tenemos mucho tiempo por delante para intentar lograrlo. Ultramuxus.

Índice

RESUMEN	1
<i>ABSTRACT</i>	
CAPÍTULO 1. PLANTEAMIENTO	7
1.1. El peróxido de hidrógeno como reactivo electrónico	9
1.2. Revisión de tecnologías para la ultrapurificación de peróxido de hidrógeno	12
1.3. La ósmosis inversa para la ultrapurificación de reactivos	16
1.4. Objetivos y estructura de la tesis	18
1.5. Referencias del Capítulo 1	20
CAPÍTULO 2. DESARROLLO	27
2.1. Instalación para la ultrapurificación de peróxido de hidrógeno a escala de laboratorio mediante membranas de ósmosis inversa	29
2.2. Herramientas para la simulación y optimización de la ultrapurificación de peróxido de hidrógeno mediante membranas de ósmosis inversa	31
2.3. Resultados	32
2.3.1. Caracterización del comportamiento de membranas comerciales de poliamida para ósmosis inversa aplicada a la ultrapurificación de peróxido de hidrógeno.	32
2.3.2. Estudio de la viabilidad técnica de la ultrapurificación de peróxido de hidrógeno mediante ósmosis inversa con membranas comerciales de poliamida.	41
2.3.3. Estudio de la evolución con el tiempo de las membranas de ósmosis inversa en ambiente oxidante	44
2.3.4. Simulación de la ultrapurificación de peróxido de hidrógeno mediante ósmosis inversa y evaluación de la viabilidad económica del proceso	52

2.3.5. Optimización del proceso de ultrapurificación de peróxido de hidrógeno mediante ósmosis inversa	65
2.4. Nomenclatura del Capítulo 2	75
2.5. Referencias del Capítulo 2	79
CAPÍTULO 3. CONCLUSIONES	85
CHAPTER 3. CONCLUSIONS	
3.1. Conclusiones y progreso de la investigación	87
3.1.1. Conclusiones	87
3.1.2. Progreso de la investigación	89
3.2. Conclusions and on-going research	90
3.2.1. Conclusions	90
3.2.2. On-going research	92
CAPÍTULO 4. ARTÍCULOS CIENTÍFICOS	93
CHAPTER 4. SCIENTIFIC ARTICLES	
4.1. Abejón, R.; Garea, A.; Irabien, A. <i>Ultrapurification of hydrogen peroxide solution from ionic metals impurities to semiconductor grade by reverse osmosis</i> . Separation and Purification Technology, 76:44-51 (2010).	95
4.2. Abejón, R.; Garea, A.; Irabien, A. <i>Analysis, modelling and simulation of hydrogen peroxide ultrapurification by multistage reverse osmosis</i> . Chemical Engineering Research and Design, 90:442-452 (2012).	105
4.3. Abejón, R.; Garea, A.; Irabien, A. <i>Integrated countercurrent reverse osmosis cascades for hydrogen peroxide ultrapurification</i> . Computers and Chemical Engineering, 41:67-76 (2012).	119
4.4. Abejón, R.; Garea, A.; Irabien, A. <i>Optimum design of reverse osmosis systems for hydrogen peroxide ultrapurification</i> . AIChE Journal, 58:3718-3730 (2012).	131
ANEXO: DIFUSIÓN DE RESULTADOS	147

Resumen

Abstract

Resumen

El descubrimiento y empleo de los semiconductores ha influido de forma decisiva en las profundas modificaciones que han vivido las sociedades avanzadas como consecuencia de la revolución tecnológica de la segunda mitad del siglo XX. De este modo se ha configurado la actual sociedad global, donde las tecnologías de la información y la comunicación se han constituido como el elemento característico e imprescindible del desarrollo científico y tecnológico en el que se basan las actuales formas de vida.

Las industrias que emplean materiales semiconductores o fabrican productos basados en los mismos demandan reactivos de calidad electrónica caracterizados por su limitado contenido en impurezas. Entre los reactivos de este tipo con mayor demanda se encuentra el peróxido de hidrógeno. Los procesos de ultrapurificación de peróxido de hidrógeno son necesarios para poder alcanzar los niveles de calidad exigidos por el sector, específicamente en lo referido a impurezas metálicas.

La revisión del estado del arte con respecto a las tecnologías disponibles para la ultrapurificación de peróxido de hidrógeno presenta diferentes alternativas que incluyen la destilación, la adsorción, el intercambio iónico y las tecnologías de membranas. El empleo de membranas de ósmosis inversa aparece como una opción prometedora desde el punto de vista del uso más sostenible de los recursos naturales (materiales, energía y agua).

En la presente Tesis Doctoral se ha estudiado el proceso de ultrapurificación de peróxido de hidrógeno mediante ósmosis inversa a escala de laboratorio. El peróxido de hidrógeno obtenido mediante un proceso de osmosis inversa con membranas de poliamida cumple con los requisitos impuestos en el contenido de impurezas metálicas para ser considerado como SEMI Grado 1, el grado menos exigente de los contemplados dentro de la calidad electrónica.

El estudio experimental del proceso a escala de laboratorio permite ajustar el modelo de Kedem-Katchalsky para el transporte de solvente y solutos a través de membranas y es capaz de explicar de forma satisfactoria la evolución de los valores de flujo de permeado y los coeficientes de rechazo de los elementos metálicos en función de la presión aplicada al sistema, evaluando los parámetros que caracterizan al proceso de separación de impurezas lo que permite simular el comportamiento del mismo.

La degradación que las membranas de ósmosis inversa sufren en un ambiente tan agresivo como el peróxido de hidrógeno es un factor a tener en cuenta durante la investigación del proceso de ultrapurificación. Por ello, a la vista de los resultados experimentales que muestran una vida útil extremadamente corta para las membranas en esta aplicación y ante la imposibilidad de encontrar en bibliografía referencias previas para la descripción de la evolución con el tiempo del

comportamiento de las membranas bajo degradación oxidativa, se propone un modelo logístico de carácter empírica que complemente el modelo de permeación con la descripción del comportamiento durante la evolución de la degradación de la membrana.

Los modelos obtenidos y los parámetros ajustados permiten simular y optimizar instalaciones para procesos de fabricación bajo la configuración de cascadas de membranas integradas en contracorriente para alcanzar las calidades de peróxido de hidrógeno ultrapuro desde el Grado SEMI 1 hasta el Grado SEMI 5. El modelo ha sido completado con un balance económico lo que permite utilizar los beneficios económicos como función objetivo en la optimización.

Finalmente se ha planteado la optimización del proceso para distintos objetivos en la ultrapurificación de peróxido de hidrógeno mediante cascadas de membranas de ósmosis inversa. Estos objetivos se han concretado en:

- (a) Número óptimo de etapas que la cascada de membranas debe incorporar para la producción de cada uno de los grados de calidad electrónica y los valores óptimos para las principales variables del proceso en cada caso, de modo que se maximice el beneficio económico del proceso.
- (b) Estudio de la influencia de los precios unitarios de los principales recursos necesarios (materia prima, membranas y energía eléctrica) y de diferentes restricciones de mercado sobre la configuración óptima del proceso.

Los resultados obtenidos y la interpretación realizada a los mismos tienen un gran interés científico-técnico y se sitúan en los límites del conocimiento actual como demuestra la publicación de los resultados en revistas del primer cuartil en cuanto a su difusión.

Abstract

The discovery and posterior use of semiconductor materials have greatly influenced the deep changes that developed societies have experienced as consequence of the technological revolution of the second half of the XX century. This way, the present global society has been configured, where the information and communication technology can be considered as the characteristic and indispensable cornerstone of the scientific and technological development which current life ways are based on.

The semiconductor industrial sector requires electronic quality chemicals which can be characterized by their very limited impurity content. Among this type of chemicals, hydrogen peroxide can be found among the ones with highest demands. Hydrogen peroxide ultrapurification processes are necessary to attain the purity levels required by the sector, specifically for the metallic impurities concentrations.

The bibliographical review about the state of the art with respect to available ultrapurification technologies for hydrogen peroxide introduces different alternatives, including distillation, adsorption, ion exchange and membrane technologies. The use of reverse osmosis membranes appears as a promising option from the point of view that considers the most sustainable use of the natural resources (raw materials, energy and water).

In this PhD Thesis, the hydrogen peroxide ultrapurification process by reverse osmosis has been investigated at lab-scale level. The hydrogen peroxide obtained by means of a reverse osmosis process with polyamide membranes fulfils with the requirements imposed about metallic impurities content to be considered as SEMI Grade 1 chemical, the least exigent grade of the electronic quality framework.

The experimental study of the process at lab scale allows the fit to the Kedem-Katchalsky model for both solvent and solute transport through membranes and it is able to explain in a satisfactory way the evolution of the permeate flux and the rejection coefficients of the metallic elements as a function of the applied pressure by evaluating the parameters that characterize the impurities separation process and lets its performance simulation.

The degradation of the reverse osmosis membranes in such a harsh medium as hydrogen peroxide is a factor to have under consideration during the investigation of the ultrapurification process. Hence, as a consequence of the analysis of the experimental results that evidence an extremely short effective lifetime for the membranes in this application and the lack of a previous bibliographic reference for the description of the time evolution of the membrane performance under oxidative degradation, an empirical logistic model was formulated to complement the permeation model with the description of the performance during the evolution of the membrane degradation.

The model that describes the lab-scale hydrogen peroxide permeation is useful to simulate and optimize industrial-scale installations for manufacturing purposes under the countercurrent integrated membrane cascade configuration to produce electronic quality hydrogen peroxide, from SEMI Grade 1 to SEMI Grade 5. The model has been completed with an economic balance which allows the use of the economic profit as an optimization target function.

Lastly, the optimization with different targets as objectives of the hydrogen peroxide ultrapurification process by reverse osmosis membrane cascades has been performed. This objectives have been specified as:

- (a) Optimum number of stages that a membrane cascade should incorporate for the production of each electronic grade and the optimum values for the main process variables have been solved to maximize the economic profit of the process.
- (b) Study of the influence of the unitary prices of the principal required resources (raw material, membranes and electric energy) and different market restrictions over the optimal process configuration.

The obtained results and the corresponding interpretation have a great scientific and technical relevance since they contribute to the current borders of knowledge as proved by the publication of the results in journals belonging to the first quartile in relation to their diffusion.

Planteamiento 1

1.1. El peróxido de hidrógeno como reactivo electrónico

Los últimos años del siglo XX vieron el nacimiento de un nuevo modelo social, la denominada sociedad del conocimiento, donde las tecnologías que facilitan la creación, distribución y manipulación de la información (tecnologías de la información y la comunicación, TICs) juegan un papel esencial en las actividades económicas, sociales y culturales (Masuda, 1980) y que ya en el siglo XXI han soportado el desarrollo del fenómeno de la globalización (Castells, 1999).

Se puede considerar que la llamada era de la información nace de la invención del transistor (un desarrollo de la física de semiconductores) en 1948, amplificando su poder con el desarrollo del circuito integrado, a finales de los años 50 y durante la década de los 60. Pero es realmente el desarrollo del microprocesador, a principios de los años 70, lo que posibilitó la aparición del ordenador personal con el que nace la revolución informacional a principios de los años 80. El desarrollo de la Internet y las TICs dio origen, durante la década de los 90, a una ola globalizadora sin precedentes, caracterizada por un entorno digital (Rúa Ceballos, 2006).

Por lo tanto queda claro que los materiales semiconductores son la base sobre la que se sustenta la actual sociedad del conocimiento. Los procesos de producción de dispositivos microelectrónicos a partir de estos materiales semiconductores son muy complejos e incluyen infinidad de tareas diferentes. Para poder llevarlas a cabo, es necesario el empleo de diversos reactivos químicos: los distintos materiales y reactivos químicos empleados para la fabricación y montaje de semiconductores son denominados reactivos electrónicos (Daigle et al., 2007). En total más de 100 productos químicos diferentes están catalogados como reactivos electrónicos.

El peróxido de hidrógeno es uno de los reactivos electrónicos en fase líquida más consumido (Sievert, 2001). Esta demanda por parte de la industria de los semiconductores se debe a su empleo para limpiar las obleas de silicio, retirar fotorresistencias o grabar el cobre de los circuitos impresos (Daigle et al., 2007). Las principales formulaciones para los baños de limpieza de las superficies de las obleas de silicio, tales como el SC1, el SC2 o el SPM, incluyen peróxido de hidrógeno (Olson et al., 2000). Estos baños son capaces de eliminar tanto las partículas indeseadas como los contaminantes orgánicos y metálicos de la superficie del silicio (Reinhardt y Kern, 2008).

La demanda de peróxido de hidrógeno de calidad electrónica a lo largo de las dos últimas décadas y una previsión para el futuro más próximo aparecen graficadas en la Figura 1.1, en la que también se ha incluido el porcentaje que supone el peróxido de hidrógeno sobre la demanda total de reactivos líquidos electrónicos (Freedonia Group, 2004). En la gráfica se puede comprobar como la demanda de peróxido de hidrógeno se mantiene en ascenso a pesar del estancamiento de la importancia relativa de este reactivo dentro del conjunto de reactivos líquidos electrónicos. Este estancamiento e incluso el descenso previsto se deben principalmente a la aparición de alternativas técnicas que no emplean peróxido de hidrógeno (Olson et al., 2000).

La preocupación por temas tales como el medio ambiente, los accidentes industriales y los riesgos laborales por parte de los sectores que trabajan con materiales semiconductores han promovido la sustitución de los reactivos peligrosos empleados en este campo, incluido el peróxido de hidrógeno. El uso de ácido sulfúrico electrolizado para retirar los materiales enmascarantes orgánicos necesarios durante el proceso que forma los circuitos en el sustrato de un chip reduce el volumen total de ácido sulfúrico empleado en el proceso en un 70% y elimina totalmente la necesidad de peróxido de hidrógeno (The Engineer, 2007). Otro ejemplo de los esfuerzos llevados a cabo por este sector para alejarse de los reactivos peligrosos es la sustitución de los clásicos baños piraña formulados con ácidos fuertes y peróxido de hidrógeno por agua ultrapura con ozono, resultando un medio mucho menos agresivo (Jeon et al., 1999).

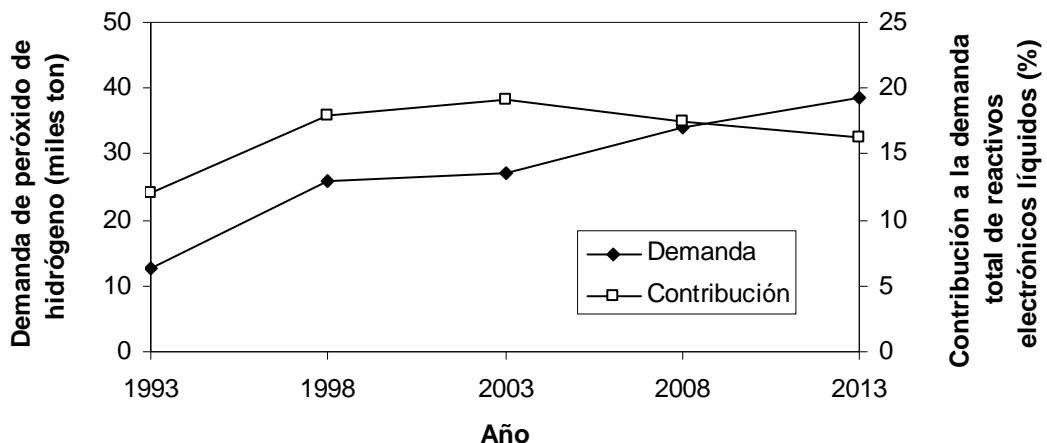


Figura 1.1. Evolución de la demanda de peróxido de hidrógeno de calidad electrónica y la contribución del mismo a la demanda total de reactivos electrónicos líquidos

Sin embargo, el peróxido de hidrógeno ha encontrado nuevas oportunidades en el seno de la revolución verde vivida en el mundo de los materiales semiconductores. El aluminio se emplea en multitud de capas no críticas presentes en microcomponentes y dispositivos lógicos y de memoria. Por muchos años, el método más usual para eliminar los residuos que quedaban en las líneas de aluminio después de haberlo sometido a grabado ha consistido en el empleo de baños de inmersión con base en reactivos con el grupo funcional amina. Las formulaciones más comunes incluían la hidroxilamina como componente activo principal y requerían de un lavado posterior con alcohol isopropílico para rebajar el pH (Sohn et al., 2005). Además, las soluciones residuales que contienen hidroxilamina necesitan un tratamiento especial. Los baños basados en compuestos fluorados, tales como el fluoruro amónico y otros fluoruros, aparecieron como alternativa a las aminas. Ya que estas nuevas formulaciones no producen un incremento del pH, la necesidad de lavar con alcohol isopropílico ha sido eliminada. De modo más reciente,

estos baños fluorados están siendo reemplazados por formulaciones que incluyen ácido sulfúrico y peróxido de hidrógeno muy diluidos (Rath et al., 2001; Ravikumar et al., 2001).

La eliminación de las máscaras foto-resistentes, bien por plasma de oxígeno o por calcinación con ozono, es un proceso que deja residuos en las obleas de silicio. A pesar de que se cuenta con varias opciones para la retirada de este tipo de residuos, la mayoría presentan el mismo problema: la necesidad de reactivos de naturaleza orgánica peligrosos para el medio ambiente (Archer et al., 2001). Nuevas formulaciones que incluyen peróxido de hidrógeno y ácido sulfúrico a las que se añade ácido fluorídico, únicamente a nivel de ppm, han demostrado su efectividad en la eliminación de los residuos poliméricos relacionados con las máscaras y así lo confirma la comercialización de mezclas comerciales ya preparadas para esta tarea (Couteau et al., 2006).

Como consecuencia del contacto directo entre el peróxido de hidrógeno y las superficies de silicio, la preocupación por la posibilidad de que el propio reactivo actúe como agente contaminante de la oblea es máxima. Las partículas que se adhieren al silicio pueden causar cortocircuitos que se manifiestan como fallos en los dispositivos microelectrónicos (Duffalo y Monkowski, 1984). Por su parte, las impurezas iónicas metálicas también entrañan problemas: ciertos metales se depositan sobre el silicio o el dióxido de silicio. Estas trazas en las superficies de la oblea de silicio influyen de forma negativa en las características eléctricas de los microdispositivos ya que causan la pérdida de integridad del óxido y producen un acortamiento de la vida útil de los portadores de carga minoritarios (Atsumi et al., 1990).

Tabla 1.1 Requisitos para el peróxido de hidrógeno de calidad electrónica de acuerdo a la norma SEMI C30-1110.

Grado Electrónico SEMI	Concentración de H ₂ O ₂	Límite al carbono total oxidable	Límites a las impurezas aniónicas	Límites a las impurezas catiónicas
1	30-32%	20 ppm	2-5 ppm	10-1000 ppb
2	30-32%	20 ppm	200-400 ppb	5-10 ppb
3	30-32%	20 ppm	200-400 ppb	1 ppb
4	30-32%	10 ppm	30 ppb	100 ppt
5	30-32%	10 ppm	30 ppb	10 ppt

SEMI (Semiconductor Equipment and Materials International) es la asociación global que sirve a las cadenas de suministro de las industrias microelectrónicas y fotovoltaicas. Esta asociación desarrolla los estándares más respetados a nivel mundial en este sector. Entre todos los temas que regula se encuentran los requerimientos que los reactivos electrónicos han de cumplir para ser aceptados por la industria. Para el caso concreto del peróxido de hidrógeno, el Documento SEMI C30-1110 se encarga de estandarizar los requisitos del reactivo de calidad electrónica

(SEMI, 2010). La Tabla 1.1 muestra las características a cumplir para cada uno de los cinco grados que el documento define. En lo referente a impurezas metálicas, se puede observar como el rango va desde los pocos ppm para el menos exigente Grado 1 hasta los 10 ppt para el más estricto Grado 5. Aunque el grado menos exigente pueda ser logrado mediante una selección experta de los lotes del reactivo de calidad técnica con menores niveles impurezas y muy poco tratamiento adicional, el resto de grados implica la necesidad de recurrir a procesos de ultrapurificación (Sievert, 2000).

1.2. Revisión de tecnologías para la ultrapurificación de peróxido de hidrógeno

En la actualidad, prácticamente la totalidad del peróxido de hidrógeno producido a escala industrial se obtiene a partir del proceso de oxidación de antraquinonas (Goor et al., 2007). En el mismo, una antraquinona (la 2-etilantraquinona es la más típica) funciona como agente cíclico de reacción para la combinación de hidrógeno y oxígeno atmosférico. El peróxido de hidrógeno obtenido es purificado y concentrado para ser comercializado como soluciones acuosas de concentraciones 35, 50 y 70% en peso, normalmente con aditivos estabilizantes (Campos-Martín et al., 2006).

El proceso de oxidación de antraquinonas implica una secuencia de hidrogenación catalítica y oxidación de la antraquinona para dar lugar a peróxido de hidrógeno que es extraído del medio orgánico de reacción con agua. La antraquinona se convierte en la correspondiente antrahidroquinona después de la etapa de hidrogenación pero su oxidación además de producir peróxido de hidrógeno conlleva la regeneración a la antraquinona de partida, por lo que idealmente no habría consumo neto de la misma (un conjunto de reacciones secundarias no deseadas impiden esta situación y obligan al acondicionamiento de la solución de trabajo y al aporte de antraquinona fresca como se puede ver en el esquema del proceso representado en la Figura 1.2).

Aunque el peróxido de hidrógeno obtenido a través del proceso de la antraquinona es sometido a tratamientos por técnicas tradicionales de purificación tales como extracción líquido-líquido, adsorción, tecnologías de membranas o destilación para disminuir su contenido en impurezas (Goor et al., 2007), los límites impuestos por la norma SEMI exigen tratamientos específicos para alcanzar la calidad electrónica. Por lo tanto, los procesos de ultrapurificación son necesarios para lograr cumplir con los requerimientos de los grados electrónicos partiendo del reactivo de calidad técnica.

Mientras que la viabilidad técnica de los procesos de ultrapurificación del peróxido de hidrógeno se puede considerar garantizada por la disponibilidad comercial de los diferentes grados electrónicos, es realmente difícil encontrar documentos científicos que traten sobre la materia y aborden los fundamentos básicos de estos procesos. Por ello, las patentes se convierten en la fuente bibliográfica que aporta más información en este ámbito (Luan et al., 2005).

Como resultado de la revisión bibliográfica llevada a cabo, se ha localizado un número notable de patentes relativas a la ultrapurificación de peróxido de hidrógeno (Tabla 1.2). Según las referencias encontradas, las técnicas más relevantes para alcanzar la calidad electrónica son la destilación, la adsorción, el intercambio iónico y las tecnologías de membranas, si bien también son mencionadas otras técnicas tales como la extracción líquido-líquido (Pennetreau y Vandenbussche, 2001) o la sublimación criogénica (Mitchell, 1976).

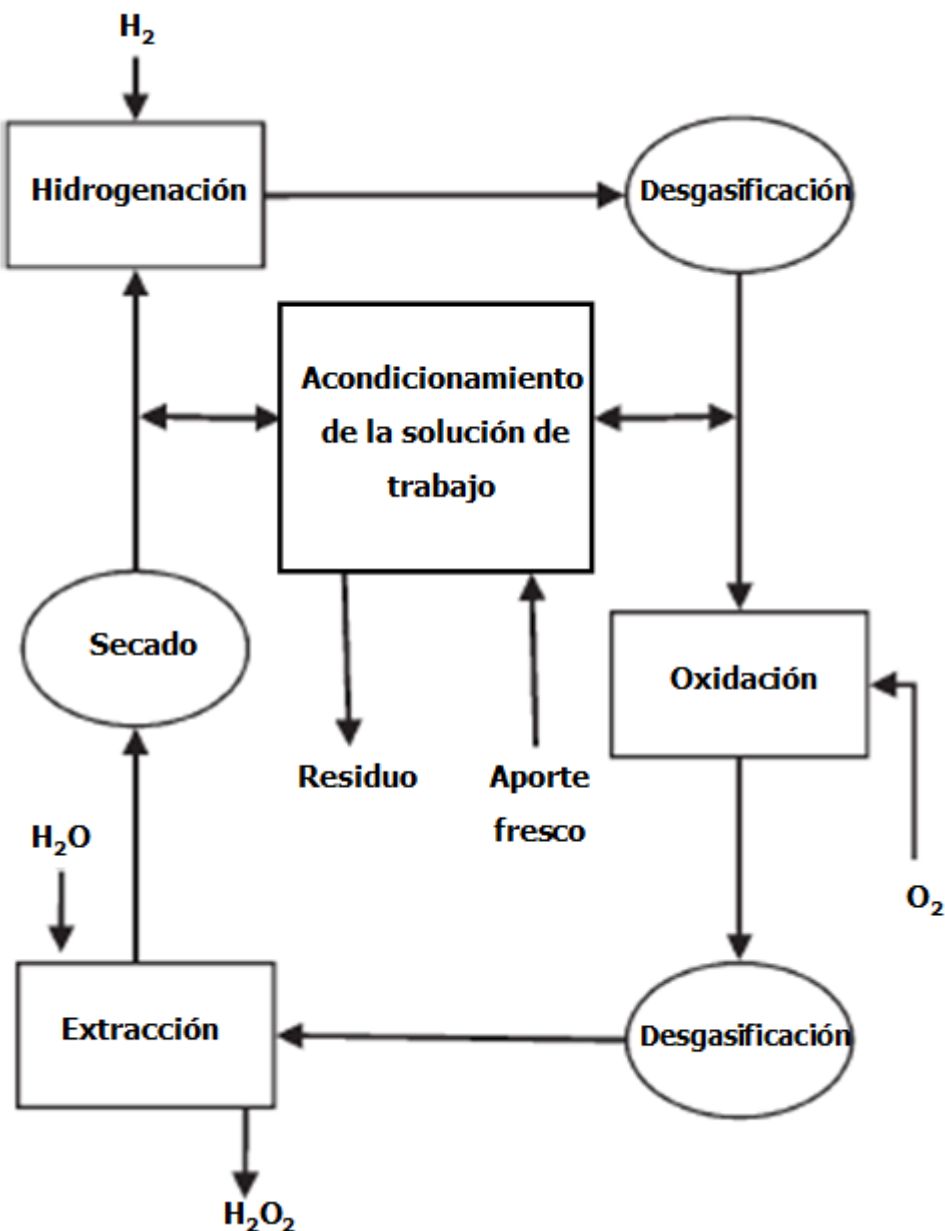


Figura 1.2. Esquema básico de las etapas del método de la antraquinona para la síntesis de peróxido de hidrógeno

De todos modos, sea cual sea la opción técnica elegida, las medidas preventivas para evitar en la medida de lo posible el riesgo de contaminación son esenciales para lograr resultados satisfactorios. Seguramente sea difícil encontrar un sector industrial más preocupado por el

control de la contaminación, ya que la producción de materiales semiconductores impone grandes restricciones al ambiente de trabajo. Todas las etapas críticas son llevadas a cabo bajo condiciones de sala limpia para minimizar la posible contaminación desde la atmósfera de trabajo. Por otra parte, la selección de los materiales más adecuados en las instalaciones y equipos empleados es también crucial, por lo que se ha de elegir materiales seguros y resistentes al contacto con peróxido de hidrógeno para reducir los riesgos de accidentes sin olvidar la necesidad de evitar la contaminación del reactivo (Mackenzie, 1990; Sinha, 2006).

El empleo de la destilación en el proceso de ultrapurificación de peróxido de hidrógeno está orientado en mayor medida a la disminución del contenido en contaminantes de origen orgánico y no tanto a reducir las impurezas metálicas (Signori y Glinos, 1994; Shimokawa et al., 1995; Inaba et al., 1997; Johnsson et al., 1998). De todas maneras, los límites para los elementos metálicos fijados para los grados electrónicos menos exigentes pueden ser alcanzados si la solución de partida no contiene concentraciones por encima de unas pocas ppm. La necesidad de emplear columnas muy inertes, normalmente fabricadas en polímeros fluorados que se caracterizan por ser malos conductores del calor, intensifica el ya de por sí elevado consumo energético del proceso (Davison, 1992; Fernández-Olmo et al., 2007).

Los ejemplos de ultrapurificación por adsorción han recurrido a muy diversos adsorbentes: óxido estánnico (Morris y Feasey, 1993), fosfato de zirconio (Manganaro et al, 1993) o distintas resinas no iónicas (Honig y Geigel, 1993; Nishide et al., 1998). Se puede disminuir la cantidad de impurezas tanto metálicas como orgánicas en función del adsorbente elegido, pero los rendimientos máximos alcanzables se encuentran por debajo de los resultados que se puede lograr con otras tecnologías tales como las membranas o el intercambio iónico. Hay que tener en consideración además la producción de desechos asociados a los adsorbentes agotados, bien de forma directa por simple sustitución por adsorbente fresco o bien de forma indirecta como efluentes consecuencia de la regeneración, y el uso en su caso de reactivos tóxicos y peligrosos como regenerantes.

El intercambio iónico es con diferencia la tecnología para ultrapurificación de peróxido de hidrógeno más mencionada por las patentes (Crofts y Williams, 1993; Sugihara et al., 1994; Millar et al., 1995; Kajiwara et al, 1999; Ledon et al., 1998; Ledon et al., 1999a; Ledon y Devos, 1999b; Devos y Demay, 2001; Miglio et al., 2005; Oeter et al., 2005). Las diversas referencias cubren un amplio rango de condiciones de operación y en ocasiones contemplan la adición de reactivos para mejorar el proceso (Shiga et al., 1993; Kajiwara y Serizawa, 1996). Los procesos con múltiples etapas son comunes cuando se busca obtener los grados electrónicos más exigentes (Ledon et al., 1999c; Saito e Izumi, 2000; Tanaka et al., 2005). El acondicionamiento de las resinas antes de entrar en contacto con el peróxido de hidrógeno es importante, ya que los grupos funcionales hidroxilo tan clásicos en las resinas aniónicas catalizan la descomposición de forma violenta del peróxido (Minamikawa et al., 1998; Kajiwara et al, 2000; Havlicek et al., 2003; Havlicek et al., 2005). Los metales de transición también pueden actuar como

catalizadores de la descomposición por lo que hay que extremar la precaución con las resinas catiónicas con cargas altas de metales de este tipo. La regeneración de las resinas agotadas implica la aparición de corrientes residuales y el empleo de reactivos peligrosos (ácidos y bases fuertes).

Tabla 1.2. Resumen de los principales trabajos de ultrapurificación de peróxido de hidrógeno localizados durante la revisión bibliográfica.

Tecnología	Patente	Título, inventores, año, empresa
Destilación	US 5296104	Process for obtaining purified aqueous hydrogen peroxide solutions Signori, L., Glinos, K., 1994, Interox Int. S.A.
	US 5456898	Method for enrichment and purification of aqueous hydrogen peroxide solution, Shimokawa, S., Minamikawa, Y., Murakami, S., 1995, Mitsubishi Gas Chemical Co.
	US 5670028	Process for preparing high purity hydrogen peroxide aqueous solution, Inaba, I., Ueno, Y., Watanabe, M., Nishida Y., 1997, UBE Industries
	US 5705040	Process for preparing a substantially pure aqueous solution of hydrogen peroxide, Johnsson, P., Mattila, T., Saari, K., 1998
Adsorción	US 5262058	Purification of hydrogen peroxide, Morris, G.W., Feasey, N.D., 1993, Interox Chemicals Ltd.
	US 5266298	Process for removing iron from hydrogen peroxide, Manganaro, J.L., Gilibisco, D., Reed, J.R., Frianeza-Kullberg, 1993, FMC Corp.
	US 5232680	Method for purifying hydrogen peroxide for microelectronics uses, Honing, H., Geigel, S., 1993, Peroxid Chemi GmbH
	US 5851505	Method of producing purified aqueous solution of hydrogen peroxide, Nishide, Y., Minamikawa, Y., Kokubu, J., 1998, Mitsubishi Gas Chemical Co.
Intercambio iónico	US 5733521	Process for producing purified aqueous hydrogen peroxide solution Minamikawa, Y., Murakami, S., Hattori, M., 1998, Mitsubishi Gas Chemical Co.
	US 5961947	Process for the preparation of an ultra pure hydrogen peroxide solution by the ion exchange by sequence: anionic-cationic-anionic-cationic Ledon, H., Carre, M., Demay, D., Devos, C., Jeanin, S., 1999, Air Liquide
	US 6054109	Method of purifying aqueous solution of hydrogen peroxide Saito, N., Izumi, M., 2000, Mitsubishi Chem. Co.
	US 6896867	Process for producing a purified aqueous hydrogen peroxide solution Tanaka, F., Sugawara, S., Adachi, T., Mine, K., 2003, Santoku Chemical Ind. Co. Ltd
	US 6939527 B2	Method for the purification of hydrogen peroxide solutions Oeter, D., Dusemund, C., Neumann, E., Freissler, K., Hostalek, M., 2005, Merck
Membranas	US 4879043	Manufacture of high purity hydrogen peroxide by using reverse osmosis Boughton, J.H., Butz, R.A., Cheng, H.C.T., Dennis, J.R., Hannon, B.T., Weigel, J.H., 1989, Du Pont
	US 5906738	Apparatus and method for removing impurities from aqueous hydrogen peroxide Morisaki, A., Sawaguri, Y., Matsuda, Y., 1999, Sumimoto Chemical Co. Ltd.
	US 6333018 B2	Process for the industrial production of high purity hydrogen peroxide Bianchi, U.P., Leone, U., Lucci, M., 2001
	US 6113798 A	Process for the purification of hydrogen peroxide Dhalluin, J.M. Wawrzyniak, J.J., Ledon, H., 2000, Air Liquide
	WO 2005/033005 A1	Process for the purification of aqueous peroxide solutions, solutions obtainable thereby and their use Owen, R., Bosse, J., Sell, M., 2005, Solvay

Las tecnologías de membranas aparecen como una adecuada opción para producir soluciones acuosas ultrapuras de peróxido de hidrógeno. La ósmosis inversa está llamada a ser la opción más apropiada para la eliminación de trazas metálicas y otras impurezas (Boughton et al., 1989; Morisaki et al., 1999; Bianchi et al., 2001; Owen et al., 2005), y la ultrapurificación también es mencionada, en este caso en combinación con agentes quelantes (Dhalluin et al., 2000). Estos aditivos ayudan a secuestrar los iones metálicos presentes en la alimentación y así se impide su paso al permeado, ya que los reactivos quelantes han de ser seleccionados de modo que sean totalmente retenidos por la membrana.

1.3. La ósmosis inversa para la ultrapurificación de reactivos

Entre todas las alternativas para la ultrapurificación de peróxido de hidrógeno propuestas en bibliografía, la ósmosis inversa aparece destacada como la opción más deseable desde el punto de vista de la sostenibilidad de procesos. La ósmosis inversa no necesita ningún tipo de reactivo químico adicional para su funcionamiento y en la aplicación concreta a la ultrapurificación de peróxido se puede lograr evitar la generación de residuos, efluentes o emisiones ya que la corriente de rechazo de la membrana puede ser considerada como un subproducto del proceso y es posible su comercialización para aplicaciones donde el contenido en impurezas metálicas del peróxido de hidrógeno no sea un factor limitante. Únicamente quedaría como residuo las membranas ya gastadas después de su vida útil, pero es posible que estas membranas puedan ser reutilizadas en procesos de ultrafiltración o microfiltración (Rodríguez et al., 2002; Veza y Rodríguez-González, 2003; Mohamedou et al., 2010; Lawler et al., 2012). Además, gran parte de la energía necesaria para incrementar la presión de la corriente que alimenta a las membranas puede ser recuperada de la corriente de rechazo por distintos sistemas (Fariñas, 1999; Harris, 1999; Semiat, 2008; Gude, 2011).

Hay que destacar que las membranas son también utilizadas para la ultrapurificación de otros reactivos electrónicos, siendo el ácido fluorhídrico el ejemplo más claro. En ocasiones, las membranas no son más que un soporte para otras técnicas tales como el intercambio iónico (Parekh y Zahka, 1996; Fyen et al., 1997; Grant et al., 1997; Weddington et al., 1999) o la adsorción con agentes quelantes (Parekh et al., 2003). Sin embargo, las membranas de ósmosis inversa han sido aplicadas de modo exitoso a la ultrapurificación de ácido fluorhídrico. Varios autores han demostrado la viabilidad del reprocesado de los baños de grabado basados en ácido fluorhídrico con membranas comerciales de ósmosis inversa capaces de separar las impurezas metálicas (Mukherjee et al., 1994; Kulkarni et al., 1995; Gill et al., 1998). Estos reprocesadores de membranas presentan unos resultados estables en el tiempo (Kulkarni et al., 1994) y son capaces de conseguir un contenido en impurezas metálicas en el baño menor al correspondiente al reactivo virgen de partida (Gill et al., 1996). Para conseguir niveles muy

exigentes de pureza, se recomienda recurrir a configuraciones con múltiples pasos por los reprocessadores (Mukherjee et al., 1996).

En el ámbito de las tecnologías de membranas, se entiende por paso a una unidad de membranas que es alimentada con la corriente de permeado de una unidad anterior. Este tipo de configuración fue en inicio desarrollada para instalaciones de desalación en las que era imposible conseguir agua potable en una única etapa, situación habitual en áreas de gran salinidad como el Golfo Pérsico (Medina San Juan, 2000). Sin embargo, las actuales membranas de ósmosis inversa, con rechazos de sales por encima del 99%, hacen viable la desalación en una etapa y los procesos en múltiples pasos parecían abocados a su desaparición. Pero la creciente preocupación por la concentración de boro en el agua potable ha dado una nueva oportunidad a las configuraciones con más de un paso (Unión Europea, 1998; Organización Mundial de la Salud, 2011), ya que el boro es retenido de modo mucho menos eficaz por las membranas de ósmosis inversa (Gorenflo et al., 2007). Por este motivo, muchas plantas desaladoras actuales funcionan en régimen de pasos múltiples para conseguir aumentar la calidad de sus permeados (Glueckstern y Priel, 2003; Redondo et al., 2003; Taniguchi et al., 2004; Faigon y Hefer, 2008).

La mayor desventaja de los procesos con múltiples pasos es la baja recuperación global del sistema. Si las corrientes de rechazo de cada unidad de membranas son descartadas, únicamente una pequeña parte de la alimentación abandona la instalación como permeado final de alta calidad. Por lo tanto es habitual recurrir a la implementación de corrientes de recirculación de manera que la corriente de rechazo de una etapa es acoplada junto a la corriente de alimentación de la etapa anterior (Zhu et al., 2009). De esta forma se configura una cascada de membranas integradas en contracorriente, cuyo esquema general se encuentra representado en la Figura 1.3.

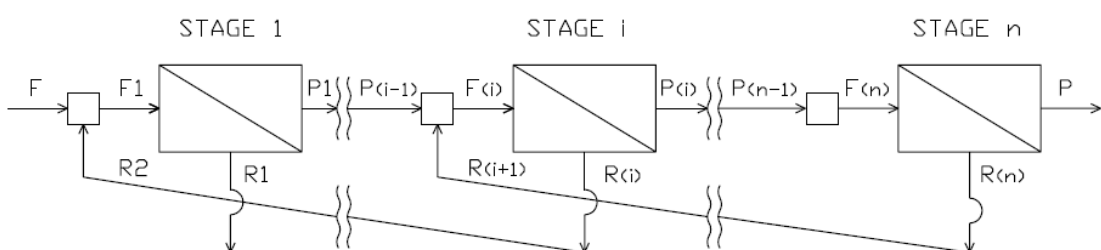


Figura 1.3. Representación esquemática de una cascada de membranas integradas por n etapas en contracorriente

La idea de configurar cascadas de membranas surgió en el campo de las separaciones de gases (Caus et al. 2009a; Gassner y Maréchal, 2010) pero rápidamente la configuración fue adoptada para otros tipos de membranas: microfiltración (Abatemarco et al., 1999; Mellal et al., 2007), ultrafiltración (Overdevest et al., 2002; Gosh, 2003; Isa et al., 2007; Mayani et al. 2009; Vanneste et al., 2011), nanofiltración (Lin y Livingstone, 2007; Caus et al., 2009b) y ósmosis inversa (Voros et al., 1997; Tanuwidjaja y Hoek, 2006).

El problema del diseño de cascadas de membranas de ósmosis inversa puede ser considerado como un caso específico de instalación de ósmosis inversa. Una instalación típica consta de una red interconectada de módulos de membranas configurada para cumplir con objetivos técnicos, económicos y medioambientales (Aboabboud y Elmasallati, 2007; Park et al., 2010; Peñate y García-Rodríguez, 2011; Voutchkov, 2011). Las herramientas de simulación y optimización ayudan en gran medida a comprender el funcionamiento de estos sistemas complejos y son imprescindibles para conseguir las condiciones más favorables de operación y explotación (Ahmetovic y Grossmann, 2011).

1.4. Objetivos y estructura de la tesis

La presente Tesis se ha desarrollado en el marco de los proyectos CTM2006-00317 "*Sostenibilidad de la Producción: Intensificación e Integración de procesos en la Industria química y transformadora*" y CTQ2010-16608 "*Ultrapurificación de productos químicos basada en tecnología de membranas para alcanzar calidad grado electrónico*". El objetivo general de este último proyecto de investigación fundamental es avanzar en el estudio y conocimiento de las tecnologías de ultrapurificación para la obtención de productos químicos de elevada calidad (grado electrónico), cuyo mercado es creciente debido a la demanda por parte de los sectores industriales vinculados con los materiales semiconductores. Este objetivo se ha concretado hasta el momento en el peróxido de hidrógeno y la evaluación de la tecnología de membrana de ósmosis inversa como opción de ultrapurificación.

En este contexto, el objetivo general de esta Tesis Doctoral es demostrar la viabilidad de las tecnologías de membranas para procesos integrados de ultrapurificación de peróxido de hidrógeno hasta alcanzar los requerimientos propios de calidad electrónica en lo referente a impurezas metálicas. Esta Tesis supone una contribución innovadora para profundizar en el conocimiento de los fundamentos de los procesos de ultrapurificación de peróxido de hidrógeno basados en las tecnologías de membranas y avanzar en el desarrollo de herramientas de ayuda para la toma de decisiones durante las etapas de diseño, operación y explotación de estos procesos.

Para alcanzar este objetivo general es necesario abordar los siguientes objetivos específicos:

- Estudio de la viabilidad técnica del proceso de ultrapurificación de peróxido de hidrógeno empleando diferentes membranas de poliamida y acetato de celulosa para ósmosis inversa con el fin de reducir los niveles de impurezas metálicas hasta valores que cumplan con los requisitos impuestos para poder ser considerado como reactivo electrónico.

- Modelado de los fenómenos de transporte a través de las membranas y simulación del proceso de ultrapurificación bajo la configuración de una cascada de membranas integradas en contracorriente.
- Estudio de la viabilidad económica de la ultrapurificación a escala industrial de peróxido de hidrógeno mediante la evaluación de los ingresos y costes del proceso.
- Análisis de la influencia de las principales condiciones de operación, precios unitarios de los recursos y restricciones de mercado sobre el proceso de ultrapurificación de peróxido de hidrógeno por ósmosis inversa.
- Optimización de las variables que definen el funcionamiento del proceso de ultrapurificación con la maximización del beneficio económico como objetivo, con la posibilidad de añadir otros criterios de optimización, como por ejemplo la calidad del producto, y planteamiento de problemas de optimización multiobjetivo.

De acuerdo con estos objetivos específicos, y considerando la normativa para una Tesis basada en un compendio de artículos, el trabajo se desarrolla en cuatro capítulos de la siguiente forma:

El Capítulo 1 presenta el planteamiento de la Tesis.

El Capítulo 2 incluye una descripción detallada de los materiales y métodos empleados para la realización de la Tesis, así como una visión global de los principales resultados obtenidos y la discusión de los mismos.

El Capítulo 3 resume las conclusiones generales extraídas y las vías de progreso de la investigación.

El Capítulo 4 supone el núcleo central de la Tesis, incluyendo copia de los artículos que la sustentan.

Referencias del Capítulo 1

- T. Abatemarco, J. Stickel, J. Belfort, B.P. Frank, P.M. Ajayan, G. Belfort, *Fractionation of multiwalled carbon nanotubes by cascade membrane microfiltration*, Journal of Physical Chemistry B, 103 (1999) 3534-3538.
- M. Aboabboud, S. Elmasallati, *Potable water production from seawater by the reverse osmosis technique in Libya*, Desalination, 203 (2007) 119-133.
- E. Ahmetovic, I.E. Grossmann, *Global superstructure optimization for the design of integrated process water networks*, AIChE Journal, 57 (2011) 434-457.
- L. Archer, S.A. Henry, D. Nachreiner, *Removing postash polymer residue from BEOL structures using inorganic chemicals*, MICRO, 6 (2001) 95-103.
- J. Atsumi, S. Ohtsuka, S. Munehira, K. Kajiyama, *Metallic contamination on Si wafers from cleaning solutions*, Proceedings of the Electrochemical Society, 90 (1990) 59-66.
- U.P. Bianchi, U. Leone, M. Lucci, *Process for the industrial production of high purity hydrogen peroxide*, US Patent 6333018 B2, 2001.
- J.H. Boughton, R.A. Butz, H.C.T. Cheng, J.R. Dennis, B.T. Hannon, J.H. Weigel, *Manufacture of high purity hydrogen peroxide by using reverse osmosis*, US Patent 4879043, 1989.
- J. M. Campos-Martín, G. Blanco-Brieva, J.L.G. Fierro, *Hydrogen peroxide synthesis: an outlook beyond the anthraquinone process*, Angewandte Chemie International Edition, 45 (2006) 6962-6984.
- M. Castells, *La era de la información, economía, sociedad y cultura*, Siglo XXI Editores, Ciudad de México, 1999.
- A. Caus, L. Braeken, K. Boussu, B. van der Bruggen, *The use of integrated countercurrent nanofiltration cascades for advanced separations*, Journal of Chemical Technology and Biotechnology, 84 (2009a) 391-398.
- A. Caus, S. Vanderhaegen, L. Braeken, B. van der Bruggen, *Integrated nanofiltration cascades with low salt rejection for complete removal of pesticides in drinking water production*, Desalination, 241 (2009b) 111-117.
- T. Couteau, G. Dawson, J. Halladay, L. Archer, *Comparing single-wafer and batch polymer cleans using inorganic chemicals in BEOL applications*, MICRO 24 (2006) 45-49.
- R.D. Crofts, J. Williams, *Purification of hydrogen peroxide*, US Patent 5215665, 1993.
- S. Daigle, E. Vogelsberg, B. Lim, I. Butcher, *Electronic chemicals*, in: *Ullmann's Encyclopedia of Industrial Chemistry*, Edición electrónica, Wiley-VCH, Weinheim, 2007.
- J. Davison, *Acid reprocessors. Part II. The HF reprocessor*, Solid State Technology, 35 (1992) S10-S14.

- C. Devos, D. Demay, *Process for the aqueous purification of hydrogen peroxide containing impurities*, US Patent 6296829 B1, **2001**.
- J.M. Dhalluin, J.J. Wawrzyniak, H. Ledon, *Process for the purification of hydrogen peroxide*, US Patent 6113798 A, **2000**.
- J.M. Duffalo, J.R. Monkowski, *Particulate contamination and device performance*, Solid State Technology, 27 (**1984**) 109-114.
- M. Faigon, D. Hefer, *Boron rejection in SWRO at high pH conditions versus cascade design*, Desalination, 223 (**2008**) 10-16.
- M. Fariñas, *Osmosis inversa: fundamentos, tecnología y aplicaciones*, McGraw-Hill, Madrid, **1999**.
- I. Fernández-Olmo, J.L. Fernández, A. Irabien, *Purification of dilute hydrofluoric acid by commercial ion exchange resins*, Separation and Purification Technology, 56 (**2007**) 118-125.
- Freedonia Group, *Electronic chemicals to 2008*, Industry Study No. 1852, Edición electrónica, **2004**.
- W. Fyen, L. Mouche, M. Meuris, M.M. Heyns, J. Zahka, *Point of use HF purification for silicon surface preparation by ion exchange*, Journal of the Electrochemical Society, 144 (**1997**) 2189-2196.
- M. Gassner, F. Maréchal, *Combined mass and energy integration in process design at the example of membrane-based gas separation systems*, Computers & Chemical Engineering, 34 (**2010**) 2033-2042.
- W.N. Gill, V. Agrawal, A.L. Gill, M. Naik, A. Kulkarni, D. Mukherjee, *Novel membrane-based systems for reprocessing hydrofluoric acid etching solutions*, Advances in Environmental Research, 2 (**1998**) 333-350.
- P. Glueckstern, M. Priel, *Optimization of boron removal in old and new SWRO systems*, Desalination, 156 (**2003**) 219-228.
- G. Goor, J. Glenneberg, S. Jacobi, *Hydrogen peroxide*, in: *Ullmann's Encyclopedia of Industrial Chemistry*, Edición electrónica, Wiley-VCH, Weinheim, **2007**.
- A. Gorenflo, M. Brusilovsky, M. Faigon, B. Liberman, *High pH operation in seawater reverse osmosis permeate: First results from the world's largest SWRO plant in Ashkelon*, Desalination, 203 (**2007**) 82-90.
- R. Gosh, *Novel cascade ultrafiltration configuration for continuous high-resolution protein-protein fractionation: A simulation study*, Journal of Membrane Science, 226 (**2003**) 85-99.

- D.C. Grant, W.P. Kelly, V. Anantharaman, J.H. Shyu, *Purity control in dilute HF baths using point of use purifiers*, Proceedings of 16th Semiconductor Pure Water and Chemicals Conference, 3-7 Marzo, Santa Clara (California), Volumen II, 1-14 ,**1997**.
- V.G. Gude, *Energy consumption and recovery in reverse osmosis*, Desalination and Water Treatment, 36 (**2011**) 239-260.
- C. Harris, *Energy recovery for membrane desalination*, Desalination, 125 (**1999**) 173-180.
- M.D. Havlicek, J.G. Hoffman, W. Yuan, *Integrated method of preconditioning a resin for hydrogen peroxide purification and purifying hydrogen peroxide*, US Patent 6537516 B2, **2003**.
- M.D. Havlicek, D.L. Snyder, J.G. Hoffman, M.E. Cummings, *Resin preconditioning methods using carbon dioxide and methods for purifying hydrogen peroxide*, US Patent 6875415 B2, **2005**.
- H. Honig, S. Geigel, *Method for purifying hydrogen peroxide for microelectronics uses*, US Patent 5232680, **1993**.
- Y. Inaba, Y. Ueno, M. Watanabe, Y. Nishida, *Process for preparing high purity hydrogen peroxide aqueous solution*, US Patent 5670028, **1997**.
- M.H.M. Isa, D.E. Coraglia, R.A. Frazier, P. Jauregui, *Recovery and purification of surfactin from fermentation broth by a two-step ultrafiltration process*, Journal of Membrane Science, 296 (**2007**) 51-57.
- J.S. Jeon, B. Ogle, M. Baeyens, P. Mertens, *Evaluation of cleaning recipes based on ozonated water for pre-gate oxide cleaning*, Solid State Phenomena, 65-66 (**1999**) 119-122.
- P. Johnsson, T. Mattila, K. Saari, *Process for preparing a substantially pure aqueous solution of hydrogen peroxide*, US Patent 5705040, **1998**.
- S. Kajiwara, H. Serizawa, *Method for the preparation of purified aqueous hydrogen peroxide solution*, US Patent 5534238, **1996**.
- S. Kajiwara, H. Serizawa, K. Nagai, *Process for purifying an aqueous solution of hydrogen peroxide*, US Patent 5976478, **1999**.
- S. Kajiwara, H. Serizawa, K. Nagai, *Method for preparing high-purity aqueous hydrogen peroxide*, US Patent 6013237, **2000**.
- A. Kulkarni, D. Mukherjee, W.N. Gill, *Reprocessing hydrofluoric acid etching solutions by reverse osmosis*, Chemical Engineering Communications, 129 (**1994**) 53-68.
- A. Kulkarni, D. Mukherjee, W.N. Gill, *Membrane reprocessing of hydrofluoric acid solutions*, Semiconductor International, 18 (**1995**) 207-211.
- W. Lawler, Z. Bradford-Hartke, M: J. Cran, M. Duke, G. Leslie, B.P. Ladewig, P. Le-Clech, *Towards new opportunities for reuse, recycling and disposal of used reverse osmosis membranes*, Desalination, 299 (**2012**) 103-112.

- H. Ledon, M. Carre, C. Devos, J.G. Hoffman, S.R. Clark, *On-site manufacture of ultra-high-purity hydrogen peroxide*, European Patent 0846654 A1, **1998**.
- H. Ledon, C. Devos, D. Demay, *Process for the preparation of an ultra pure solution of hydrogen peroxide by ion exchange with recycling*, US Patent 5928621, **1999a**.
- H. Ledon, C. Devos, *Process for the preparation of an ultra pure hydrogen peroxide solution by ionic exchange in beds having defined H/D ratios*, US Patent 5932187, **1999b**.
- H. Ledon, M. Carre, D. Demay, C. Devos, S. Jeanin, *Process for the preparation of an ultra pure hydrogen peroxide solution by the ion exchange by sequence: anionic-cationic-anionic-cationic*, US Patent 5961947, **1999c**.
- J.C.T. Lin, A.G. Livingston, *Nanofiltration membrane cascade for continuous solvent exchange*, Chemical Engineering Science, 62 (**2007**) 2728-2736.
- G.Y. Luan, W.P. Gao, P.J. Yao, *Progress in purification of total organic carbon compounds in highly pure hydrogen peroxide production*, Xiandai Huagong / Modern Chemical Industry, 25 (**2005**) 20-24.
- J. Mackenzie, *Hydrogen peroxide without accidents*, Chemical Engineering, 97 (**1990**) 84–90.
- J.L. Manganaro, D. Gibilisco, J.R. Reed, T. Frianeza-Kullberg, *Process for removing iron from hydrogen peroxide*, US Patent 5266298, **1993**.
- Y. Masuda, *The Information Society as Post-Industrial Society*, Institute for the Information Society, Tokio, **1980**.
- M. Mayani, K. Mohanty, C. Filipe, R. Gosh, *Continuous fractionation of plasma proteins HSA and IgG using cascade ultrafiltration systems*, Separation and Purification Technology, 70 (**2009**) 231-241.
- J.A. Medina San Juan, *Desalación de aguas salobres y de mar. Osmosis inversa*. Mundi-Prensa, Madrid, **2000**.
- M. Mellal, L.H. Ding, M.Y. Jaffrin, C. Delattre, P. Michaud, J. Courtois, *Separation and fractionation of oligouronides by shear-enhanced filtration*, Separation Science and Technology, 42 (**2007**) 349-361.
- R. Miglio, G. Paparatto, G. De Alberti, *Process for the removal of the inorganic acids and metal impurities present in essentially alcoholic solutions of H₂O₂ coming from direct synthesis*, WO Patent 2005/063619, **2005**.
- M.H. Millar, F.R.F. Hardy, G.W. Morris, J.R. Crampton, *Purification of hydrogen peroxide*, US Patent 5397475, **1995**.
- Y. Minamikawa, S. Murakami, M. Hattori, *Process for producing a purified aqueous hydrogen peroxide solution*, US Patent 5733521, **1998**.

- J.W. Mitchell, *Process for purification by cryogenic sublimation*, US Patent 3992159, **1976**.
- E.O. Mohamedou, D.B. Penate Suarez, F. Vince, P. Jaouen, M. Pontie, *New lives for old reverse osmosis (RO) membranes*, Desalination, 253 (**2010**) 62-70.
- A. Morisaki, Y. Sawaguri, Y. Matsuda, *Apparatus and method for removing impurities from aqueous hydrogen peroxide*, US Patent 5906738, **1999**.
- G.W. Morris, N.D. Feasey, *Purification of hydrogen peroxide*, US Patent 5262058, **1993**.
- D. Mukherjee , A. Kulkarni, A. Chawla, W.N. Gill, *Ultrapurification and recycling of hydrofluoric acid etching solutions by reverse osmosis: membrane performance and multicomponent rejection*, Chemical Engineering Communications, 130 (**1994**) 127-138.
- D. Mukherjee , A. Kulkarni, W.N. Gill, *Membrane based system for ultrapure hydrofluoric acid etching solutions*, Journal of Membrane Science, 109 (**1996**) 205-217.
- Y. Nishide, Y. Minamikawa, J. Kokubu, *Method of producing purified aqueous solution of hydrogen peroxide*, US Patent 5851505, **1998**.
- D. Oeter, C. Dusemund, E. Neumann, K. Freissler, M. Hostalek, *Method for the purification of hydrogen peroxide solutions*, US Patent 6939527 B2, **2005**.
- E.D. Olson, C.A. Reaux, W.C., Ma, J.W. Butterbaugh, *Alternatives to standard wet cleans*, Semiconductor International, 23 (**2000**) 70-75.
- Organización Mundial de la Salud (OMS), *Guías para la calidad del agua potable*, 4^a edición, Ginebra, **2011**.
- P.E.M. Overdevest, M.H.J. Hoenders, K. van't Riet, A. van der Padt, J.T.F. Keurentjes, *Enantiomer separation in a cascaded micellar-enhanced ultrafiltration system*, AIChE Journal, 48 (**2002**) 1917-1926.
- R. Owen, J. Bosse, M. Sell, *Process for the purification of aqueous peroxygen solutions, solutions obtainable thereby and their use*, WO Patent 2005/033005 A1, **2005**.
- B. Parekh, J. Zahka, *Point-of-use purification in DHF baths*, Solid State Technology, 39 (**1996**) 155-161.
- B.S. Parekh, A.J. DiLeo, E. Deane, R.L. Bruening, *Filtration and purification method for aqueous acids*, US Patent 6649064 B2, **2003**.
- C. Park, P.K. Park, P.P. Mane, H. Hyung, V. Gandhi, S.H. Kim, J.H. Kim, *Stochastic cost estimation approach for full-scale reverse osmosis desalination plants*, Journal of Membrane Science, 364 (**2010**) 52-64.
- P. Pennetreau, A. Vandebussche, *Process for manufacturing an aqueous hydrogen peroxide solution*, US Patent 6224845 B1, **2001**.

- B. Peñate, L. García-Rodríguez, *Retrofitting assessment of the Lanzarote IV seawater reverse osmosis desalination plant*, Desalination, 266 (2011) 244-255.
- D.L. Rath, R. Ravikumar, D.J. Delehanty, R.G. Filippi, E.W. Kiewra, G. Stojakovic, K.J. McCullough, D.D. Miura, B.N. Rhoads, *New aqueous clean for aluminium interconnects: Part I. Fundamental*, Solid State Phenomena, 76-77 (2001) 31-34.
- R. Ravikumar , D.L. Rath, D.J. Delehanty, R.G. Filippi, E.W. Kiewra, G. Stojakovic, K.J. McCullough, D.D. Miura, J. Gambino, F. Schnabel, B.N. Rhoads, *New aqueous clean for aluminium interconnects: Part II. Applications*, Solid State Phenomena, 76-77 (2001) 51-54.
- J. Redondo, M. Busch, J.P. De Witte, *Boron removal from seawater using FILMTECTM high rejection SWRO membranes*. Desalination, 156 (2003) 229-238.
- K.A. Reinhardt, W. Kern, *Handbook of silicon wafer cleaning technology*, William Andrew, Norwich, Nueva York, 2008.
- J.J. Rodríguez, V. Jiménez, O. Trujillo, J.M. Veza, *Reuse of reverse osmosis membranes in advanced wastewater treatment*, Desalination, 150 (2002) 219-225.
- N. Rúa Ceballos, *La globalización del conocimiento científico-tecnológico y su impacto sobre la innovación en los países menos desarrollados*, I Congreso Iberoamericano de Ciencia, Tecnología, Sociedad e Innovación, 19-23 Junio, Ciudad de México, Volumen 6, 1-13 2006.
- N. Saito, M. Izumi, *Method of purifying aqueous solution of hydrogen peroxide*, US Patent 6054109, 2000.
- SEMI (Semiconductor Equipment and Materials International), *Specifications for Hydrogen Peroxide*, SEMI Document C30-1110, San Jose (California), 2010.
- R. Semiat, *Energy issues in desalination processes*, Environmental Science and Technology, 42 (2008) 8193-8201.
- W.J. Sievert, *A European perspective on electronic chemicals*, Semiconductor Fabtech, 10 (2000) 199-204.
- W.J. Sievert, *Setting standards. The developments of standards in the field of electronic chemicals*, Semiconductor Fabtech, 13 (2001) 175-179.
- D. Sinha, *Metal contamination from process materials used for wet cleaning of silicon wafer*, The Electrochemical Society Transactions, 2 (2006) 91-98.
- S. Shiga, Y. Sawaguri, K. Kabasawa, T. Momobayashi, *Purification of hydrogen peroxide solution*, US Patent 5200166, 1993.
- S. Shimokawa, Y. Minamikawa, S. Murakami, *Method for enrichment and purification of aqueous hydrogen peroxide solution*, US Patent 5456898, 1995.

- H.S. Sohn, J.W. Butterbaugh, E.D. Olson, J.Diedrick, N.P. Lee, *Using cost-effective dilute acid chemicals to perform postetch interconnect cleans*, MICRO, 23 (2005) 67-76.
- L. Signori, K. Glinos, *Process for obtaining purified aqueous hydrogen peroxide solutions*, US Patent 5296104, 1994.
- Y. Sugihara, K. Tanaka, H. Sakaitani, *Process for purification of hydrogen peroxide*, US Patent 5614165, 1994.
- F. Tanaka, S. Sugawara, T. Adachi, K. Mine, *Process for producing a purified aqueous hydrogen peroxide solution*, US Patent 6896867, 2005.
- M. Taniguchi, Y. Fusaoka, T. Nishikawa, M. Kurihara, *Boron removal in RO seawater desalination*, Desalination, 167 (2004) 419-426.
- D. Tanuwidjaja, E.M.V. Hoek, *High-efficiency seawater desalination via NF/RO multi-pass arrays*, AIChE Annual Meeting Conference Proceedings, 12-17 Noviembre, San Francisco (California), 1-6, 2006.
- The Engineer, *Electrolysed acid strips for semiconductors*, Edición on-line, Marzo, 2007.
- Unión Europea, *Directiva 98/83/CE del Consejo de 3 de Noviembre de 1998 relativa a la calidad de las aguas destinadas al consumo humano*, Diario Oficial L 330 de 05/12/1998, 32-54, 1998.
- J. Vanneste, S. de Ron, S. Vandecruys, S. A. Soare, S. Darvishmanesh, B. van der Bruggen, *Techno-economic evaluation of membrane cascades relative to simulated moving bed chromatography for the purification of mono- and oligosaccharides*, Separation and Purification Technology, 80 (2011) 600-609.
- J.M. Veza, J.J. Rodríguez-González, *Second use for old reverse osmosis membranes: wastewater treatment*, Desalination, 157 (2003) 65-72.
- N.G. Voros, Z.B. Maroulis, D. Marinos-Kouris, *Short-cut structural design of reverse osmosis desalination plants*, Journal of Membrane Science, 127 (1997) 47-68.
- N. Voutchkov, *Overview of seawater concentrate disposal alternatives*, Desalination, 273 (2011) 205-219.
- D. Weddington, J. Bodnar, M. Jahanbani, R. Blum, *An assessment of a dilute hydrofluoric acid purifier*, Semiconductor Internacional, 22/6 (1999) 151-158.
- A. Zhu, P.D. Christofides, Y. Cohen, *Minimization of energy consumption for a two-pass membrane desalination: Effect of energy recovery, membrane rejection and retentate recycling*, Journal of Membrane Science, 339 (2009) 126-137.

Desarrollo 2

CAPÍTULO 2. DESARROLLO

2.1. Instalación para la ultrapurificación de peróxido de hidrógeno a escala de laboratorio mediante membranas de ósmosis inversa

El corazón de la instalación experimental de laboratorio diseñada para poder llevar a cabo la ultrapurificación de peróxido de hidrógeno fue una celda SEPA CF II (Osmonics), unidad para test de membranas planas en régimen de flujo cruzado (Figura 2.1). La celda es capaz de alojar cualquier muestra de membrana plana con dimensiones 19 x 14 cm, dando como resultado una superficie efectiva de membrana de 140 cm².



Figura 2.1. Vista de la celda plana para membranas

La alimentación a la celda se realizó mediante una bomba de diafragma Hydra-Cell G-03 (Wanner Engineering) equipada con un variador digital de frecuencia para ajustar los caudales. Los materiales de todos los componentes del sistema fueron elegidos para buscar la máxima compatibilidad con peróxido de hidrógeno concentrado. Para todos los tubos que componen la instalación se seleccionó Teflón HP PFA (perfluroalcoído de alta pureza) excepto para el tubo de conexión entre la bomba y la celda (el único que trabaja a presión). En este caso se eligió un tubo con el interior de Teflón PTFE (politetrafluoroetileno) y reforzado exteriormente con acero inoxidable trenzado. Los tanques de alimentación y recogida de permeado están fabricados en PE (polietileno). Un simple esquema de la instalación se puede observar en la Figura 2.2.

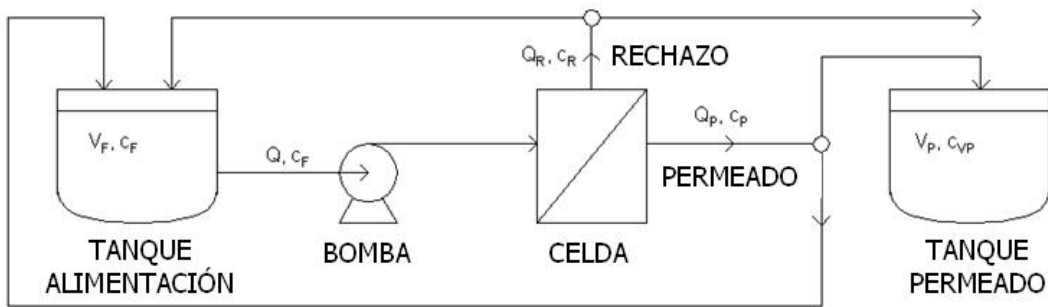


Figura 2.2. Esquema general de la instalación experimental

Para minimizar en todo lo posible la contaminación por metales presentes en el ambiente del laboratorio, los elementos más críticos de sistema de ultrapurificación fueron localizados bajo condiciones de sala limpia. Para conseguirlo, se recurrió a una cabina de flujo laminar vertical Bio-48-M (Faster) que garantiza una atmósfera de trabajo de clase ISO 5.

La instalación fue diseñada para trabajar bajo dos modos de operación distintos. El modo de recirculación total se puede configurar mediante la devolución total al tanque de alimentación de las corrientes de permeado y rechazo que abandonan la celda. Por el contrario, si la corriente de permeado es recogida en el tanque de permeado en vez de ser recirculada al tanque de alimentación, se obtiene el modo semicontinuo de operación (Figura 2.2).

Antes de comenzar los experimentos, el tanque de alimentación (220 l de volumen) era llenado con aproximadamente 200 l de peróxido de hidrógeno de calidad técnica. Como peróxido de calidad técnica se empleó una solución acuosa de peróxido de hidrógeno al 35% en peso sin ningún tipo de estabilizante: Interox ST-35 hydrogen peroxide H₂O₂ (Solvay).

El caudal de alimentación a la celda se ajustaba mediante el variador digital de frecuencia, lo normal era trabajar con un caudal de 3.4 l/min, correspondiente con una velocidad en flujo cruzado de 0.5 m/s dentro de la celda, el cual es un valor representativo de las velocidades de operación en los módulos de membranas en espiral empleados a escala industrial (GE Water & Process Technologies, 2004). La experimentación se llevó a cabo a temperatura ambiente y la presión de trabajo se ajustó por la válvula de control integrada en la salida de la corriente de rechazo de la celda.

Con el objetivo de asegurar la correcta hidratación y compactación de las membranas, antes de comenzar el experimento la membrana se mantenía en remojo por al menos 12 h en agua ultrapura (resistividad de 18.2 MΩcm) y, una vez ya instalada dentro de la celda, se sometía posteriormente a 5 h de compactación con el fluido de operación a 40 bar.

Las medidas de producción de permeado se llevaron a cabo mediante balanza de precisión y cronómetro. Para determinar la concentración de los diferentes metales, las muestras fueron

analizadas por espectrofotometría de masas con fuente de plasma de acoplamiento inductivo (ICP-MS) con un equipo 7500ce (Agilent). Un sistema especial de introducción de muestras (ESI Upgrade Kit) fabricado en PFA fue necesario para poder tolerar la presencia de peróxido de hidrógeno concentrado.

Tanto las medidas de permeado como las muestras para analizar el contenido en metales se llevaron a cabo por triplicado con un intervalo de 10 minutos entre repeticiones y siempre esperando 15 minutos desde el ajuste de la presión hasta la toma de la primera muestra.

2.2. Herramientas para la simulación y optimización de la ultrapurificación de peróxido de hidrógeno mediante membranas de ósmosis inversa

La inclusión de tareas de modelado, simulación y optimización en la presente Tesis requiere la selección de las herramientas informáticas más apropiadas, lo suficientemente potentes como para poder llevar a cabo los trabajos previstos y lo suficientemente flexibles para permitir el desarrollo de nuevos modelos en ingeniería de procesos.

La simulación de una instalación química consiste básicamente en la creación de un modelo que describa el comportamiento de los procesos reales y sea capaz de predecir la salida del sistema en función de las entradas al mismo (Walas, 1990; Peters et al., 2003).

Hoy en día, la simulación ha alcanzado una madurez total y hay una amplia variedad de simuladores disponibles específicos para el sector químico. Desde hace ya bastantes años se han impuesto los paquetes de software comerciales frente a los desarrollos específicos de cada empresa.

El simulador seleccionado para realizar las fases de modelado y simulación de la presente Tesis ha sido Aspen Custom Modeler. Este simulador está diseñado por Aspen Technology y permite la creación de modelos rigorosos para distintos equipos de procesado y la simulación de dichos equipos tanto en condiciones continuas como discontinuas y semicontinuas (Aspen Technology, 2009). La versión empleada durante este trabajo ha sido la 2004.1 v.

Por su parte, la optimización dentro de la ingeniería de procesos es un ámbito en continua evolución. Desde que en la década de los años 50 del pasado siglo se comenzara a desarrollar códigos computacionales y algoritmos para la resolución de problemas de optimización de gran envergadura, el progreso en este campo ha sido sustancial. Un paso muy importante en este avance fue el desarrollo durante la década de los 80 de los primeros sistemas basados en modelado, dentro de los cuales se puede destacar a GAMS (McCarl et al., 2009). El software GAMS fue la herramienta de optimización escogida para resolver los modelos de optimización. GAMS (General Algebraic Modeling System) es un sistema de modelado de alto nivel para programación matemática y optimización. Consiste en un compilador y una librería de resolviédores integrados de alto rendimiento (Rosenthal, 2012).

2.3. Resultados

2.3.1. Caracterización del comportamiento de membranas comerciales de poliamida para ósmosis inversa aplicadas a la ultrapurificación de peróxido de hidrógeno.

Caracterización del peróxido de hidrógeno de calidad técnica empleado como materia prima

La caracterización del peróxido de hidrógeno de calidad técnica llevada a cabo mediante ICP-MS para los 21 metales contemplados en la norma SEMI C30 (SEMI, 2010) se muestra en la Tabla 2.1. Se puede comprobar el amplio rango de concentraciones de las impurezas metálicas, que abarca desde 20 ppm para Na hasta concentraciones por debajo de 1 ppb para varios elementos.

Tabla 2.1. Caracterización del contenido en metales del peróxido de hidrógeno técnico por ICP-MS

Elemento	Concentración (ppb)	Elemento	Concentración (ppb)	Elemento	Concentración (ppb)
Li	< 1	Ti	72	Zn	13
B	6	V	< 1	As	< 1
Na	20895	Cr	48	Cd	< 1
Mg	17	Mn	3	Sn	< 1
Al	1067	Fe	161	Sb	< 1
K	36	Ni	24	Ba	< 1
Ca	89	Cu	2	Pb	< 1

A la vista de los resultados de caracterización, se pudo concluir que el peróxido de hidrógeno de calidad técnica de partida supera los límites fijados para el grado electrónico menos exigente (Grado SEMI 1) para tres metales: Na (1000 ppb), Al (1000 ppb) y Fe (100 ppb). Cuando se comparó con un grado más exigente como puede ser el Grado SEMI 3, el número de elementos cuya concentración supera los límites permitidos aumenta hasta 13: B, Na, Mg, Al, K, Ca, Ti, Cr, Mn, Fe, Ni, Cu y Zn.

Comportamiento de las membranas con agua ultrapura y dopada

Las membranas preseleccionadas fueron sometidas a experimentos preliminares con agua ultrapura y dopada para comparar su comportamiento y elegir a la más apropiada para el proceso de ultrapurificación (Tabla 2.2).

Tabla 2.2. Principales características (aportadas por el suministrador) de las membranas

Modelo	Fabricante	Material	Flujo de permeado ($\text{m}^3/\text{m}^2 \text{ d}$)	Rechazo (%)
AD	GE Osmonics	Poliamida	0.61	99.5
CE	GE Osmonics	Acetato de celulosa	0.96	97
BE	Woongjin Chemical	Poliamida	1.12	99.5
CRM	Woongjin Chemical	Poliamida	0.92	99.5
SW30HR	Filmtec	Poliamida	0.66	99.7
UTC 80 B	Toray	Poliamida	0.57	99.75

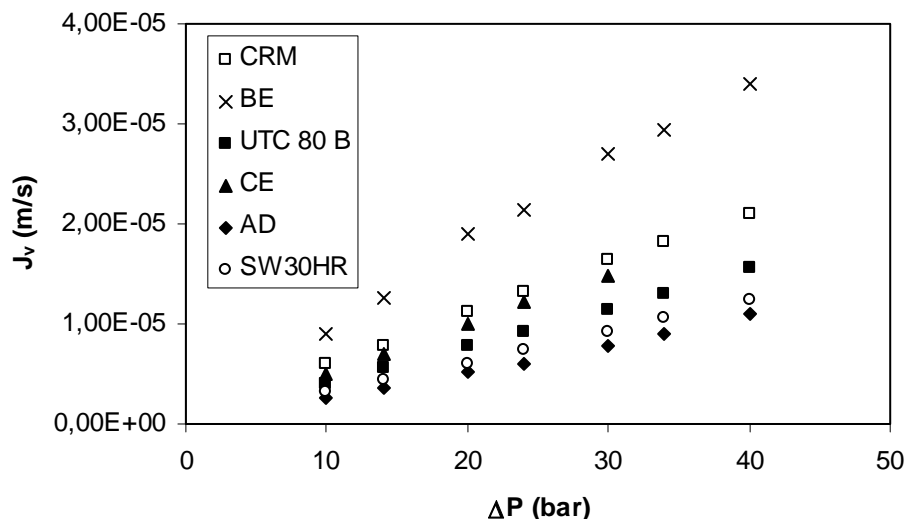


Figura 2.3. Determinación de la permeabilidad de las membranas en agua ultrapura

Los experimentos con agua ultrapura sirvieron para demostrar la dependencia lineal del flujo de permeado con respecto a la presión aplicada, de donde se puede estimar la permeabilidad de cada membrana como la pendiente de la recta correspondiente (Benítez et al., 2006). Las dos membranas fabricadas por Woongjin Chemical (BE y CRM) destacaron por encima del resto en términos de producción de permeado (Figura 2.3). Las otras membranas de poliamida (AD, SW30HR y UTC 80 B) mostraron un comportamiento muy similar, siendo los flujos de permeado obtenidos cercanos a la mitad del valor de la membrana BE. Por su parte, la permeabilidad de la membrana de acetato de celulosa (CE) resultó ser intermedia entre la membrana BE y el resto de membranas de poliamida.

Tabla 2.3. Valores medios de permeabilidad de las membranas basados en los experimentos con agua ultrapura y dopada y comparación con valores obtenidos de bibliografía para otras membranas de ósmosis inversa

Membrana	Permeabilidad L_p ($m/s \cdot bar$)
AD	$2.86 \pm 0.31 \cdot 10^{-7}$
SW30HR	$3.11 \pm 0.01 \cdot 10^{-7}$
UTC 80 B	$3.83 \pm 0.06 \cdot 10^{-7}$
CE	$5.04 \pm 0.06 \cdot 10^{-7}$
CRM	$5.64 \pm 0.34 \cdot 10^{-7}$
BE	$8.29 \pm 0.71 \cdot 10^{-7}$
Otras membranas referenciadas	
UTC 80 AB (Koseoglu y Kitis, 2009)	$2.33 \cdot 10^{-7}$
UTC 80 AB (Koseoglu et al., 2008)	$2.62 \cdot 10^{-7}$
LFC1 (Kwon y Leckie, 2006)	$8.20 \cdot 10^{-7}$
TFC-HR (Xu y Drewes, 2006)	$9.72 \cdot 10^{-7}$

Cuando se realizaron los experimentos con agua ultrapura dopada (15000 ppb de sodio y 1400 ppb de aluminio), la misma relación de linealidad fue observada y se hizo el cálculo de las pendientes de las curvas. Los valores de permeabilidad obtenidos resultaron muy parecidos

para ambas matrices como se puede observar en la Tabla 2.3 (Abejón et al., 2010). Esta coincidencia entre los valores era fácilmente predecible bajo la consideración de que la presión osmótica atribuible a concentraciones tan bajas de soluto es despreciable. Los valores de permeabilidad calculados están en sintonía con los valores que se pueden encontrar en bibliografía para otras membranas planas de ósmosis inversa y también incluidos en la Tabla 2.3 (Kwon y Leckie, 2006; Xu y Drewes, 2006, Koseoglu et al., 2008; Koseoglu y Kitis, 2009).

Los experimentos con agua ultrapura dopada fueron útiles para determinar la eficiencia de las membranas preseleccionadas para reducir el contenido en impurezas metálicas a concentraciones muy bajas. Los coeficientes de rechazos, definidos por la siguiente ecuación:

$$R = \frac{C_F - C_P}{C_F} \quad (2.1)$$

donde C_F y C_P representan las concentraciones de los metales (Na y Al) en las corrientes de alimentación y permeado respectivamente, fueron calculados para las diferentes membranas los casos de Na y Al (Figura 2.4).

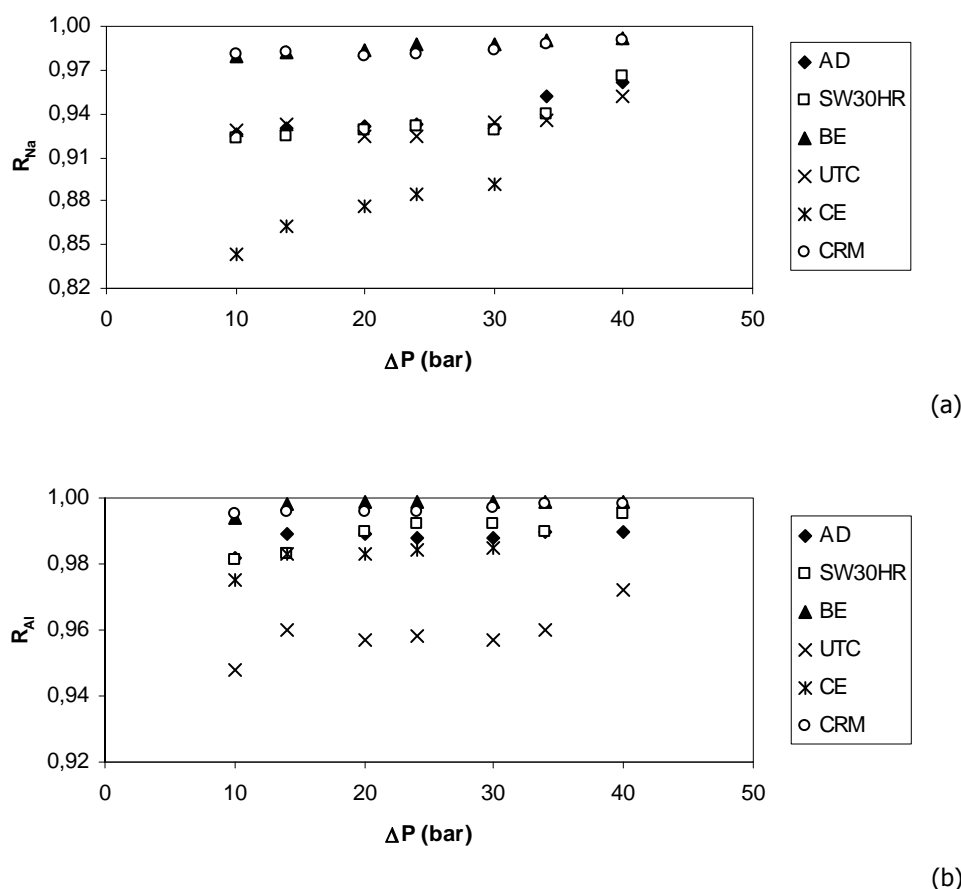


Figura 2.4. Influencia de la presión aplicada sobre los coeficientes de rechazo de sodio (a) y aluminio (b) en agua ultrapura dopada

La membrana BE mostró los mejores resultados para los dos metales: 0.992 para Na y 0.999 para Al. Los valores de la membrana CRM fueron muy cercanos a los de la BE (0.990 para Na y 0.998 para Al). Como ocurría con las permeabilidades, los coeficientes de rechazo obtenidos con las membranas fabricadas por Woongjin Chemical son superiores al del resto de membranas de poliamida. Estas tres membranas mostraron otra vez un comportamiento muy similar entre ellas, a excepción del coeficiente de rechazo de Al correspondiente a la membrana UTC 80 B, que destaca por ser algo menor. La membrana CE fue la menos efectiva para la separación de Na, pero mostró un valor superior a la membrana UTC 80 B en lo relativo a Al.

Como conclusión de los experimentos preliminares con agua ultrapura y dopada con Na y Al, la membrana BE fue considerada como la más prometedora para su aplicación a la ultrapurificación de peróxido de hidrógeno debido a su mayor permeabilidad y mejores coeficientes de rechazo.

Permeabilidad de la membrana en peróxido de hidrógeno

El modelo de exclusión iónica puede ser considerado como una buena herramienta para hacerse una primera idea acerca de la permeación de peróxido de hidrógeno a través de membranas de ósmosis inversa. Este mismo modelo ha sido aplicado para estimar la permeación de otros compuestos débilmente disociados en procesos de ultrapurificación con membranas (Kulkarni et al., 2004).

El desarrollo del modelo se basa en los siguientes supuestos:

- Todos los iones son excluidos por la membrana (efecto doble capa).
- Todas las especies en formas moleculares neutras atraviesan por completo la membrana.
- Las condiciones de mezcla perfecta a ambos lados de la membrana son asumibles.
- No se considera polarización de la concentración.

La ecuación final que resulta para el cálculo de la concentración en el permeado a partir de la concentración de alimentación es:

$$x_p = x_F - \sqrt{K_A \cdot x_F} - \sqrt{K_A(x_F - \sqrt{K_A \cdot x_F})} \quad (2.2)$$

donde K_A es la constante de disociación ($K_A = 1.78 \cdot 10^{-12}$ para el caso concreto del peróxido de hidrógeno). Cuando la concentración del peróxido de hidrógeno de alimentación es 35% en peso ($x_F = 10.3M$), el coeficiente de rechazo calculado es despreciable ($R < 10^{-6}$).

Este resultado demuestra de forma teórica la inexistencia de efectos de dilución de las soluciones acuosas de peróxido de hidrógeno cuando son forzadas a permear a través de membranas de ósmosis inversa. La determinación experimental de la concentración de peróxido de hidrógeno a ambos lados de la membrana durante distintos ensayos de permeación

confirmaron esta hipótesis (Figura 2.5), por lo que quedó demostrada la validez de la ósmosis inversa para soluciones acuosas de peróxido de hidrógeno sin que sufran dilución o concentración alguna.

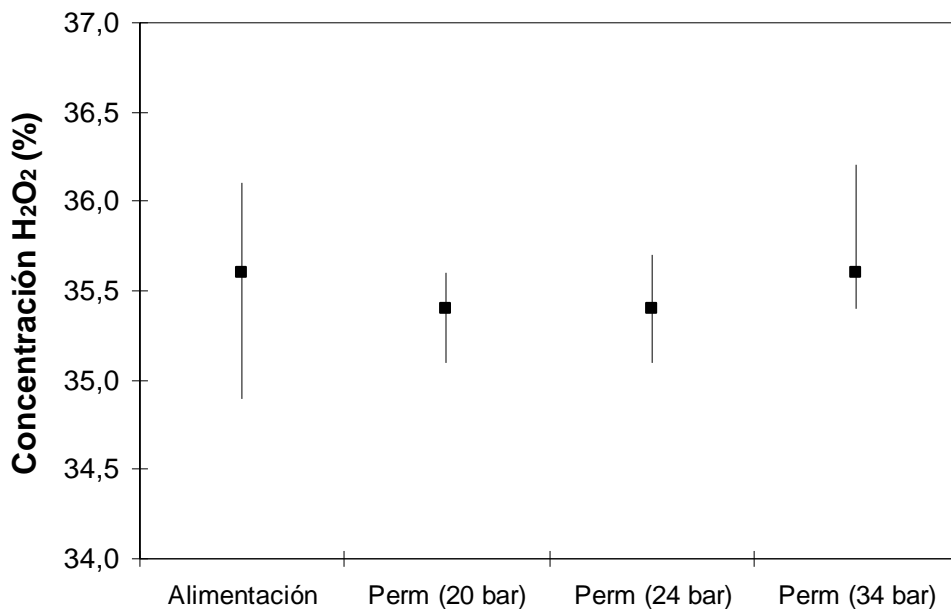


Figura 2.5. Concentración del peróxido de hidrógeno en la alimentación y en diferentes permeados (aparecen representados los valores medios, máximos y mínimos)

La relación de dependencia entre el flujo de permeado y la presión aplicada mantiene la linealidad también para el caso del peróxido de hidrógeno al 35% (Figura 2.6). La comparación de los distintos valores de permeabilidad para los dos casos mostró un descenso del 44% para la permeabilidad de la membrana BE en el peróxido de hidrógeno con respecto a la del agua ultrapura.

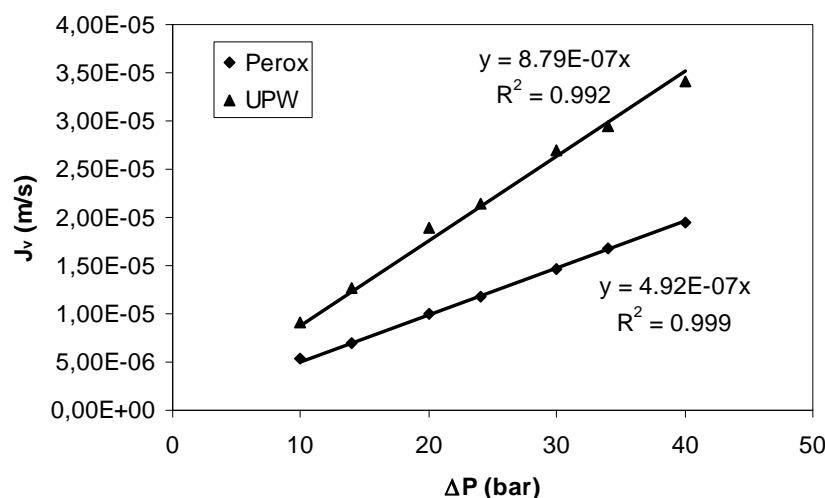


Figura 2.6. Comparación de los valores de permeabilidad de la membrana BE en agua ultrapura (UPW) y peróxido de hidrógeno (Perox)

A través de una interpretación de la permeabilidad basada en la ecuación de Hagen-Poiseuille, se puede concluir una relación de proporcionalidad inversa entre la permeabilidad y la viscosidad del líquido (Tsuru et al., 2006). Los valores de viscosidad del agua ultrapura y del peróxido de hidrógeno al 35% a 20 °C son respectivamente 1.00 y 1.11 mPa s (Goor et al., 2007), por lo que solamente un descenso de la permeabilidad alrededor del 10% puede ser justificado de esta forma. Todo hace indicar que la existencia de interacciones químicas más complejas entre el peróxido de hidrógeno y la membrana de poliamida podría explicar esta disminución en la producción de permeado.

Rechazo de los componentes metálicos presentes en el peróxido de hidrógeno

Los coeficientes de rechazo obtenidos para todos los elementos metálicos estudiados fueron altos, con valores por encima de 0.9 excepto para el caso del boro, que alcanzó un valor de 0.825. De igual modo que sucedía para el agua ultrapura, mayores presiones aplicadas conllevan mejores coeficientes de rechazo.

El comportamiento de la membrana es muy similar para todos los elementos metálicos, sin discriminación aparente por causa de la masa atómica, la carga iónica o la concentración inicial (Tabla 2.4).

Tabla 2.4. Coeficientes de rechazo de la membrana BE en peróxido de hidrógeno
(aparecen representados valores medios ± desviación estándar)

Elemento	Coeficientes de rechazo (R)			
	10	20	30	40
B	0.504 ± 0.010	0.663 ± 0.024	0.725 ± 0.024	0.769 ± 0.008
Na	0.930 ± 0.024	0.954 ± 0.012	0.960 ± 0.007	0.966 ± 0.005
Al	0.973 ± 0.004	0.979 ± 0.002	0.979 ± 0.003	0.981 ± 0.004
Ti	0.968 ± 0.005	0.977 ± 0.003	0.978 ± 0.005	0.980 ± 0.006
Cr	0.942 ± 0.013	0.962 ± 0.005	0.967 ± 0.006	0.971 ± 0.007
Mn	0.899 ± 0.015	0.939 ± 0.008	0.948 ± 0.006	0.955 ± 0.009
Fe	0.906 ± 0.023	0.936 ± 0.016	0.940 ± 0.025	0.952 ± 0.021
Ni	0.926 ± 0.007	0.949 ± 0.007	0.951 ± 0.005	0.955 ± 0.005
Cu	0.900 ± 0.057	0.951 ± 0.012	0.961 ± 0.013	0.972 ± 0.010
Zn	0.852 ± 0.059	0.912 ± 0.045	0.928 ± 0.020	0.954 ± 0.017

El permeado que se obtuvo no cumple con los requisitos impuestos para el Grado SEMI 1, ya que la concentración de sodio supera el límite impuesto (1565 ppb frente al máximo de 1000 ppb fijado). Esto impone la necesidad de recurrir a múltiples etapas de ósmosis inversa en serie para el permeado con el objetivo de cumplir con las especificaciones SEMI.

Modelado del proceso de ósmosis inversa para peróxido de hidrógeno: ecuaciones de transporte

Cuatro de los modelos más comunes para relacionar el flujo de permeado y con los coeficientes de rechazo con la presión aplicada fueron seleccionados para representar el comportamiento de las membranas de ósmosis inversa con el peróxido de hidrógeno (Soltanieh y Gill, 1981). Los modelos propuestos son:

Solución-Difusión (SD), con dos parámetros (A , K_1)

$$J_w = A(\Delta P - \Delta \Pi) \quad (2.3)$$

$$J_s = K_1(C_r - C_p) \quad (2.4)$$

$$R = \frac{J_w}{J_w + K_1} \quad (2.5)$$

Solución-Difusión con Imperfecciones (SDI), con tres parámetros (A' , K_2 , K_3)

$$N_w = A'(\Delta P - \Delta \Pi) + K_3 \Delta P X_w \quad (2.6)$$

$$N_s = K_2(X_r - X_p) + K_3 \Delta P X_r \quad (2.7)$$

Spliegler-Kedem (SK), con tres parámetros ($p_h/\Delta x$, σ , P_M)

$$J_v = \frac{p_h}{\Delta x}(\Delta P - \sigma \Delta \Pi) \quad (2.8)$$

$$R = \frac{\sigma(e^\beta - 1)}{e^\beta - \sigma} \quad (2.9)$$

$$\beta = J_v \frac{1 - \sigma}{P_M} \quad (2.10)$$

Kedem-Katchalsky (KK), con tres parámetros (L_P , ω' , σ)

$$J_v = L_P(\Delta P - \sigma \Delta \Pi) \quad (2.11)$$

$$J_s = \omega \Delta \Pi + (1 - \sigma) J_v (C_s)_{ln} \quad (2.12)$$

$$R = \sigma \frac{J_v}{J_v + \omega'} \quad (2.13)$$

donde

$$\omega' = \omega \nu \mathfrak{R} T \quad (2.14)$$

Los valores experimentales obtenidos de flujo de permeado y coeficientes de rechazo en función de las diferentes presiones aplicadas fueron ajustados a los modelos propuestos. La herramienta informática Aspen Custom Modeler fue empleada para la estimación de los parámetros de cada modelo y la determinación de su grado de ajuste, cuantificado como el porcentaje de variación explicada para el sistema global. Se consideró adecuado despreciar el término relacionado con la presión osmótica en las ecuaciones que describen el flujo de solvente a la vista de la coincidencia entre los flujos de permeado con agua ultrapura y dopada. Los mejores resultados fueron obtenidos para el modelo Kedem-Katchalsky (Tabla 2.5) y los

parámetros obtenidos para este modelo están recogidos en la Tabla 2.6 (Abejón et al., 2010). Para el rango de presiones estudiadas, el modelo describe de forma adecuada el comportamiento exhibido por la membrana (Figura 2.7).

Tabla 2.5. Evaluación del grado de ajuste de los diferentes modelos a los datos experimentales

Modelo	SD	SDI	KK	SK
Porcentaje de variación explicada para el sistema global (%)	79.0	88.8	94.4	94.1

En relación a los parámetros de transporte del modelo Kedem-Katchalsky, son necesarios tres parámetros para la caracterización del sistema: L_P , la permeabilidad hidráulica de la membrana; ω , la movilidad o permeabilidad del soluto; y σ , el coeficiente de reflexión del soluto. Los parámetros pueden ser definidos por las fórmulas siguientes:

$$L_P = \left(\frac{J_V}{\Delta P} \right)_{\Delta \Pi=0} \quad (2.15)$$

$$\sigma = \left(\frac{\Delta P}{\Delta \Pi} \right)_{J_V=0} \quad (2.16)$$

$$\omega = \left(\frac{J_S}{\Delta \Pi} \right)_{J_V=0} \quad (2.17)$$

Estas definiciones plasman el significado físico de los parámetros y, en cierta medida, orientan sobre las técnicas a emplear para su medida experimental (Kargol y Kargol, 2003).

Tabla 2.6. Parámetros del modelo KK para peróxido de hidrógeno y agua ultrapura dopada

Peróxido de hidrógeno										
B	Na	Al	Ti	Cr	Mn	Fe	Ni	Cu	Zn	
ω' (m/s)	$5.58 \cdot 10^{-6}$	$2.60 \cdot 10^{-7}$	$3.38 \cdot 10^{-7}$	$5.11 \cdot 10^{-7}$	$7.19 \cdot 10^{-7}$	$2.50 \cdot 10^{-6}$	$1.40 \cdot 10^{-6}$	$4.03 \cdot 10^{-7}$	$1.17 \cdot 10^{-6}$	$1.53 \cdot 10^{-6}$
σ	1.000	0.926	0.920	0.917	0.925	1.000	0.928	0.920	1.000	0.964
L_P (m/s bar)					$4.92 \cdot 10^{-7}$					
Porcentaje de variación explicada para el sistema global (%) = 94.4										
Agua ultrapura dopada										
B	Na	Al	Ti	Cr	Mn	Fe	Ni	Cu	Zn	
ω' (m/s)		$1.36 \cdot 10^{-7}$	$3.15 \cdot 10^{-8}$							
σ		0.995	1.000							
L_P (m/s bar)				$7.79 \cdot 10^{-7}$						
Porcentaje de variación explicada para el sistema global (%) = 89.4										

La permeabilidad hidráulica de la membrana L_P expresa el volumen de flujo a través de membrana inducido por unidad de presión aplicada cuando la presión osmótica es nula. En otras palabras, da idea de las propiedades de una membrana dada con respecto a la permeación global. La permeabilidad hidráulica puede ser fácilmente relacionada con la ley de Hagen-Poiseuille o comparada por analogía con la ley de Darcy que describe de manera fenomenológica el flujo de un fluido a través de un medio poroso (Jarzyńska y Pietruszka,

2011). La permeabilidad hidráulica no depende únicamente de las propiedades físicas y químicas de la membrana, ya que también de las propiedades del líquido que permea, especialmente de su viscosidad. Por otra parte, también depende de manera importante del espesor de la capa selectiva por lo que la correlación de estos parámetros para comparar diferentes membranas solamente es válida cuando los resultados se normalizan a capas del mismo espesor.

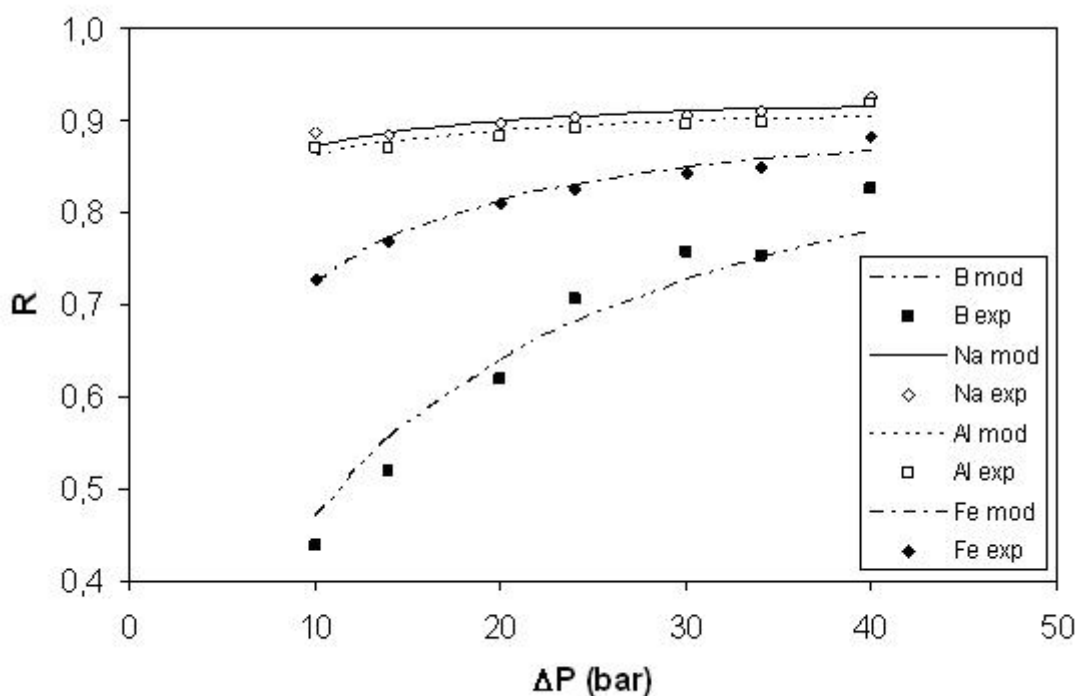


Figura 2.7. Aplicación del modelo Kedem-Katchalsky a los resultados experimentales de la membrana BE en peróxido de hidrógeno

La movilidad del soluto ω expresa el valor del flujo de soluto por unidad de diferencia de presiones osmóticas cuando el flujo de solvente es nulo. Esto significa que el flujo de soluto en este modelo se entiende como consecuencia de la presencia simultánea de gradientes de presión osmótica, que también puede ser expresado como gradiente de concentración en función de la ley de Morse (Morse y Frazer, 1905; Lewis, 1908) y de presión mecánica. Este parámetro depende en gran medida de la naturaleza de cada soluto.

El último de los parámetros, el coeficiente de reflexión del soluto σ , representa la ratio entre la diferencia de presión mecánica a flujo nulo y la diferencia de presión osmótica. Este parámetro expresa la selectividad de la membrana. Cuando su valor es 1, la membrana es perfectamente semipermeable (permeable para el solvente y totalmente impermeable para los solutos). Este es el caso de una membrana ideal de ósmosis inversa, con estructura densa y carente de poros. Por el contrario, cuando su valor es 0, la membrana es totalmente permeable y no presenta selectividad alguna (al ser permeable al solvente y a los solutos). Para los valores intermedios

entre 0 y 1, se considera que la membrana es selectiva, ya que favorece la permeación del solvente en comparación con los solutos.

Reorganizando la Ecuación 2.12 de la siguiente forma:

$$J_S = \omega' \Delta C_S + (1 - \sigma) J_V (C_S)_{ln} \quad (2.18)$$

el flujo de soluto queda expresado como la suma de dos términos, el primero difusivo y el segundo convectivo: un gradiente de concentraciones a ambos lados de la membrana causa transporte por difusión mientras que el transporte por convección tiene lugar gracias al gradiente aplicado de presión (Pontié et al., 2008).

Para cuantificar la importancia de la difusión y la convección en el transporte de soluto para el caso concreto de los metales presentes en el peróxido de hidrógeno objeto de estudio, se calculó la contribución de cada término a partir de los datos experimentales y los parámetros de transporte del modelo (expresado como porcentaje del flujo total de soluto en la Tabla 2.7). Se puede comprobar la existencia de casos muy diferentes, desde el transporte totalmente difusivo de B, Mn y Cu hasta elementos tales como Na, Al, Ti y Ni para los que el término convectivo se vuelve mayoritario cuando las presiones aplicadas son superiores a 20 bar (Abejón et al., 2010).

Tabla 2.7. Porcentaje de la contribución del término de difusión al flujo total de soluto para la membrana BE

ΔP	Contribución del término de difusión al flujo total de soluto (%)									
	Elemento									
	B	Na	Al	Ti	Cr	Mn	Fe	Ni	Cu	Zn
10	100	59	62	68	75	100	83	65	100	92
14	100	52	55	62	71	100	80	59	100	90
20	100	45	48	55	66	100	76	52	100	89
24	100	41	44	52	63	100	74	49	100	88
30	100	36	39	47	58	100	71	43	100	85
34	100	34	37	45	55	100	69	40	100	84
40	100	32	35	43	53	100	68	38	100	85

2.3.2. Estudio de la viabilidad técnica de la ultrapurificación de peróxido de hidrógeno mediante ósmosis inversa con membranas comerciales de poliamida.

Tal como se ha observado en los resultados obtenidos experimentalmente, el permeado producto de una etapa de ósmosis inversa con la membrana BE no cumple los requerimientos para peróxido de hidrógeno de calidad electrónica, lo que implica la necesidad de añadir más etapas en el proceso de ultrapurificación.

Con este objetivo, se planificó la experimentación a escala de laboratorio en múltiples etapas para poder demostrar la viabilidad técnica del proceso de ultrapurificación de peróxido de hidrógeno mediante membranas de ósmosis inversa hasta alcanzar calidad electrónica.

Para la primera etapa, el modo de operación en semicontinuo fue el seleccionado para poder

recoger cantidad suficiente de permeado y alimentar con él la segunda etapa. Las concentraciones de la alimentación inicial y del permeado finalmente recogido después de 130 h de experimento se muestran en la Tabla 2.8, donde únicamente aparecen los elementos metálicos cuyas concentraciones iniciales exceden los límites para Grado SEMI 1. Como ya había ocurrido en los experimentos de caracterización del comportamiento de la membrana, el sodio fue el único metal que permanecía por encima de los límites en el permeado recogido, después de la disminución de las concentraciones de Al y Fe por debajo de los requerimientos.

Tabla 2.8. Concentraciones de los principales metales en el peróxido de hidrógeno de alimentación y en los permeados obtenidos del proceso experimental de ultrapurificación y comparación con los requisitos para Grado SEMI 1

Concentraciones (ppb)	Metales		
	Na	Al	Fe
Alimentación	23682	1091	181
Límites para Grado SEMI 1	1000	1000	100
Permeado de la primera etapa	5748	245	44
Permeado de la segunda etapa	515	17	5

Después de 100 h de operación, se detectó un pequeño aumento de la producción de permeado. Aunque el periodo de operación para la recogida de permeado se acabó después de 130 h, se decidió prolongar el experimento, esta vez en modo de recirculación total, hasta completar 300 h de operación para poder observar la evolución del flujo de permeado (Figura 2.8). Una vez transcurrido este tiempo, se pudo comprobar que el flujo de permeado era más de 7 veces superior a la inicial.

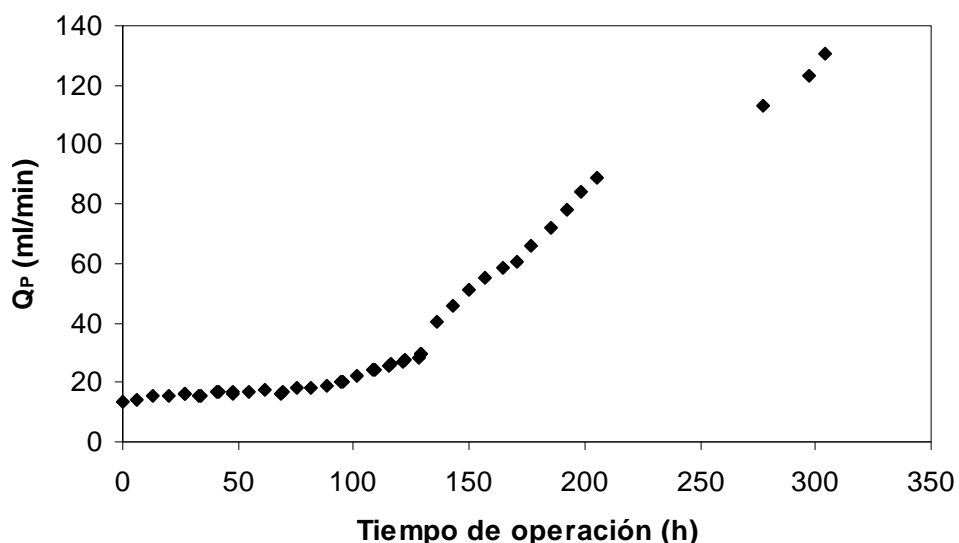


Figura 2.8. Evolución del caudal de permeado (Q_p) a lo largo del tiempo durante la primera etapa del proceso experimental de ultrapurificación

Como la presión aplicada se mantuvo constante, el aumento del flujo de permeado ocurrido tiene que ser consecuencia de cambios en el valor de la permeabilidad hidráulica de la membrana. El incremento de la permeabilidad de las membranas de poliamida tipo composite para ósmosis inversa como resultado del contacto con oxidantes (típicamente derivados del cloro utilizados para desinfectar) está bien reportada (Gabelich et al., 2002; Rouaix et al. 2006; Shintani et al, 2007; Buch et al., 2008; Antony et al, 2010; Raval et al., 2010; Shemer y Semiat, 2011). También se puede encontrar información sobre el contacto con peróxido de hidrógeno y el comportamiento de la membrana es similar (Wu et al., 1996). Este aumento del flujo de permeado sería positivo si el comportamiento de la membrana frente a los solutos no se viese afectado, pero no es el caso. Los coeficientes de rechazo observados siempre muestran una tendencia descendente frente al tiempo de contacto de la membrana con el oxidante.

La Figura 2.9 muestra la evolución de los coeficientes de rechazo de Na, Al y Fe durante el transcurso del experimento y los resultados concuerdan con las expectativas: después de una fase inicial (inferior a 100 h) en la que los valores se muestran estables, los coeficientes de rechazo caen primeramente de forma lenta y después de modo repentino hasta alcanzar el valor cero después de 170 h de contacto.

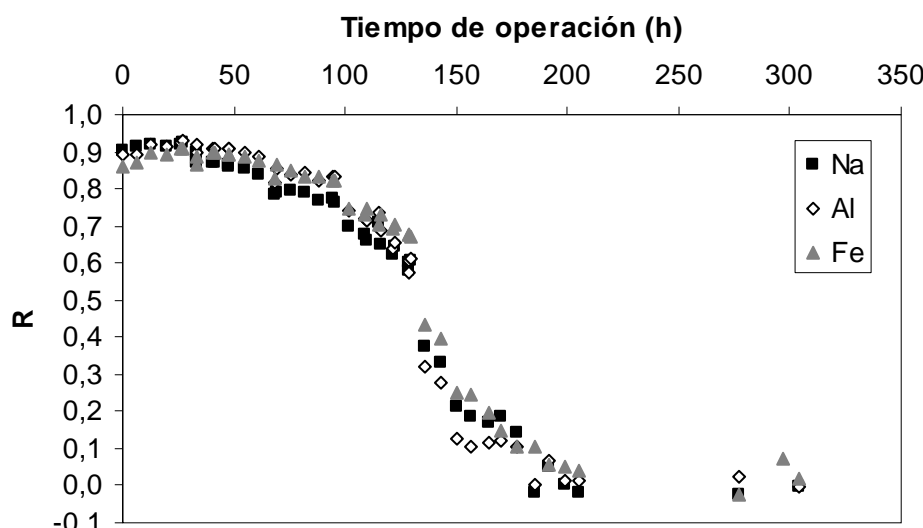


Figura 2.9. Evolución de los coeficientes de rechazo de los metales (R) a lo largo del tiempo durante la primera etapa del proceso experimental de ultrapurificación

Los coeficientes globales de rechazo, definidos mediante la siguiente expresión:

$$R_f = \frac{c_{F0} - c_{VPf}}{c_{F0}} \quad (2.19)$$

fueron calculados para cada uno de los elementos metálicos, obteniéndose valores de 0.757, 0.775 y 0.757 para Na, Al y Fe respectivamente. Estos coeficientes son sensiblemente inferiores a lo que se había predicho de acuerdo a los parámetros de transporte calculados en base a la

experimentación previa y que se rondaban el valor de 0.9 (Abejón et al., 2010).

A la vista de los resultados obtenidos, una segunda etapa de ósmosis inversa (en este caso en modo de recirculación total) alimentada con el permeado recogido durante la primera etapa habría de ser suficiente para alcanzar los requerimientos del Grado SEMI 1. Las características del permeado que se obtuvo de la segunda etapa aparece en la Tabla 2.8. La concentración de Na, la única que quedaba por cumplir con su limitación, alcanzó un valor cercano a los 500 ppb, justo la mitad del límite, así que efectivamente este permeado cumplía ya con los requisitos para poder ser considerado reactivo de calidad electrónica. En esta etapa, los coeficientes de rechazo fueron 0.910, 0.931 y 0.886 para Na, Al y Fe respectivamente.

De esta forma, quedó demostrada la viabilidad técnica del proceso de ultrapurificación de peróxido de hidrógeno para Grado SEMI 1 a escala de laboratorio mediante la instalación experimental basada en dos etapas de ósmosis inversa, sin necesidad de ninguna otra técnica auxiliar, todo ello a pesar de la duración excesivamente larga de la primera etapa, en la que puso de manifiesto la degradación de la membrana en un medio tan oxidante.

2.3.3. Estudio de la evolución con el tiempo de las membranas de ósmosis inversa en ambiente oxidante

A la vista de los resultados observados, en los que se comprueba una evolución a lo largo del tiempo del comportamiento de la membrana de poliamida para ósmosis inversa en contacto con peróxido de hidrógeno, se decidió estudiar con mayor detenimiento los cambios que sufren las membranas de ósmosis inversa en un medio tan oxidante.

Además de la membrana BE de poliamida, se estudió el comportamiento de la membrana CE de acetato de celulosa, ya que las membranas de este material son generalmente más resistentes a la oxidación (Glater et al., 1983). Efectivamente, la evolución del flujo de permeado con peróxido de hidrógeno al 35% muestra como la membrana de acetato de celulosa es mucho más estable que la de poliamida, ya que no muestra cambios en la permeabilidad de la membrana hasta después de 500 h (Figura 2.10). Cuando se decidió parar el experimento, pasadas ya 670 h, el valor de flujo de permeado era 4 veces superior al inicial (para el caso de la membrana de poliamida se había llegado a un valor más de 7 veces superior en menos de la mitad de tiempo). El aumento de la permeabilidad de las membranas de acetato de celulosa en medios oxidantes está también bien documentado (Farooque et al., 1999; Khedr, 2002; Xu et al., 2010).

La degradación de las membranas podía ser observada directamente a simple vista (Figura 2.11): la aparición de un patrón de color ocre sirvió como evidencia de oxidación de la membrana de poliamida, mientras que la membrana de acetato de celulosa apareció con la capa efectiva desgarrada, fenómeno que se conoce como peeling off (Kucera, 2008).

La determinación de la estructura física de las membranas degradadas fue determinada por medio de SEM (Scanning Electron Microscopy). Las microfotografías obtenidas mostraron las características superficiales de las distintas membranas (la Figura 2.12 muestra la membrana BE y la Figura 2.13 la membrana CE).

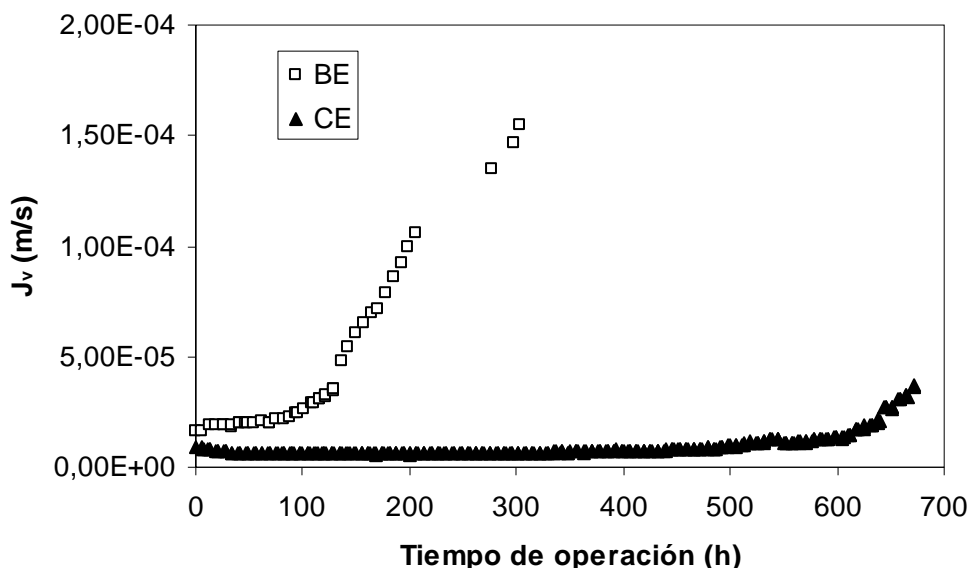


Figura 2.10. Evolución de los flujos de permeado (J_V) de las membranas BE y CE a lo largo del tiempo

La degradación resultó obvia a la vista de los resultados obtenidos. Las superficies de las membranas vírgenes, antes del contacto con el peróxido de hidrógeno, parecen caracterizadas por la presencia de partículas granuladas de polímero con una morfología suave (Figuras 2.12a y 2.13a). Sin embargo, después de la exposición durante los experimentos, las características de las superficies habían cambiado. La membrana de poliamida mostraba una mayor rugosidad e incluso agrietamiento de la superficie (Figura 2.12b). En el caso de la membrana de acetato de celulosa, el aumento de la rugosidad era también evidente pero en vez de agrietamiento aparecía un proceso de rasgado mucho más definido (Figura 2.13b). Estos pequeños jirones y desprendimientos podrían ser los precursores del posterior peeling off, que acaba sacando a la superficie visible la capa de soporte sobre la que se apoya la capa efectiva de la membrana.

Los coeficientes de rechazo de los elementos metálicos mostraron otra vez que la membrana de poliamida es más sensible al contacto con peróxido de hidrógeno. El intervalo de tiempo durante el que los coeficientes de rechazo mantienen su valor inicial es mucho mayor para el caso de la membrana de acetato de celulosa (Figura 2.14). Mientras que la membrana de poliamida sufría el descenso de los valores antes de 100 h, los coeficientes de rechazo de la membrana de acetato de celulosa se muestran estables por más de 200 h. Además este descenso no es tan brusco como el que caracteriza a la membrana de poliamida.

A pesar de la existencia de referencias que mencionan la degradación de membranas por causa

de su exposición a reactivos oxidantes (Iborra et al., 1996; da Silva et al., 2006; Kang et al., 2007), hay muy poca información disponible sobre la evolución del comportamiento de las membranas durante la degradación y no se ha podido encontrar referencia alguna que intente buscar un modelo matemático para describir esta evolución temporal.

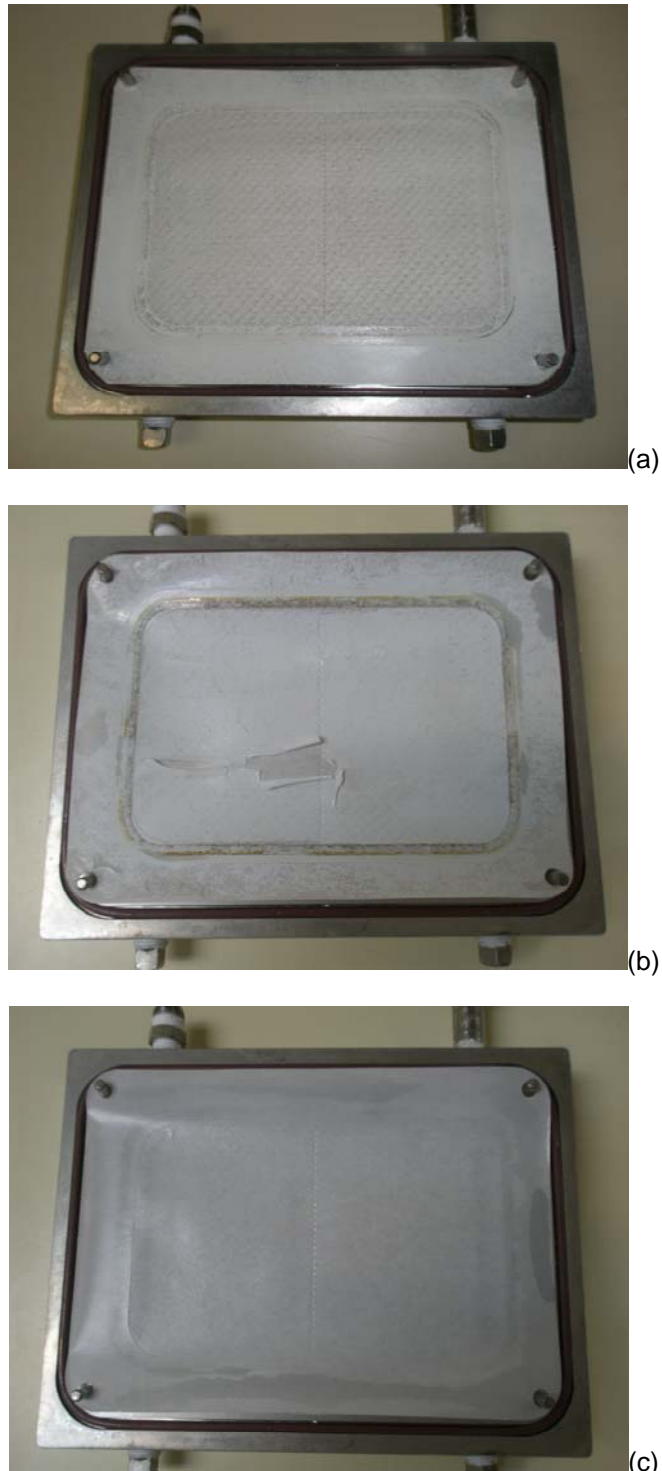


Figura 2.11. Fotografías de las membranas después del contacto con peróxido de hidrógeno: membrana BE después de más de 300 horas (a) y membrana CE después de 700 horas (b) y 8 horas (c)

Las causas de la degradación pueden ser englobadas en las diferentes contribuciones de naturaleza química, física y térmica. Como primer acercamiento a la descripción matemática, se optó por chequear por analogía algunos de los modelos usados para representar la desactivación de catalizadores a lo largo del tiempo (Fogler, 1999).

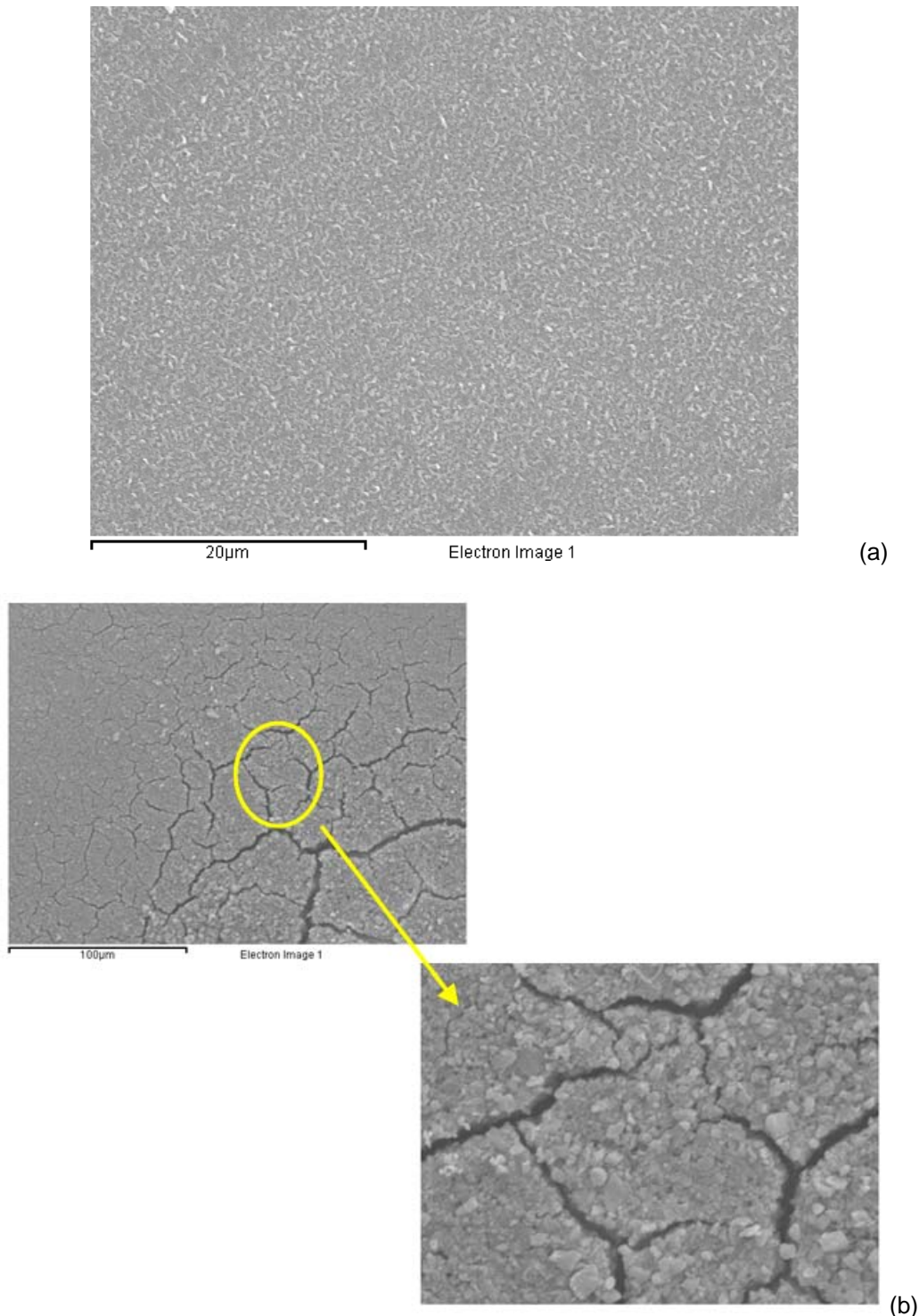


Figura 2.12. Microfotografías SEM de la membrana BE: antes del contacto con peróxido de hidrógeno (a) y después de 300 horas de contacto con peróxido de hidrógeno (b)

Sin embargo ninguno de los modelos seleccionados (lineal, exponencial, hiperbólico y potencial) describía de modo adecuado la evolución de forma sigmoidal de los coeficientes experimentales de rechazo.

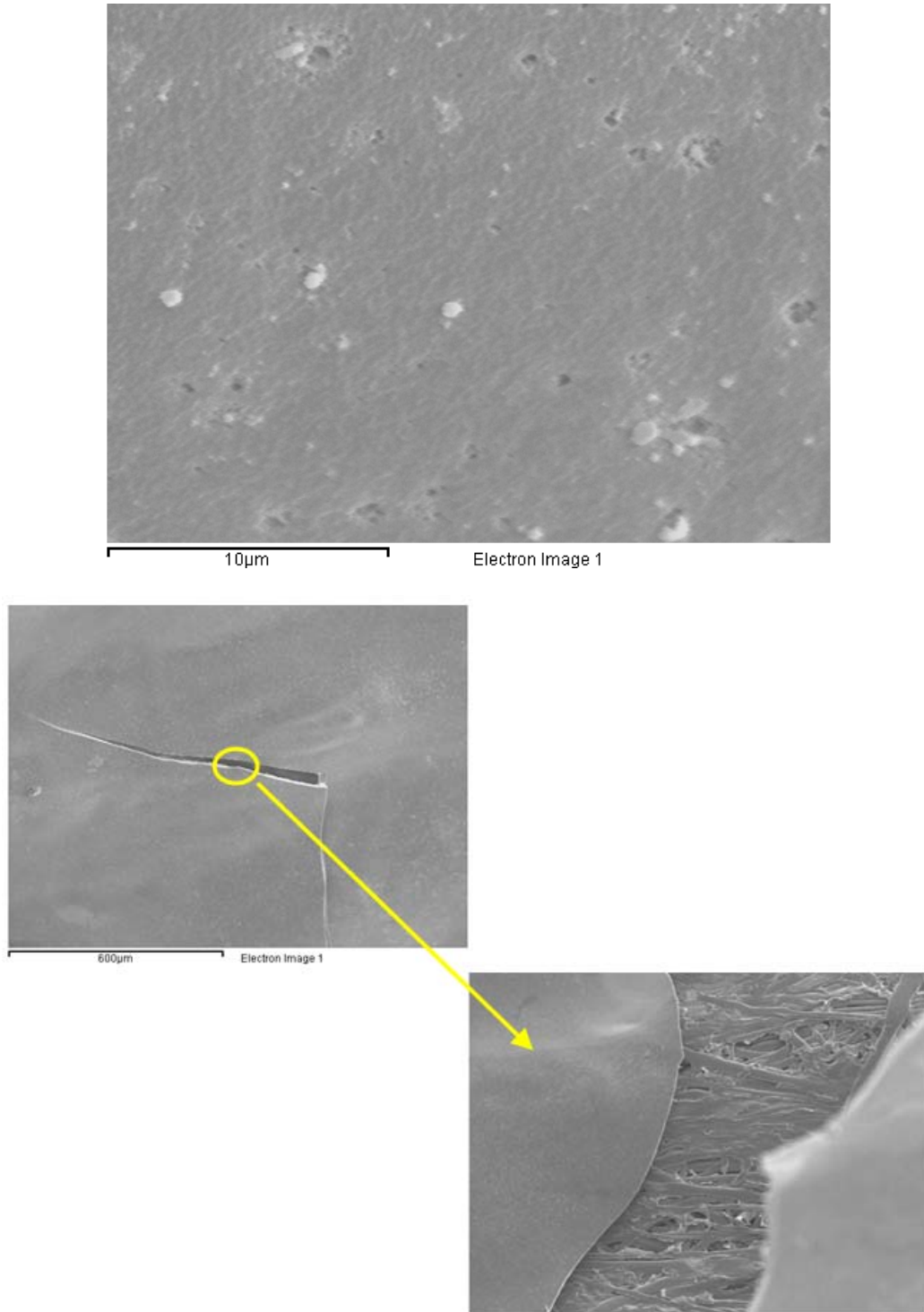


Figura 2.13. Microfotografías SEM de la membrana CE: antes del contacto con peróxido de hidrógeno (a) y después de 700 horas de contacto con peróxido de hidrógeno (b)

Es por ello que se decidió buscar una curva logística para ajustar la evolución de los coeficientes de rechazo, ya que este tipo de curvas han sido muy utilizadas en diferentes ámbitos para describir una gran variedad de procesos (Kaplan y Glass, 1995; Fekedulegn et al., 1999; Augusto et al., 2012).

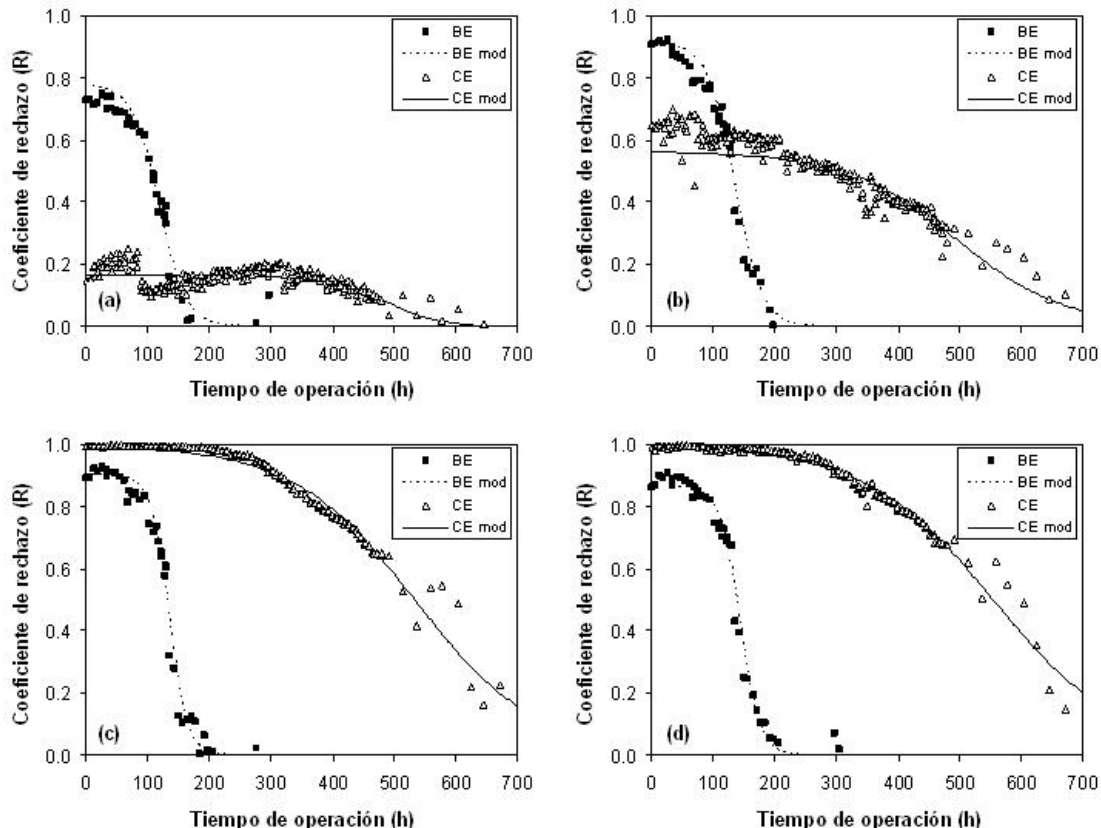


Figura 2.14. Evolución de los coeficientes de rechazo experimentales y modelados de las membranas BE y CE para las principales impurezas metálicas: boro (a), sodio (b), aluminio (c) y hierro (d).

De entre las curvas logísticas se eligió esta:

$$f(t) = 1 - \frac{1}{1 + e^{-k(t-t_{1/2})}} \quad (2.20)$$

La función $f(t)$ definida en la Ecuación 2.20 se propone como herramienta para calcular la evolución de los coeficientes de rechazo en función del valor inicial calculable a partir de los parámetros del modelo Kedem-Katchalsky:

$$R(t) = R_0 \cdot f(t) \quad (2.21)$$

La función logística del tiempo elegida considera una degradación total de la membrana para un tiempo suficientemente largo por lo que se puede asumir que el límite asintótico final para el coeficiente de rechazo es cero. El modelo logístico propuesto se basa en dos parámetros: el tiempo medio $t_{1/2}$ y la resistencia τ , teniendo en consideración que la constante logística k de la

Ecuación 2.20 puede ser definida como la inversa de la resistencia τ :

$$k = \frac{1}{\tau} \quad (2.22)$$

el tiempo medio indica el punto donde la velocidad de degradación es máxima, que coincide con el tiempo al que $R(t)$ toma exactamente el valor medio entre sus límites superior e inferior, que corresponden con R_0 y 0 respectivamente. La resistencia es la propiedad que determina la rapidez con la que una membrana es degradada (Bartholomew y Farrauto, 2006).

La evaluación del ajuste entre el modelo y los datos experimentales fue evaluada a través del valor de la suma de residuales cuadrados Φ :

$$\Phi = \sum (X_{\text{exp}} - X_{\text{mod}})^2 \quad (2.23)$$

donde X_{exp} y X_{mod} representan los valores de los coeficientes de rechazo experimentales y modelados respectivamente. La herramienta informática GAMS fue empleada para la estimación de los parámetros del modelo logístico de degradación, bajo la consideración de la minimización del valor de Φ como objetivo de optimización.

El modelo propuesto sirvió para describir de modo adecuado el comportamiento de la membrana (Figura 2.14), por lo que también fue aplicado al resto de elementos metálicos para cada una de las dos membranas y la Tabla 2.9 recoge los valores de los parámetros del modelo ($t_{1/2}$ y τ).

La comparación de los tiempos medio de ambas membranas y los correspondientes valores medios muestra que los tiempos medios son muy similares para los distintos elementos metálicos para una misma membrana. Por lo tanto, parece viable considerar un único valor de tiempo medio capaz de caracterizar a cada membrana ($t_{1/2 \text{ med}}$), calculado como la media de los valores de este parámetro para cada uno de los metales. De este modo se consideran unos valores de tiempo medio de 138 y 542 h para las membranas BE y CE respectivamente para el caso de peróxido de hidrógeno.

Tabla 2.9. Parámetros del modelo de degradación de las membranas BE y CE

Membrana BE										
B	Na	Al	Ti	Cr	Mn	Fe	Ni	Cu	Zn	
$t_{1/2}$ (h)	118	134	134	138	140	144	143	140	146	138
τ (h)	22	22	15	20	17	16	16	15	14	18
Membrana CE										
B	Na	Al	Ti	Cr	Mn	Fe	Ni	Cu	Zn	
$t_{1/2}$ (h)	486	494	534	560	585	533	556	548	573	547
τ (h)	43	89	99	80	118	107	105	106	78	98

La definición de este nuevo parámetro, único para cada membrana y común para todos los metales, permite el desarrollo de una forma normalizada del modelo logístico de degradación:

$$\rho(\theta) = 1 - \frac{1}{1 + e^{-(\theta-1)/\psi}} \quad (2.24)$$

donde

$$\rho = \frac{R(t)}{R_0} \quad (2.25)$$

$$\theta = \frac{t}{t_{1/2 \text{ mean}}} \quad (2.26)$$

$$\psi = \frac{\tau}{t_{1/2 \text{ mean}}} \quad (2.27)$$

Los resultados del modelo de degradación demostraron una vez más la mayor sensibilidad de la membrana de poliamida a la oxidación en comparación con la membrana de acetato de celulosa. El valor del tiempo medio de la membrana CE es más de tres veces superior y, teniendo en mente que cuando el tiempo de operación de la membrana alcanza el valor del tiempo medio el coeficiente de rechazo se reduce a la mitad del valor inicial, resulta obvio que la vida efectiva de la membrana debe ser más larga en una magnitud similar. Además, los valores de resistencia de la membrana de acetato de celulosa son también mayores, lo que supone que las curvas de degradación no sufren un descenso tan brusco como en el caso de la membrana de poliamida. Hay que mencionar, que entre los valores de resistencia estimados, los valores de B y Zn para la membrana de acetato de celulosa CE se apartan bastante de los del resto de elementos estudiados y su comportamiento parece más cercano al de la membrana de poliamida BE.

El modelo de degradación propuesto es una herramienta muy útil para el cálculo de la vida efectiva de las membranas. Hasta ahora, se contaba con valores de vida efectiva basados en resultados experimentales (Abejón et al., 2012a). Para la membrana de poliamida BE, se proponía una vida efectiva de 72 h (3 días). El descenso de los coeficientes de rechazo en base al modelo logístico de degradación correspondiente a la vida efectiva sugerida fue calculado (Tabla 2.10). Como se puede comprobar, todos los porcentajes de descenso se limitan al 5%, excepto para el caso del B. Teniendo en cuenta que este elemento no es una de las principales impurezas del peróxido de grado técnico, se concluye que una vida efectiva de 72 h puede ser aceptada como un valor adecuado por debajo del cual poder considerar el comportamiento de las membranas frente a las impurezas metálicas como constante.

Se operó de forma análoga para el caso de la membrana de acetato de celulosa CE y, como se puede observar en la Tabla 2.10, un límite de 216 h (9 días) fue propuesto como valor válido de vida efectiva, ya que mantiene todos los porcentajes de descenso del coeficiente de rechazo por debajo del 5%.

Tabla 2.10. Disminución de los coeficientes de rechazo al final de la vida útil de las membranas BE y CE de acuerdo al modelo de degradación

Membrana BE									
	B	Na	Al	Ti	Cr	Mn	Fe	Ni	Zn
R_0	0.776	0.912	0.904	0.893	0.892	0.887	0.866	0.902	0.893
R_{72}	0.695	0.863	0.890	0.864	0.876	0.877	0.855	0.892	0.869
Disminución (%)	10.4	5.4	1.5	3.2	1.8	1.1	1.3	1.1	2.7
Membrana CE									
	B	Na	Al	Ti	Cr	Mn	Fe	Ni	Zn
R_0	0.162	0.561	0.992	0.901	0.987	0.980	0.990	0.982	0.890
R_{216}	0.162	0.539	0.958	0.890	0.953	0.938	0.958	0.947	0.864
Disminución (%)	0.2	3.9	3.4	1.2	3.4	4.3	3.2	3.6	2.9

En relación con los flujos de permeado, ambas membranas presentan un comportamiento que puede ser considerado como constante para las vidas efectivas propuestas en virtud de la reducción de los coeficientes de rechazo. Como se muestra en la Tabla 2.11, los valores experimentales de flujo de permeado cuando las membranas se acercan al final de su vida útil no son significativamente distintos de los correspondientes valores medios hasta esos momentos, con una dispersión con respecto al valor medio menor que la desviación estándar en el período efectivo de cada membrana.

Tabla 2.11. Flujos de permeado de las membranas de BE y CE en el final de su vida útil

Membrana	BE	CE
Valor medio J_V (m/s)	$1.91 \cdot 10^{-5}$	$6.53 \cdot 10^{-6}$
Desviación estándar experimental (%)	6.71	9.58
J_V tras 69 h (m/s)	$2.00 \cdot 10^{-5}$	
J_V tras 214 h (m/s)		$5.96 \cdot 10^{-6}$
Dispersión con respecto al valor medio (%)	+ 4.54	- 8.72

2.3.4. Simulación de la ultrapurificación de peróxido de hidrógeno mediante ósmosis inversa y evaluación de la viabilidad económica del proceso.

Formulación del modelo de simulación para la instalación experimental de ultrapurificación

El modelo adoptado para describir el comportamiento de la instalación a escala laboratorio empleada para demostrar la viabilidad técnica del proceso de ultrapurificación por ósmosis inversa se basa en el modelo de Kedem-Katchalsky para el transporte a través de la membrana y en los correspondientes balances de materia.

Las ecuaciones de transporte de Kedem-Katchalsky, simplificadas bajo la consideración de presión osmótica despreciable, sirven para definir las principales variables que caracterizan el comportamiento de la membrana de ósmosis inversa, el flujo específico de permeado (J_P) y los coeficientes de rechazo de cada soluto (R_{metal}):

$$J_P = L_P \Delta P \quad (2.28)$$

$$R_{(metal)} = \sigma_{(metal)} \frac{J_p}{J_p + \omega'_{(metal)}} \quad (2.29)$$

Los valores de los parámetros del modelo para el caso de ultrapurificación de peróxido de hidrógeno con la membrana BE están recogidos en la Tabla 2.6 (Abejón et al., 2010).

Cuando la instalación experimental opera en modo de recirculación completa, el sistema queda completamente definido si se determina el caudal de permeado (Q_p) y las concentraciones de los metales en la corriente de permeado ($C_{P\ metal}$):

$$Q_p = A J_p \quad (2.30)$$

$$c_{P(metal)} = (1 - R_{(metal)}) c_{F(metal)} \quad (2.31)$$

donde A es el área efectiva de la membrana y $C_{F(metal)}$ la concentración de cada metal en la corriente de alimentación.

Por otra parte, el modo de operación en semicontinuo requiere de más ecuaciones ya que las variables evolucionan con el tiempo (comportamiento dinámico). Según transcurre el tiempo de operación, el volumen del tanque de alimentación disminuye al mismo ritmo al que aumenta el del tanque de permeado. Esta transferencia de materia implica también cambios en las concentraciones de los metales, ya que el permeado que abandona la celda de la membrana se encuentra purificado en comparación con la corriente de rechazo que vuelve al tanque de alimentación. Por lo tanto, es necesario aplicar balances de materia (globales y por componentes) a la celda y a los tanques de alimentación y permeado:

Tanque de alimentación

$$\frac{dV_F}{dt} = Q_R - Q \quad (2.32)$$

$$t = 0 \Rightarrow V_F = V_{Fo}$$

$$\frac{d(V_F c_F)}{dt} = Q_R c_R - Q c_F \quad (2.33)$$

$$t = 0 \Rightarrow c_F = c_{Fo}$$

Celda de ósmosis inversa

$$Q = Q_R + Q_p \quad (2.34)$$

$$Q c_F = Q_R c_R + Q_p c_p \quad (2.35)$$

Tanque de permeado

$$\frac{dV_p}{dt} = Q_p \quad (2.36)$$

$$t = 0 \Rightarrow V_p = 0$$

$$\frac{d(V_p c_{VP})}{dt} = Q_p c_p \quad (2.37)$$

$$t = 0 \Rightarrow c_{VP} = 0$$

Validación del modelo de simulación para la instalación experimental de ultrapurificación

El caudal de permeado calculado a partir de la Ecuación 2.30 para la primera etapa (operación en modo semicontinuo) fue 16.5 ml/min. Cuando este valor se compara con la media de las varias medidas de caudal de permeado realizadas durante las primeras 75 h de operación (16.1 ml/min), se observa gran similitud, con un error calculado inferior al 3% (Abejón et al., 2012a).

Los resultados experimentales y los valores simulados de las concentraciones de las principales impurezas metálicas (Na, Al y Fe) en el tanque de permeado y en la corriente de permeado durante el transcurso de la primera etapa experimental se muestran en la Figura 2.15 (Abejón et al., 2012a). Las variables aparecen como concentraciones normalizadas ya que han sido divididas por las respectivas concentraciones iniciales en la alimentación (C_{F0}). De acuerdo a las gráficas, el modelo propuesto describe la evolución de las concentraciones de un modo satisfactorio. Para cuantificar el grado de ajuste, se realizó un estudio estadístico por el que se calcularon algunas variables estadísticas. Primeramente, se obtuvo la concentración media normalizada y la correspondiente desviación estándar de los resultados experimentales y modelados. El sesgo también fue incluido en el estudio, así como dos diferentes indicadores de error, raíz del error cuadrático de la media (RMSE) y error absoluto porcentual de la media (MAPE) (Abejón et al., 2012a):

$$\text{Sesgo} = \frac{1}{n} \sum_{i=1}^n X_{\text{modi}} - X_{\text{expi}} \quad (2.38)$$

$$\text{RMSE} = \sqrt{\frac{\sum_{i=1}^n (X_{\text{modi}} - X_{\text{expi}})^2}{n}} \quad (2.39)$$

$$\text{MAPE} = 100 \frac{1}{n} \sum_{i=1}^n \left| \frac{X_{\text{modi}} - X_{\text{expi}}}{X_{\text{expi}}} \right| \quad (2.40)$$

La dispersión de los puntos experimentales ha de ser mencionada, especialmente para el caso de las concentraciones en la corriente de permeado, ya que sus valores de desviación estándar son comparables con los de la correspondiente al tanque de alimentación, a pesar de la diferencia de un orden de magnitud entre estas concentraciones.

Como consecuencia, los errores cuadráticos de la media (RMSE) son también comparables, pero las concentraciones en el permeado presentan un error absoluto porcentual de la media (MAPE) mayor debido a sus menores concentraciones en comparación con los correspondientes errores.

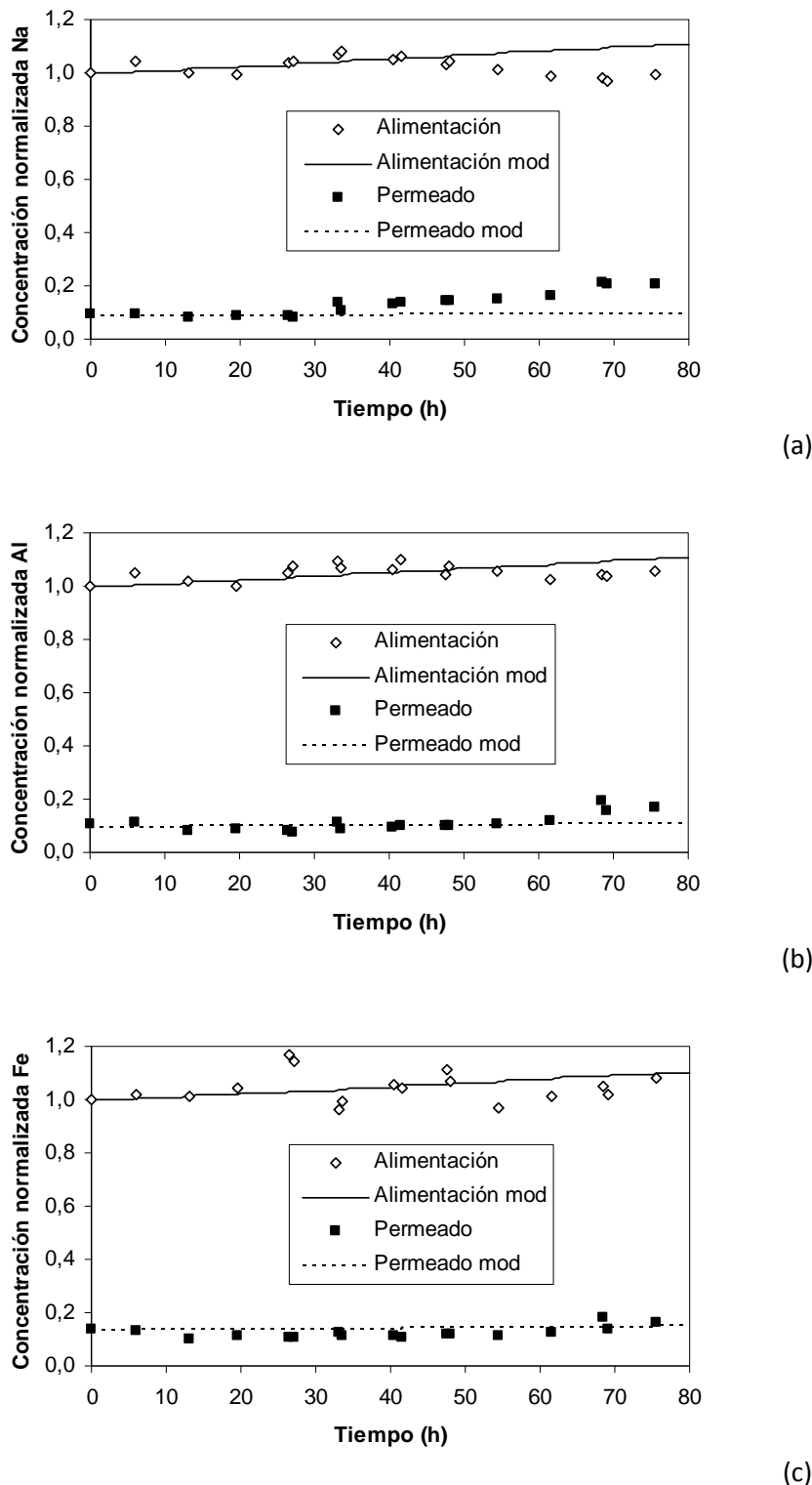


Figura 2.15. Concentraciones normalizadas de Na (a), Al (b) y Fe (c) tanto experimentales como modeladas en el tanque de alimentación y en la corriente de permeado a lo largo de la primera etapa experimental

Sin embargo, el valor MAPE más alto obtenido a partir de los datos modelados es 26.2%, que pertenece a la concentración de Na en la corriente de permeado. Este valor puede considerarse equivalente a los obtenidos a partir de modelos de mayor complejidad para el transporte a

través de membranas (Silva et al., 2010). Las concentraciones del tanque de alimentación fueron predichas con mayor exactitud, como demuestra que ninguno de sus valores MAPE superó el 5%.

El análisis del sesgo mostró que los valores positivos y negativos estaban distribuidos de forma equitativa entre los diferentes elementos metálicos y puntos de muestreo (tanque de alimentación y corriente de permeado), por lo que el modelo puede ser considerado como no sesgado.

Los resultados experimentales de la segunda etapa (operación en modo de recirculación total) fueron comparados con el comportamiento predicho por el modelo (Ecuaciones 2.28-2.31). El caudal medio de permeado calculado a partir de varias medidas distintas fue 19.9 ml/min. En este caso, el error con respecto al valor modelado (16.5 ml/min) fue 20.6%, por lo que quedó de nuevo ejemplificada la gran variabilidad existente entre diferentes muestras de membrana.

Con respecto a los coeficientes de rechazo, la Figura 2.16 muestra los valores experimentales comparados con los modelados. La coincidencia dentro de cada par de valores es muy elevada, con porcentajes de error por debajo de 3% para todos los casos.

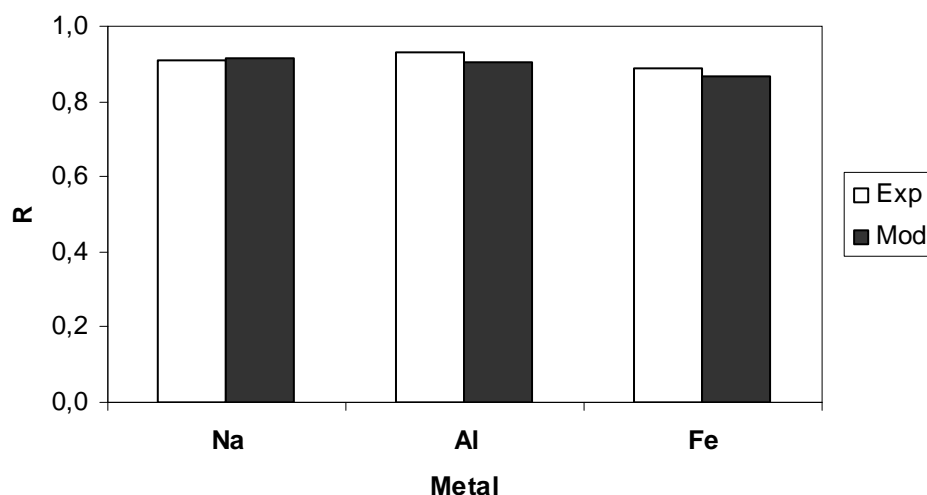


Figura 2.16. Coeficientes de rechazo de las principales impurezas metálicas experimentales y modelados en la segunda etapa experimental

Formulación del modelo de simulación para una instalación industrial de ultrapurificación

El diseño de una cascada de membranas en contracorriente es análogo al de una columna de destilación fraccional. El rechazo, que se recircula al módulo de membranas previo, se enriquece en los componentes con elevados coeficientes de rechazo (similar a la corriente líquida en la columna de destilación) mientras que el permeado enriquecido en los componentes con menores coeficientes de rechazo (similar a la corriente de vapor en la columna de

destilación) se emplea como corriente de alimentación del módulo de membrana siguiente.

El esquema general de una cascada de membranas integradas en contracorriente se muestra en la Figura 2.17. Del sistema únicamente salen dos corrientes, el permeado de la etapa final, que es producto ultrapurificado y el rechazo de la primera etapa, que para el caso concreto de la ultrapurificación de peróxido de hidrógeno es una corriente de subproducto caracterizado por un contenido en impurezas metálicas superior al de partida.

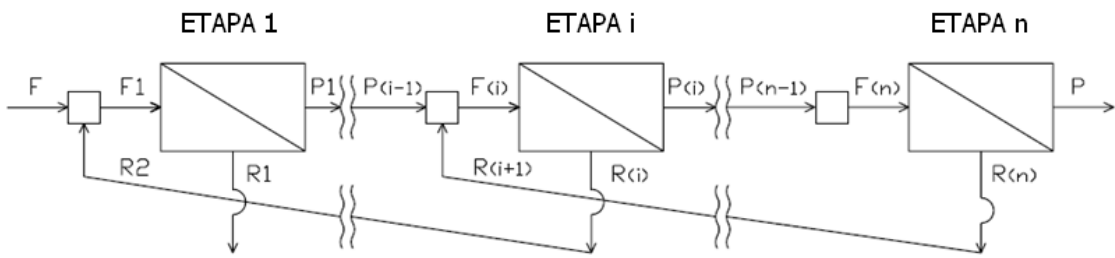


Figura 2.17. Representación esquemática de una cascada de membranas integrada por n etapas en contracorriente

Para la simulación del comportamiento del proceso de ultrapurificación por membranas de ósmosis inversa a escala industrial se empleó como software Aspen Custom Modeler (Aspen Technology, 2009). El modelo de simulación vuelve a basarse en las ecuaciones de transporte de Kedem-Katchalsky y en los correspondientes balances de materia.

Primeramente, se plantean los balances de materia tanto globales como por componentes:

Etapa inicial

$$F + R_2 = F_1 \quad (2.41)$$

$$F C_F^{\text{metal}} + R_2 C_{R_2}^{\text{metal}} = F_1 C_{F_1}^{\text{metal}} \quad (2.42)$$

$$F_1 = P_1 + R_1 \quad (2.43)$$

$$F_1 C_{F_1}^{\text{metal}} = P_1 C_{P_1}^{\text{metal}} + R_1 C_{R_1}^{\text{metal}} \quad (2.44)$$

Etapas intermedias

$$P(i-1) + R(i+1) = F(i) \quad (2.45)$$

$$P(i-1) C_{P(i-1)}^{\text{metal}} + R(i+1) C_{R(i+1)}^{\text{metal}} = F(i) C_{F(i)}^{\text{metal}} \quad (2.46)$$

$$F(i) = P(i) + R(i) \quad (2.47)$$

$$F(i) C_{F(i)}^{\text{metal}} = P(i) C_{P(i)}^{\text{metal}} + R(i) C_{R(i)}^{\text{metal}} \quad (2.48)$$

Etapa final

$$P(n-1) = F(n) \quad (2.49)$$

$$P(n-1) C_{P(n-1)}^{\text{metal}} = F(n) C_{F(n)}^{\text{metal}} \quad (2.50)$$

$$F(n) = P + R(n) \quad (2.51)$$

$$F(n) C_{F(n)}^{\text{metal}} = P C_P^{\text{metal}} + R(n) C_{R(n)}^{\text{metal}} \quad (2.52)$$

Después, las ecuaciones de transporte del modelo Kedem-Katchalsky sirven para definir las variables características del comportamiento de la membrana de ósmosis inversa (flujo específico de permeado y coeficientes de rechazo para cada metal):

$$J_{V(i)} = L'_P \Delta P_{(i)} \quad (2.53)$$

$$R_{(i)}^{\text{metal}} = \frac{\sigma^{\text{metal}} J_{V(i)}}{J_{V(i)} + \omega'_{\text{metal}}} \quad (2.54)$$

Con el transporte a través de la membrana ya definido, se puede calcular las características de las corrientes de permeado (caudales y concentraciones):

$$P(i) = A_{(i)} J_{V(i)} \quad (2.55)$$

$$C_{P(i)}^{\text{metal}} = (1 - R_{(i)}^{\text{metal}}) C_{F(i)}^{\text{metal}} \quad (2.56)$$

Por último, únicamente queda por definir la tasa de recuperación de cada etapa:

$$\text{Rec}_{(i)} = \frac{P(i)}{F(i)} \quad (2.57)$$

Resultados de la simulación de una instalación industrial de ultrapurificación y análisis de sensibilidad del sistema a las principales variables de operación

A continuación, se muestran los resultados de la simulación de una planta industrial para la ultrapurificación de peróxido de hidrógeno hasta calidad Grado SEMI 1 mediante dos etapas de ósmosis inversa integradas como cascada en contracorriente fue llevada a cabo.

Tabla 2.12. Concentraciones asumidas de los distintos metales en el peróxido de hidrógeno de partida para los casos de simulación

Elemento	Concentración (ppb)	Elemento	Concentración (ppb)
B	8	Mn	5
Na	25000	Fe	200
Al	1300	Ni	30
Ti	80	Cu	3
Cr	55	Zn	15

Como primer paso, se definió la escala del proceso y se fijaron las variables de operación. Con respecto a la escala, se planeó una planta capaz de tratar 9000 toneladas anuales de peróxido de hidrógeno de grado técnico (asumiendo que se acoplaría a una planta de producción de peróxido de hidrógeno de grado técnico con dicha producción anual), lo que implica un caudal diario de alimentación de 24.2 m³/d (supuestos 330 días de operación por año). La calidad del peróxido de partida se basó en los análisis realizados al reactivo suministrado por Solvay

(Interox ST-35 hydrogen peroxide H₂O₂) y que se puede considerar como representativo del contenido en impurezas metálicas de los peróxidos de grado técnico. La Tabla 2.12 recoge las concentraciones de los diferentes metales en la materia prima del proceso. En cuanto a las variables de operación, las tasas de recuperación de los módulos se fijaron en 0.7 y la presión aplicada en todos los módulos en 25 bar.

Los resultados de la simulación se recogen en la Tabla 2.13, donde se muestran los flujos de cada corriente y las concentraciones de los metales en las mismas. Como se esperaba, el producto final cumple los requisitos del Grado SEMI 1. La recuperación total del sistema, calculada como la ratio entre el caudal de la corriente de producto final entre el caudal de la corriente de alimentación del sistema, es 0.621 y los coeficientes de rechazo globales cuando se comparan las mismas corrientes están comprendidos entre 0.913 para B y 0.994 para Cu. Sobre el dimensionado de los módulos, la primera etapa requiere una superficie total de membrana de 20.2 m², mientras que para la segunda etapa basta con 14.1 m².

Tabla 2.13. Balance de materia de una cascada de dos etapas integradas en contracorriente

	Corrientes					Límites Grado SEMI 1
	F	R1	P1	R2	P2	
Caudal (m ³ /d)	24.19	9.19	21.44	6.43	15.01	
Concentración (ppb)						
Al	1300	3405	115	356	12.1	1000
B	8	20	2.4	6.2	0.7	100
Cr	55	144	6.0	18	0.8	50
Cu	3	8	0.2	0.7	0.0	50
Fe	200	519	29	87	4.9	100
Mn	5	13	0.7	2.2	0.1	50
Na	25000	65535	1960	6105	182.6	1000
Ni	30	79	2.8	8.6	0.3	50
Ti	80	209	8.2	25	1.0	300
Zn	15	39	1.9	5.6	0.3	100

La influencia de las dos principales variables de operación (las tasas de recuperación y las presiones aplicadas) sobre el comportamiento de la planta simulada de dos etapas (para calidad Grado SEMI 1) fue estudiada mediante un análisis de sensibilidad. Los efectos de variar las tasas de recuperación entre 0.45 y 0.95 mientras las presiones aplicadas en las dos etapas se mantenían constantes en 40 bar están graficados en la Figura 2.18. La decisión acerca de la tasa de recuperación a elegir tiene que tener en cuenta los efectos contraproducentes que aparecen en el sistema. Obviamente, tasas de recuperación alta implican mayor producción de producto final (gráficamente expresado como recuperación total en la Figura 2.18c), ya que la pérdida de materia fuera del sistema como rechazo en la primera etapa se reduce. El contrapunto a la mayor producción del proceso es el incremento en la demanda de superficie de membrana, ya que se necesita más área para permitir caudales más elevados (Figura 2.18a).

La situación con mayor superficie de membrana es aquella en la que la tasa de recuperación es máxima para la primera etapa y mínima para la segunda. Este escenario conlleva el caudal máximo de recirculación y como consecuencia, el caudal de entrada a la primera etapa alcanza también el máximo después de la mezcla entre alimentación y recirculación.

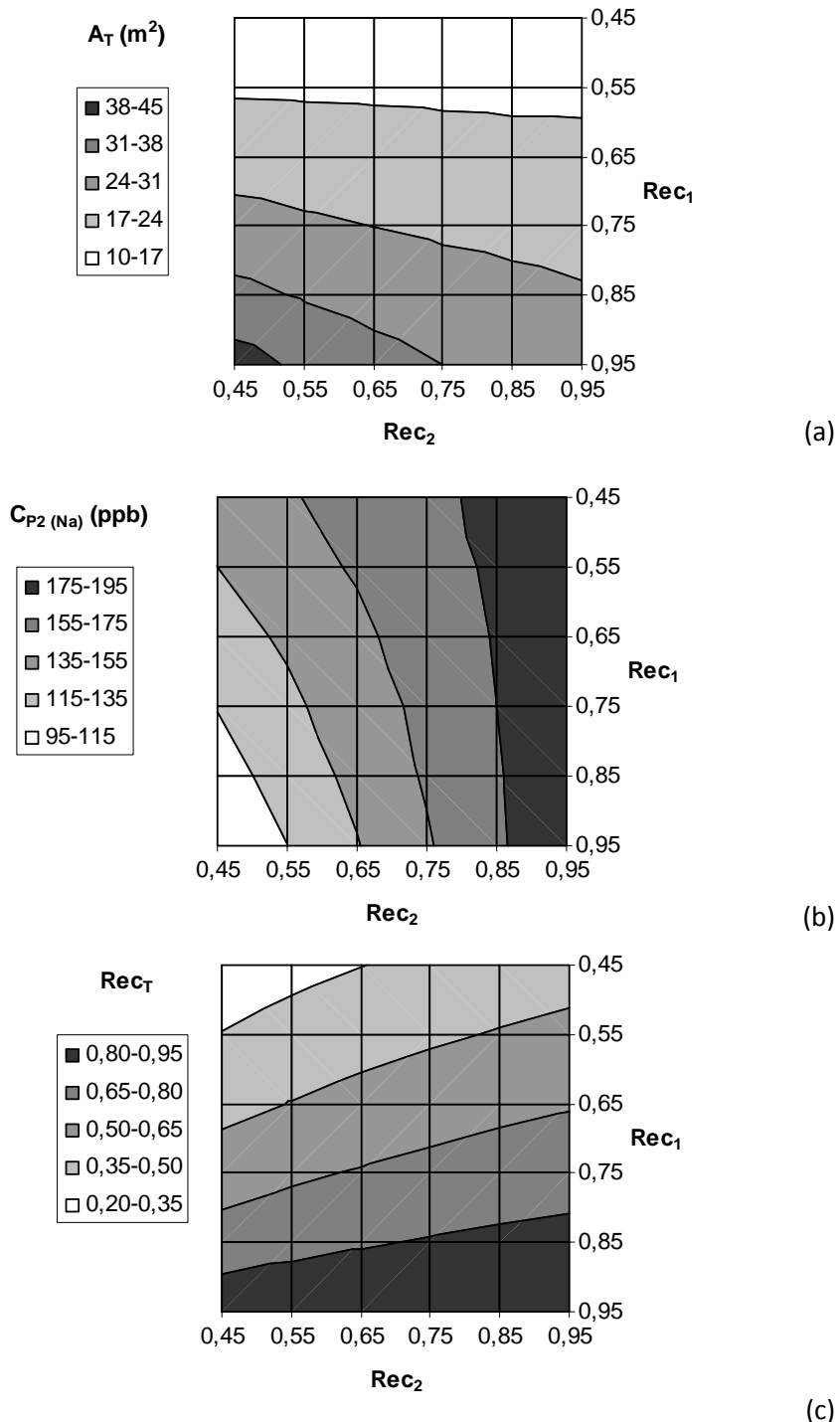


Figura 2.18. Relación de dependencia entre las tasas de recuperación en las etapas de la cascada de membranas (Rec_1 y Rec_2) y el área total de membrana A_T (a), la concentración de Na en el permeado de la segunda etapa $C_{P2\text{Na}}$ (b) y la tasa global de recuperación Rec_T (c).

Por otra parte, cuando la tasa de recuperación en la primera etapa es baja, el sistema se vuelve bastante insensible en términos de variación del área de membrana a los cambios en la operación de la segunda etapa, por lo que si se desea reducir la superficie total de membrana del sistema el modo más efectivo es disminuir la tasa de recuperación en la primera etapa.

El caso en el que se necesita más superficie total de membrana se caracteriza también por ser la situación que alcanza mayor calidad en el producto final (Figura 2.18b). La gran tasa de recuperación de la segunda etapa implica una mayor dilución de la corriente de entrada a la primera etapa, por la mezcla de la alimentación con un caudal importante de producto purificado. En lo que se refiere al control de las concentraciones de metales en el producto final, la segunda etapa se muestra como la preponderante, por lo que el modo más efectivo de reducir el contenido en impurezas del producto final es rebajar la tasa de recuperación de la segunda etapa.

En un modo similar, las presiones aplicadas fueron modificadas entre 5 y 40 bar para estudiar la evolución del proceso, mientras que las tasas de recuperación de ambas etapas se mantuvieron fijas en un valor de 0.95. Los resultados obtenidos se muestran en la Figura 2.19. En este caso, aplicar altas presiones de operación es beneficioso tanto en términos de menor área total de membrana requerida como de mayor calidad del producto: la superficie total de membrana necesaria es menor para altas presiones siempre que la tasa de recuperación se mantenga constante (Figura 2.19a) y el producto final se obtiene con menores concentraciones metálicas (Figura 2.19b). Estos resultados son consecuencia directa del mayor flujo de permeado y mejores coeficientes de rechazo resultantes de emplear altas presiones en los módulos de membranas. El contrapunto a estas ventajas es un mayor consumo energético.

Estudio de la viabilidad económica de la ultrapurificación de peróxido de hidrógeno mediante ósmosis inversa con membranas comerciales de poliamida.

Para evaluar la viabilidad económica del proceso de ultrapurificación a escala industrial se planteó un modelo económico simple basado en ingresos y gastos.

El beneficio diario (Z) se puede definir como la diferencia entre los ingresos diarios (Rev) y los costes totales diarios (TC):

$$Z = Rev - TC \quad (2.58)$$

Se consideraron ingresos por dos vías distintas: la principal aportación es la venta del producto final ultrapurificado como peróxido de hidrógeno de calidad electrónico mientras que el rechazo de la primera etapa del proceso puede ser comercializado como un sub-producto del proceso aprovechable para aplicaciones donde el contenido en impurezas metálicas del peróxido no es un factor limitante:

$$Rev = P Y_{EG} + R1 Y_{by} \quad (2.59)$$

Los costes totales del sistema se calcularon como la suma de los costes de capital (CC) y los costes de operación (OC). Dentro de los costes de capital, se hizo distinción entre la inversión en membranas y la necesaria para el resto de la instalación. Los costes de operación fueron desglosados en los correspondientes a materia prima, mano de obra, energía y mantenimiento:

$$TC = CC + OC \quad (2.60)$$

$$CC = CC_{memb} + CC_{ins} \quad (2.61)$$

$$OC = OC_{raw} + OC_{lab} + OC_{en} + OC_m \quad (2.62)$$

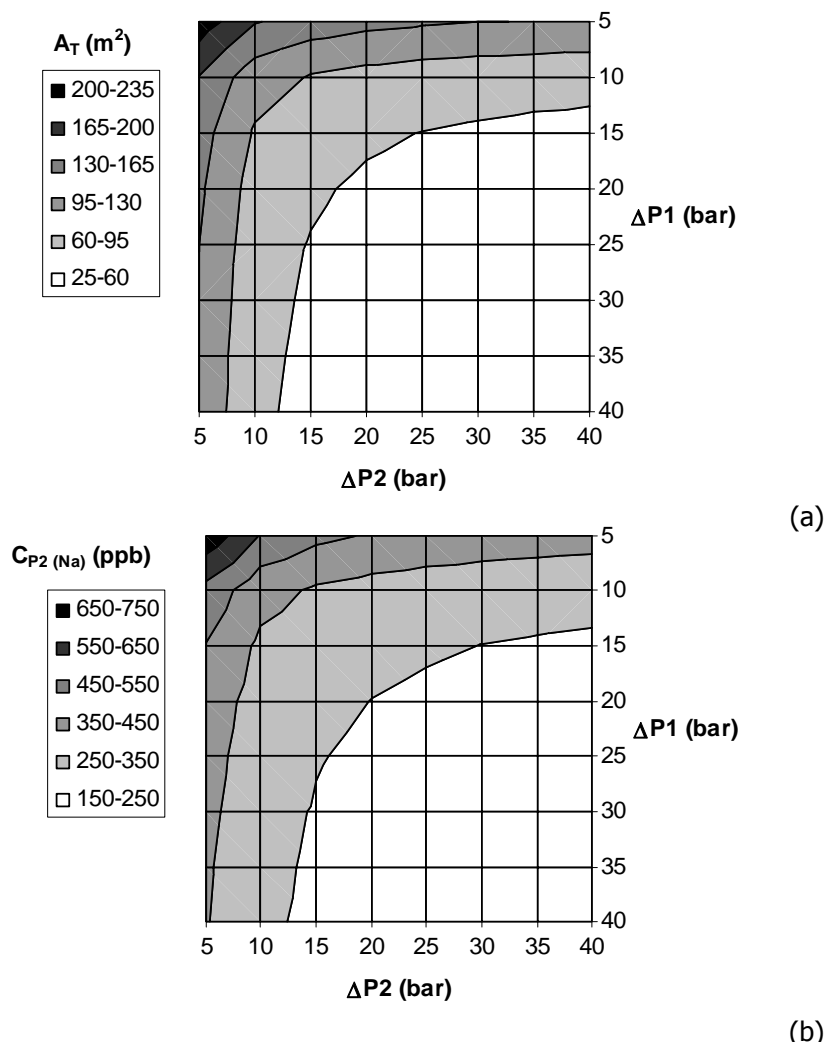


Figura 2.19. Relación de dependencia entre las presiones aplicadas en las etapas de la cascada de membranas (ΔP_1 y ΔP_2) y el área total de membrana A_T (a) y la concentración de Na en el permeado de la segunda etapa $C_{P2\text{Na}}$ (b)

Los costes diarios de capital achacables a los módulos de membranas considerando un modelo de depreciación lineal constante se expresaron en función del área total de membrana de la instalación:

$$CC_{\text{memb}} = \frac{Y_{\text{memb}} \sum A_i}{LT_{\text{memb}}} \quad (2.63)$$

La aplicación de la ósmosis inversa al proceso de ultrapurificación de peróxido de hidrógeno conlleva una tasa de reemplazo de las membranas inusualmente alta en comparación con el resto de aplicaciones de ósmosis inversa. La vida efectiva de las membranas de poliamida previamente calculada para esta aplicación concreta (3 días) no es comparable con los usos más habituales de este tipo de membranas, donde períodos útiles de varios años son típicos cuando se planifica y se lleva a cabo un correcto mantenimiento de las mismas que incluya limpieza química y tratamientos físicos para el lavado en contracorriente de las membranas (El-Manharawy y Hafez, 2000; Avlonitis et al., 2003; Goosen et al, 2005; Sanz et al., 2007; Sehn, 2008).

Una vez el coste de las membranas quedó definido, éste se tomó como base para relacionarlo con los costes de capital del resto de la instalación a través de un coeficiente (K_{memb}) que indica la contribución que supone el gasto en membranas al total de los costes de capital. Según referencias bibliográficas (Fariñas, 1999; Medina San Juan, 2000), el porcentaje estimado de contribución de las membranas a los costes de capital está comprendido en el rango 12-30%, por lo que se seleccionó un valor de K_{memb} de 0.12 para cubrir el peor escenario posible (una instalación de ultrapurificación requiere materiales inertes de alta calidad por lo que su precio resulta más elevado que el de los materiales más tradicionales):

$$CC_{\text{ins}} = CC_{\text{memb}} \frac{(1 - K_{\text{memb}})}{K_{\text{memb}}} \frac{LT_{\text{memb}}}{LT_{\text{inst}}} + CC_{\text{clean}} \quad (2.64)$$

Por otra parte, hay que tener en cuenta que los procesos de ultrapurificación necesitan un estricto control de la contaminación, por lo que la instalación debe ser incluida dentro de una sala limpia para mantenerse en condiciones de atmósfera controlada. Los costes de la sala limpia se calcularon de acuerdo a un modelo propuesto para salas limpias de pequeño tamaño (Yang y Eng Gan, 2007), considerando un espacio de 200 m² en Clase 100, lo que implica 200 cambios horarios de aire (Rumsey Engineers, 2009), con suelo levantado y ventilación tipo FFU:

$$CC_{\text{clean}} = -1645051 + 5156.6CA + 68.8MAV + 34EAV + 2996627AFC + AN \quad (2.65)$$

El término AN, que no aparece en la formulación original del modelo, fue incluido para contemplar los costes debidos al análisis y control de la calidad. Su valor fue calculado a partir de la experiencia del grupo investigador en la gestión de equipamiento analítico, principalmente espectrometría de masas con fuente de plasma de acoplamiento inductivo (ICP-MS) y cromatografía iónica (IC).

Los costes de operación se basaron esencialmente en el consumo del recurso correspondiente, excepto para el caso de los costes de mantenimiento, los cuales se decidió definir como función de los costes totales de capital (Shaalan et al., 2000). La única materia prima necesaria fue el peróxido de hidrógeno de calidad técnica utilizado como alimentación del sistema y la

instalación fue diseñada para operar bajo el mando de un único empleado:

$$OC_{\text{raw}} = F Y_{\text{raw}} \quad (2.66)$$

$$OC_{\text{lab}} = 24 Y_{\text{lab}} \quad (2.67)$$

$$OC_{\text{en}} = \frac{\sum (F(i) \Delta P_i)}{36 \eta} Y_{\text{elec}} \quad (2.68)$$

$$OC_m = 0.05 CC \quad (2.69)$$

En base al caso de estudio simulado y a los parámetros de cálculo recogidos en la Tabla 2.14, se llevó a cabo la evaluación económica del proceso y se calculó el beneficio resultante. Los principales indicadores económicos se muestran en la Tabla 2.15 (Abejón et al., 2012a). A la vista de estos resultados, se puede concluir que la viabilidad económica del proceso es obvia, ya que se estimó un beneficio diario de 21793\$ (equivalente a 7.19 millones de dólares por año).

Tabla 2.14. Parámetros del modelo económico

Parámetro	Unidad	Valor
Y_{memb}	(\$/m ²)	50
$L T_{\text{memb}}$	(d)	3
$L T_{\text{inst}}$	(d)	1825
K_{memb}		0.12
Y_{raw}	(\$/m ³)	790
Y_{EG}	(\$/m ³)	2592
Y_{by}	(\$/m ³)	600
Y_{lab}	(\$/h)	7
Y_{elec}	(\$/kWh)	0.08
η		0.70
CC_{clean}	(\$/d)	2590

Cuando se observó el desglose de los costes totales de la planta simulada, destacó la importancia de los costes de materia prima, ya que la adquisición del peróxido de hidrógeno de grado técnico suponía el 84.5% de los costes totales del proceso. Por comparación, el resto de costes de operación podrían ser considerados despreciables porque ninguno de ellos llega al 1% de contribución.

Tabla 2.15. Resultados de la evaluación económica

Indicador económico	Valor diario (\$/d)	Contribución a los gastos totales (%)
Z	21793	
Rev	44402	
TC	22609	
CC	3169	14.0
CC_{memb}	572	2.5
CC_{inst}	2597	11.5
OC	19441	86.0
OC_{raw}	19110	84.5
OC_{lab}	168	0.7
OC_{en}	4	0.1
OC_m	159	0.7

Por otra parte, al fijarse en los costes de capital, la inversión en membranas únicamente aportó

el 2.5% de los costes totales a pesar de la elevada tasa de renovación consecuencia de una vida útil muy corta en un medio tan agresivo para las membranas.

2.3.5. Optimización del proceso de ultrapurificación de peróxido de hidrógeno mediante ósmosis inversa

Optimización de una instalación para obtener un determinado Grado SEMI

Se decidió aplicar una rutina de optimización para obtener los valores óptimos que maximizaran el beneficio económico del proceso de producción de cada uno de los grados de calidad electrónica.

Como función objetivo para la optimización se eligió el beneficio diario Z (definido según la Ecuación 2.58). Todas las variables del modelo se formularon en función de las variables independientes del sistema, esto es, las principales variables de operación (tasas de recuperación y presiones aplicadas). Las variables de operación fueron sometidas a rangos válidos definidos por los correspondientes límites inferiores y superiores (Tabla 2.16). El intervalo para las tasas de recuperación fue limitado entre 0.5 y 0.9 teniendo en consideración los valores referenciados para instalaciones industriales de procesos con membranas (Shaanan et al., 2000; Noronha et al., 2002; Zhu et al., 2010). Las tasas de recuperación muy cercanas a 1 pueden causar problemas de polarización de la concentración y valores cercanos a 0 conllevan producciones bajas. En lo que respecta al rango de presiones, se decidió operar bajo condiciones de seguridad totalmente contrastadas por lo que se fijó el límite superior siguiendo las recomendaciones de los fabricantes de las membranas.

Tabla 2.16. Formulación del problema de optimización

Función objetivo	Z
Tipo de optimización	Maximización
Variables independientes	$Rec_{(i)}, \Delta P_{(i)}$
Restricciones a las variables independientes	$0.5 < Rec_{(i)} < 0.9$
Otras restricciones	$10 < \Delta P_{(i)} < 40$ $Conc\ Prod < Conc\ SEMI$

En términos matemáticos propios del ámbito de los problemas de optimización, el modelo de optimización propuesto queda expresado de la siguiente manera:

$$\begin{aligned} \max Z &= f(x) \\ \text{s.t. } h(x) &= 0 \\ w(x) &\leq 0 \\ x &\in \Re^n \\ x_L < x &< x_U \end{aligned}$$

siendo Z el beneficio diario, x el vector de las variables continuas (Rec(i) y P(i)), h el vector de las funciones de restricción como igualdades (las Ecuaciones 2.41-2.52 de los balances de materia y las Ecuaciones 2.53-2.57 de transporte en la membrana) y w el vector de las funciones de restricción como desigualdades (exigencias de calidad del producto como límites a la concentración máxima admitida de cada metal):

$$C_P^{\text{metal}} < C_{\text{SEMI}} \quad (2.70)$$

Los valores óptimos para maximizar el beneficio diario de una instalación de dos etapas para la obtención del Grado SEMI 1 fueron estimados después de la ejecución del correspondiente programa no lineal (NLP) en el software informático. Los resultados están recogidos en la Tabla 2.17 y mostraron que ambas variables de operación tomaban sus valores máximos dentro del rango definido para cada una de ellas (presiones de 40 bar y tasas de recuperación de 0.9). Bajo estas condiciones, el beneficio diario alcanzó un valor de 34928\$, lo que equivale a un beneficio anual superior a 11.5 M\$.

Tabla 2.17. Resultados de la optimización

Grado H ₂ O ₂	Grado 1		Grado 2		Grado 3		Grado 4		Grado 5	
	Caso simulado (2 etapas)	Caso optimizado (2 etapas)	Caso optimizado (4 etapas)	Caso optimizado (5 etapas)	Caso optimizado (6 etapas)	Caso optimizado (7 etapas)				
ΔP _(i) (bar)	25	40	40	40	40	40				
Rec _(i)	0.7	0.9	0.9	0.9	0.9	0.9				
P (m ³ /d)	15.0	21.5	21.5	21.5	21.5	21.5				
C _P ^(Na) (ppb)	183	182	1.3	0.1	0.01	0.001				
Σ A (m ²)	34.3	26.8	54.2	68.2	82.2	96.2				
Términos económicos (\$/d)										
Z	21793	34928	54696	59668	165657	232170				
Rev	44402	57405	77677	82891	189132	255896				
TC	22609	22477	22972	23223	23474	23726				
CC	3169	3041	3505	3741	3977	4213				
CC _{memb}	572	446	904	1137	1371	1604				
CC _{inst}	2597	2595	2601	2604	2607	2609				
OC	19441	19436	19467	19482	19497	19512				
OC _{raw}	19110	19110	19110	19110	19110	19110				
OC _{lab}	168	168	168	168	168	168				
OC _{en}	4	6	13	17	20	23				
OC _m	159	152	175	187	199	211				

De modo similar a lo realizado para el Grado SEMI 1, se planteó la optimización de la obtención de cada uno del resto de grados de calidad electrónica mediante instalaciones que incluían desde 4 a 7 etapas (Abejón et al., 2011). De nuevo, los valores óptimos para las variables de operación mantuvieron el valor máximo fijado en cada una de las etapas para todas las instalaciones (presiones de 40 bar y tasas de recuperación de 0.9). La Figura 2.20 muestra los beneficios obtenidos para cada uno de los Grados, así como los correspondientes ingresos y costes totales del proceso. Como se puede comprobar, el beneficio de los dos Grados más

exigentes (Grados SEMI 4 y 5) aumenta de forma muy importante cuando se compara con el resto de Grados, básicamente como consecuencia de sus elevados precios de mercado. Por otra parte, los costes totales son mucho más estables, ya que apenas aumentan, especialmente en contraste con el gran aumento de los beneficios.

En lo que respecta al desglose de los costes (Tabla 2.18), el coste de adquisición de la materia prima sigue siendo el gasto más significativo al contribuir por encima del 80%. El resto de costes de operación siguen en niveles despreciables (sin llegar ninguno de ellos al 1%). Además, la inversión en membranas incluso para la cascada integrada por siete etapas no llega a suponer más del 7% de los costes totales.

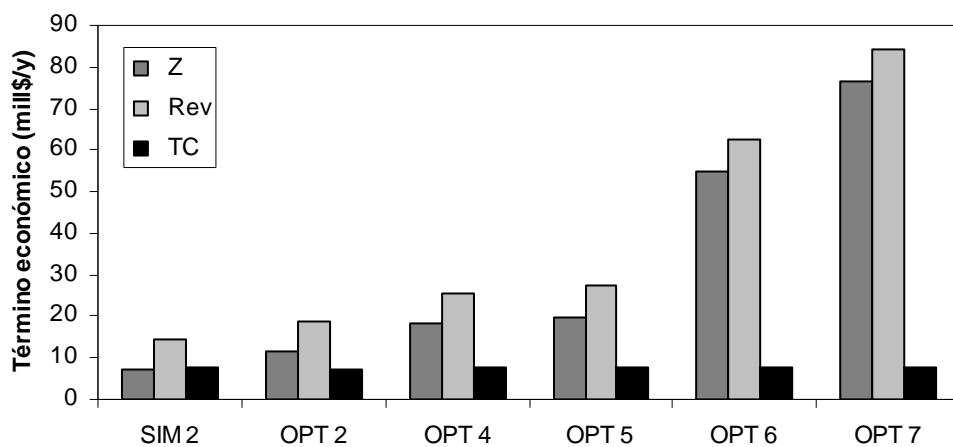


Figura 2.20. Beneficio óptimo y sus correspondientes ingresos y gastos para cada grado electrónico

Tabla 2.18. Desglose de los gastos totales para las diferentes instalaciones

Grado H_2O_2	Contribución a los costes totales (%)					
	Grado 1		Grado 2		Grado 3	
	Caso simulado (2 etapas)	Caso optimizado (2 etapas)	Caso optimizado (4 etapas)	Caso optimizado (5 etapas)	Caso optimizado (6 etapas)	Caso simulado (7 etapas)
CC	14.0	13.5	15.3	16.1	16.9	17.8
CC _{memb}	2.5	2.0	4.0	4.9	5.8	6.8
CC _{inst}	11.5	11.5	11.3	11.2	11.1	11.0
OC	86.0	86.5	84.7	83.9	83.1	82.2
OC _{raw}	84.5	85.0	83.2	82.3	81.4	80.5
OC _{lab}	0.7	0.8	0.7	0.7	0.7	0.7
OC _{en}	<0.1	<0.1	0.1	0.1	0.1	0.1
OC _m	0.7	0.7	0.7	0.8	0.9	0.9

Optimización de una instalación para obtener de forma simultánea todos los Grados SEMI

Después de la optimización de las instalaciones para producir los diferentes Grados SEMI de manera individual (cada instalación produce únicamente un Grado), se planteó el diseño de una instalación capaz de producir los 5 Grados SEMI de peróxido de hidrógeno de forma simultánea.

Para representar esta instalación se optó por recurrir a una superestructura. El empleo de superestructuras para optimizar distintas redes de gestión de aguas y sistemas de desalinización ha sido muy habitual (Voros et al., 1997; Galán y Grossmann, 1998; Saif et al., 2008; Ahmetovic et al., 2010; Khor et al., 2011; Sassi y Mujtaba, 2011; Alnouri y Linke, 2012). La superestructura planteada para la producción de peróxido de hidrógeno ultrapuro se muestra en la Figura 2.21.

El diseño representa una cascada de siete etapas integradas en contracorriente capaz de producir de forma simultánea todos los Grados SEMI. La red está formada principalmente por módulos de membranas, mezcladores y divisores. El modelo matemático de la superestructura se basa en los balances de materia correspondientes y las ya conocidas ecuaciones de transporte de Kedem-Katchalsky. Entre los balances de materia se añade los correspondientes a los splits:

$$Q(j)_{\text{spin}} = Q(j)_{\text{spo1}} + Q(j)_{\text{spo2}} \quad (2.71)$$

$$Q(j)_{\text{spin}} X(j)_{\text{sp}} = Q(j)_{\text{spo1}} \quad (2.72)$$

$$C(j)_{\text{spin}}^{\text{metal}} = C(j)_{\text{spo1}}^{\text{metal}} = C(j)_{\text{spo2}}^{\text{metal}} \quad (2.73)$$

Los resultados de la optimización de la superestructura volvieron a mostrar que los valores óptimos para las presiones aplicadas en todas las etapas es 40 bar (el límite superior de la restricción). De modo análogo, las tasas de recuperación también alcanzan el valor máximo de su rango de definición (0.9). En lo que respecta a la configuración óptima, la superestructura se adapta para la producción del Grado SEMI 5 únicamente, lo que implica que todas las variables de división toman el valor 1 para evitar la salida de materia del sistema como otros Grados distintos del 5 (Figura 2.22). Bajo estas condiciones, el beneficio diario asciende a 232170 \$/d, equivalente a un beneficio anual de 76.6 M\$.

Optimización de una instalación para obtener de forma simultánea todos los Grados SEMI bajo restricciones de mercado

Como ha mostrado la optimización de instalaciones individuales y la superestructura para la producción simultánea de varios Grados SEMI, la economía del proceso invita claramente a promover la producción de los Grados de mayor calidad, pero la existencia de determinadas exigencias de mercado vendría a contrarrestar esta situación. Y es que parece más razonable considerar que la demanda de los grados más exigentes va a estar limitada, impidiendo la comercialización de toda la producción obtenida dentro de una estrategia general orientada a producir todo lo que se pueda del producto lo más ultrapurificado posible. Este marco comercial más realista puede incluir además algunos compromisos adquiridos con los clientes para suministrarles con otros productos distintos del peróxido de mayor calidad (ya que el Grado SEMI 5 únicamente es necesario para tareas muy exigentes dentro de los procesos de

obtención de materiales semiconductores y fabricación de dispositivos microelectrónicos, siendo totalmente reemplazable por peróxido de menor calidad para el resto de etapas productivas).

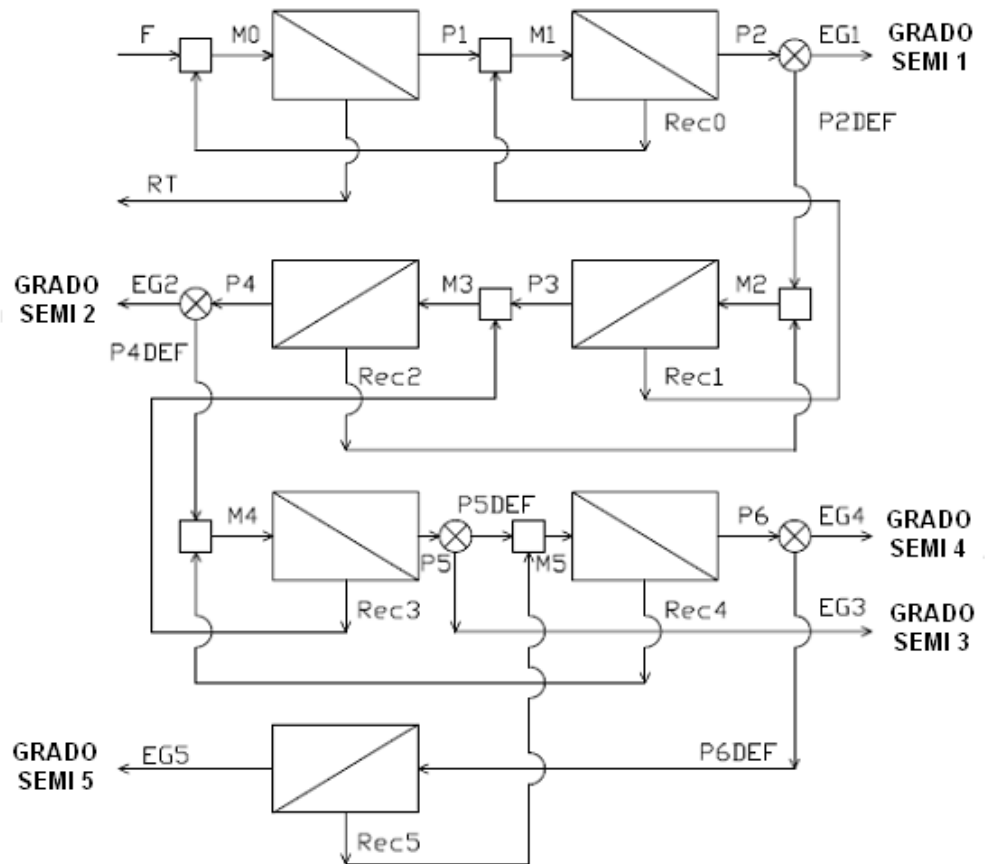


Figura 2.21. Configuración de la superestructura

Inicialmente, se planteó la optimización de la superestructura bajo diferentes restricciones de mercado para lo que se propuso el estudio de tres escenarios distintos. Cada uno de los escenarios quedó definido por un caudal mínimo y otro máximo para cada Grado SEMI (Tabla 2.19).

El Escenario 1 representa la situación base, donde se imponen límites inferiores y superiores a las distintas corrientes de producto. Por un lado, se debe obtener una producción mínima de cada Grado para satisfacer los compromisos adquiridos con los clientes y, por otra parte, hay una producción máxima por encima de la cual el mercado no es capaz de absorber más producto.

Los Escenarios 2 y 3 consideran circunstancias de alta y baja demanda respectivamente. En cada situación, tanto los límites inferiores como los superiores son, respectivamente, aumentados o rebajados con respecto al valor del Escenario 1.

Los resultados de la optimización de los distintos escenarios básicos se detallan en la Tabla 2.20. Una vez más, todos los valores óptimos de las variables de operación coincidieron con sus límites superiores (presiones aplicadas de 40 bar y tasas de recuperación de 0.9) para cada uno

de los escenarios. Los aspectos económicos de los diferentes escenarios están recogidos en la Tabla 2.22. Si se comparan los beneficios obtenidos con el correspondiente a una instalación de siete etapas que solamente produce el Grado SEMI 5, se observa una severa reducción del beneficio: la caída más importante es la del Escenario 3 de baja demanda (61%), seguido del Escenario 2 de alta demanda (54%), quedando así el Escenario 1 como el más beneficioso (40% de reducción).

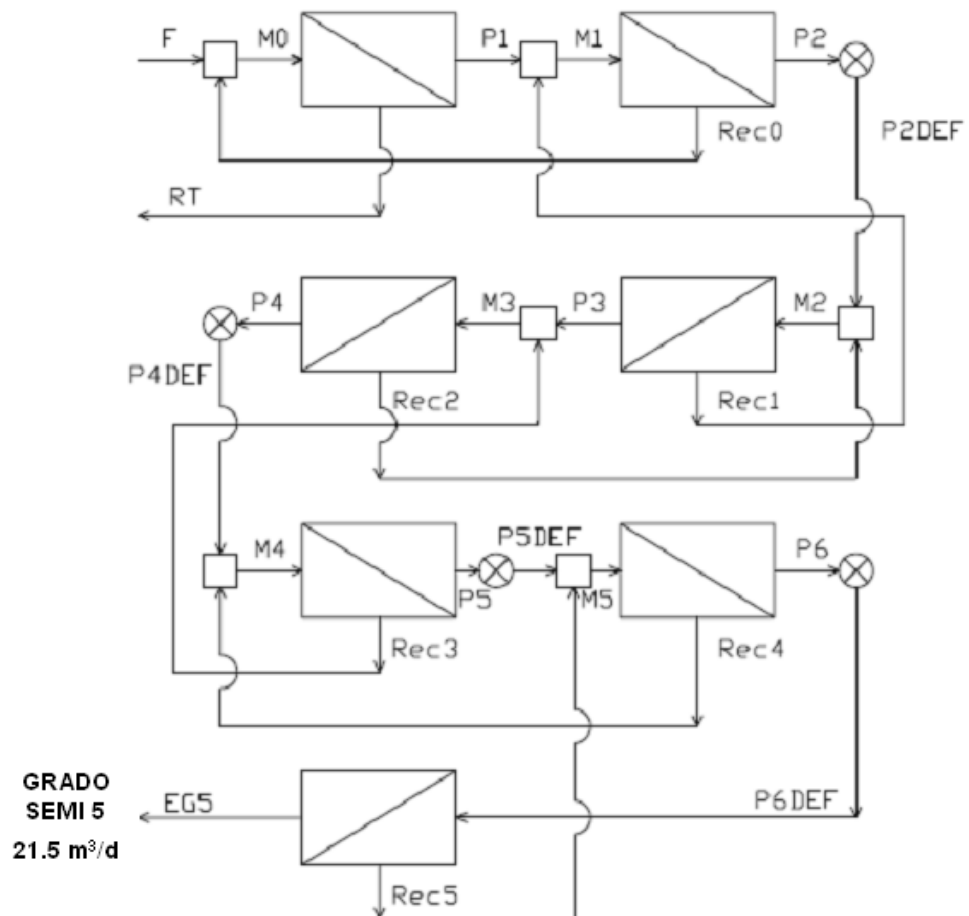


Figura 2.22. Configuración óptima del proceso

La principal causa de la disminución del beneficio económico tiene que ver con la reducción de los ingresos por comercializar productos de menor valor en el mercado. Los costes totales del proceso también se reducen, pero no de un modo comparable, ya que el mayor descenso corresponde al Escenario 3, donde la rebaja de 2% de los costes totales no compensa la caída de 55% en los ingresos del mismo Escenario.

Analizando la configuración del sistema, el Escenario 1 se caracteriza por cumplir con las demandas mínimas de los grados menos exigentes (Grados SEMI 1, 2 y 3), producir la máxima cantidad posible del Grado 5 y dedicar el resto de materia prima disponible al Grado 4.

Se podía esperar que el Escenario 2, con sus condiciones de mayor demanda, fuese más rentable que la situación base. Sin embargo, los resultados dejan claro que el Escenario 1 es

más beneficioso. La configuración del Escenario 2 muestra como el sistema produce únicamente la demanda mínima de todos los productos, a excepción del Grado 5. Bajo estas condiciones, la mayoría de la alimentación se destina a cumplir los compromisos de los Grados menos exigentes, disponiéndose de poca materia prima para producir los Grados más valiosos. Por el contrario, en el Escenario 3, la baja demanda hace que todos los Grados menos el Grado 1 sean producidos hasta el límite máximo fijado. De todos modos, estos límites son inferiores a los correspondientes al caso base, por lo que el beneficio económico se ve reducido (en este caso porque la baja demanda de los Grados de alto valor obliga a destinar gran parte de la materia prima a la obtención de productos de bajo valor).

Tabla 2.19. Restricciones de mercado para los diferentes escenarios definidos

Escenario	Restricciones de caudal para las corrientes de productos (m^3/d)									
	Grado SEMI 1		Grado SEMI 2		Grado SEMI 3		Grado SEMI 4		Grado SEMI 5	
	$Q_{EG1\min}$	$Q_{EG1\max}$	$Q_{EG2\min}$	$Q_{EG2\max}$	$Q_{EG3\min}$	$Q_{EG3\max}$	$Q_{EG4\min}$	$Q_{EG4\max}$	$Q_{EG5\min}$	$Q_{EG5\max}$
1	2	30	1	3	5	30	2	10	1	5
2	4	40	2.5	9	7	38	3.7	18	1.9	8
3	1	14	0.6	1.3	2	12	0.8	3.6	0.6	2.1
4	4	40	2.5	9	7	38	0.8	3.6	0.6	2.1
5	1	14	0.6	1.3	2	12	3.7	18	1.9	8

A la vista de estos resultados, se decidió plantear dos nuevos escenarios de mercado: los Escenarios 4 y 5 caracterizados por situaciones de demanda mixta. El Escenario 4 incluye las condiciones de alta demanda para los Grados 1, 2 y 3 (como en el Escenario 2) y las condiciones de baja demanda para los Grados 4 y 5 (como en el Escenario 3). De modo contrario, el Escenario 5 supone los límites de baja demanda para los Grados 1, 2 y 3 (como en el Escenario 3) y los valores de alta demanda para los Grados 4 y 5 (como en el Escenario 2).

Los resultados de la optimización de estos dos nuevos escenarios aparecen en la Tabla 2.21 (Abejón et al., 2012c). Otra vez, todos los valores óptimos de las variables tomaron su valor límite superior. Los aspectos económicos de los nuevos escenarios aparecen incluidos en la Tabla 2.22.

Como cabía esperar, el Escenario 4 es el menos beneficioso de todos porque combina dos factores no deseables: alta demanda de los grados menos valiosos y baja demanda de los grados de alta calidad preferibles por su alto valor. Esta situación implica una distribución muy desigual de la materia prima entre las dos clases de grados, convirtiendo a los de baja calidad en los preponderantes.

Por su parte, el Escenario 5 también representa un desequilibrio en las condiciones del mercado, pero en este caso hace que los grados de alto valor sean los dominantes, por lo que el beneficio del sistema alcanza un valor mejor al correspondiente a la situación base (23% de beneficio extra).

Todos los resultados de la optimización de los diferentes casos de estudio habían demostrado

un comportamiento muy robusto del sistema, ya que las variables de operación adquirían el valor máximo definido dentro del rango para todas las situaciones. Por ello, se decidió llevar a cabo un simple análisis de sensibilidad para investigar la influencia de los parámetros que definen los costes asociados a las principales variables: (I) el precio de la electricidad influye en los costes de energía debido a la presurización de las corrientes que entran a los módulos de membranas y (II) el coste unitario de las membranas determina la inversión en este apartado para cada etapa. En cada caso, el área disponible de membrana define la cantidad de permeado que se puede obtener y, por consiguiente, la correspondiente tasa de recuperación.

Tabla 2.20. Resultados de la optimización para los escenarios básicos de mercado

k	Etapas de membranas			Splits		Corrientes de producto	
	$\Delta P(k)$ (bar)	Rec(k) (-)	A(k) (m ²)	j	X(j) _{split} (-)	n	$Q_{EG(n)}$ (m ³ /d)
ESCENARIO 1							
1	40	0.9	14.0	1	0.916	1	2.0
2	40	0.9	13.9	2	0.954	2	1.0
3	40	0.9	12.7	3	0.751	3	5.0
4	40	0.9	12.6	4	0.395	4	8.5
5	40	0.9	11.6			5	5.0
6	40	0.9	8.1				
7	40	0.9	2.9				
ESCENARIO 2							
1	40	0.9	14.0	1	0.831	1	4.0
2	40	0.9	13.7	2	0.870	2	2.5
3	40	0.9	11.4	3	0.561	3	7.0
4	40	0.9	11.1	4	0.564	4	3.7
5	40	0.9	9.2			5	4.3
6	40	0.9	4.9				
7	40	0.9	2.5				
ESCENARIO 3							
1	40	0.9	14.0	1	0.895	1	2.5
2	40	0.9	13.8	2	0.938	2	1.3
3	40	0.9	12.3	3	0.346	3	12.0
4	40	0.9	12.2	4	0.393	4	3.6
5	40	0.9	10.6			5	2.1
6	40	0.9	3.4				
7	40	0.9	1.2				

Además, los costes de membrana sirven como base de cálculo para el resto de costes de capital e incluso los costes de mantenimiento depende directamente del coste total de capital. También se incluyó en el análisis la influencia del precio del peróxido de hidrógeno de calidad técnica que se emplea como materia prima.

Los resultados del análisis de sensibilidad (Tabla 2.23) muestran que el beneficio total de la superestructura bajo las condiciones definidas en el Escenario 1 es muy poco sensible a los cambios en los precios unitarios de la electricidad, la membrana o la materia prima. Las variaciones del beneficio se sitúan en el rango $\pm 1\%$ incluso para cambios de un orden de

magnitud en el precio de la electricidad o cuando el precio de la membrana se duplica. Como el coste de la materia prima es el principal coste del proceso, la influencia de su coste unitario es mayor, pero los ingresos son tan dominantes que un incremento o descenso del precio del 20% afecta únicamente en el intervalo $\pm 3\%$ al beneficio económico del sistema.

Tabla 2.21. Resultados de la optimización para los escenarios de mercado con demandas mixtas

k	Etapas de membranas			Splits		Corrientes de producto	
	$\Delta P(k)$ (bar)	Rec(k) (-)	A(k) (m ²)	j	X(j) _{split} (-)	n	$Q_{EG(n)}$ (m ³ /d)
ESCENARIO 4							
1	40	0.9	14.0	1	0.831	1	4.0
2	40	0.9	13.7	2	0.870	2	2.5
3	40	0.9	11.4	3	0.406	3	9.3
4	40	0.9	11.1	4	0.393	4	3.6
5	40	0.9	9.1			5	2.1
6	40	0.9	3.4				
7	40	0.9	1.2				
ESCENARIO 5							
1	40	0.9	14.0	1	0.958	1	1.0
2	40	0.9	13.9	2	0.974	2	0.6
3	40	0.9	13.3	3	0.909	3	2.0
4	40	0.9	13.3	4	0.473	4	9.9
5	40	0.9	12.7			5	8.0
6	40	0.9	10.9				
7	40	0.9	4.6				

En todos los casos, no se produjo ninguna novedad en los valores óptimos de las variables de operación durante el análisis de sensibilidad a los precios (valores de 40 bar y 0.9). Para confirmar la robustez de los valores óptimos de las variables, se buscó unas condiciones tales que modificaran los valores óptimos. Para el caso de las presiones aplicadas, un precio unitario de 6 \$/kWh da como resultado un nuevo valor óptimo (39.4 bar) para todas las presiones aplicadas a la superestructura bajo las condiciones del Escenario 1. Una situación con un precio de la electricidad tan elevado es definitivamente muy improbable, ya que exigiría multiplicar el valor base de la electricidad por un factor cercano a 100.

Tabla 2.22. Resultados económicos de los diferentes escenarios

Término económico (M\$/y)	Sin restricciones de mercado	Escenario 1	Escenario 2	Escenario 3	Escenario 4	Escenario 5
Z	76.616	45.928	35.407	30.057	29.399	56.555
Rev	84.445	53.636	43.062	37.717	37.037	64.305
TC	7.829	7.708	7.655	7.660	7.638	7.750
CC	1.390	1.276	1.227	1.231	1.210	1.315
CC _{memb}	0.529	0.417	0.368	0.372	0.351	0.455
CC _{inst}	0.861	0.860	0.859	0.859	0.859	0.860
OC	6.439	6.432	6.428	6.429	6.427	6.434
OC _{raw}	6.306	6.306	6.306	6.306	6.306	6.306
OC _{lab}	0.055	0.055	0.055	0.055	0.055	0.055
OC _{en}	0.008	0.006	0.005	0.005	0.005	0.007
OC _m	0.070	0.064	0.061	0.062	0.061	0.066

Se obtuvo un resultado muy similar después de estudiar condiciones para lograr un valor óptimo de las tasas de recuperación distinto de 0.9: un precio desorbitado de las membranas de ósmosis inversa ($6000 \text{ \$/m}^2$) darían como resultado como resultado óptimo para la tasa de recuperación de la primera etapa de 0.647. Sin embargo, el resto de etapas mantendrían su valor óptimo en 0.9. De nuevo, el incremento en el precio de la membrana exige multiplicar casi por 100 el precio base, por lo que no puede ser considerado como un panorama lógico. Además, en caso de llegarse a esta situación, el proceso ya no sería viable económicoamente.

Tabla 2.23. Análisis de sensibilidad a los precios de la electricidad y las membranas

Término económico (M\$/y)	Precio electricidad (\$/kWh)			Precio membrana (\$/m ²)		
	0.02	0.08	0.80	10	50	100
CC_{memb}				0.083	0.417	0.833
CC_{inst}				0.856	0.860	0.865
OC_m				0.047	0.064	0.085
OC_{en}	0.002	0.006	0.061			
Z	45.933	45.928	45.873	46.282	45.928	45.486
Variación Z (%)	+0.01		-0.12	0.77		-0.96

2.4. Nomenclatura del Capítulo 2

A	Coeficiente de permeabilidad del solvente en el modelo SD (m/s·bar)
A'	Coeficiente de permeabilidad del solvente en el modelo SDI (kg/m ² ·s·bar)
A	Área de membrana (m ²)
A _(i)	Área de membrana de la etapa i en una cascada (m ²)
AFC	Coeficiente de área cubierta por filtros
AN	Costes vinculados a análisis y control de la calidad en la sala limpia (\$/d)
C _F	Concentración de soluto en la alimentación (mol/m ³)
C _{F0}	Concentración de soluto en la alimentación inicial del proceso experimental (mol/m ³)
C _P	Concentración de soluto en el permeado (mol/m ³)
C _R	Concentración de soluto en el rechazo (mol/m ³)
C _{SEMI}	Concentración de soluto máxima permitida por la norma SEMI (ppb)
C _{VP}	Concentración de soluto en el producto final del proceso experimental (mol/m ³)
C _{V Pf}	Concentración de soluto en el tanque de permeado (mol/m ³)
CA	Superficie de la sala limpia (m ²)
CC	Costes de capital totales (\$/d)
CC _{clean}	Costes de capital asignables a la sala limpia (\$/d)
CC _{inst}	Costes de capital asignables a la instalación sin considerar las membranas (\$/d)
CC _{memb}	Costes de capital asignables a las membranas (\$/d)
(CS)ln	Concentración media logarítmica del soluto a través de la membrana (mol/m ³)
C _{F(i)} ^{metal}	Concentración del metal correspondiente en la corriente de alimentación i (ppb)
C _{P(i)} ^{metal}	Concentración del metal correspondiente en la corriente de permeado i (ppb)
C _{R(i)} ^{metal}	Concentración del metal correspondiente en la corriente de rechazo i (ppb)
C(j) _{spin} ^{metal}	Concentración del metal correspondiente en la corriente entrante al divisor j (ppb)
C(j) _{spo1} ^{metal}	Concentración del metal correspondiente en la corriente 1 saliente del divisor j (ppb)
C(j) _{spo2} ^{metal}	Concentración del metal correspondiente en la corriente 2 saliente del divisor j (ppb)
EAV	Volumen de aire exhausto (m ³ /d)
f(t)	Función logística de degradación en función del tiempo
F	Caudal de alimentación de una cascada (m ³ /d)

$F(i)$	Caudal de alimentación de la etapa i de una cascada (m^3/d)
k	Constante logística ($1/h$)
K_1	Coeficiente de transporte de soluto de la membrana en el modelo SD (m/s)
K_2	Coeficiente de transporte de soluto de la membrana en el modelo SDI ($kg/m^2 \cdot s$)
K_3	Coeficiente de acoplamiento debido a las imperfecciones de la membrana ($kg/m^2 \cdot s \cdot bar$)
J_p	Flujo de permeado bajo consideración de presiones osmóticas despreciables (m/s)
J_s	Flujo de soluto debido al gradiente de potencial químico ($mol/m^2 \cdot s$)
J_v	Flujo volumétrico total de permeado (m/s)
$J_{v(i)}$	Flujo volumétrico de permeado en la etapa i de una cascada (m/d)
J_w	Flujo de solvente debido al gradiente de potencial químico (m/s)
K_A	Constante de disociación (mol/l)
K_{memb}	Constante de ratio entre los costes de membranas y los costes totales de capital
L_p	Coeficiente de permeabilidad hidráulica ($m/s \cdot bar$)
L'_p	Coeficiente de permeabilidad hidráulica ($m/d \cdot bar$)
LT_{inst}	Vida útil de la instalación (d)
LT_{memb}	Vida útil de las membranas de ósmosis inversa (d)
MAV	Volumen de aire para acondicionamiento de la sala limpia (m^3/h)
n	Número de observaciones experimentales
N_s	Flujo total de soluto ($kg/m^2 \cdot s$)
N_w	Flujo total de solvente ($kg/m^2 \cdot s$)
OC	Costes de operación totales (\$/d)
OC_{en}	Costes de operación asignables al consumo energético (\$/d)
OC_{lab}	Costes de operación asignables a la mano de obra (\$/d)
OC_m	Costes de operación asignables al mantenimiento (\$/d)
OC_{raw}	Costes de operación asignables a la materia prima (\$/d)
P	Caudal de permeado de la etapa final de una cascada (m^3/d)
p_h	Permeabilidad hidráulica local de la membrana ($m^2/s \cdot bar$)
$P(i)$	Caudal de permeado de la etapa i de una cascada (m^3/d)
P_M	Permeabilidad local del soluto (m/s)

Q	Caudal de alimentación a la celda (m^3/s)
$Q(j)_{\text{spin}}$	Caudal de la corriente entrante al divisor j (m^3/d)
$Q(j)_{\text{spo1}}$	Caudal de la corriente 1 que sale del divisor j con destino a la siguiente etapa (m^3/d)
$Q(j)_{\text{spo2}}$	Caudal de la corriente 2 que sale del divisor j con destino fuera del sistema (m^3/d)
Q_p	Caudal de permeado (m^3/s)
Q_R	Caudal de recirculación (m^3/s)
R	Coeficiente de rechazo
\mathfrak{R}	Constante universal de los gases ideales ($\text{bar}\cdot\text{m}^3/\text{K}\cdot\text{mol}$)
R_f	Coeficiente global de rechazo
$R(i)$	Caudal de rechazo de la etapa i de una cascada (m^3/d)
$R(t)$	Coeficiente de rechazo correspondiente al tiempo t durante la degradación
R_0	Coeficiente inicial de rechazo en una membrana virgen
$R_{(i)}^{\text{metal}}$	Coeficiente de rechazo del metal correspondiente en la etapa i de una cascada
$\text{Rec}(i)$	Tasa de recuperación de la etapa i en una cascada
Rev	Ingresos diarios ($$/\text{d}$)
t	tiempo (h)
$t_{1/2}$	tiempo medio (h)
T	Temperatura (K)
TC	Costes totales diarios ($$/\text{d}$)
V_F	Volumen en el tanque de alimentación (m^3)
V_p	Volumen en el tanque de permeado (m^3)
x_F	Concentración de peróxido de hidrógeno en la alimentación (mol/l)
x_p	Concentración de peróxido de hidrógeno en el permeado (mol/l)
X_{exp}	Valor experimental de una variable
X_{mod}	Valor modelado de una variable
X_p	Fracción másica de soluto en el permeado
X_R	Fracción másica de soluto en el rechazo
X_w	Fracción másica de solvente en la alimentación
$X(j)_{\text{sp}}$	Variable de decisión del divisor j

Y_{by}	Precio del peróxido de hidrógeno de menor calidad obtenido como subproducto (\$/m ³)
Y_{EG}	Precio del peróxido de hidrógeno de calidad electrónica (\$/m ³)
Y_{elec}	Precio de la electricidad (\$/kWh)
Y_{lab}	Salario de la mano de obra (\$/h)
Y_{memb}	Precio de las membranas de ósmosis inversa (\$/m ²)
Y_{raw}	Precio del peróxido de hidrógeno utilizado como materia prima (\$/m ²)
Z	Beneficio diario (\$/d)

β	Parámetro Spiegler-Kedem
Δx	Espesor total de la membrana (m)
ΔP	Diferencia de presión aplicada sobre la membrana (bar)
$\Delta P_{(i)}$	Diferencia de presión aplicada sobre la membrana en la etapa i de una cascada (bar)
$\Delta \Pi$	Diferencia de presión osmótica entre las caras de la membrana (bar)
Φ	Suma de residuales cuadrados
v	Coeficiente estequiométrico basado en el factor de van't Hoff
θ	Tiempo adimensional
ρ	Coeficiente de rechazo adimensional
σ	Coeficiente de reflexión
σ^{metal}	Coeficiente de reflexión del metal correspondiente
τ	Resistencia (h)
ω	Coeficiente de permeabilidad del soluto (mol/m ² ·s·bar)
ω'	Coeficiente modificado de permeabilidad del soluto (m/s)
ω^{metal}	Coeficiente modificado de permeabilidad del soluto para el metal correspondiente (m/d)
ψ	Resistencia adimensional

2.5. Referencias del Capítulo 2

- R. Abejón, A. Garea, A. Irabien, *Ultrapurification of hydrogen peroxide solution from ionic metals impurities to semiconductor grade by reverse osmosis*, Separation and Purification Technology, 76 (2010) 44-51.
- R. Abejón, A. Garea, A. Irabien, *Membrane process optimization for hydrogen peroxide ultrapurification*, Computer Aided Chemical Engineering, 29 (2011) 678-682.
- R. Abejón, A. Garea, A. Irabien, *Analysis, modelling and simulation of hydrogen peroxide ultrapurification by multistage reverse osmosis*, Chemical Engineering Research and Design, 90 (2012a) 442-452.
- R. Abejón, A. Garea, A. Irabien, *Integrated countercurrent reverse osmosis cascades for hydrogen peroxide ultrapurification*, Computers and Chemical Engineering, 41 (2012b) 67-76.
- R. Abejón, A. Garea, A. Irabien, *Optimum design of reverse osmosis systems for hydrogen peroxide ultrapurification*, AIChE Journal, 58:3718-3730 (2012c).
- E. Ahmetović, M. Martín, I.E. Grossmann, *Optimization of energy and water consumption in corn-based ethanol plants*, Industrial and Engineering Chemistry Research, 49 (2010) 7972-7982.
- S.Y. Alnouri, P. Linke, *A systematic approach to optimal membrane network synthesis for seawater desalination*, Journal of Membrane Science, 417-418 (2012) 96-112.
- A. Antony, R. Fudianto, S. Cox, G. Leslie, *Assessing the oxidative degradation of polyamide reverse osmosis membrane - Accelerated ageing with hypochlorite exposure*, Journal of Membrane Science, 347 (2010) 159-164.
- Aspen Technology, Inc., *Aspen simulation workbook*, Versión V7.1., Burlington (Iowa), 2009.
- P.E.D. Augusto, B.M.C. Soares, M.C. Chiu, L.A.G. Gonçalves, *Modelling the effect of temperature on the lipid solid fat content (SFC)*, Food Research International, 45 (2012) 132-135.
- S.A. Avlonitis, K. Kouroumbas, N. Vlachakis, *Energy consumption and membrane replacement cost for seawater RO desalination plants*, Desalination, 157 (2003) 151-158.
- C.H. Bartholomew, R.J. Farrauto, *Fundamentals of industrial catalytic processes*, Wiley, Hoboken (Nueva Jersey), 2006.
- F.J. Benítez, J.L. Acero, A.I. Leal, *Application of microfiltration and ultrafiltration processes to cork processing wastewaters and assessment of the membrane fouling*, Separation and Purification Technology, 50 (2006) 354–364.
- R.E. Rosenthal, *GAMS: A user's guide*, GAMS Development Corporation, Washington, 2012.

- P.R. Buch, D. Jagan Mohan, A.V.R. Reddy, *Preparation, characterization and chlorine stability of aromatic-cycloaliphatic polyamide thin film composite membranes*, Journal of Membrane Science, 309 (2008) 36-44.
- M.K. da Silva, I.C Tessaro, K. Wada, *Investigation of oxidative degradation of polyamide reverse osmosis membranes by monochloramine solutions*, Journal of Membrane Science, 282 (2006) 375-382.
- S. El-Manharawy, A. Hafez, *Technical management of RO system*, Desalination, 131 (2000) 173-188.
- M. Fariñas, *Osmosis inversa: fundamentos, tecnología y aplicaciones*. McGraw-Hill, Madrid, 1999.
- A. M. Farooque, A. Al-Amoudi, K. Numata, *Degradation study of cellulose triacetate hollow fine-fiber SWRO membranes*, Desalination, 123 (1999) 165-171.
- D. Fekedulegn, M.P. Mac Siurtain, J.J. Colbert, *Parameter estimation of nonlinear growth models in forestry*, Silva Fennica, 33 (1999) 327-336.
- H. S. Fogler, *Elements of chemical reaction engineering*, Prentice Hall, Upper Saddle River (Nueva Jersey), 1999.
- C.J. Gabelich, T.I. Yun, B.M Coffey, I.H.M Suffet, *Enhanced oxidation of polyamide membranes using monochloramine and ferrous iron*, Desalination, 150 (2002) 15-30.
- B.Galán, I.E. Grossmann, *Optimal design of distributed wastewater treatment networks*, Industrial and Engineering Chemistry Research, 37 (1998) 4036-4048.
- GE Water & Process Technologies, *SEPA CF II Membrane Element Cell instruction manual*, Minnetonka (Minnesota), 2004.
- J. Glater, M.R. Zachariah, S.B. McCray, J.W. McCutchan, *Reverse osmosis membrane sensitivity to ozone and halogen disinfectants*, Desalination, 48 (1983) 1-16.
- G. Goor, J. Glenneberg, S. Jacobi, Hydrogen peroxide, in: *Ullmann's Encyclopedia of Industrial Chemistry*, Edición electrónica, Wiley-VCH, Weinheim, 2007.
- M. F. A. Goosen, S. S. Sablani, H. Al-Hinai, S. Al-Obeidani, R. Al-Belushi, D. Jackson, *Fouling of reverse osmosis and ultrafiltration membranes: a critical review*, Separation Science and Technology, 39 (2005) 2261-2297.
- M.I. Iborra, J. Lora, M.I. Alcaina, J.M. Arnal, *Effect of oxidation agents on reverse osmosis membrane performance to brackish water desalination*, Desalination, 108 (1996) 83-89.
- M. Jarzyńska, M. Pietruszka, *The application of the Kedem-Katchalsky equations to membrane transport of ethyl alcohol and glucose*, Desalination, 280 (2011) 14-19.

- G.D. Kang, C.J. Gao, W.D. Chen, X.M Jie, Y.M. Cao, Q. Yuan, *Study on hypochlorite degradation of aromatic polyamide reverse osmosis membrane*, Journal of Membrane Science, 300 (2007) 165-171.
- D. Kaplan, L. Glass, *Understanding nonlinear dynamics*, Springer-Verlag, Nueva York, 1995.
- M. Kargol, A. Kargol, *Mechanistic equations for membrane substance transport and their identity with Kedem-Katchalsky equations*, Biophysical Chemistry, 103 (2003) 117-127.
- M.G.A. Khedr, *Development of reverse osmosis desalination membranes composition and configuration: future prospects*, Desalination, 153 (2002) 295-304.
- C.S. Khor, D.C.Y. Foo, M.M. El-Halwagi, R.R. Tan, N. Shah, *A superstructure optimization approach for membrane separation-based water regeneration network synthesis with detailed nonlinear mechanistic reverse osmosis model*, Industrial and Engineering Chemistry Research, 50 (2011) 13444-13456.
- H. Koseoglu, N. Kabay, M. Yüksel, S. Sarp, Ö. Arar, M. Kitis, *Boron removal from seawater using high rejection SWRO membranes - impact of pH, feed concentration, pressure and cross-flow velocity*, Desalination, 227 (2008) 253–263.
- H. Koseoglu, M. Kitis, *The recovery of silver from mining wastewaters using hybrid cyanidation and high-pressure membrane process*, Minerals Engineering 22 (2009) 440–444.
- J. Kucera, *Understanding RO membrane performance*, Chemical Engineering Progress, 104 (2008) 30-34.
- A. Kulkarni, D. Mukherjee, D. Mukherjee, W.N. Gill, *Reprocessing hydrofluoric acid etching solutions by reverse osmosis*, Chemical Engineering Communications, 129 (1994) 53–68.
- Y.N. Kwon, J.O. Leckie, *Hypochlorite degradation of crosslinked polyamide membranes II. Changes in hydrogen bonding behavior and performance*, Journal of Membrane Science, 282 (2006) 456–464.
- G.N. Lewis, *The osmotic pressure of concentrated solutions, and the laws of the perfect solution*, Journal of Agricultural and Food Chemistry, 30 (1908) 668-683.
- B.A. McCarl, A. Meeraus, P. van der Eijk, M. Bussieck, S. Dirkse, P. Steacy, *GAMS user guide*, Versión 23.3, 2009.
- J.A. Medina San Juan, *Desalación de aguas salobres y de mar. Osmosis inversa*. Mundi-Prensa, Madrid, 2000.
- H.N. Morse, J.C.W. Frazer, *The osmotic pressure and freezing points of solutions of cane sugar*, American Chemical Journal, 34 (1905) 1-99.
- M. Noronha, V. Mavrov, H. Chmiel, *Efficient design and optimisation of two-stage NF processes by simplified process simulation*, Desalination, 145 (2002) 207-215.

- M. Peters, K. Timmerhaus, R. West, *Plant design and economics for chemical engineers*, McGraw-Hill, Nueva York, **2003**.
- M. Pontié, H. Dach, J. Leparc, M. Hafsi, A. Lhassan, *Novel approach combining physico-chemical characterizations and mass transfer modelling of nanofiltration and low pressure reverse osmosis membranes for brackish water desalination intensification*, Desalination, 221 (2008) 174-191.
- H.D. Raval, J.J Trivedi, S.V. Joshi, C.V. Devmurari, *Flux enhancement of thin film composite RO membrane by controlled chlorine treatment*, Desalination, 250 (2010) 945-949.
- S. Rouaix, C. Causserand, P. Aimar, *Experimental study of the effects of hypochlorite on polysulfone membrane properties*, Journal of Membrane Science, 277 (2006) 137-147.
- Rumsey Engineers Inc, *Energy efficiency baselines for cleanrooms*, Non-Residential New Construction and Retrofit Incentive Programs of PG&E, Oakland (California) **2009**.
- Y. Saif, A. Elkamel, M. Pritzker, *Optimal design of reverse-osmosis networks for wastewater treatment*, Chemical Engineering and Processing, 47 (2008) 2163-2174.
- M. A. Sanz, V. Bonnélye, G. Cremer, *Fujairah reverse osmosis plant: 2 years of operation*, Desalination, 203 (2007) 91-99.
- K. Sassi, I. Mujtaba, *Optimal design of reverse osmosis based desalination process with seasonal variation of feed temperature*, Chemical Engineering Transactions, 25 (2011) 1055-1060.
- P. Sehn, *Fluoride removal with extra low energy reverse osmosis membranes: three years of large scale field experience in Finland*, Desalination, 223 (2008) 73-84.
- SEMI (Semiconductor Equipment and Materials International), *Specifications for Hydrogen Peroxide*, SEMI Document C30-1110, San Jose (California), **2010**.
- H.F. Shaalan, M.H. Sorour, S.R. Tewfik, *Simulation and optimization of a membrane system for chromium recovery from tanning wastes*, Desalination, 141 (2000) 315-324.
- H. Shemer, R. Semiat, *Impact of halogen based disinfectants in seawater on polyamide RO membranes*, Desalination, 273 (2011) 179-183.
- T. Shintani, H. Matsuyama, N. Kurata, *Development of a chlorine-resistant polyamide reverse osmosis membrane*, Desalination, 207 (2007) 340-348.
- P. Silva, L.G. Peeva, A.G. Livingston, *Organic solvent nanofiltration (OSN) with spiral-wound membrane elements -Highly rejected solute system*, Journal of Membrane Science, 349 (2010) 167-174.
- M. Soltanieh, W.N. Gill, *Review of reverse osmosis membranes and transport models*, Chemical Engineering Communications, 12 (1981) 279-363.

- T. Tsuru, M. Miyawaki, T. Yoshioka, M. Asaeda, *Reverse osmosis of nonaqueous solutions through porous silica-zirconia membranes*, AIChE Journal, 52 (2006) 522-531.
- N.G. Voros, Z.B. Maroulis, D. Marinos-Kouris, *Short-cut structural design of reverse osmosis desalination plants*, Journal of Membrane Science, 127 (1997) 47-68.
- S.M. Walas, *Chemical process equipment - Selection and design*, Butterworth-Heinemann, Newton (Massachusetts), 1990.
- S. Wu, C. Zheng, G. Zheng, *Effective interface of a composite membrane serving as an ideally ultrathin barrier layer*, Polymer, 37 (1996) 4193-4195.
- P. Xu, J.E. Drewes, *Viability of nanofiltration and ultra-low pressure reverse osmosis membranes for multi-beneficial use of methane produced water*, Separation and Purification Technology, 52 (2006) 67-76.
- J. Xu, G. Ruan, L. Zou, C. Gao, *Effect of chlorine and acid injection on hollow fiber RO for SWRO*, Desalination, 262 (2010) 115-120.
- L. Yang, C. Eng Gan, *Costing small cleanrooms*, Building and Environment, 42 (2007) 743-751.
- A. Zhu, A. Rahardianto, P.D. Christofides, Y. Cohen, *Reverse osmosis desalination with high permeability membranes - cost optimization and research needs*, Desalination and Water Treatment, 15 (2010) 256-266.

Conclusiones 3

Conclusions

3.1. Conclusiones y progreso de la investigación

3.1.1. Conclusiones

Las conclusiones obtenidas a lo largo de la presente Tesis Doctoral han sido difundidas fundamentalmente en revistas científicas de impacto internacional incluidas en el *Journal of Citation Reports-Science Edition (JCR)*. Las publicaciones se listan a continuación indicando su posición con respecto al número total de citas hasta Junio de 2012, extraídas del *Essential Science Indicators-Citations*, disponible en plataforma *ISI Web of Knowledge*:

1. Abejón, R.; Garea, A.; Irabien, A. *Ultrapurification of hydrogen peroxide solution from ionic metals impurities to semiconductor grade by reverse osmosis*. Separation and Purification Technology, 76:44-51 (2010). Ranking de la revista: 798/6048 (Cuartil Q1).
2. Abejón, R.; Garea, A.; Irabien, A. *Analysis, modelling and simulation of hydrogen peroxide ultrapurification by multistage reverse osmosis*. Chemical Engineering Research and Design, 90:442-452 (2012). Ranking de la revista: 2414/6048 (Cuartil Q2).
3. Abejón, R.; Garea, A.; Irabien, A. *Integrated countercurrent reverse osmosis cascades for hydrogen peroxide ultrapurification*. Computers and Chemical Engineering, 41:67-76 (2012). Ranking de la revista: 1388/6048 (Cuartil Q1).
4. Abejón, R.; Garea, A.; Irabien, A. *Optimum design of reverse osmosis systems for hydrogen peroxide ultrapurification*. AIChE Journal, 58:3718-3730 (2012). Ranking de la revista: 797/6048. (Cuartil Q1).

Las conclusiones principales de este trabajo son:

- 1) Se ha demostrado experimentalmente a escala laboratorio la **viabilidad técnica de un proceso basado en ósmosis inversa** con membranas comerciales de poliamida para la **ultrapurificación de peróxido de hidrógeno** desde calidad técnica hasta grado electrónico, obteniendo peróxido de hidrógeno de calidad **Grado SEMI 1** mediante dos etapas en serie.
- 2) El comportamiento del proceso de ósmosis inversa para la ultrapurificación de peróxido de hidrógeno con **membranas de poliamida** se caracteriza por: **flujo diario máximo de permeado** de $1.9 \text{ m}^3/\text{m}^2$, **coeficientes de rechazo** para la mayoría de los elementos metálicos con valores cercanos a **0.9** y una **vida útil** de las membranas de unos **3 días**.

- 3) La producción de permeado en función de la presión aplicada se puede describir mediante el modelo de **Kedem-Katchalsky** que describe el comportamiento experimental del **flujo de permeado** y de los **coeficientes de rechazo**.
- 4) El comportamiento de las membranas como consecuencia de la **degradación** oxidativa se puede describir mediante un **modelo logístico** de degradación con el tiempo. El modelo propuesto permite estimar dos parámetros: el **tiempo medio $t_{1/2}$** y la **resistencia τ** .
- 5) Se ha desarrollado un modelo de **simulación** para el proceso que se ha aplicado para **la escala industrial** bajo la configuración de cascadas de membranas integradas en contracorriente. Mediante este modelo se ha simulado la **influencia de las principales variables del proceso** (presiones aplicadas y tasas de recuperación) y se ha evaluado la **viabilidad económica** del mismo.
- 6) A partir de los modelos desarrollados se ha llevado a cabo la optimización del proceso para diferentes objetivos de ultrapurificación de peróxido de hidrógeno. Se ha calculado el **número óptimo de etapas** que la cascada de membranas debe incorporar para la producción de cada uno de los grados de calidad electrónica y los **valores óptimos para las presiones aplicadas y tasas de recuperación**, de modo que se **maximice el beneficio económico del proceso**.
- 7) **Los precios unitarios de los principales recursos necesarios** (materia prima, membranas y energía eléctrica) y las **restricciones del mercado** permiten establecer una **baja sensibilidad** del óptimo económico con estas variables, ya que los beneficios mayores corresponden a la fabricación de los **grados más exigentes** (Grados SEMI 4 y 5) por su elevado precio de mercado.

3.1.2. Progreso de la investigación

Para el progreso científico-técnico futuro en relación a los contenidos desarrollados en esta Tesis, las siguientes líneas de trabajo son consideradas de especial relevancia:

- 1) **Estudio del comportamiento de membranas de ósmosis inversa fabricadas en materiales distintos a los testados.** La principal limitación que se ha encontrado al empleo de membranas de poliamida para la ultrapurificación de peróxido de hidrógeno ha sido la vida útil tan corta que muestran. Los resultados experimentales preliminares llevados a cabo con membranas de acetato de celulosa han puesto de manifiesto que presentan una vida útil más larga, pero a costa de perder productividad en términos de flujo de permeado y capacidad de rechazo de ciertos elementos metálicos.

Por tanto, se estima oportuno el estudio de membranas específicamente diseñadas para presentar alta resistencia frente a la oxidación, la degradación de las mismas y el diseño de procesos "híbridos", en los que se integren membranas de distintas características.

- 2) **Integración de objetivos distintos de los económicos en estrategias complejas de optimización.** En esta Tesis se ha planteado únicamente la maximización del beneficio económico o en su caso la minimización de los costes totales del proceso como objetivos para la optimización. El trabajo futuro deberá incluir nuevos criterios en la estrategia de optimización que tengan en consideración otros aspectos importantes del proceso, por ejemplo la calidad de producto obtenido o el impacto del consumo energético y el resto de cargas ambientales asociadas al proceso de ultrapurificación, planteándose la optimización multiobjetivo para la toma de decisión en escenarios de mayor complejidad.

La inclusión de cuestiones tales como incertidumbre y variabilidad a lo largo del tiempo de los parámetros en los que basa el sistema es también una cuestión importante a tener en cuenta.

- 3) **Evaluación de procesos innovadores para la fabricación de peróxido de hidrógeno.** El proceso tradicional de oxidación de antraquinonas requiere grandes cantidades de energía e implica una importante generación de residuos. Si se tiene además en consideración el empleo de mezclas de disolventes orgánicos para dar lugar a una solución de trabajo de muy baja productividad, el proceso no puede ser evaluado de forma positiva en términos de sostenibilidad. Por lo tanto es necesaria una visión global que además de centrarse en la mejora del proceso de ultrapurificación tenga en mente avanzar en la sostenibilidad de la etapa productiva previa.

La síntesis directa de peróxido de hidrógeno a partir de hidrógeno y oxígeno mediante el uso de catalizadores se plantea como la alternativa más viable para la sustitución del proceso de la antraquinona. La elección del catalizador así como los factores de diseño y operación del proceso que influyen en la formación y descomposición del peróxido de hidrógeno deben ser fruto de investigación mediante técnicas de ingeniería de proceso.

3.2. Conclusions and on-going research

3.2.1. Conclusions

The conclusions obtained in the present PhD Thesis have been spread principally in scientific journals of worldwide relevance, all of them included in the *Journal of Citation Reports-Science Edition (JCR)*. The publications are listed below, showing the journal ranking as a function of the number of total citations up to June 2012, from the *Essential Science Indicators-Citations*, available in the *ISI Web of Knowledge* Platform:

1. Abejón, R.; Garea, A.; Irabien, A. *Ultrapurification of hydrogen peroxide solution from ionic metals impurities to semiconductor grade by reverse osmosis*. Separation and Purification Technology, 76:44-51 (**2010**). Journal ranking: 798/6048 (Quartile Q1).
2. Abejón, R.; Garea, A.; Irabien, A. *Analysis, modelling and simulation of hydrogen peroxide ultrapurification by multistage reverse osmosis*. Chemical Engineering Research and Design, 90:442-452 (**2012**). Journal ranking: 2414/6048 (Quartile Q2).
3. Abejón, R.; Garea, A.; Irabien, A. *Integrated countercurrent reverse osmosis cascades for hydrogen peroxide ultrapurification*. Computers and Chemical Engineering, 41:67-76 (**2012**). Journal ranking: 1388/6048 (Quartile Q1).
4. Abejón, R.; Garea, A.; Irabien, A. *Optimum design of reverse osmosis systems for hydrogen peroxide ultrapurification*. AIChE Journal, 58:3718-3730 (**2012**). Journal ranking: 797/6048. (Quartile Q1).

The main conclusions which can be withdrawn from this work are:

- 1) The **technical viability** of a process based on commercially available polyamide **reverse osmosis** membranes for **hydrogen peroxide ultrapurification** from technical grade to electronic grade has been experimentally demonstrated at lab scale, producing **SEMI Grade 1** hydrogen peroxide by a two-stage process.
- 2) The performance of reverse osmosis **polyamide membranes** for the ultrapurification process has been characterized by: a **maximum daily permeate flow** of $1.9 \text{ m}^3/\text{m}^2$, the **rejection coefficients** for most of the metallic elements around 0.9 and the **effective lifetime** of the membranes about just 3 days.
- 3) The permeate production as a function of the pressure applied can be described by the **Kedem-Katchalsky** model that describes the experimental performance of the **permeate flux** and the **rejection coefficients**.

- 4) The reverse osmosis membranes behaviour as a result of the oxidative **degradation** can be described by a **logistic model** of degradation along time. The proposed model allows the determination of two parameters: the **halftime** $t_{1/2}$ and the **resistance** τ .
- 5) A **simulation model** has been developed to be applied to **industrial scale installations** under the **countercurrent integrated membrane cascade** configuration. The model has been used to simulate the **influence of the main process variables** (applied pressures and recovery rates) and to evaluate the **economic viability**.
- 6) From the developed models, the process optimization has been carried out for several objectives in the framework of the hydrogen peroxide ultrapurification process. The **optimum number of stages** a membrane cascade should incorporate for the production of each electronic grade and the **optimum values for applied pressures and recovery rates** have been solved to **maximize the economic profit** of the process.
- 7) The **unitary prices of the principal required resources** (raw material, membranes and electric energy) and the **market restrictions** allows the assessment of a **low sensitivity** of the optimal economic point, as the highest profits correspond to the production of **the most exigent grades** (SEMI Grades 4 and 5) because of their high market price.

3.2.2. On-going research

Based on the results presented on this PhD Thesis, the following relevant lines are considered for the future scientific-technical progress:

- 1) **Study of the performance of reverse osmosis membranes made of materials different from the tested ones.** The main limitation that has been found to the use of polyamide membranes for hydrogen peroxide ultrapurification is their extremely short effective lifetime. The preliminary experimental results with cellulose acetate membranes have showed that they have a longer effective lifetime, but at the expense of decreasing the productivity in terms of permeate flux and rejection coefficients of some metallic elements.

Therefore, the study of membranes specifically designed to exhibit high resistance to oxidation, their degradation and the design of new "hybrid" processes which integrate membranes with different characteristics should also be considered.

- 2) **Integration of objectives different from the economic one in complex optimization strategies.** In this PhD Thesis, only the maximization of the economic profit and, in some particular cases, the minimization of the total costs of the process have been considered as optimization targets. The future work should include new criteria to the optimization strategy to take into consideration other important aspects of the process, such as the obtained product quality or the impact of the energy consumption and the rest of environmental loads related to the ultrapurification process, resorting to multiobjective optimization problems as useful decision tools in scenarios involving more complexity.

The inclusion of topics such as uncertainty and time depending parameters that govern the system performance is an issue to take into account for the on-going work to be completed in this investigation project.

- 3) **Evaluation of new innovative processes for the hydrogen peroxide production.** The traditional process based on the oxidation of anthraquinones requires large amounts of energy and implies a considerable waste generation. In addition, when the use of organic solvent mixtures to obtain a very low productivity working solution is taken into account, the process can not be evaluated in a positive way in terms of sustainability. Hence, a global vision that adds to the progress in the ultrapurification process new advances in the sustainability of the previous productive stages is nowadays needed.

The direct synthesis of hydrogen peroxide from hydrogen and oxygen with the assistance of catalysis is proposed as the most viable alternative to replace the anthraquinone process. The choice of the best catalysts and the process design and operation factors which influence on the formation and decomposition of hydrogen peroxide must be investigated by process engineering techniques.

Artículos científicos 4

Scientific articles

4.1. Abejón, R.; Garea, A.; Irabien, A. *Ultrapurification of hydrogen peroxide solution from ionic metals impurities to semiconductor grade by reverse osmosis. Separation and Purification Technology*, **76**:44-51 (2010).

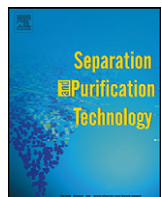
Resumen

El presente trabajo se centra en la aplicación de ósmosis inversa a la ultrapurificación de soluciones acuosas de peróxido de hidrógeno (35% en peso). La organización Semiconductor Equipment and Materials International (SEMI) desarrolla los estándares más respetados a nivel global a la hora de establecer los requisitos de calidad para los reactivos usados en este sector; uno de estos estándares, SEMI C30, se refiere al peróxido de hidrógeno. El peróxido de hidrógeno de calidad electrónica se limita a niveles de impurezas metálicas por debajo de 1 ppm (concentraciones por debajo de 1 ppb son necesarias para los grados más exigentes), así que varios elementos presentes como impurezas en el peróxido de hidrógeno de calidad técnica superan los límites fijados. Se llevó a cabo un estudio experimental preliminar en una instalación a escala laboratorio (celda para membranas planas) con 6 membranas comerciales para ósmosis inversa diferentes para elegir la más apropiada para la ultrapurificación de peróxido de hidrógeno. La membrana BE (producida por Woongjin Chemical) fue seleccionada para un estudio de viabilidad más profundo por sus mayores flujo de permeado ($1.95 \cdot 10^{-5} \text{ m}^3/\text{m}^2 \text{ s}$ a 40 bar) y valores de rechazo de los metales (comprendidos entre 0,825 para B y 0,961 para Cu). El modelo Kedem-Katchalsky resultó ser el más representativo para caracterizar el comportamiento de la membrana seleccionada ya que alcanzó un porcentaje de variación global explicada superior al 94%.

Original abstract

The present research is centred upon the application of reverse osmosis to the ultrapurification of aqueous hydrogen peroxide (35%, w/w). Semiconductor Equipment and Materials International (SEMI) organization develops the globally most respected standards to establish the quality requirements for the chemicals used in this sector; one of these standards, SEMI C30, is proposed for hydrogen peroxide. Electronic grade hydrogen peroxide accounts for sub-ppm metallic impurity levels (sub-ppb concentrations are required for the most exigent grades), so various elements present as impurities in technical grade hydrogen peroxide exceed the fixed limits. A preliminary experimental study was carried out with a laboratory-scale facility (flat-sheet membrane unit) with 6 different commercial reverse osmosis membranes in order to choose the most appropriate one for hydrogen peroxide ultrapurification. BE membrane (manufactured by Woongjin Chemical) was selected for further viability study because of its

higher permeate flux ($1.95 \cdot 10^{-5} \text{ m}^3/\text{m}^2 \text{ s}$ at 40 bar) and metal rejections values (ranging from 0.825 for B to 0.961 for Cu). The Kedem–Katchalsky model resulted as the most representative for characterizing the selected membrane behaviour as it achieved a percentage of overall variation explained upper than 94%.



Ultrapurification of hydrogen peroxide solution from ionic metals impurities to semiconductor grade by reverse osmosis

R. Abejón, A. Garea*, A. Irabien

Departamento de Ingeniería Química y Química Inorgánica, Universidad de Cantabria, Avda. Los Castros s/n, 39005 Santander, Cantabria, Spain

ARTICLE INFO

Article history:

Received 21 June 2010

Received in revised form

10 September 2010

Accepted 15 September 2010

Keywords:

Ultrapurification

Hydrogen peroxide

Reverse osmosis

High-purity chemicals

Metallic ion traces

ABSTRACT

The present research is centred upon the application of reverse osmosis to the ultrapurification of aqueous hydrogen peroxide (35%, w/w). Semiconductor Equipment and Materials International (SEMI) organization develops the globally most respected standards to establish the quality requirements for the chemicals used in this sector; one of these standards, SEMI C30 is proposed for hydrogen peroxide. Electronic grade hydrogen peroxide accounts for sub-ppm metallic impurity levels (sub-ppb concentrations are required for the most exigent grades), so various elements present as impurities in technical grade hydrogen peroxide exceed the fixed limits. A preliminary experimental study was carried out with a laboratory-scale facility (flat-sheet membrane unit) with 6 different commercial reverse osmosis membranes in order to choose the most appropriate one for hydrogen peroxide ultrapurification. BE membrane (manufactured by Woongjin Chemical) was selected for further viability study because of its higher permeate flux ($1.95 \times 10^{-5} \text{ m}^3/\text{m}^2 \text{ s}$ at 40 bar) and metal rejections values (ranging from 0.825 for B to 0.961 for Cu). The Kedem–Katchalsky model resulted as the most representative for characterizing the selected membrane behaviour as it achieved a percentage of overall variation explained upper than 94%.

© 2010 Elsevier B.V. All rights reserved.

1. Introduction

Hydrogen peroxide is considered a key chemical for the semiconductor industry. The preparation of semiconductor materials and the manufacture of printed circuit boards employ aqueous hydrogen peroxide solutions for cleaning silicon wafers, removing photoresists or etching copper on printed circuit boards. Most usual cleaning baths for silicon wafer surface cleaning (SC1, SC2 or SPM) include hydrogen peroxide in their formulations [1]. The said baths remove particulate, organic and metallic pollutants from silicon surface, avoiding electric inoperativeness and decreased minority carrier lifetime caused by pollution [2]. In order to avoid contamination because of the bath itself, extremely high levels of purity are required for all the components, so strict control about impurity concentration in these chemicals becomes necessary.

Semiconductor Equipment and Materials International (SEMI) organization is the global industry association serving the manufacturing supply chains for the microelectronic, display and photovoltaic industries. This organization facilitates the development of the globally most respected technical standards in this field. Among all the topics regulated, some refer to process chemicals and indicate the requirements to be fulfilled in order to be accepted as

electronic chemicals. For the particular case of hydrogen peroxide, the SEMI C30 document is applicable [3], where six different electronic grades are defined in function of the allowed maximum pollutant concentration, as can be seen in Table 1.

Although typically commercialized grades of aqueous hydrogen peroxide solutions have been treated by traditional purification techniques (L-L extraction, adsorption, membrane technologies, distillation...) for lowering impurity levels [4], hydrogen peroxide for use in electronics demands very low content of pollutants. Hence, ultrapurification processes are needed to achieve electronic grade requirements from standard grade product.

While technical viability of hydrogen peroxide ultrapurification is well solved as commercialization of the different electronic grades demonstrates, scientific papers hinting process fundamentals cannot be found. Therefore, patents become the only available bibliographic source.

As result of the bibliographical review over the last twenty years, more than 25 patents relative to purification of hydrogen peroxide have been found. According to the noticed references, distillation, adsorption, ion exchange and membranes technologies are the most relevant techniques when electronic grade chemical is desired.

Whichever technology is selected, prevention measures to avoid as much as possible contamination from environment and materials are essentials for successful results. The use of cleanroom is a solution for the maintenance of low levels of environmental

* Corresponding author.

E-mail address: garea@unican.es (A. Garea).

Nomenclature

A	solvent permeability coefficient in the SD model (m/s bar)
A'	solvent permeability coefficient in the SDI model (kg/m ² s bar)
C_F	solute feed concentration (mol/m ³)
C_P	solute permeate concentration (mol/m ³)
C_R	solute reject concentration (mol/m ³)
$(C_S)_{ln}$	logarithmic average solute concentration across the membrane (mol/m ³)
J_S	flux of the solute due to the gradient of chemical potential (mol/m ² s)
J_V	permeate volume flux (m/s)
J_W	flux of the solvent due to the gradient of chemical potential (m/s)
K_1	membrane transport coefficient in SD model (m/s)
K_2	membrane transport coefficient in SDI model (kg/m ² s)
K_3	coupling coefficient due to the membrane imperfections (kg/m ² s bar)
K_A	dissociation constant (mol/l)
L_P	hydraulic permeability coefficient (m/s bar)
N_S	total solute flux (kg/m ² s)
N_W	total solvent flux (kg/m ² s)
p_h	local hydraulic permeability in the membrane (m ² /s bar)
P_M	local solute permeability (m/s)
R	rejection coefficient
R	gas constant (bar m ³ /K mol)
T	temperature (K)
x_F	hydrogen peroxide feed concentration (mol/l)
x_P	hydrogen peroxide permeate concentration (mol/l)
X_P	solute mass fraction on the permeate
X_S	solute mass fraction on the upstream side of the membrane
X_W	solvent mass fraction on the upstream side of the membrane

Greek symbols

β	= $J_V(1-\sigma)/P_M$, Spiegler–Kedem parameter
ΔP	pressure difference across the membrane (bar)
Δx	total membrane thickness (m)
$\Delta \Pi$	osmotic pressure difference across the membrane (bar)
ΔC_s	difference between the concentration of solute on either side of the membrane (mol/m ³)
ν	stoichiometric coefficient
σ	reflection coefficient
ω	coefficient of solute permeability (mol/m ² s bar)
ω'	modified coefficient of solute permeability (m/s)

pollutants. On the other hand, selection of adequate equipment materials is crucial in order to minimize contamination and risk of accidents [5].

The employment of distillation for purifying hydrogen peroxide is oriented to organic pollutant diminution in greater extension than to inorganic impurities [6–8]. Requirements for the least strict electronic grades can be satisfied if metal concentrations in the feed solution do not exceed the low ppm level. The requirement of inert columns made of fluorinated polymers (poor heat conductors) stresses the energy intensiveness of this technique.

Very different adsorbents have been tested with aqueous hydrogen peroxide solutions: stannic oxide [9], α -zirconium phosphate

Table 1

Concentration and impurity limits for electronic grade hydrogen peroxide according to SEMI standards.

Grade	[H ₂ O ₂]	[Most exigent anion]	[Most exigent cation]
1	30–32%	<2 ppm	<10 ppb
2	30–32%	<200 ppb	<5 ppb
3	30–32%	<200 ppb	<1 ppb
4	30–32%	<30 ppb	<100 ppt
5	30–32%	<30 ppb	<10 ppt
VLSI	30–32% or 34–36%	<500 ppb	<10 ppt

[10] and various non-ionic resins [11,12]. Both organic and inorganic pollutants can be removed from the chemical, but attained maximum efficiencies (below 80%) are not comparable with results reachable by ion exchange or membranes technologies (above 99%). Exhausted adsorbents imply waste production, either directly when substituted with fresh adsorbent or indirectly when regenerated. Besides, in the latter case, toxic and hazardous chemicals could be needed as regenerants.

Ion exchange is the most mentioned ultrapurification technology, covering a wide range of conditions [13–18]. Multiple-pass processes are common when strictest electronic grades are desired. Special caution should be recommended when ion exchange resins contacts with hydrogen peroxide solutions, since hydroxyl groups as functional moieties in anionic resins or cationic resins highly charged with transition metallic ions can catalyze violently hydrogen peroxide decomposition. Again, regeneration of exhausted resins implies waste streams and employment of hazardous chemicals (strong acids and bases).

Membrane technologies appear as adequate options for ultrapurifying aqueous hydrogen peroxide. Reverse osmosis is expected to be the most appropriate membrane technique for elimination of metallic traces and other impurities [19–22] and ultrafiltration has also reported its potentiality when employed jointly with chelating chemicals [23]. These chelating agents sequester metallic ions from feed solution and keep these pollutants away from permeate, since non-permeant chelators must be chosen. Polyamides, polypiperazine amides, polyacronitriles, polysulphones and fluoropolymers are recommended materials for the membranes, although all examples illustrating patents resort to polyamide membranes.

Among all the ultrapurification alternatives, reverse osmosis emerges as the most desirable technology according to environmentally friendly criteria. Auxiliary chemicals are not needed and virtual zero waste generation is achieved (only damaged membranes become residue when replaced after lifetime), since the retentate stream can be recirculated or commercialized as non-electronic grade for other industrial uses. In addition, a great percentage of the energy supplied for increasing the pressure of the feed stream can be recovered from the retentate by different systems [24].

Taking into account the lack of published papers concerning to the fundamentals of membrane technologies applied to the ultrapurification of aqueous hydrogen peroxide, the present work is focused on this objective with the study of reverse osmosis to the further purification of industrial grade hydrogen peroxide solutions in order to achieve electronic specifications. The ionic metal impurities rejections and permeate flux were evaluated, paying special attention to the assessment of the permeation parameters of the membranes.

2. Experimental

2.1. Chemicals

Interox ST-35 hydrogen peroxide H₂O₂ was kindly supplied by Solvay Química Torrelavega as raw material for the

Table 2

Main characteristics of the flat-sheet membranes from the supplier.

Designation	Manufacturer	Material	Permeate flow (m ³ /m ² day)	Rejection (%)
AD	GE Osmonics	Polyamide	0.61	99.5
CE	GE Osmonics	Cellulose acetate	0.96	97
BE	Woongjin Chemical	Polyamide	1.12	99.5
CRM	Woongjin Chemical	Polyamide	0.92	99.5
SW30HR	Filmtec	Polyamide	0.66	99.7
UTC 80 B	Toray	Polyamide	0.57	99.75

ultrapurification process. It is an aqueous 35% (w/w) hydrogen peroxide solution without any type of stabilizers. Preliminary membrane characterization was performed with ultrapure and doped water. Ultrapure water (18.2 MΩ cm resistivity) was obtained by a Milli-Q Element (Millipore). Doped water was prepared by adding both sodium chloride NaCl (PA-ACS-ISO from Panreac) as sodium source and aluminium chloride anhydrous AlCl₃ (98% PS from Panreac) as aluminium source to ultrapure water in order to achieve metal concentrations similar to those in Interox ST-35 hydrogen peroxide. Na and Al were selected for doping the water because these components are the major impurities in Interox ST-35 technical grade hydrogen peroxide.

2.2. Installation and reverse osmosis membranes

A lab-scale cross-flow flat-sheet configuration test unit SEPA CF II from Osmonics was purchased for reverse osmosis experiments. The membrane cell can accommodate any 19 cm × 14 cm flat-sheet membranes, resulting 140 cm² of effective membrane area. Diverse commercially available polymeric flat sheet RO membranes from different manufacturers were preselected for this ultrapurification study. After revision of the patents which employ reverse osmosis [19–22], it was clear that polyamide was the preferred membrane material, so manufacturers were contacted for request of their most appropriate polyamide membrane for the present application. It was also suggested by a manufacturer to include a cellulose acetate membrane among the preselected ones because of its lower susceptibility to degradation by oxidizing agents such as chlorine, hydrogen peroxide or ozone. Information about the preselected membranes is summarized in Table 2.

The membrane cell was fed by a Hydra-Cell G-03 (Wanner Engineering) diaphragm pump equipped with digital variable frequency drive to adjust flowrate. Materials of all the components were chosen to maximize compatibility with concentrated hydrogen peroxide. HP PFA tubing was selected for all the installation except for the tube joining the pump and the cell (which worked under pressure), where a PTFE tube enhanced with braided stainless steel has been preferred; and the feed tank, which is made of polyethylene (PE). A simple scheme of the entire installation is showed in Fig. 1.

To minimize as possible the contamination by metals coming from the laboratory environment, the most critical components of the ultrapurification system were located under cleanroom condi-

tions. A Bio-48-M vertical laminar flow cabinet (Faster) guaranteed ISO Class 5 atmosphere.

2.3. Reverse osmosis experiments

Different tests were carried out with ultrapure and doped waters and aqueous hydrogen peroxide. The feed tank (220 l max. volume) was filled with 180 l of the corresponding fluid and a constant feed flow of 3.4 l/min was maintained (corresponding to a cross-flow velocity of 0.5 m/s in the membrane cell, value representative for cross-flow velocities in spiral-wound elements in full-scale RO plants [25]). The different applied pressures were adjusted by the high-pressure concentrate control valve supplied with the membrane cell. The experiments were performed at room temperature (temperature control was not needed as the temperature rise of the chemical in the feed tank during the operation time was negligible taking into account the large volume of this tank) and in total recycling mode; that is, with permeate and retentate streams being continuously recycled to the reservoir vessel, which assured constant characteristics in the feed stream during the whole experiment.

As a first step prior to the experiments, membranes were put in ultrapure water to soak at least 12 h before the start of the experiments. Then, each membrane is flushed with the feed liquid for 5 h at a feed pressure of 40 bar to ensure compaction of the membranes. In the experiments, the applied pressure in the system was varied between 10 and 40 bar. After 15 min of operation under each pressure, time enough for reaching steady state conditions, the permeate flux was measured and, for the cases of doped water and hydrogen peroxide, samples for determining metal concentrations were taken. Triplicate flux measures and samples were performed with 10 min intervals among them. All samples were analyzed by inductively coupled plasma mass spectrometry (ICP-MS) with an Agilent 7500ce ICP-MS system for the most exigent SEMI Grade defined metals. A special sample introduction system (ESI Upgrade Kit) made of PFA for resistance to hydrogen peroxide was necessary. Determination of hydrogen peroxide concentration was carried out also for triplicate following the procedure of the supplier [26].

3. Results and discussion

3.1. Characterization of technical grade hydrogen peroxide

The characterization of technical grade H₂O₂ 35% (w/w) by ICP-MS for the 21 metals required in SEMI C30 most exigent grade is showed in Table 3. It can be observed a broad range of concentrations of impurities, ranging from more than 20,000 ppb of Na to concentrations below 1 ppb [27].

The technical grade H₂O₂ exceeds the fixed limits of the less stringent electronic grade (Grade 1) for 3 metals: Na (1000 ppb), Al (1000 ppb) and Fe (100 ppb). When compared with a more demanding grade as Grade 3, the number of elements that fail the specifications (1 ppb for all the metals) increase to 13: B, Na, Mg, Al, K, Ca, Ti, Cr, Mn, Fe, Ni, Cu and Zn.

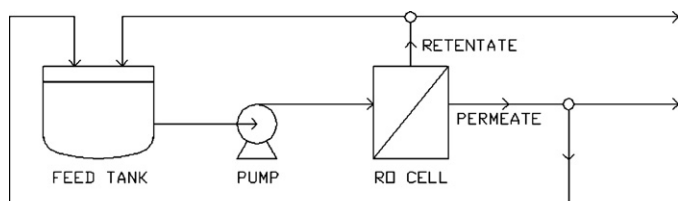


Fig. 1. General schematic of the experimental installation for ultrapurification by reverse osmosis.

Table 3Characterization of technical grade H₂O₂ by ICP-MS.

	Concentration (ppb)	Element		Concentration (ppb)	Element		Concentration (ppb)
Li	<1	Ti	72	Zn	13		
B	6	V	<1	As	<1		
Na	20895	Cr	48	Cd	<1		
Mg	17	Mn	3	Sn	<1		
Al	1067	Fe	161	Sb	<1		
K	36	Ni	24	Ba	<1		
Ca	89	Cu	2	Pb	<1		

3.2. Membranes performance with ultrapure and doped water

The preselected membranes were used in preliminary experiments with ultrapure and doped water in order to compare them and choose the most appropriate one for the ultrapurification process. Ultrapure water experiments were useful to establish the dependence of the permeate flux (J_v) on the applied pressure (ΔP). As it is showed in Fig. 2 the water fluxes increased with increasing pressures, obtaining a linear relationship with high correlation coefficients. The linear evolution of fluxes shows that Darcy's law is verified. The slope of this straight line is the solvent permeability L_p which is defined as J_v divided by ΔP [28].

Both membranes manufactured by Woongjin Chemical (BE and CRM) stood out from the rest when their permeate productions were compared. The other polyamide based membranes (UTC 80 B, AD and SW30HR) showed a very similar L_p value, but it was not comparable with that of the BE membrane, as it was more than double. The cellulose acetate membrane CE permeability was intermediate between Woongjin Chemical membranes and the rest of polyamide membranes.

When experiments with doped water (15,000 ppb of Na and 1,400 ppb of Al) were carried out, the same linear relationship was observed and slopes could be calculated. The values of solvent permeability obtained for ultrapure and doped water are quite similar for both matrixes as shown in Table 4 (this coincidence between both values was expected as osmotic pressure related to these low levels of solute concentrations can be considered negligible), where some information about the solvent permeability values reported in the literature for other flat-sheet reverse osmosis membranes is also included [29–32]. The experiments with doped water were also suitable for the determination of the efficiency of the preselected membranes for metal removal at low ppm concentrations. Their rejection coefficients (R) were defined by the equation:

$$R = \frac{C_F - C_P}{C_F} \quad (1)$$

where C_F and C_P represent the metal concentrations measured in the feed and permeate streams, respectively. These coefficients for

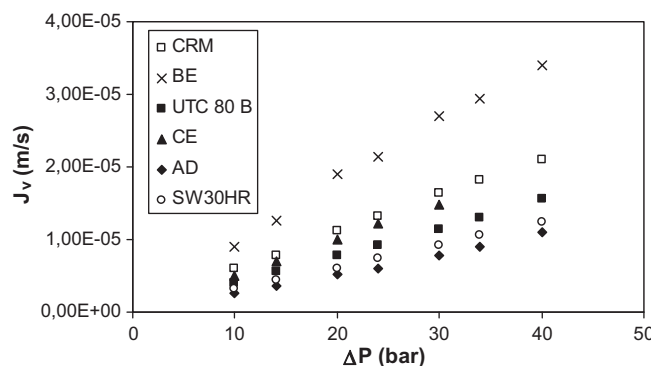


Fig. 2. Determination of the solvent permeability of the membranes for ultrapure water.

Table 4

Mean membrane solvent permeability values from ultrapure and doped water experiments and comparison with literature References.

Membrane	Solvent permeability, L_p (m/s bar)
AD	$2.86 \pm 0.31 \times 10^{-7}$
SW30HR	$3.11 \pm 0.01 \times 10^{-7}$
UTC 80 B	$3.83 \pm 0.06 \times 10^{-7}$
CE	$5.04 \pm 0.06 \times 10^{-7}$
CRM	$5.64 \pm 0.34 \times 10^{-7}$
BE	$8.29 \pm 0.71 \times 10^{-7}$
Other referenced membranes	
UTC 80 AB [29]	2.33×10^{-7}
UTC 80 AB [30]	2.62×10^{-7}
LFC1 [31]	8.20×10^{-7}
TFC-HR [32]	9.72×10^{-7}

Na and Al were determined in the doped water experiments performed with the membranes and the results obtained are plot in Fig. 3.

BE membrane reached the greatest values of rejection coefficients: 0.992 and 0.999 for sodium and aluminium respectively. CRM membrane performance was very close to BE (0.990 and 0.998). As occurred with permeabilities, Woongjin Chemical membranes obtained rejection coefficients were higher than those of the other three polyamide membranes. These three membranes showed again a very similar behaviour except for the UTC 80 B lower values for aluminium. CE was the least effective membrane for sodium removal but exceeded UTC 80 B for aluminium.

As a conclusion of the preliminary experiments carried out with ultrapure and doped with sodium and aluminium water, BE was considered as the most promising membrane for hydrogen peroxide ultrapurification, as showed the highest values for both solvent permeability and rejection coefficients [33].

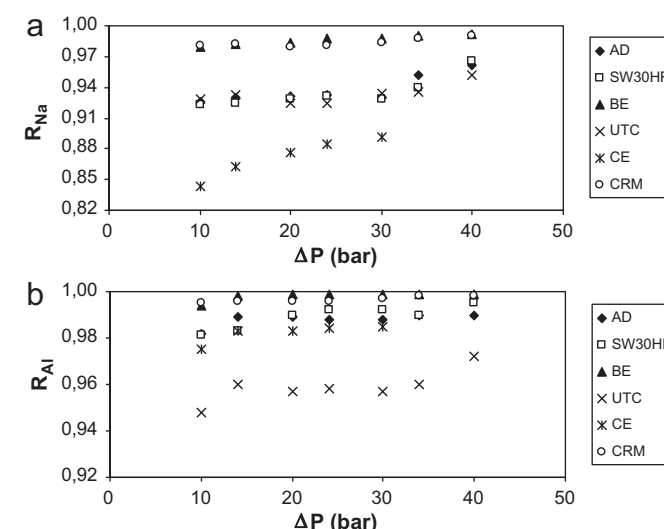


Fig. 3. Influence of the operating pressure on sodium (a) and aluminium (b) rejection coefficients for doped ultrapure water.

3.3. Ultrapurification of commercial grade hydrogen peroxide

3.3.1. Permeation of hydrogen peroxide

The ion exclusion model can be considered for a first approximation to assess the permeation of hydrogen peroxide through reverse osmosis membranes. This model has been applied for estimating permeation of weakly dissociated compounds in ultrapurification processes by membranes technology [34]. The following assumptions are made in its derivation:

- All ions are excluded by the membrane (double layer effect).
- All species in molecular form permeate the membrane completely.
- Perfect mixing conditions prevail on the retentate and permeate sides of the membrane.
- Concentration polarization is ignored.

The final equation for estimating the permeate concentration (x_p) from the feed concentration (x_F) is:

$$x_p = x_F - \sqrt{K_A \cdot x_F} - \sqrt{K_A(x_F - \sqrt{K_A \cdot x_F})} \quad (2)$$

where K_A is the dissociation constant ($K_A = 1.78 \times 10^{-12}$ M for the particular case of hydrogen peroxide). When the feed concentration is 35% (w/w) (corresponding to $x_F = 10.3$ M), the rejection coefficient became negligible ($R < 10^{-6}$). This means no theoretical dilution of aqueous hydrogen peroxide solutions when forced to permeate through reverse osmosis membranes. Experimental determination of hydrogen peroxide concentration in both feed and permeate streams confirmed the hypothesis as showed in Fig. 4, so the validity of reverse osmosis for aqueous hydrogen peroxide solutions without dilution or concentration effects was asserted.

The variation of the experimental permeate flux, J_v , with the increase in the applied pressure for both ultrapure water and 35% hydrogen peroxide is shown in Fig. 5. The linear relationship with high correlation coefficient was also observed for the hydrogen peroxide case and a L_p value of 4.92×10^{-7} was calculated from the slope, which entailed a decrease of 44% in comparison with ultrapure water. The L_p parameter can be interpreted based on the Hagen–Poiseuille flow and an inversely proportional relationship between L_p and the viscosity of the solution is obtained [35]. The values of viscosity of ultrapure water and 35% hydrogen peroxide at 20 °C are 1.00 and 1.11 mPa s respectively [4], so a decrease of only about 10% can be explained in terms of viscosity variation of the liquid phase. Complex chemical interactions deserving of further investigation between 35% hydrogen peroxide and the membrane could explain the drop of permeate production.

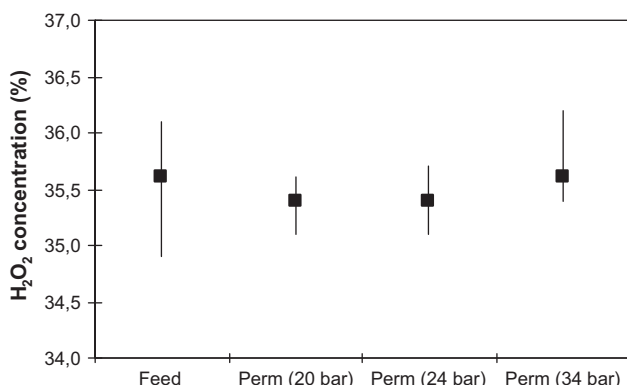


Fig. 4. Hydrogen peroxide concentration on feed and BE membrane permeate streams (maximum, medium and minimum values are plotted)

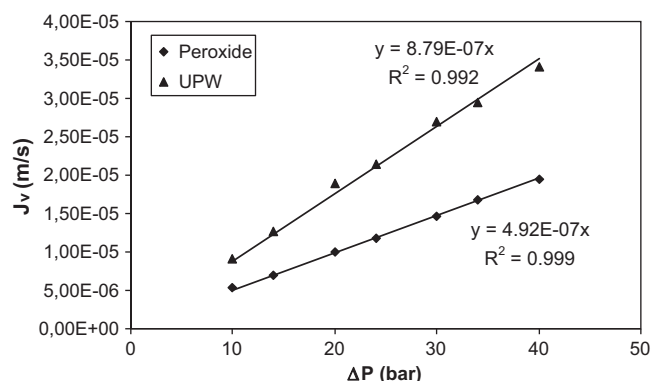


Fig. 5. Comparison of BE membrane solvent permeability for ultrapure water (UPW) and 35% H_2O_2 (Peroxide).

Experimental tests were designed to investigate the ability of the selected membrane to withstand the highly oxidative environment of H_2O_2 . Fresh samples of the BE membrane (without previous exposition to H_2O_2 and designed as Membrane2 and Membrane3) were subjected to 8-hours lasting experiments during several consecutive days until total operation times of at least 64 hours were completed. The applied pressure was maintained at 40 bar except for the characterization intervals when the influence of this operation variable upon permeate flux and metal rejections was studied (8 regularly spaced over time characterization intervals of 2 hours each were fixed).

The evolution of the Membrane2 permeate production through the test when operating at 40 bar is shown in Fig. 6 and a very stable behaviour can be observed. The influence of applied pressure upon permeate flux of the different membrane samples is depicted in Fig. 7: the results of 3 characterization intervals for Membrane2 and a single result for Membrane3 were chosen for representing the performance during the experiment. The permeate flux maintained again a constant performance, as proved by the superposition of the data from different intervals. An assessed standard deviation of 3.17% for the Membrane2 permeability coefficient L_p confirmed the flux stability.

When compared with the sample used during the preliminary experiments (designed as Membrane1 in Fig. 7), the Membranes 2 and 3 were noted for its slightly lower permeate flux. In terms of L_p values, this difference is below 5% in the case of Membrane3 ($L_p = 4.68 \times 10^{-7}$ m/s bar) and is lesser than 22% for Membrane2 ($L_p = 3.86 \times 10^{-7}$ m/s bar) and the discrepancy can be explained by the intrinsic variability among samples of the reverse osmosis membranes. Woongjin Chemical, the manufacturer of BE membrane, informs about this small uncertainty as permeate flow rate

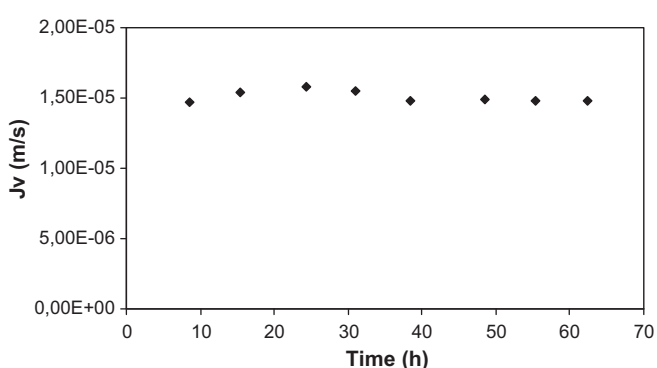


Fig. 6. Measured permeate fluxes through the hydrogen peroxide ultrapurification process by Membrane2 sample at 40 bar.

Table 5

Metal concentrations on BE membrane permeate and corresponding rejection coefficients operating at 40 bar.

	Concentration (ppb)									
	B	Na	Al	Ti	Cr	Mn	Fe	Ni	Cu	Zn
Feed	6	>20000	>1000	72	48	3	161	24	2	13
Permeate (at 40 bar)	1.0	1565	87	6.7	4.6	0.3	19	2.2	0.1	1.0
Rejection coefficients (<i>R</i>)	0.825	0.925	0.919	0.906	0.903	0.912	0.883	0.909	0.961	0.920

for each element may vary but will be no more than 10% below the specified value [36], but there is no notice about the percentage that can typically exceeds the specification. On the other hand, another membrane manufacturer such as Filmtec accepts 15% of uncertainty over the permeate flux both by excess or defect [37]. These margins can accommodate relative differences greater than 25% between the maximum and minimum values of the range, so the variability found in this experimental case lies within the expected interval.

3.3.2. Rejection of metallic components

The concentrations of metals in the permeated hydrogen peroxide stream obtained with the maximum tested applied pressure (40 bar) are shown in Table 5, also including the metal rejection coefficients. High rejections were found for all the studied elements, with values around 0.9 except for the case of boron, which reached a value of 0.825. As occurred with ultrapure water, better rejections were obtained at higher applied pressures and quite similar performance could be observed for whichever chosen metal but boron, with no discrimination because of atomic mass, ionic charge or feed concentration. The rejection coefficients corresponding to the characterizations for Membrane2 during the 64 hours lasted experiment are tabulated (Table 6). Highly stable values were obtained for all the metals through the tested time. Further investigation is planned in order to study the membrane behaviour for longer time periods (more than 64 hours) in both permeate production and rejection terms.

The permeated hydrogen peroxide solution comply with SEMI Grade 1 requirements for all the metals but sodium (1565 ppm is above the 1000 ppm fixed limit). Based on a value of rejection coefficient of 0.9 as representative of the metal rejections, and taking into account the requirements of metal traces in electronic grades of hydrogen peroxide (SEMI C30, Table 1), an estimation of the multistage membrane process was calculated based on the reverse osmosis results: 2 stages required for Grade 1 quality, 4 stages for Grade 2, and 5 stages for Grade 3, which is the aim of further experimental work in the H₂O₂ ultrapurification: multistage operation for flat membranes and spiral-wound configuration in module for

intensification [38] and integrated reverse osmosis membrane cascades [39].

3.4. Transport equations

Four frequent reverse osmosis models [40] that relate permeate fluxes and rejection coefficients with applied pressure were chosen as approximations to represent the behaviour of the hydrogen peroxide ultrapurification process:

Solution-Diffusion (SD) model, two parameters (*A*, *K*₁)

$$J_W = A(\Delta P - \Delta \Pi) \quad (3)$$

$$J_S = K_1(C_R - C_P) \quad (4)$$

$$\frac{1}{R} = 1 + \frac{K_1}{J_W} \quad (5)$$

Solution-Diffusion-Imperfections (SDI) model, three parameters (*A'*, *K*₂, *K*₃)

$$N_W = A'(\Delta P - \Delta \Pi) + K_3 \Delta P X_W \quad (6)$$

$$N_S = K_2(X_R - X_P) + K_3 \Delta P X_R \quad (7)$$

Spiegler-Kedem (SK) model, three parameters (*p*_h/*Δx*, *σ*, *P*_M)

$$J_V = \frac{p_h}{\Delta x} (\Delta P - \sigma \Delta \Pi) \quad (8)$$

$$R = \frac{\sigma(e^\beta - 1)}{e^\beta - \sigma} \quad (9)$$

$$\beta = J_V \frac{1 - \sigma}{P_M} \quad (10)$$

Kedem-Katchalsky (KK) model, three parameters (*L*_P, *ω'*, *σ*)

$$J_V = L_P (\Delta P - \sigma \Delta \Pi) \quad (11)$$

$$J_S = \omega \Delta \Pi + (1 - \sigma) J_V (C_S)_{ln} \quad (12)$$

$$\frac{1}{R} = \frac{1}{\sigma} + \frac{\omega'}{\sigma} \frac{1}{J_V} \quad (13)$$

$$\omega' = \omega v R T \quad (14)$$

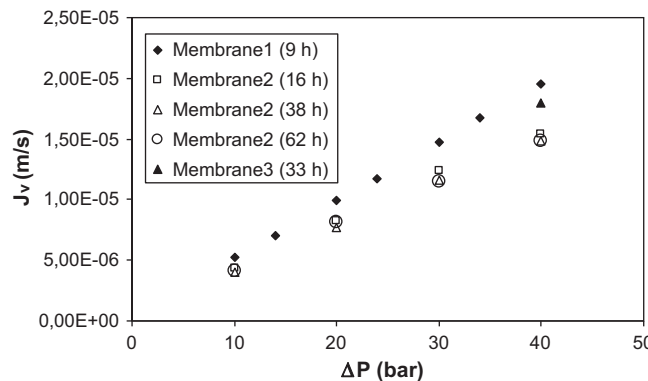


Fig. 7. Evolution of permeated hydrogen peroxide flux at different times for the different BE membrane samples.

Table 6

Calculated rejection coefficients for Membrane2 (mean values ± experimental standard deviation calculated from samples taken during operation up to 64 h).

Element	Rejections coefficients (<i>R</i>)			
	ΔP (bar)	10	20	30
B	0.504 ± 0.010	0.663 ± 0.024	0.725 ± 0.024	0.769 ± 0.008
Na	0.930 ± 0.024	0.954 ± 0.012	0.960 ± 0.007	0.966 ± 0.005
Al	0.973 ± 0.004	0.979 ± 0.002	0.979 ± 0.003	0.981 ± 0.004
Ti	0.968 ± 0.005	0.977 ± 0.003	0.978 ± 0.005	0.980 ± 0.006
Cr	0.942 ± 0.013	0.962 ± 0.005	0.967 ± 0.006	0.971 ± 0.007
Mn	0.899 ± 0.015	0.939 ± 0.008	0.948 ± 0.006	0.955 ± 0.009
Fe	0.906 ± 0.023	0.936 ± 0.016	0.940 ± 0.025	0.952 ± 0.021
Ni	0.926 ± 0.007	0.949 ± 0.007	0.951 ± 0.005	0.955 ± 0.005
Cu	0.900 ± 0.057	0.951 ± 0.012	0.961 ± 0.013	0.972 ± 0.010
Zn	0.852 ± 0.059	0.912 ± 0.045	0.928 ± 0.020	0.954 ± 0.017

Table 7

Evaluation of the fitting of the experimental data by the proposed osmosis reverse models.

Model	SD	SDI	KK	SK
Percentage of overall variation explained (%)	79.0	88.8	94.4	94.1

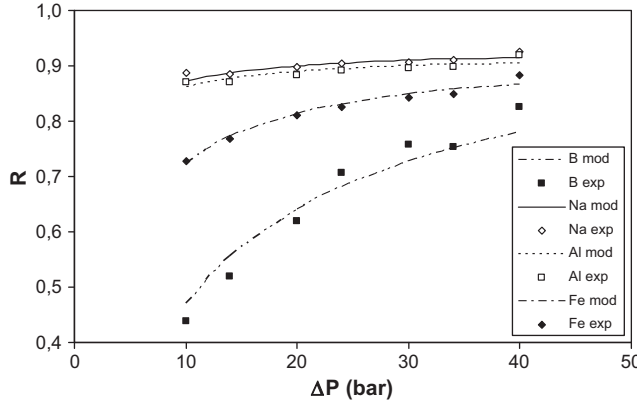


Fig. 8. Kedem–Katchalsky model applied to the experimental rejection coefficients of the main metallic impurities.

With the experimentally obtained values for permeate flux (J_V) and metal rejections (R) as functions of the applied pressure, the estimation of the parameters in these models was performed by a software tool (Aspen Custom Modeler). The osmotic pressure related term in the equations describing the solvent flux was considered as negligible (as suggested by the agreement between the values of solvent permeability for ultrapure and doped water) for all the models. The agreement of the models to the experimental data was quantified as the percentage of variation explained for the overall system. As reported in [Table 7](#), best results were obtained with the Kedem–Katchalsky model, which obtained parameters are summarized in [Table 8](#). In the pressure operation range, the model adequately describes the experimental data permeate flux and metal rejections (see [Fig. 8](#)).

Related to the transport parameters in the Kedem–Katchalsky model, Eqs. (11)–(14), three practical parameters are required to characterize each membrane + solution system: L_p , is the hydraulic permeability of the membrane; ω , is called the solute mobility (or solute permeability); and σ , the reflection coefficient. The parameters L_p and ω depend strongly on the thickness of the selective membrane and correlations between the practical parameters in order to compare different membranes are valid only when the results are normalized to layers of the same thickness. Moreover, σ and ω depend strongly on the nature of each solute and they may be used to relate the ability of the separation respect to the solute or solutes (also expressed in the values of rejection coefficients, R).

Table 8
Assessm

Assessment of the Kedem-Katchalsky model parameters: transports coefficients ω , σ and L_p for both hydrogen peroxide solution and doped ultrapure water.

Table 9

Percentage contribution of the diffusive term to the total solute fluxes.

ΔP	Diffusive contribution to total solute flux (%)									
	Element									
	B	Na	Al	Ti	Cr	Mn	Fe	Ni	Cu	Zn
10	100	59	62	68	75	100	83	65	100	92
14	100	52	55	62	71	100	80	59	100	90
20	100	45	48	55	66	100	76	52	100	89
24	100	41	44	52	63	100	74	49	100	88
30	100	36	39	47	58	100	71	43	100	85
34	100	34	37	45	55	100	69	40	100	84
40	100	32	35	43	53	100	68	38	100	85

The physical meaning of ω can be clearly seen by applying Eq. (12) to a situation in which J_V is zero or no net volume flux. Keeping in mind the van't Hoff equation for the osmotic pressure of an ideal solution ($\pi = vRTC_S$) and setting J_V equal to zero in Eq. (12) gives

$$(J_s)_{v=0} = v \omega R T \Delta C_S \quad (15)$$

where ΔC_S is the difference between the concentration of solute on either side of the membrane.

Comparing Eq. (15) with Fick's law of diffusion, it is seen that ω gives a measure of the diffusion mobility of each solute across the membrane.

Eq. (13), which relates the rejection coefficient of each solute, R , to the transport parameters can be rearranged as

$$R = \frac{\sigma J_v}{J_v + \omega'} \quad (16)$$

showing that the rejection increases with increasing solution flux and reaches a limiting value σ at infinitely high J_v . As the diffusive flux of the solutes can be neglected in the range of high J_v (operation at high pressures), the reflection coefficient σ is a characteristic of the convective transport of each solute; a value of 1 means that no transport by convection takes place at all. This may be the case for ideal RO membranes where the membranes have dense structure and no pores are available for convective transport.

As can be seen in Eq. (12), also expressed as follows

$$J_S = \omega' \Delta C_S + (1 - \sigma) J_V(C_S)_{\ln} \quad (17)$$

the flux of each solute across the membrane is the sum of diffusive and convective terms: a concentration difference on both sides of the membrane causes diffusive transport, and solute transport by convection takes place because of an applied pressure gradient across the membrane.

In order to quantify these convective and diffusive terms [41] for the case of the metal components present in the hydrogen peroxide RO system under study, the contribution of both terms has been calculated from the experimental data and the transport parameters; and it is shown in Table 9 as the percentage of solute flux due to diffusion for each metal and pressure related to the total solute flux J_s . At low pressures, when J_v is low, the first term of the solute flux

(diffusive term) is dominant, while at high pressures the second term (convective) increases to be dominant.

The obtained results of the contribution of the diffusive term to each total solute flux (Table 9), show that the elements B, Mn and Cu are controlled totally by diffusive transport (in concordance with the value of the parameter $\sigma = 1$ obtained for these components). Components as Zn, Fe, and Cr show diffusional contributions higher than 50% to their total flux in the range of pressure operation, while for the rest of the components: Na, Al, Ti and Ni, the convective transport contributes significantly (values of diffusive term lower than 50%) when the system operates at pressures higher than 20 bar.

Related to the application of the selected transport model through the membrane lifetime, satisfactory results were obtained in terms of percentage of overall variation explained by the Kedem–Katchalsky model as a mean value of 93.4% was obtained for the different characterization intervals of the experiment.

4. Conclusions

Commercially available RO polyamide membrane BE (manufactured by Woongjin Chemical) has been successfully applied to the diminution of metallic contents of 35% Technical Grade hydrogen peroxide in the pressure range between 10 and 40 bar for exposition time up to 64 h. Rejection coefficients above 0.9 were obtained for most metals.

The Kedem–Katchalsky model can be considered suitable for representing the performance of the reverse osmosis process when employed in the ultrapurification of aqueous hydrogen peroxide solutions from technical to electronic grade, as 94.4% of the overall variation of the system was explained by the proposed model.

Acknowledgements

This research has been financially supported by the Ministry of Science and Innovation of Spain (MICINN) through CTM2006-00317 Project. R. Abejón acknowledges also the assistance of MICINN for the award of a FPI grant (BES-2008-003622). We gratefully thank Dow Filmtec and Woongjin Chemicals for the supplied membranes and Solvay Torrelavega for the industrial grade hydrogen peroxide.

References

- [1] E.D. Olson, C.A. Reaux, W.C. Ma, J.W. Butterbaugh, Alternatives to standard wet cleans, *Semicond. Int.* 23 (2000) 70–75.
- [2] J. Atsumi, S. Ohtsuka, S. Munehira, K. Kajiyama, Metallic contamination on Si wafers from cleaning solutions, *Proc. Electrochem. Soc.* 90 (1990) 59–66.
- [3] Semiconductor Equipment and Material International Association (SEMI®), Specifications and Guidelines for Hydrogen Peroxide, SEMI Document C30-1101, 2001.
- [4] G. Goor, J. Glenneberg, S. Jacobi, Hydrogen peroxide, in: Ullmann's Encyclopedia of Industrial Chemistry, Electronic Release, Wiley-VCH, Weinheim, 2007.
- [5] J. Mackenzie, Hydrogen peroxide without accidents, *Chem. Eng.* 97 (1990) 84–90.
- [6] L. Signori, K. Glinos, Process for obtaining purified aqueous hydrogen peroxide solutions, US Patent 5296104 (1994).
- [7] Y. Inaba, Y. Ueno, M. Watanabe, Y. Nishida, Process for preparing high purity hydrogen peroxide aqueous solution, US Patent 5670028 (1997).
- [8] P. Johnsson, T. Mattila, K. Saari, Process for preparing a substantially pure aqueous solution of hydrogen peroxide, US Patent 5705040 (1998).
- [9] G.W. Morris, N.D. Feasey, Purification of hydrogen peroxide, US Patent 5262058 (1993).
- [10] J.L. Manganaro, D. Gibilisco, J.R. Reed, T. Frianeza-Kullberg, Process for removing iron from hydrogen peroxide, US Patent 5266298 (1993).
- [11] H. Honig, S. Geigel, Method for purifying hydrogen peroxide for microelectronics uses, US Patent 5232680 (1993).
- [12] Y. Nishide, Y. Minamikawa, J. Kokubu, Method of producing purified aqueous solution of hydrogen peroxide, US Patent 5851505 (1998).
- [13] Y. Minamikawa, S. Murakami, M. Hattori, Process for producing a purified aqueous hydrogen peroxide solution, US Patent 5733521 (1998).
- [14] H. Ledon, M. Carre, D. Demay, C. Devos, S. Jeanin, Process for the preparation of an ultra pure hydrogen peroxide solution by the ion exchange by sequence: anionic-cationic-anionic-cationic, US Patent 5961947 (1999).
- [15] N. Saito, M. Izumi, Method of purifying aqueous solution of hydrogen peroxide, US Patent 6054109 (2000).
- [16] M.D. Havlicek, J.G. Hoffman, W. Yuan, Integrated method of preconditioning a resin for hydrogen peroxide purification and purifying hydrogen peroxide, US Patent 6537516 B2 (2003).
- [17] F. Tanaka, S. Sugawara, T. Adachi, K. Mine, Process for producing a purified aqueous hydrogen peroxide solution, US Patent 6896867 (2005).
- [18] D. Oeter, C. Dusemund, E. Neumann, K. Freissler, M. Hostalek, Method for the purification of hydrogen peroxide solutions, US Patent 6939527 B2 (2005).
- [19] J.H. Boughton, R.A. Butz, H.C.T. Cheng, J.R. Dennis, B.T. Hannon, J.H. Weigel, Manufacture of high purity hydrogen peroxide by using reverse osmosis, US Patent 4879043 (1989).
- [20] A. Morisaki, Y. Sawaguri, Y. Matsuda, Apparatus and method for removing impurities from aqueous hydrogen peroxide, US Patent 5906738 (1999).
- [21] U.P. Bianchi, U. Leone, M. Lucci, Process for the industrial production of high purity hydrogen peroxide, US Patent 6333018 B2 (2001).
- [22] R. Owen, J. Bosse, M. Sell, Process for the purification of aqueous peroxygen solutions, solutions obtainable thereby and their use, WO Patent 2005/033005 A1 (2005).
- [23] J.M. Dhalluin, J.J. Wawrzyniak, H. Ledon, Process for the purification of hydrogen peroxide, US Patent 6113798 A (2000).
- [24] M. Fariñas, Osmosis inversa: fundamentos, tecnología y aplicaciones, McGraw-Hill, Madrid, 1999.
- [25] GE Water & Process Technologies, SEPA CF II Membrane Element Cell instruction manual, 2004.
- [26] Solvay Chemicals Incorporation, Determination of hydrogen peroxide concentration (20% to 70%). Technical Data Sheet, 2008.
- [27] R. Abejón, A. Garea, A. Irabien, Use of reverse osmosis for ultrapurification of hydrogen peroxide to semiconductor grade, in: II International Green Process Engineering Congress and European Process Intensification Conference (GPE-EPIC 2009), 2009.
- [28] F.J. Benítez, J.L. Aceró, A.I. Leal, Application of microfiltration and ultrafiltration processes to cork processing wastewaters and assessment of the membrane fouling, *Sep. Purif. Technol.* 50 (2006) 354–364.
- [29] H. Koseoglu, M. Kitis, The recovery of silver from mining wastewaters using hybrid cyanidation and high-pressure membrane process, *Miner. Eng.* 22 (2009) 440–444.
- [30] H. Koseoglu, N. Kabay, M. Yüksel, S. Sarp, Ö. Arar, M. Kitis, Boron removal from seawater using high rejection SWRO membranes – impact of pH, feed concentration, pressure and cross-flow velocity, *Desalination* 227 (2008) 253–263.
- [31] Y.N. Kwon, J.O. Leckie, Hypochlorite degradation of crosslinked polyamide membranes II. Changes in hydrogen bonding behavior and performance, *J. Membr. Sci.* 282 (2006) 456–464.
- [32] P. Xu, J.E. Drewes, Viability of nanofiltration and ultra-low pressure reverse osmosis membranes for multi-beneficial use of methane produced water, *Sep. Purif. Technol.* 52 (2006) 67–76.
- [33] R. Abejón, A. Garea, A. Irabien, Reverse osmosis for the ultrapurification of aqueous hydrogen peroxide to electronic grade, EUROMEMBRANE 2009.
- [34] A. Kulkarni, D. Mukherjee, D. Mukherjee, W.N. Gill, Reprocessing hydrofluoric acid etching solutions by reverse osmosis, *Chem. Eng. Commun.* 129 (1994) 53–68.
- [35] T. Tsuru, M. Miyawaki, T. Yoshioka, M. Asaeda, Reverse osmosis of nonaqueous solutions through porous silica-zirconia membranes, *AIChE J.* 52 (2006) 522–531.
- [36] Woongjin Chemical Company, Model RE 4040-BE Product Specification Sheet, Specification Sheet Rev. 2411112 04/15/07 (2007).
- [37] Filmtec, FILMTEC SW30HR-380 High Rejection Seawater RO Element, Form N° 609-00390-1008.
- [38] E. Bringas, M.F. San Román, J.A. Irabien, I. Ortiz, An overview of the mathematical modelling of liquid membrane separation processes in hollow fibre contactors, *J. Chem. Technol. Biotechnol.* 84 (2009) 1583–1614.
- [39] A. Caus, L. Braeken, K. Boussu, B. Van der Bruggen, The use of integrated countercurrent nanofiltration cascades for advanced separations, *J. Chem. Technol. Biotechnol.* 84 (2009) 391–398.
- [40] M. Soltanieh, W.N. Gill, Review of reverse osmosis membranes and transport models, *Chem. Eng. Commun.* 12 (1981) 279–363.
- [41] M. Pontié, H. Dach, J. Leparc, M. Hafsi, A. Lhassan, Novel approach combining physico-chemical characterizations and mass transfer modelling of nanofiltration and low pressure reverse osmosis membranes for brackish water desalination intensification, *Desalination* 221 (2008) 174–191.

4.2. Abejón, R.; Garea, A.; Irabien, A. *Analysis, modelling and simulation of hydrogen peroxide ultrapurification by multistage reverse osmosis*. Chemical Engineering Research and Design, 90:442-452 (2012).

Resumen

La preparación de los materiales semiconductores y la producción de circuitos impresos requiere de reactivos de elevada pureza porque se necesita un contenido muy bajo en impurezas metálicas para evitar defectos en la superficie del silicio. El peróxido de hidrógeno es uno de los reactivos con mayor demanda por parte de la industria semiconductora y debe ser sometido a procesos de ultrapurificación para alcanzar los exigentes requisitos necesarios para ser aceptado en el sector de los semiconductores. En este documento, se investiga el potencial de los procesos multietapa de ósmosis inversa para reducir el contenido metálico del peróxido de hidrógeno de grado técnico por debajo de los límites fijados por la industria de los semiconductores. Se obtuvo peróxido de hidrógeno de Grado SEMI 1 a escala de laboratorio mediante un proceso en dos pasos de ósmosis inversa. Un modelo basado en las ecuaciones de transporte de Kedem-Katchalsky junto con los balances de materia del sistema ha sido propuesto para describir el comportamiento de la instalación. Se llevó a cabo un completo análisis de la influencia de las variables de diseño (tasas de recuperación) y operación (presiones aplicadas) sobre el comportamiento de una planta de escala industrial simulada. La viabilidad económica de la planta simulada ha quedado demostrada.

Original abstract

Very high purity chemicals are required for preparation of semiconductor materials and manufacture of printed circuit boards because low presence of metallic impurities is needed to avoid defects on silicon surface. Hydrogen peroxide is one of the most demanded chemical by the semiconductor industry and it must be submitted to ultrapurification processes to achieve the exigent requirements the chemical must fulfill to be accepted for semiconductor uses. In this paper, the potential of multistage reverse osmosis processes to reduce the metallic content of technical grade hydrogen peroxide below the limits fixed by the semiconductor industry is investigated. SEMI Grade 1 quality hydrogen peroxide was obtained by a two-pass reverse osmosis process in an experimental lab scale. A model based on Kedem-Katchalsky transport equations together with system material balances was proposed to describe the behavior of the installation. A full analysis of the influence of the design (recovery rates) and operation (applied pressures) variables over the performance of a simulated industrial scale plant was carried out. The economic viability of the simulated plant was demonstrated.



Analysis, modelling and simulation of hydrogen peroxide ultrapurification by multistage reverse osmosis

R. Abejón, A. Garea*, A. Irabien

Departamento de Ingeniería Química y Química Inorgánica, Universidad de Cantabria, Avda. Los Castros s/n, 39005 Santander, Cantabria, Spain

ABSTRACT

Very high purity chemicals are required for preparation of semiconductor materials and manufacture of printed circuit boards because low presence of metallic impurities is needed to avoid defects on silicon surface. Hydrogen peroxide is one of the most demanded chemical by the semiconductor industry and it must be submitted to ultrapurification processes to achieve the exigent requirements the chemical must fulfill to be accepted for semiconductor uses. In this paper, the potential of multistage reverse osmosis processes to reduce the metallic content of technical grade hydrogen peroxide below the limits fixed by the semiconductor industry is investigated. SEMI Grade 1 quality hydrogen peroxide was obtained by a two-pass reverse osmosis process in an experimental lab scale. A model based on Kedem-Katchalsky transport equations together with system material balances was proposed to describe the behavior of the installation. A full analysis of the influence of the design (recovery rates) and operation (applied pressures) variables over the performance of a simulated industrial scale plant was carried out. The economic viability of the simulated plant was demonstrated.

© 2011 The Institution of Chemical Engineers. Published by Elsevier B.V. All rights reserved.

Keywords: Ultrapurification; Electronic grade chemicals; Hydrogen peroxide; Reverse osmosis

1. Introduction

There is probably no industry more concerned for and committed to contamination control than the semiconductor industry. The production of semiconductor devices requires very exigent demands for the environment and the equipment. All the critical manufacturing steps are performed under cleanroom conditions in order to minimize contamination in the working environment and semiconductor manufacturing equipment is made of non-contaminating materials. The chemicals and materials used to manufacture and package semiconductors and printed circuit boards are considered electronic chemicals (Daigle et al., 2007). The purity of these electronic chemicals is as important as the environment and the equipment. A typical silicon wafer might be treated with several different liquids (wet electronic chemicals) during the manufacturing process. Because the wet chemicals are in intimate contact with silicon surfaces, their particulate and ionic impurity levels are of great concern. Particles that adhere to the wafers can cause short circuits or open

circuits resulting in devices failure (Duffalo and Monkowski, 1984). Metallic ionic impurities also entail problems: certain metals and other ionic impurities are known to deposit on bare silicon or silicon dioxide. These trace impurities on the surfaces of silicon wafers adversely affect the electrical characteristics of silicon devices: they cause a loss of oxide integrity and act as minority carrier lifetime killers (Atsumi et al., 1990).

Hydrogen peroxide (H_2O_2) is one of the most employed wet electronic chemical (Sievert, 2001) because of its use for cleaning silicon wafer surfaces of foreign contaminants, removing photoresists or etching copper on printed circuit boards (Daigle et al., 2007). Most usual cleaning baths for silicon wafer surface cleaning (SC1, SC2 or SPM) include hydrogen peroxide in their formulations (Olson et al., 2000). Said baths remove particulate, organic and metallic pollutants from silicon surfaces. Semiconductor Equipment and Materials International (SEMI) is the global industry association serving the manufacturing supply chains for the micro-electronic, display and photovoltaic industries. This entity

* Corresponding author.

E-mail addresses: abejonr@unican.es (R. Abejón), gareaa@unican.es (A. Garea).

Received 23 March 2011; Received in revised form 28 June 2011; Accepted 27 July 2011
0263-8762/\$ – see front matter © 2011 The Institution of Chemical Engineers. Published by Elsevier B.V. All rights reserved.
doi:[10.1016/j.cherd.2011.07.025](https://doi.org/10.1016/j.cherd.2011.07.025)

Nomenclature

A	membrane area (m^2)
AFC	average filter coverage ratio
AN	capital costs attributable to analysis and quality control (\$/d)
CA	cleanroom area (m^2)
c_F	feed concentration (ppb)
c_{F0}	initial feed concentration (ppb)
c_P	permeate concentration (ppb)
c_R	recirculation concentration (ppb)
c_{VP}	permeate tank concentration (ppb)
CC	capital costs (\$/d)
CC _{clean}	capital costs attributable to cleanroom (\$/d)
CC _{inst}	capital costs attributable to installation (\$/d)
CC _{memb}	capital costs attributable to membranes (\$/d)
C_F	feed concentration in the industrial scale simulation (ppb)
C_{IN}	concentration of the stage inlet stream (ppb)
C_{P1}	first stage permeate concentration in the industrial scale simulation (ppb)
C_{P2}	second stage permeate concentration in the industrial scale simulation (ppb)
C_{R1}	first stage retentate concentration in the industrial scale simulation (ppb)
C_{R2}	second stage retentate concentration in the industrial scale simulation (ppb)
EAV	exhaust air volume (m^3/h)
F	feed flow (m^3/d)
J_P	permeate flux (m/s)
K _{memb}	ratio membrane capital costs to total capital costs
L_P	hydraulic permeability coefficient (m/s bar)
LT _{memb}	membrane lifetime (d)
LT _{inst}	installation lifetime (d)
MAPE	mean absolute percentage error (%)
MAV	make-up air volume (m^3/h)
n	number of experimental observations
OC	operation costs (\$/d)
OC _{en}	energy costs (\$/d)
OC _{lab}	labor costs (\$/d)
OC _m	maintenance costs (\$/d)
OC _{raw}	raw material costs (\$/d)
P1	permeate flow of the first stage (m^3/d)
P2	permeate flow of the second stage (m^3/d)
Q	cell feed flow (m^3/s)
Q_{IN}	flow of the stage inlet stream (m^3/s)
Q_P	permeate flow (m^3/s)
Q_R	recirculation flow (m^3/s)
R	rejection coefficient
R1	retentate flow of the first stage (m^3/d)
R2	retentate flow of the second stage (m^3/d)
Rec	recovery rate
Rev	revenues (\$/d)
RMSE	root mean square error
t	time (s)
TC	total costs (\$/d)
V_F	volume in the feed tank (m^3)
V_{F0}	initial volume in the feed tank (m^3)
V_P	volume in the permeate tank (m^3)
x_{exp}	experimentally observed value of a variable
x_{mod}	modeled value of a variable

Y_{by}	price of by-product hydrogen peroxide from first stage retentate (\$/ m^3)
Y_{EG}	price of SEMI 1 electronic grade hydrogen peroxide (\$/ m^3)
Y_{elec}	electricity price (\$/kWh)
Y_{lab}	salary (\$/h)
Y_{memb}	price of reverse osmosis membranes (\$/ m^2)
Y_{raw}	price of technical grade hydrogen peroxide (\$/ m^3)
Z	profit (\$/d)

Greek symbols

ΔP	pressure difference across the membrane
η	pump efficiency
σ	reflection coefficient
ω'	modified coefficient of solute permeability (m/s)

facilitates the worldwide development of the most respected technical standards in this manufacturing sector. Among all the topics regulated, some refer to wet chemicals and indicate the requirements to be fulfilled in order to be accepted as electronic chemicals. For the particular case of hydrogen peroxide, the SEMI C30 document is available (Semiconductor Equipment and Material International Association, 2010), where five different electronic grades are defined in function of the allowed maximum concentration of contaminant impurities.

The least strict electronic grade could be achieved by just expertly selecting from technical grade chemical produced by qualified manufacturers and little additional treatment (filtration). Nevertheless, when more stringent electronic grades are required, selection and filtration are not enough and further ultrapurification technology must be employed. Different ultrapurification techniques are reported in the literature to obtain high-purity hydrogen peroxide, including distillation, adsorption, ion exchange or membrane technologies (Abejón et al., 2010).

Besides the traditional application to desalination processes of seawater and brackish water, reverse osmosis technology has been successfully implemented for several other practical purposes: municipal wastewater treatment (García-Figueroel et al., 2009; Tam et al., 2007), concentration, dewatering and other functional separations in the food processing and nutraceutical industries (Cuellar et al., 2009; Gurak et al., 2010; Kawachale and Kumar, 2010; Pilipovik and Riverol, 2005), water and byproduct recovery in the pulp and paper sector (Pizzichini et al., 2005; Restolho et al., 2009), metal and other chemical recovery from mining and metallurgical activities (Kalderis et al., 2008; Koseoglu and Kitis, 2009) or treatment of many industrial effluents (Ahmad et al., 2009; Benito and Ruiz, 2002; Das et al., 2010; Rajamanickam and Rajamohan, 2010; Ryan et al., 2009).

Also the semiconductor industry has been recognized as an emerging new field for the application of reverse osmosis membranes based technology (Gill et al., 1998; Juang et al., 2008; Tang et al., 2006; You et al., 2001). Focusing on hydrogen peroxide, several patents refer to ultrapurification by reverse osmosis (Bianchi et al., 2001; Boughton et al., 1989; Morisaki et al., 1999; Owen et al., 2005). For the particular case of hydrogen peroxide ultrapurification, metallic impurities are

considered as the high rejected component in opposition to aqueous hydrogen peroxide matrix which does not suffer any rejection as ion exclusion model predicts (Abejón et al., 2010). The achievement of exigent electronic grades by reverse osmosis without any auxiliary technique is a great challenge and a multistage process becomes indispensable. To realize a high removal of metallic impurities combined with a high recovery rate, recirculation of the subsequent retentates is proposed for multistage integrated schemes (Caus et al., 2009).

The present paper examines the potential of multistage reverse osmosis for ultrapurification of hydrogen peroxide from technical to electronic grade. The technical viability of the process is investigated through lab scale experimental installation while the economic viability is evaluated by a simple profit/costs economic scheme applied to a simulated industrial plant based on models contrasted with the experimental results.

2. Methods and materials

2.1. Chemicals and experimental installation

The technical grade hydrogen peroxide employed as raw material for the ultrapurification process was kindly supplied by Solvay Química Torrelavega: Interox ST-35 hydrogen peroxide H₂O₂ is an aqueous 35% (w/w) hydrogen peroxide solution without any type of stabilizers.

A lab-scale cross-flow flat-sheet configuration test unit SEPA CF II from Osmonics was purchased. The membrane cell can accommodate any 19 × 14 cm flat-sheet membrane coupons, resulting 140 cm² of effective membrane area. BE membrane, a thin-film composite polyamide membrane from Woongjin Chemical, was previously selected as the most competitive one for hydrogen peroxide ultrapurification among all the preselected reverse osmosis membranes (Abejón et al., 2010).

The membrane cell was fed by a Hydra-Cell G-03 (Wanner Engineering) diaphragm pump equipped with digital variable frequency drive to adjust flowrate. Materials of all the components were chosen to maximize compatibility with concentrated hydrogen peroxide. HP PFA tubing was selected for all the installation except for the tube joining the pump and the cell (which worked under pressure), where a PTFE tube enhanced with braided stainless steel has been preferred; and the feed and permeate tanks, which were made of polyethylene (PE). A simple scheme of the entire installation is shown in Fig. 1.

To minimize as possible the contamination by metals coming from the laboratory environment, the most critical components of the ultrapurification system were located under cleanroom conditions. A Bio-48-M vertical laminar flow cabinet (Faster) guaranteed ISO Class 5 atmosphere.

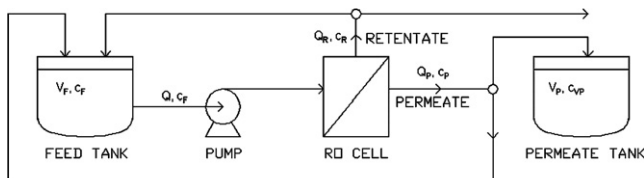


Fig. 1 – General schematic of the experimental installation for ultrapurification by reverse osmosis.

2.2. Reverse osmosis experiments

The ultrapurification installation was designed to work at different operations modes: the total recycling mode was configured by returning both permeate and retentate streams to the feed tank; on the other hand, if the permeate was collected in a permeate tank instead of returned while retentate continued coming back to the feed tank, the semicontinuous mode for permeate mode operated. For the particular case of hydrogen peroxide ultrapurification by two-stage reverse osmosis, a first stage in semicontinuous mode was carried out, followed by a total recycling mode second stage, where the permeate collected during the first stage became the feed of the second one.

For the first stage, the feed tank (220 l max. volume) was filled with 200 l of technical grade hydrogen peroxide and a constant feed flow of 3.4 l/min was maintained; corresponding to a cross-flow velocity of 0.5 m/s in the membrane cell, value representative for cross-flow velocities in spiral-wound elements in full-scale RO plants (GE Water & Process Technologies, 2004). A fresh BE membrane coupon (without previous contact with hydrogen peroxide) was installed in the cell. The experiments were performed at room temperature and the applied pressure was adjusted to 40 bar by the high-pressure concentrate control valve supplied with the membrane cell. In order to assure the membrane compactness, cycles of total recycling mode of 5 h of duration were interspersed. As a result, the first stage lasted for 130 h, 36 of them in semicontinuous mode. Throughout this time, the permeate was collected in the permeate tank.

For the second stage, the collected permeate was employed as feed. The total recycling mode was established and the same operation values in relation to temperature and applied pressure of the first stage were maintained. Once again, the cell was equipped with a fresh BE membrane coupon. This stage lasted for 9 h.

The permeate flow was measured by means of precision scale and chronometer. To determinate metal concentrations, all samples were analyzed by inductively coupled plasma mass spectrometry (ICP-MS) with an Agilent 7500ce ICP-MS system. A special sample introduction system (ESI Upgrade Kit) made of PFA for resistance to hydrogen peroxide was necessary.

2.3. Formulated simulation model for the experimental installation

The model adopted in this work to describe the behavior of the lab-scale experimental installation is based on Kedem-Katchalsky equations for solvent and solute transport through reverse osmosis membranes (Soltanieh and Gill, 1981), as previous work demonstrated that this model was the most representative of ultrapurification of hydrogen peroxide by BE reverse osmosis membrane (Abejón et al., 2010). The Kedem-Katchalsky model, simplified by consideration of negligible osmotic pressure, define the characteristic variables of the reverse osmosis membrane behavior, the specific permeate flux (J_P) and the retention coefficient of each metal ($R_{(metal)}$):

$$J_P = L_P \Delta P \quad (1)$$

$$\frac{1}{R_{(metal)}} = \frac{1}{\sigma_{(metal)}} + \frac{\omega'_{(metal)}}{\sigma_{(metal)}} \frac{1}{J_P} \quad (2)$$

Table 1 – Kedem-Katchalsky model parameters.

	B	Na	Al	Ti	Cr	Mn	Fe	Ni	Cu	Zn
ω' (m/s)	5.58×10^{-6}	2.60×10^{-7}	3.38×10^{-7}	5.11×10^{-7}	7.19×10^{-7}	2.50×10^{-6}	1.40×10^{-6}	4.03×10^{-7}	1.17×10^{-6}	1.53×10^{-6}
σ	1.000	0.926	0.920	0.917	0.925	1.000	0.928	0.920	1.000	0.964
L_p (m/s bar)	4.92×10^{-7}									

where ΔP is the applied pressure and L_p , σ and ω' are the Kedem-Katchalsky parameters hydraulic permeability coefficient, reflection coefficient and modified coefficient of solute permeability respectively. The values of the model parameters for hydrogen peroxide ultrapurification with BE membrane are shown in Table 1 (Abejón et al., 2010). When the experimental installation is running under total recycling operation mode, the system is completely defined by just determinating the flow (Q_p) and concentrations ($c_{P(\text{metal})}$) of the permeate stream. Both variables can be directly calculated from Eqs. (1) and (2):

$$Q_p = AJ_p \quad (3)$$

$$c_{P(\text{metal})} = (1 - R_{(\text{metal})})c_{F(\text{metal})} \quad (4)$$

where A is the effective membrane area and $c_{F(\text{metal})}$ the metal concentration in the feed stream. On the other hand, the semicontinuous operation mode requires more equations as variables changes throughout time. As operation time passes, the feed volume decrease at the same rate that the collected permeate volume increase. This matter transference also implies changes on the metal concentrations, as permeate leaving the cell is more purified than the recirculated stream. Mass balances (global and by components) must be applied to the cell and feed and permeate tanks:

Feed tank

$$\frac{dV_F}{dt} = Q_R - Q \quad (5)$$

$$t=0 \Rightarrow V_F = V_{FO}$$

$$\frac{d(V_F c_F)}{dt} = Q_R c_R - Q c_F \quad (6)$$

$$t=0 \Rightarrow V_F = c_{FO}$$

Cell

$$Q = Q_R + Q_p \quad (7)$$

$$Q c_F = Q_R c_R + Q_p c_P \quad (8)$$

Permeate tank

$$\frac{dV_p}{dt} = Q_p \quad (9)$$

$$t=0 \Rightarrow V_p = 0$$

$$\frac{d(V_p c_{VP})}{dt} = Q_p c_P \quad (10)$$

$$t=0 \Rightarrow c_{VP} = 0$$

3. Results and discussion

3.1. Experimental multistage operation

3.1.1. Results of the first stage of the ultrapurification process

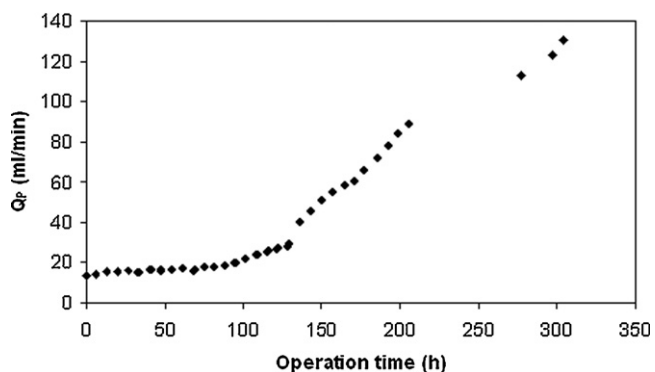
In the first stage, the semicontinuous operation mode was selected in order to collect permeate that would feed the second stage. The initial feed and finally collected permeate (after 130 h of experiment) concentrations are presented in Table 2 (only the metals exceeding the SEMI Grade 1 limit for the initial feed are shown). Na remained as the only element exceeding the corresponding SEMI Grade 1 limit, as Al and Fe concentration in the collected permeate during the first stage fulfill the requirement.

After approximately 70 h of operation, an initially small increase on the permeate production rate was found and, as shown in Fig. 2, evidences of faster rise appeared after 100 h. Although the collection of permeate was finished when an operation time of 130 h was completed, it was decided to prolong the experiment in total recycling mode until 300 h in order to observe the evolution of the permeate flow. Even after this time, the permeate production rate continued increasing, reaching values higher than 7 times the initial value.

As the applied pressure was maintained constant, the permeate flow variation had to be consequence of changes in the hydraulic permeability coefficient of the membrane L_p . The increase of the permeability of composite reverse osmosis membranes as a result of contact with oxidant chemicals (typically chlorine derivatives) is well reported (Raval et al., 2010;

Table 2 – Concentrations of the initial feed and obtained permeates in the experimental ultrapurification process and comparison with SEMI Grade 1 limits.

Concentrations (ppb)	Metals		
	Na	Al	Fe
Initial feed	23,682	1091	181
SEMI Grade 1 limit	1000	1000	100
First stage permeate	5748	245	44
Second stage permeate	515	17	5

**Fig. 2 – Evolution of the permeate flow (Q_p) along time during the first stage of the ultrapurification process.**

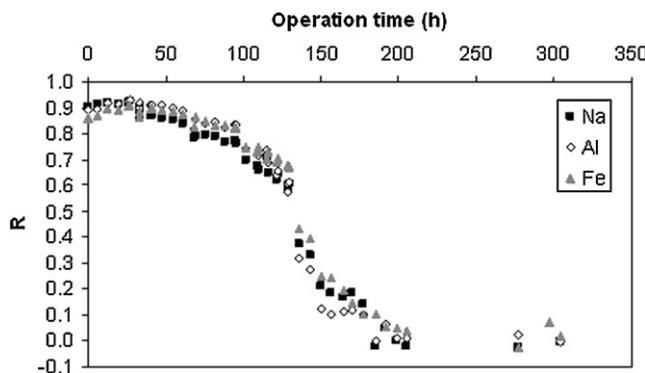


Fig. 3 – Evolution of the rejection coefficients (R) of the metals along time during the first stage of the ultrapurification process.

Rouaix et al., 2006). Information about contact with hydrogen peroxide is also published (Wu et al., 1996) and similar membrane behavior is found. The rise of the permeate production rate would be a positive result of the oxidative degradation of polyamide membranes if rejection was not affected, but this is not the case. The observed retention always decreases with time as an effect of oxidation and retention tends to zero for contact time long enough. The evolution of the rejection coefficients of Na, Al and Fe during the experiment showed clearly the expected performance: after the initial phase where values were maintained constant for around 70 h, the rejection coefficients fell down first slowly and then drastically until reaching the zero level after 170 h of contact between the membrane and the hydrogen peroxide (Fig. 3). No discrimination to the different metals by reverse osmosis membrane because of atomic mass, ionic charge or initial feed concentration could be found, as demonstrated by the high similarity of the rejection values.

The global rejection coefficients (ratio of difference between initial feed and final permeate tank concentrations to initial feed concentration) were calculated for each metal, obtaining values of 0.757, 0.775 and 0.757 for Na, Al and Fe, respectively. These coefficients are quite lower than the predictions according to previous experimentation (Abejón et al., 2010), as values close to 0.9 were expected. It is clear that the duration of the first stage should have been designed shorter to avoid membrane degradation. Therefore, it can be concluded that the effective lifetime for the BE membrane in 35% hydrogen peroxide medium working under pressure of 40 bar should not be extended for more than 75 h (3 full days, corresponding to 72 h, would be an adequate limit).

3.1.2. Results of the second stage of the ultrapurification process

Electronic grade requirements were expected to be reached for the first stage permeate by a second reverse osmosis stage. The characteristics of the permeate obtained in the second

stage are presented in Table 2. Na concentration was close to 500 ppb, just half of the demanded limit, so permeate obtained by the second stage of the ultrapurification process fulfilled the SEMI Grade 1 requirements referring to metallic content. In this case, the rejection coefficients were 0.910, 0.931 and 0.886 for Na, Al and Fe, respectively. The average value of the several permeate flow measures was 18.4 ml/min, equivalent to 1.9 m³/m² d.

The designed lab-scale experimental ultrapurification installation, based on two stages of reverse osmosis, has demonstrated the technical viability of this technology to reach electronic grade quality from technical grade hydrogen peroxide without any auxiliary technique.

3.1.3. Model validation

The permeate flux calculated for the first stage (semicontinuous operation mode) by the proposed model (Eq. (3)) was 16.5 ml/min. When this value was compared with the mean of the several experimental measures taken before 75 h of experiment (16.1 ml/min), a great agreement was observed, with an estimation error lesser than 3%. It should be mentioned that previous work has demonstrated that variability between different membrane coupons can accommodate relative differences greater than 25% between the maximum and minimum values of the permeate flux range (Abejón et al., 2010).

The experimental and predicted results for the concentrations of the main metallic impurities (Na, Al and Fe) in the feed tank and the permeate stream through the first stage evolution are presented in Fig. 4. The variables appear as normalized concentrations as they have been divided by the respective initial feed concentration (c_{F0}).

According to the graphs, the proposed model describes the experimental concentration trends reasonably well. To measure this fitting, some statistic variables were assessed and shown in Table 3. Firstly, the average normalized concentrations (\bar{x}) and standard deviations (σ) of the experimental and modeled results were calculated. The biases were also included and both root mean square error (RMSE) and mean absolute percentage errors (MAPE) were chosen as error indicators:

$$\text{Bias} = \frac{1}{n} \sum_{i=1}^n x_{\text{modi}} - x_{\text{expi}} \quad (11)$$

$$\text{RMSE} = \sqrt{\frac{\sum_{i=1}^n (x_{\text{modi}} - x_{\text{expi}})^2}{n}} \quad (12)$$

$$\text{MAPE} = 100 \frac{1}{n} \sum_{i=1}^n \left| \frac{x_{\text{modi}} - x_{\text{expi}}}{x_{\text{expi}}} \right| \quad (13)$$

The dispersion of the experimental points has to be pointed out, specially for the case of the permeate stream

Table 3 – First stage model summary statistics.

		\bar{X}_{exp}	\bar{X}_{mod}	σ_{exp}	σ_{mod}	Bias	RMSE	MAPE
Na	Feed tank	1.026	1.047	0.034	0.030	0.021	0.055	3.9
	Permeate stream	0.128	0.090	0.042	0.003	-0.038	0.054	26.2
Al	Feed tank	1.050	1.046	0.030	0.029	-0.004	0.036	2.8
	Permeate stream	0.106	0.100	0.030	0.003	-0.006	0.028	15.2
Fe	Feed tank	1.042	1.044	0.058	0.028	0.002	0.064	4.6
	Permeate stream	0.121	0.140	0.019	0.004	0.018	0.025	19.7

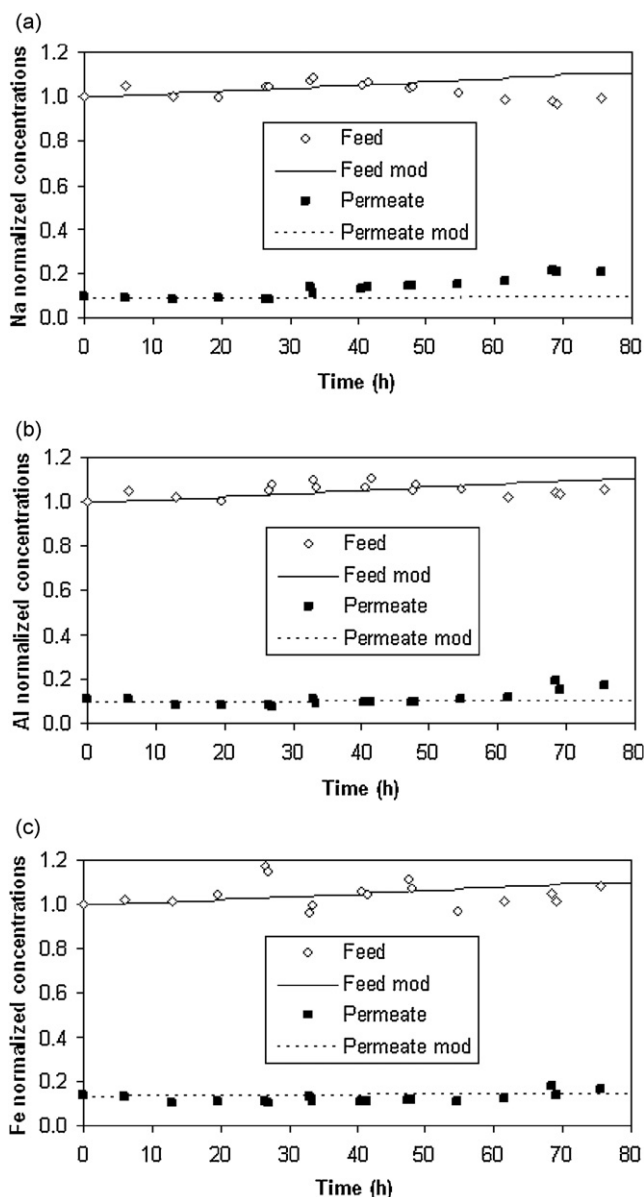


Fig. 4 – Observed and modeled normalized concentrations of the main metallic impurities Na (a), Al (b) and Fe (c) in the feed tank and the permeate stream through the first experimental stage evolution.

concentrations, as their standard deviation values are comparable to those of the feed tank in spite of the difference of an order of magnitude among them. As a consequence, the root mean square errors (RMSE) are also comparable but higher mean absolute percentage errors (MAPE) correspond to the permeate streams because of their lower concentrations when compared to the related errors. However, the highest MAPE value given by the model is 26.2% for Na concentration in the permeate stream, similar to figures obtained by more complex membrane models (Silva et al., 2010). The feed tank concentrations are predicted with more accuracy, since their MAPE values do not exceed 5%. According to the biases analysis, positive and negative values are equally distributed among metallic elements and sample points (feed tank or permeate stream), so the model can be considered unbiased.

The performance during the second stage (total recycling operation mode) was also compared with the predicted behavior by the proposed model (Eqs. (1–4)). The mean experimental permeate flux obtained as the average value of six different

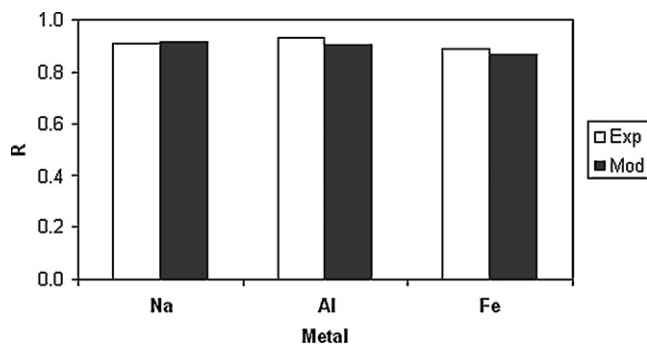


Fig. 5 – Observed and modeled rejection coefficients of the main metallic impurities Na, Al and Fe in the second experimental stage.

samples was 19.9 ml/min. This value implied an estimation error of 20.6% with respect to the modeled permeate flux (16.5 ml/min). This fact exemplified the abovementioned variability among membrane coupons. With respect to the main metallic impurities, the experimental and modeled rejection coefficients (R) were represented in Fig. 5. The agreement between each pair of values is great, with percentages of estimation error of 0.5, 2.9 and 2.7% for Na, Al and Fe, respectively.

3.2. Design of an industrial scale process

The design of integrated countercurrent membrane cascades is analogous to those of fractional distillation columns. The retentate which is recycled to the previous membrane module is enriched in the component with the highest rejection (similar to the depleted liquid stream in the distillation column), while the permeate enriched in the component with the lowest rejection (similar to the vapor stream in the distillation column) is employed as feed stream for the next module. A general scheme of the simplest (only two stages) integrated countercurrent membrane cascade is shown in Fig. 6. Two streams are obtained as result of the membrane cascade: the permeate of the final stage, which is the purified aqueous hydrogen peroxide solution and the retentate of the feed stage, a by-product stream characterized by higher metal content if compared with feed chemical.

3.2.1. Formulated simulation mode for the industrial scale process

The Aspen Custom Modeler software was employed to simulate the behavior of the designed membrane process. The simulation model was based on overall mass balances and the Kedem-Katchalsky equations for solvent and solute transport through reverse osmosis membranes. To illustrate the model, the simulation of the two-stage installation (as shown in Fig. 6) is detailed.

Firstly, the overall and component (metal) mass balances for both modules are composed:

$$F + R_2 = P_1 + R_1 \quad (14)$$

$$P_1 = P_2 + R_2 \quad (15)$$

$$F C_{F(\text{metal})} + R_2 C_{R_2(\text{metal})} = P_1 C_{P_1(\text{metal})} + R_1 C_{R_1(\text{metal})} \quad (16)$$

$$P_1 C_{P_1(\text{metal})} = P_2 C_{P_2(\text{metal})} + R_2 C_{R_2(\text{metal})} \quad (17)$$

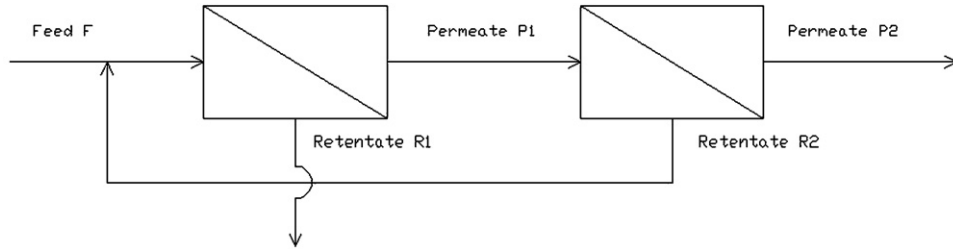


Fig. 6 – General scheme of a two-module integrated reverse osmosis process.

where P_i and R_i are the permeate and retentate volume flows respectively of the corresponding i membrane module, F is the initial feed flow and $C_{i(\text{metal})}$ the metal concentration of the corresponding stream.

Secondly, the transport equations based on the simplified Kedem-Katchalsky model, define the characteristic variables of the reverse osmosis membrane behavior, the specific permeate flux (J_P) and the retention coefficient of each metal ($R_{i(\text{metal})}$):

$$J_{Pi} = L_P \Delta P_i \quad (18)$$

$$\frac{1}{R_{i(\text{metal})}} = \frac{1}{\sigma_{(\text{metal})}} + \frac{\omega'_{(\text{metal})}}{\sigma_{(\text{metal})}} \frac{1}{J_{Pi}} \quad (19)$$

where ΔP_i is the applied pressure in each stage and L_P , σ and ω' are the Kedem-Katchalsky parameters. Once the membrane transport model is described, the characteristics of the permeate streams (flow and metal concentrations) can be calculated:

$$P_i = A_i J_P \quad (20)$$

$$C_{Pi(\text{metal})} = (1 - R_{i(\text{metal})}) C_{INi(\text{metal})} \quad (21)$$

where A_i is the membrane area of the corresponding stage and C_{INi} the metal concentration of the inlet stream of the corresponding stage. Finally the recovery ratio of each module (Rec_i) is defined:

$$Rec_i = \frac{P_i}{P_i + R_i} \quad (22)$$

3.2.2. Simulation results and sensibility analysis

As a first step, the scale of the process and both design and operation variables were fixed. A plant able to treat 9000 t of technical grade hydrogen peroxide annually was planned, that implies a feed flow of 24.19 m³/d (330 operating days per year were considered). The quality of the feed peroxide is based on previous analysis of Interox ST-35 hydrogen peroxide H₂O₂ (Solvay), which can be representative of technical grade chemical and its metallic content is shown in Table 4. The recovery ratios of the modules were chosen as design variables and a value of 0.7 was selected. The applied pressure was the only remaining operation variable and it was decided to work under 40 bar pressure.

The simulation results for the hydrogen peroxide ultra-purification performance of a two-stage integrated reverse osmosis cascade are presented in Table 5, where the flows and metallic contents of each stream can be observed. The final product achieved impurities concentrations that satisfied the SEMI Grade1 requirements. The total recovery ratio, the quotient between the ultrapurified and feed streams, was 0.620 and the global rejection coefficients obtained when compared

the same streams ranged from 0.956 for B to 0.997 for Cu. In relation to the modules, 12.6 and 8.8 m² of membrane area were required for stages 1 and 2, respectively.

The influence of the main design and operation variables (recovery rates and applied pressures) on the simulated installation was studied by means of a sensibility analysis. The effects of varying the recovery rates in the range of 0.45–0.95 while keeping the applied pressures in both stages constant at 40 bar is graphed in Fig. 7. The design decision about the recovery rates should ride out the conflicting effects those variables produce over the process performance. Obviously, high recovery rates imply high product stream flow (graphically expressed as total recovery in Fig. 7c) as less material is able to leave the system by the first stage retentate stream. The counterpoint to the greater ultrapure chemical production is the higher demanded membrane area required to permit the increased permeate flow (Fig. 7a). The maximum membrane area corresponds to the case where the maximum recovery rate is wanted for the first stage while the second stage works at its minimum value. This situation implies the highest flow for the recirculation stream and, as a consequence, the flow entering the first stage reaches its maximum after feed and recirculation mixing. On the other hand, when the recovery in the first stage is low, the system becomes very little sensitive in terms of membrane area variation to changes in the second stage recovery design, so the total membrane area of the system can be mainly reduced by diminishing the recovery rate of the first stage. The maximum membrane area case is also characterized because it is the situation where the best final product quality is achieved (Fig. 7b). The high recovery rate implies the dilution of the stream entering the first stage with retentate from the second stage. For the consideration of impurities concentration in final product stream, the second stage emerges as the controlling one, so the most efficient way to improve the product quality is the reduction of the second stage recovery rate instead of action over the first stage.

In a similar way, the applied pressures were changed in the range from 5 to 40 bar to study the evolution of the installation

Table 4 – Assumed metal concentrations of 35% Technical Grade hydrogen peroxide.

Element	Concentration (ppb)
B	8
Na	25,000
Al	1300
Ti	80
Cr	55
Mn	5
Fe	200
Ni	30
Cu	3
Zn	15

Table 5 – Material flow for the two-module countercurrent integrated reverse osmosis cascade.

	Streams	R1	P1	R2	P2	SEMI Grade 1 limits
	F					
Flow (m ³ /d)	24.19	9.19	21.43	6.43	15.00	
Concentration (ppb)						
Al	1300	3407	105	325	10.0	1000
B	8	20	1.6	4.5	0.4	100
Cr	55	144	5.0	15	0.5	50
Cu	3	7.9	0.1	0.4	0.0	50
Fe	200	522	23	70	3.1	100
Mn	5	13	0.5	1.5	0.1	50
Na	25,000	65,580	1802	5646	155.2	1000
Ni	30	79	2.5	7.7	0.2	50
Ti	80	209	7.2	22	0.8	300
Zn	15	39	1.3	4.1	0.1	100

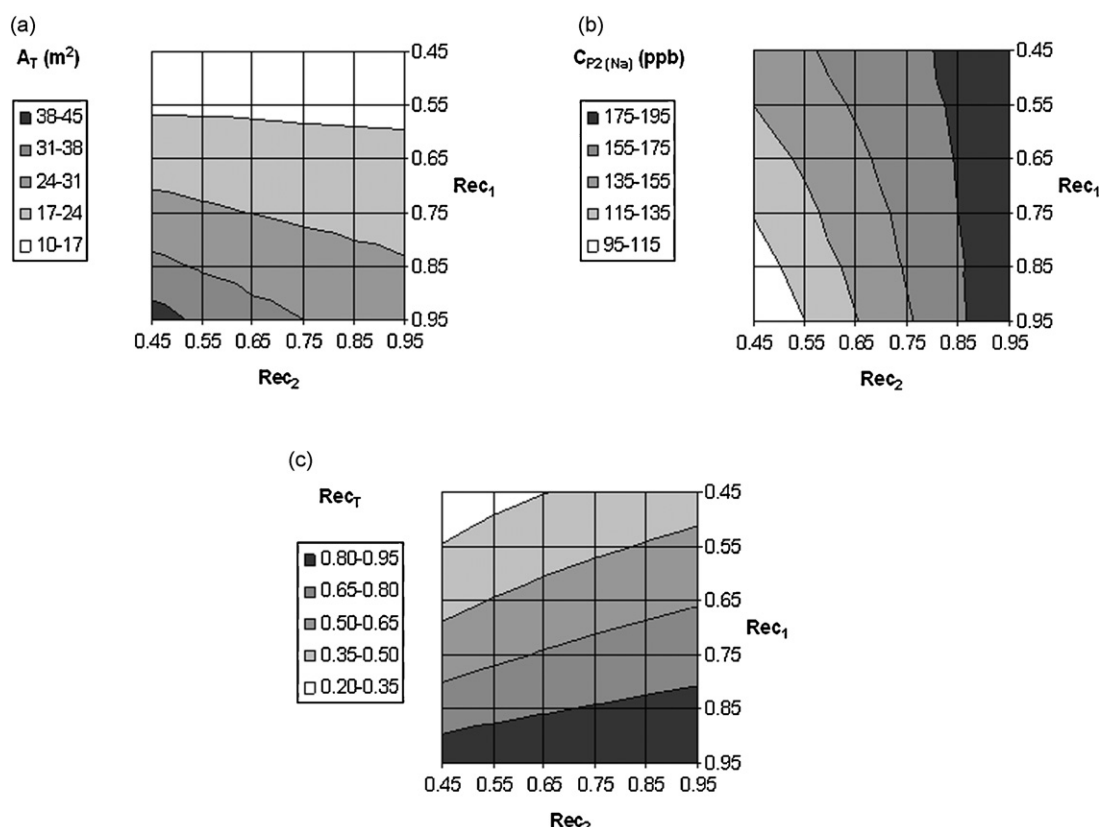


Fig. 7 – Dependence relation of the recovery rates (Rec_1 and Rec_2) of the two reverse osmosis stages upon (a) the total membrane area (A_T), (b) the concentration of Na in the second stage permeate ($C_{P2(Na)}$) and (c) the total recovery rate (Rec_T).

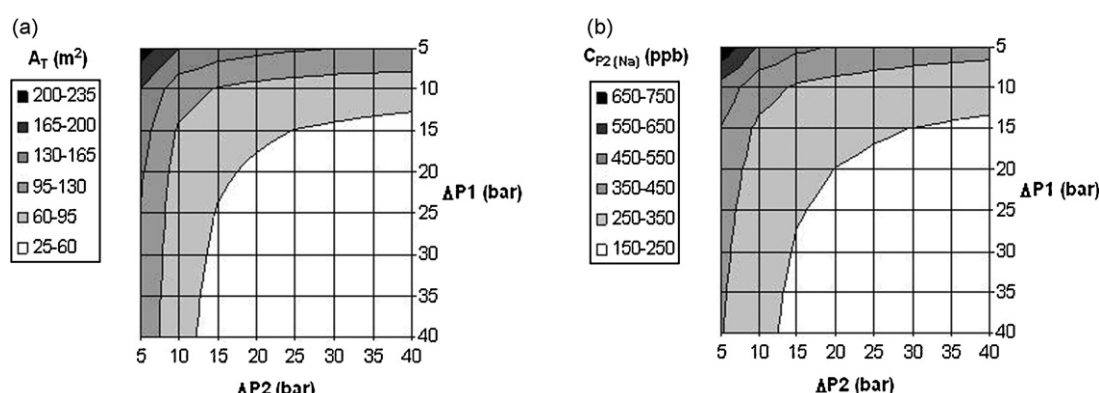


Fig. 8 – Dependence relation of the applied pressures (ΔP_1 and ΔP_2) over the two reverse osmosis stages upon (a) the total membrane area (A_T) and (b) the concentration of Na in the second stage permeate ($C_{P2(Na)}$).

performance while the recovery rates of both stages was fixed at 0.95. The obtained results can be observed in Fig. 8. In this case, high applied pressures in both stages are beneficial for the process in both equipment and product quality terms: the total membrane area required for a constant recovery rate is smaller when high pressures are chosen (Fig. 8a) and a final product stream with lower metallic content can be produced (Fig. 8b). This is a direct effect of the greater permeate flux and rejection coefficients resulting from higher applied pressures (Eqs. (1) and (2)). Upper energy consumption is the counterbalance to these advantages.

3.2.3. Economic evaluation

Some basic economic assumptions were considered to formulate a simple model based on costs and revenues to evaluate the economic viability of the simulated industrial scale process. The daily profit of the process (Z) was defined as the difference between daily revenues (Rev) and total costs (TC):

$$Z = \text{Rev} - \text{TC} \quad (23)$$

Two different revenues were considered: the main one corresponding to the sale of the second stage permeate (P_2) as electronic grade hydrogen peroxide, while the retentate of the first stage (R_1) could be commercialized as a by-product useful for hydrogen peroxide applications when metallic content is not a limiting factor:

$$\text{Rev} = P_2 Y_{\text{EG}} + R_1 Y_{\text{by}} \quad (24)$$

The total costs of the system were calculated by the addition of the capital costs (CC) and the operation costs (OC). The capital costs attributable to membranes or to the rest of the installation were differentiated, while the operation costs were itemized into raw materials, labor, energy and maintenance costs:

$$\text{TC} = \text{CC} + \text{OC} \quad (25)$$

$$\text{CC} = \text{CC}_{\text{memb}} + \text{CC}_{\text{ins}} \quad (26)$$

$$\text{OC} = \text{OC}_{\text{raw}} + \text{OC}_{\text{lab}} + \text{OC}_{\text{en}} + \text{OC}_m \quad (27)$$

The diarized capital costs of the membranes modules considering straight-line depreciation were expressed as function of the total membrane area of the installation:

$$\text{CC}_{\text{memb}} = \frac{Y_{\text{memb}} \sum A_i}{LT_{\text{memb}}} \quad (28)$$

The application of reverse osmosis membranes to ultrapurification of hydrogen peroxide involves unusually high membrane replacement rates as previously demonstrated when the membrane lifetime limit for this particular case was fixed at 3 days. This short resistance is not comparable to the most classic membranes uses, when durations longer than years can be typically expected when the correct maintenance (including chemical cleaning and physical flushing) is planned and executed.

Once the membranes costs were defined, the capital costs corresponding to the rest of the installation were related to them by mean of a coefficient (K_{memb}) that expressed the contribution of the investment in membranes to the total capital costs. Bibliographic references (Fariñas, 1999; Medina San

Table 6 – Economic model parameters.

Parameter	Unit	Value
Y_{memb}	(\$/m ²)	50
LT_{memb}	(d)	3
LT_{inst}	(d)	1825
K_{memb}		0.12
Y_{raw}	(\$/m ³)	790
Y_{EG}	(\$/m ³)	2592
Y_{by}	(\$/m ³)	600
Y_{lab}	(\$/h)	7
Y_{elec}	(\$/kWh)	0.08
η		0.70
CC_{clean}	(\$/d)	2590

Juan, 2000) estimate the percentage of the total investment attributable to the membranes in the range of 12–30%, so value of K_{memb} of 0.12 was selected:

$$CC_{\text{ins}} = CC_{\text{memb}} \frac{(1 - K_{\text{memb}})}{K_{\text{memb}}} \frac{LT_{\text{memb}}}{LT_{\text{inst}}} + CC_{\text{clean}} \quad (29)$$

Ultrapurification processes require contamination control, so the installation needed to be included in a cleanroom to provide the necessary controlled atmosphere. The capital costs attributable to the cleanroom were calculated according to the model proposed by Yang and Eng Gan (2007) for a Class 100 space of 200 m² (200 air changes per hour (Rumsey Engineers Inc., 2009)) with raised floor and FFU type air ventilation:

$$CC_{\text{clean}} = -1645051 + 5156.6CA + 68.8MAV + 34EAV + 2996627AFC + AN \quad (30)$$

The term AN, that did not appear in the originally formulated model, was added to include the costs related to analysis and quality control. Its value was assessed according to the research group experience in analytical equipment management, mainly inductively coupled plasma mass spectrometry (ICP-MS) and ion chromatography (IC).

The operation costs are essentially based on the consumption of the corresponding resource, except for the case of maintenance costs, which are function of the total capital costs (Shaalan et al., 2000). The only required raw material was the technical grade hydrogen peroxide employed as feed and the installation was designed to be totally managed by a single worker:

$$OC_{\text{raw}} = FY_{\text{raw}} \quad (31)$$

$$OC_{\text{lab}} = 24Y_{\text{lab}} \quad (32)$$

$$OC_{\text{en}} = \frac{\sum(Q_{\text{INi}} \Delta P_i)}{36\eta} Y_{\text{elec}} \quad (33)$$

$$OC_m = 0.05CC \quad (34)$$

Based on the aforesaid simulated study case and the parameters required for calculation purposes listed in Table 6, economic evaluation including the assessment of the resulting profit was carried out. The main economic indicators are given in Table 7. It is noted that the economic viability of the process is obvious as 22018\$ would result as daily profit (this is equivalent to 7.27\$mill per year).

When the breakdown of the total costs of the proposed plant is observed, it is worth mentioning that raw material

Table 7 – Economic evaluation results.

Economic indicator	Daily value (\$/d)	Contribution to total costs (%)
Z	21,793	
Rev	44,402	
TC	22,609	
CC	3169	14.0
CC _{memb}	572	2.5
CC _{inst}	2597	11.5
OC	19,441	86.0
OC _{raw}	19,110	84.5
OC _{lab}	168	0.7
OC _{en}	4	0.1
OC _m	159	0.7

costs are the most significant as the purchase of technical grade hydrogen peroxide comprises 85.4% of the total costs of the process. The rest of the operation costs could be considered negligible when compared to raw material ones, since none of them reach the 1% level of contribution. On the other hand, when focusing on capital costs, the investment on membranes contributes by only 1.6% to the total costs in spite of the high replacement rate consequence of the short membrane lifetime in such a harsh medium.

4. Conclusions

Commercially available 35% technical grade hydrogen peroxide has been successfully purified to the achievement of SEMI Grade 1 chemical by a two-stage reverse osmosis process without any auxiliary technique. The rejection coefficients of the metals kept around 0.90 as average value, and the permeate flow of H₂O₂ purified, SEMI 1 production, was equivalent to 1.9 m³/m² d. The effective lifetime for the BE membrane (thin-film composite polyamide membrane from Woongjin Chemical) in such an oxidant medium was analyzed and a limit of 75 h is suggested from this experimental work, for the membrane operation at 40 bar in contact to H₂O₂ 35%. Further work related to the process behavior in the terms of membrane lifetime is under study.

The proposed simulation model defined by system material balances together with Kedem-Katchalsky transport equations has predicted adequately the performance of a lab scale installation in both semicontinuous and continuous operation modes. In addition, simulation of the industrial scale process was carried out and the influence of the design and operation parameters, such as recovery rates and applied pressures, over the system operation was investigated. For the consideration of impurities concentration in final product stream, the second stage emerges as the controlling one, so the most efficient way to improve the product quality is the reduction of the second stage recovery rate instead of actions over the first stage.

The economic viability of the industrial process was demonstrated by the formulated economic model, as an annual profit upper to 7 mill\$ was estimated when the capacity of the simulated plant was fixed at 9000 t of feed chemical per year.

Acknowledgements

This research has been financially supported by the Ministry of Science and Innovation of Spain (MICINN) through CTM2006-00317 Project. R. Abejón acknowledges also the assistance

of MICINN for the award of a FPI grant (BES-2008-003622). We gratefully thank Woongjin Chemicals for the supplied membranes and Solvay Torrelavega for the technical grade hydrogen peroxide.

References

- Abejón, R., Garea, A., Irabien, A., 2010. Ultrapurification of hydrogen peroxide solution from ionic metals impurities to semiconductor grade by reverse osmosis. *Sep. Purif. Technol.* 76, 44–51.
- Ahmad, A.L., Chong, M.F., Bhatia, S., 2009. A comparative study on the membrane based palm oil mill effluent (POME) treatment plant. *J. Hazard. Mater.* 171, 166–174.
- Atsumi, J., Ohtsuka, S., Munehira, S., Kajiyama, K., 1990. Metallic contamination on Si wafers from cleaning solutions. *Proc. Electrochem. Soc.* 90, 59–66.
- Benito, Y., Ruiz, M.L., 2002. Reverse osmosis applied to metal finishing wastewater. *Desalination* 142, 229–234.
- Bianchi, U.P., Leone, U., Lucci, M., 2001. Process for the industrial production of high purity hydrogen peroxide. US Patent 6333018 B2.
- Boughton, J.H., Butz, R.A., Cheng, H.C.T., Dennis, J.R., Hannon, B.T., Weigel, J.H., 1989. Manufacture of high purity hydrogen peroxide by using reverse osmosis. US Patent 4879043.
- Caus, A., Braeken, L., Boussu, K., Van der Bruggen, B., 2009. The use of integrated countercurrent nanofiltration cascades for advanced separations. *J. Chem. Technol. Biotechnol.* 84, 391–398.
- Cuellar, M.C., Herreilers, S.N., Straathof, A.J.J., Heijnen, J.J., van der Wielen, L.A.M., 2009. Limits of operation for the integration of water removal by membranes and crystallization of L-phenylalanine. *Ind. Eng. Chem. Res.* 48, 1566–1573.
- Daigle, S., Vogelsberg, E., Lim, B., Butcher, I., 2007. Electronic chemicals. In: Ullmann's Encyclopedia of Industrial Chemistry. Wiley-VCH, Weinheim, Electronic Release.
- Das, C., DasGupta, S., De, S., 2010. Treatment of dyeing effluent from tannery using membrane separation processes. *Int. J. Environ. Waste Manag.* 5, 354–367.
- Duffalo, J.M., Monkowski, J.R., 1984. Particulate contamination and device performance. *Solid State Technol.* 27, 109–114.
- Fariñas, M., 1999. Osmosis Inversa: Fundamentos, Tecnología y Aplicaciones. McGraw-Hill, Madrid.
- García-Figueroa, C., Bes-Piá, A., Mendoza-Roca, J.A., Lora-García, J., Cuartas-Uribe, B., 2009. Reverse osmosis of the retentate from the nanofiltration of secondary effluents. *Desalination* 240, 274–279.
- GE Water & Process Technologies, 2004. SEPA CF II Membrane Element Cell instruction manual.
- Gill, W.N., Agrawal, V., Gill, A.L., Naik, M., Kulkarni, A., Mukherjee, D., 1998. Novel membrane-based systems for reprocessing hydrofluoric acid etching wastes. *Adv. Environ. Res.* 2, 333–350.
- Gurak, P.D., Cabral, L.M.C., Rocha-Leao, M.H.M., Matta, V.M., Freitas, S.P., 2010. Quality evaluation of grape juice concentrated by reverse osmosis. *J. Food Eng.* 96, 421–426.
- Juang, L.C., Tseng, D.H., Lin, H.Y., Lee, C.K., Liang, T.M., 2008. Treatment of chemical mechanical polishing wastewater for water reuse by ultrafiltration and reverse osmosis separation. *Environ. Eng. Sci.* 25, 1091–1098.
- Kalderis, D., Tsolaki, E., Antoniou, C., Diamadopoulos, E., 2008. Characterization and treatment of wastewater produced during the hydro-metallurgical extraction of germanium from fly ash. *Desalination* 230, 162–174.
- Kawachale, N., Kumar, A., 2010. Simulation, scale-up and economics of adsorption and membrane based processes for isoflavones recovery. *Chem. Eng. Res. Des.*, doi:10.1016/j.cherd.2010.07.015.
- Koseoglu, H., Kitil, M., 2009. The recovery of silver from mining wastewaters using hybrid cyanidation and high-pressure membrane process. *Miner. Eng.* 22, 440–444.
- Medina San Juan, J.A., 2000. Desalación de aguas salobres y de mar: osmosis inversa. Mundi-Prensa, Madrid.

- Morisaki, A., Sawaguri, Y., Matsuda, Y., 1999. Apparatus and method for removing impurities from aqueous hydrogen peroxide. US Patent 5906738.
- Olson, E.D., Reaux, C.A., Ma, W.C., Butterbaugh, J.W., 2000. Alternatives to standard wet cleans. *Semiconduct. Int.* 23, 70–75.
- Owen, R., Bosse, J., Sell, M., 2005. Process for the purification of aqueous peroxygen solutions, solutions obtainable thereby and their use. WO Patent 2005/033005 A1.
- Pilipovik, M.V., Riverol, C., 2005. Assessing dealcoholization systems based on reverse osmosis. *J. Food Eng.* 69, 437–441.
- Pizzichini, M., Russo, C., di Meo, C., 2005. Purification of pulp and paper wastewater, with membrane technology, for water reuse in a closed loop. *Desalination* 178, 351–359.
- Rajamanickam, R., Rajamohan, T.S., 2010. Study on quality of effluent discharge from textile bleaching and dyeing units CETPs in Karur, Tamil Nadu. *Pollut. Res.* 29, 1–6.
- Raval, H.D., Trivedi, J.J., Joshi, S.V., Devmurari, C.V., 2010. Flux enhancement of thin film composite RO membrane by controlled chlorine treatment. *Desalination* 250, 945–949.
- Restolho, J.A., Prates, A., de Pinho, M.N., Afonso, M.D., 2009. Sugars and lignosulphonates recovery from eucalyptus spent sulphite liquor by membrane processes. *Biomass Bioenergy* 33, 1558–1566.
- Rouaix, S., Causserand, C., Aimar, P., 2006. Experimental study of the effects of hypochlorite on polysulfone membrane properties. *J. Membr. Sci.* 277, 137–147.
- Rumsey Engineers Inc., 2009. Energy efficiency baselines for cleanrooms. Non-Residential New Construction and Retrofit Incentive Programs of PG&E, Oakland.
- Ryan, D., Gadd, A., Kavanagh, J., Barton, G.W., 2009. Integrated biorefinery wastewater design. *Chem. Eng. Res. Des.* 87, 1261–1268.
- Semiconductor Equipment and Material International Association (SEMI®), 2010. Specifications for Hydrogen Peroxide. SEMI Document C30-1110.
- Shaalan, H.F., Sorour, M.H., Tewfik, S.R., 2000. Simulation and optimization of a membrane system for chromium recovery from tanning wastes. *Desalination* 141, 315–324.
- Sievert, W.J., 2001. Setting standards. The developments of standards in the field of electronic chemicals. *Semiconduct. Fabtech.* 13, 175–179.
- Silva, P., Peeva, L.G., Livingston, A.G., 2010. Organic solvent nanofiltration (OSN) with spiral-wound membrane elements—Highly rejected solute system. *J. Membr. Sci.* 349, 167–174.
- Soltanieh, M., Gill, W.N., 1981. Review of reverse osmosis membranes and transport models. *Chem. Eng. Commun.* 12, 279–363.
- Tam, L.S., Tang, T.W., Lau, G.N., Sharma, K.R., Chen, G.H., 2007. A pilot study for wastewater reclamation and reuse with MBR/RO and MF/RO systems. *Desalination* 202, 106–113.
- Tang, C.Y., Fu, Q.S., Robertson, A.P., Criddle, C.S., Leckie, J.O., 2006. Use of reverse osmosis membranes to remove perfluorooctane sulfonate (PFOS) from semiconductor wastewater. *Environ. Sci. Technol.* 40, 7343–7349.
- Yang, L., Eng Gan, C., 2007. Costing small cleanrooms. *Build. Environ.* 42, 743–751.
- You, S.H., Tseng, D.H., Guo, G.L., 2001. A case study on the wastewater reclamation and reuse in the semiconductor industry. *Resour. Conserv. Recycl.* 32, 73–81.
- Wu, S., Zheng, C., Zheng, G., 1996. Effective interface of a composite membrane serving as an ideally ultrathin barrier layer. *Polymer* 37, 4193–4195.

4.3. Abejón, R.; Garea, A.; Irabien, A. *Integrated countercurrent reverse osmosis cascades for hydrogen peroxide ultrapurification.* Computers and Chemical Engineering, 41:67-76 (2012).

Resumen

Los reactivos y materiales empleados para fabricar y embalar los semiconductores y los circuitos impresos son conocidos como reactivos electrónicos. La pureza de estos reactivos electrónicos, fijada por la asociación industrial Semiconductor Equipment and Materials International (SEMI), es una preocupación muy comprometedora para el sector industrial de los semiconductores, por lo que se imponen requisitos muy estrictos para evitar fallos en los dispositivos microelectrónicos por culpa del contenido en impurezas metálicas de los reactivos electrónicos. Para el caso particular del peróxido de hidrógeno como uno de los reactivos electrónicos en fase líquida de mayor consumo, el Documento SEMI C30-1110 presenta cinco grados electrónicos diferentes definidos por su contenido límite en impurezas.

La industria de los semiconductores aparece como una aplicación emergente para los procesos basados en membranas de ósmosis inversa. Después de revisar las patentes publicadas a lo largo de los últimos veinte años sobre ultrapurificación para la producción industrial de peróxido de hidrógeno de grado electrónico de alta pureza, las técnicas de separación referenciadas pueden ser reemplazadas por ósmosis inversa con menores costes de energía y reactivos. Este trabajo propone un proceso de membranas cuyo diseño se basa en cascadas de membranas integradas en contracorriente, con el propósito de determinar la cascada óptima para cada uno de los grados SEMI de peróxido de hidrógeno con el beneficio económico como función objetivo de la estrategia de optimización. Los resultados muestran las ventajas del proceso de ósmosis inversa, con valores de beneficio entre 20 y 85 millones \$/año, requiriéndose cascadas de ósmosis inversa integradas por dos etapas para la producción del Grado 1 y por siete etapas para el más estricto Grado 5.

Original abstract

The chemicals and materials used to manufacture and package semiconductors and printed circuit boards are called electronic chemicals. The purity of these electronic chemicals, given by the industry association Semiconductor Equipment and Materials International (SEMI), is a very compromising concern for the semiconductor industrial sector, so very strict requirements are set to avoid microelectronic devices failures because of the content of impurities of electronic chemicals. For the particular case of hydrogen peroxide as one of the most consumed wet electronic chemicals, SEMI Document C30-1110 indicates five different electronic grades defined by their limiting impurities content.

The semiconductor industry is appearing as an emerging application of reverse osmosis membranes based processes. After reviewing the patents published over the last twenty years about ultrapurification for industrial production of high purity electronic grade hydrogen peroxide, the referenced separation techniques can be replaced by reverse osmosis with lower operating expenses due to energy and chemicals. This work proposes a membrane process design based on an integrated countercurrent membrane cascade, in order to determine the optimum osmosis cascade for each SEMI Grade hydrogen peroxide, with the economic profit as the objective function in the optimization strategy. The results show the benefits of the reverse osmosis process, with profit values of 20–85 million \$/year, for a target annual production of 9000 tons of electronic hydrogen peroxide, requiring the integrated reverse osmosis cascades of two stages for the production of Grade 1 to seven stages for the strictest Grade 5.



Integrated countercurrent reverse osmosis cascades for hydrogen peroxide ultrapurification

R. Abejón*, A. Garea, A. Irabien

Departamento de Ingeniería Química y Química Inorgánica, Universidad de Cantabria, Avda. Los Castros s/n, 39005 Santander, Cantabria, Spain

ARTICLE INFO

Article history:

Received 13 July 2011

Received in revised form 20 February 2012

Accepted 22 February 2012

Available online xxx

Keywords:

Reverse osmosis

Membrane cascades

Hydrogen peroxide

Ultrapurification

Wet electronic chemicals

ABSTRACT

The chemicals and materials used to manufacture and package semiconductors and printed circuit boards are called electronic chemicals. The purity of these electronic chemicals, given by the industry association Semiconductor Equipment and Materials International (SEMI), is a very compromising concern for the semiconductor industrial sector, so very strict requirements are set to avoid microelectronic devices failures because of the content of impurities of electronic chemicals. For the particular case of hydrogen peroxide as one of the most consumed wet electronic chemicals, SEMI Document C30-1110 indicates five different electronic grades defined by their limiting impurities content.

The semiconductor industry is appearing as an emerging application of reverse osmosis membranes based processes. After reviewing the patents published over the last twenty years about ultrapurification for industrial production of high purity electronic grade hydrogen peroxide, the referenced separation techniques can be replaced by reverse osmosis with lower operating expenses due to energy and chemicals. This work proposes a membrane process design based on an integrated countercurrent membrane cascade, in order to determine the optimum osmosis cascade for each SEMI Grade hydrogen peroxide, with the economic profit as the objective function in the optimization strategy. The results show the benefits of the reverse osmosis process, with profit values of 20–85 million \$/year, for a target annual production of 9000 tons of electronic hydrogen peroxide, requiring the integrated reverse osmosis cascades of two stages for the production of Grade 1 to seven stages for the strictest Grade 5.

© 2012 Elsevier Ltd. All rights reserved.

1. Introduction

Membrane separation processes have experienced a great development in the last two decades allowing a wide range of industrial applications. Abundant alternatives can be configured through adequate combinations of microfiltration (MF), ultrafiltration (UF), nanofiltration (NF) and reverse osmosis (RO). The exact system design is dependant of multiple factors, including physical and chemical properties of the stream to be treated, nature of target separation substances, intrinsic separation efficiencies and economic considerations. The main advantage of a membrane based process is that separation is achieved with neither a change of state (no thermal energy required) nor use of auxiliary chemicals. Membranes provide a fine separation barrier, allowing for specific chemicals to be separated mainly as function of their size or molecular weight (Fig. 1).

Focusing on reverse osmosis, it was the first membrane based separation process to be widely commercialized (Baker et al., 1991). The characteristic dense semipermeable reverse

osmosis membrane (highly permeable to water and impermeable to microorganisms, colloids, dissolved salts and organics) was the key that paved the way to desalination boom. Desalination of sea and brackish waters is nowadays the main source for supplying fresh water in the regions suffering scarcity of natural freshwater sources (Ibáñez Mengual, 2009). Besides the typical application to desalination purposes, reverse osmosis has been successfully implemented for several other technical practices in various productive sectors: food processing industries (Gurak, Cabral, Rocha-Leao, Matta, & Freitas, 2010), mining and metallurgical activities (Benito & Ruiz, 2002), pulp and paper sector (Restolho, Prates, de Pinho, & Afonso, 2009) and municipal wastewater (Pérez, Fernández-Alba, Urtiaga, & Ortiz, 2010) and many industrial effluent treatments (Das, DasGupta, & De, 2010).

Also the semiconductor industry is appearing as an emerging new guest for the application of reverse osmosis membranes based processes. The chemicals and materials used to manufacture and package semiconductors and printed circuit boards are called electronic chemicals (Daigle, Vogelsberg, Lim, & Butcher, 2007). The purity of these electronic chemicals is a very compromising concern for the semiconductor industrial sector, so very strict requirements are set to avoid microelectronic devices failures because of the content of impurities of electronic

* Corresponding author. Tel.: +34 942201579; fax: +34 942201591.

E-mail address: abejonr@unican.es (R. Abejón).

Nomenclature

$A_{(i)}$	membrane area of the i stage (m^2)
AFC	average filter coverage ratio
AN	capital costs attributable to analysis and quality control ($\$/\text{d}$)
CA	cleanroom area (m^2)
CC	capital costs ($\$/\text{d}$)
CC _{clean}	capital costs attributable to cleanroom ($\$/\text{d}$)
CC _{inst}	capital costs attributable to installation ($\$/\text{d}$)
CC _{memb}	capital costs attributable to membranes ($\$/\text{d}$)
$C_{\text{metal}}^{(i)}$	concentration of the corresponding metal in the i feed stream (ppb)
$C_{P(i)}^{\text{metal}}$	concentration of the corresponding metal in the i permeate stream (ppb)
$C_{R(i)}^{\text{metal}}$	concentration of the corresponding metal in the i retentate stream (ppb)
EAV	exhaust air volume (m^3/h)
F	initial feed flow (m^3/d)
$F(i)$	feed flow of the i stage (m^3/d)
J_V	permeate flux (m/s)
$J_{V(i)}$	permeate flux of the i stage (m/d)
K_{memb}	ratio membrane capital costs to total capital costs
L_P	hydraulic permeability coefficient ($\text{m}/\text{s bar}$)
L'_P	hydraulic permeability coefficient ($\text{m}/\text{d bar}$)
LT _{memb}	membrane lifetime (d)
LT _{inst}	installation lifetime (d)
MAV	make-up air volume (m^3/h)
OC	operation costs ($\$/\text{d}$)
OC _{en}	energy costs ($\$/\text{d}$)
OC _{lab}	labor costs ($\$/\text{d}$)
OC _m	maintenance costs ($\$/\text{d}$)
OC _{raw}	raw material costs ($\$/\text{d}$)
P	permeate flow of the final stage (m^3/d)
$P(i)$	permeate flow of the i stage (m^3/d)
R	rejection coefficient
$R_{(i)}^{\text{metal}}$	rejection coefficient of the corresponding metal in the i stage
$R(i)$	retentate flow of the i stage (m^3/d)
Rec _(i)	recovery rate of the i stage
Rev	daily revenues ($\$/\text{d}$)
TC	total costs ($\$/\text{d}$)
Y_{by}	price of by-product hydrogen peroxide from first stage retentate ($\$/\text{m}^3$)
Y_{EG}	price of SEMI electronic grade hydrogen peroxide ($\$/\text{m}^3$)
Y_{elec}	electricity price ($\$/\text{kWh}$)
Y_{lab}	salary ($\$/\text{h}$)
Y_{memb}	price of reverse osmosis membranes ($\$/\text{m}^2$)
Y_{raw}	price of technical grade hydrogen peroxide ($\$/\text{m}^3$)
Z	daily profit ($\$/\text{d}$)

Greek symbols

ΔP	pressure difference across the membrane (bar)
$\Delta P_{(i)}$	pressure difference across the membrane in the i stage (bar)
η	pump efficiency
σ	reflection coefficient
σ^{metal}	reflection coefficient of the corresponding metal
ω'	modified coefficient of solute permeability (m/s)
ω^{metal}	modified coefficient of solute permeability of the corresponding metal (m/d)

chemicals (Atsumi, Ohtsuka, Munehira, & Kajiyama, 1990; Duffalo & Monkowski, 1984). Semiconductor Equipment and Materials International (SEMI) is the global industry association serving the manufacturing supply chains for the microelectronic, display and photovoltaic industries. SEMI assists the worldwide development of the most respected technical standards in this technological sector. Among all the topics regulated, some refer to the electronic chemicals characteristics and fix the maximum permitted impurities limits in order to be accepted as electronic grade chemicals. Although the least strict electronic grade can be achieved by expert selection from technical grade and little additional treatment, the more stringent electronic grades require employment of further ultrapurification technology to obtain high-purity electronic chemicals, including distillation, adsorption, ion exchange and membrane technologies.

For the particular case of hydrogen peroxide as one of the most consumed wet electronic chemicals (Freedonia Group, 2004), SEMI has recently updated the applicable specifications through SEMI Document C30-1110 (Semiconductor Equipment and Material International Association, 2010). Five different electronic grades remain defined by their limiting impurities content, as shown in Table 1. After reviewing the patents published over the last twenty years about ultrapurification for industrial production of high purity electronic grade hydrogen peroxide (Abejón, Garea, & Irabien, 2010), ion exchange emerges as the most frequently mentioned technology; but distillation is also widely employed, especially for organic pollutant diminution. Despite the wide number of different adsorbents that have been tested for hydrogen peroxide ultrapurification, this technology has become obsolete because of its low maximum efficiency when compared to other competitive options.

All these referenced separation techniques can be replaced by reverse osmosis, as indicated in Fig. 1, with lower operating expenses due to energy and chemicals. Some patents based on reverse osmosis can be found (Bianchi, Leone, & Lucci, 2001; Morisaki, Sawaguri, & Matsuda, 1999), being the membranes employed in combination with other separation techniques (mainly ion exchange) in hybrid processes. This conservative stance on the replacement of conventional separations has been based on some objections to different aspects of the implementation of membrane processes. Firstly, when the retentate stream has to be considered like a waste, careful consideration to its treatment and disposal must be taken. Secondly, membrane fouling can deteriorate the process performance by decrease of the permeation rate. Thirdly, adequate membranes (free of defects and with high permeate flux and effective lifetime) on the most appropriate industrial configuration for each application must be commercially available. Lastly, the required permeate and/or retentate quality has to be achieved by a good separation between components. But the alleged drawbacks can be refuted for the case of hydrogen peroxide ultrapurification by reverse osmosis: the retentate stream can be considered as a valuable by-product useful for hydrogen peroxide applications when metallic impurities content is not a limiting factor; previous work demonstrated that technical grade hydrogen peroxide produces no membrane fouling at any moment of the reverse osmosis membrane lifetime (Abejón, Garea, & Irabien, 2012); despite the implicit harsh conditions of concentrated hydrogen peroxide medium, research efforts have resulted in the development of oxidation-resistant reverse osmosis membranes (Baker, 2010) and multi-pass arrangement is an effective way of achieving stringent permeate quality requirements when poor retention is such that the membrane is unavailable to reach the desired rejection in a single stage (Zhu, Rahardianto, Christofides, & Cohen, 2010).

In reverse osmosis terms, a pass is defined as a membrane unit fed with permeate from a previous membrane unit. A multipass

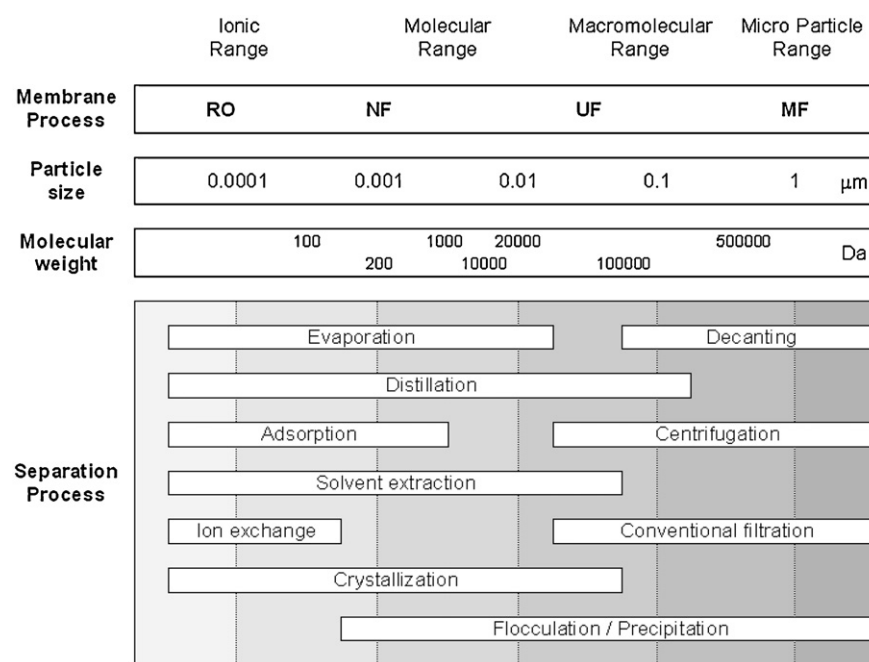


Fig. 1. The filtration spectrum (based on Scholz & Lucas, 2003 and Schweitzer, 1988).

configuration is arranged when product permeate stream is re-pumped after a membrane stage to rise its pressure before entering a new stage. This type of installation is employed to upgrade the quality of the permeate: initially it was used in seawater desalination installations where it was impossible to attain potable water by a single stage, typically high salinity areas like the Persian Gulf. But current reverse osmosis membranes (with salt rejection above 99.3%) make single-stage seawater purification possible, so multipass processes seemed bound to giving up. However, emerging concern about boron concentration in drinking water has bring another opportunity for multipass configuration, as the passage of boron through RO membranes is approximately 30 times higher than the passage of other ionic species such as sodium (Gorenflo, Brusilovsky, Faigon, & Liberman, 2007). Multipass installations are adequate solutions to the poor rejection of boron and desalination plants configured in this way are running all over the world (Faigon & Hefer, 2008; Glueckstern & Priel, 2003; Redondo, Busch, & De Witte, 2003; Taniguchi, Fusaoka, Nishikawa, & Kurihara, 2004). Other desalination plants try to extend membrane lifetime by multipass arrangement and some industrial sectors resort to it when specific high quality permeates are required (Medina San Juan, 2000).

The main drawback of multipass processes is that only poor total recoveries can be achieved. This can be solved by implementation of recycle streams, where the retentate of a stage is coupled back to the feed stream of the previous stage (Zhu, Christofides, & Cohen, 2009). This way, an integrated countercurrent membrane cascade is designed, which general scheme for n stages can be observed in Fig. 2. The idea of using countercurrent membrane cascades was initially developed for gas separation (Caus, Braeken, Boussu, &

van der Bruggen, 2009; Gassner & Maréchal, 2010), but membranes cascades have been employed for different separation purposes by use of every type of the most usual membranes: microfiltration (Abatemozzo et al., 1999; Mellal et al., 2007), ultrafiltration (Gosh, 2003; Isa, Coraglia, Frazier, & Jauregui, 2007; Mayani, Mohanty, Filipe, & Gosh, 2009; Overdevest, Hoenders, van't Riet, van der Padt, & Keurentjes, 2002), nanofiltration (Caus, Vanderhaegen, Braeken, & van der Bruggen, 2009; Lin & Livingston, 2007) and reverse osmosis (Tanuwidjaja & Hoek, 2006; Voros, Maroulis, & Marinos-Kouris, 1997).

The problem of membrane cascade design has been considered from the optimization techniques by the generation of the configurations and their optimization using a superstructure concept, with mass and energy integration (Gassner & Maréchal, 2010) and multi-objective optimization (Guria, Bhattacharya, & Gupta, 2005), mainly for desalination units of seawater and brackish networks by multistage reverse osmosis in order to minimize costs, energy consumption and to maximize permeate production (Guria et al., 2005; Sassi & Mujtaba, 2010; Voros, Maroulis, & Marinos-Kouris, 1996), as well as for process water networks with the development of algorithms for the global optimization of the integrated networks (Ahmetović & Grossmann, 2010, 2011; Karuppiah & Grossmann, 2006).

This work is focused to the ultrapurification of chemicals by membrane processes, selected the hydrogen peroxide as one of the most consumed wet electronic chemicals, being proposed as a problem of membrane cascade in order to achieve the requirements of quality specified for each electronic grade, with the simulation and optimization of the based on revenues and costs for a determined plant capacity. All the model variables are expressed in terms

Table 1

Concentration and impurity limits for electronic grade hydrogen peroxide according to SEMI standard.

SEMI electronic grade	Assay (H_2O_2)	Total oxidizable carbon limit	Anion limit range	Cation limit range
1	30–32%	20 ppm	2–5 ppm	10–1000 ppb
2	30–32%	20 ppm	200–400 ppb	5–10 ppb
3	30–32%	20 ppm	200–400 ppb	1 ppb
4	30–32%	10 ppm	30 ppb	100 ppt
5	30–32%	10 ppm	30 ppb	10 ppt

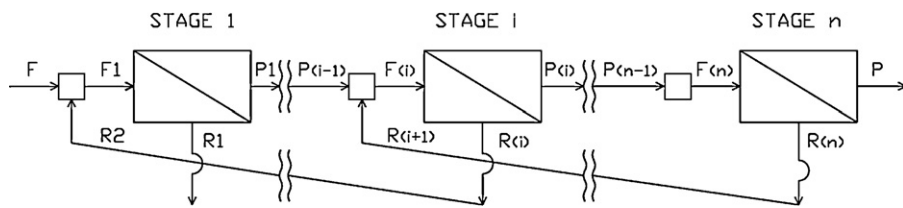


Fig. 2. Schematic representation of n -stage membrane cascade with integration of retentate streams.

of the independent design and operation variables, recovery rates and applied pressures, and the number of membrane units in the integrated cascade are calculated for each electronic grade, Grade 1 (less strict) to Grade 5 (strictest) from the chemical feed which is the technical grade hydrogen peroxide.

2. Characterization of RO process in single-stage experiments

The characterization of RO process for hydrogen peroxide ultrapurification in single-stage experiments is the essential first step for the design of a membrane cascade. The performance of a RO membrane when employed to diminish the metallic content of aqueous solutions of hydrogen peroxide has previously been experimentally studied by this research group (Abejón et al., 2010, 2012). The main results of this previous work are compiled and commented below.

Several commercially available polymeric flat-sheet RO membranes were preselected in accordance with the references appearing in the related patents and the membrane manufacturers' criteria. Experiments with ultrapure water (also doped with Na and Al to 15,000 and 1400 ppb respectively, which are concentrations typically found in technical grade hydrogen peroxide) revealed the leadership of BE polyamide membrane (commercially manufactured by Woongjin Chemical, previously known as Saehan Industries Corporation) among all the candidates in both terms of permeate rate and quality, so it was the unique membrane tested with hydrogen peroxide. The main characteristics of the BE membrane can be consulted in the technical data sheet of the manufacturer (Saehan Industries Corporation, 2007).

Interox ST-35 hydrogen peroxide H_2O_2 was the technical grade peroxide selected as raw material for the ultrapurification process. It is an aqueous 35% (w/w) hydrogen peroxide solution manufactured by Solvay. Its characterization by ICP-MS for the 21 metals required by SEMI C30 document proved that only 10 metals were present above the 1 ppb level as showed in Table 2. The ion exclusion model predicts neither theoretical dilution nor concentration of aqueous hydrogen peroxide solutions when forced to permeate through BE membrane, as experimental determination of hydrogen peroxide concentration in both feed and permeate

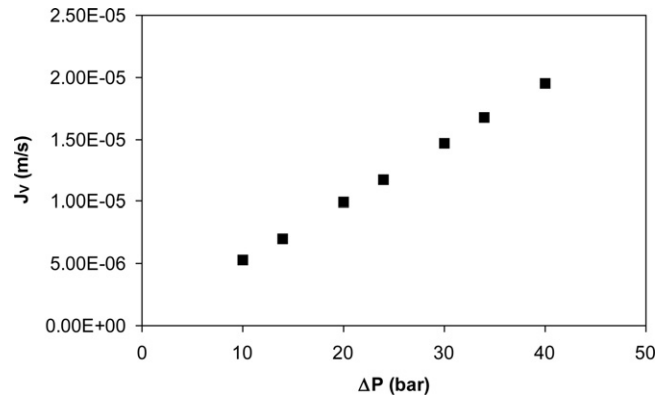


Fig. 3. Hydrogen peroxide flux characterization of BE membrane.

streams confirmed. The rejection coefficients (defined as the ratio of difference between feed and permeate concentrations to feed concentration) of metals obtained for single stage experiments in a lab-scale flat-sheet unit SEPA CF II with BE membrane as function of the applied pressure to the feed technical grade hydrogen peroxide can be observed in Table 2. These rejection coefficients were calculated from experimental data of metal ions concentrations compiled from previous experimental work (Abejón et al., 2010). The repeatability of the data (included as the mean rejection coefficients of the metal ions calculated at different pressures and the corresponding standard deviation values calculated from samples taken during the process operation) can also be consulted in the same reference. On the other hand, the variation of the permeate flux (J_v) with respect to the variation of the applied pressure is showed in Fig. 3.

The Kedem-Katchalsky model, a membrane transport model commonly employed for relating RO permeate fluxes (J_v) and rejection coefficients (R) with applied pressures (ΔP), which is based on three practical parameters (the hydraulic permeability of the membrane L_P , the solute permeability ω' and the reflection coefficient σ) to characterize membrane and solution systems, can be summed

Table 2

Calculated metal rejection coefficients for BE membrane as function of the applied pressure in a single-stage hydrogen peroxide ultrapurification process.

Concentration (ppb)										
Feed	B	Na	Al	Ti	Cr	Mn	Fe	Ni	Cu	Zn
6	>20,000	>1000	72	48	3	161	24	2	13	
Applied pressure (bar)	Rejection coefficients									
	B	Na	Al	Ti	Cr	Mn	Fe	Ni	Cu	Zn
10	0.438	0.887	0.869	0.840	0.812	0.662	0.727	0.854	0.798	0.739
14	0.519	0.884	0.869	0.845	0.834	0.737	0.769	0.865	0.854	0.780
20	0.618	0.897	0.883	0.862	0.859	0.805	0.810	0.883	0.896	0.834
24	0.706	0.904	0.891	0.878	0.873	0.817	0.826	0.893	0.930	0.877
30	0.758	0.907	0.895	0.882	0.880	0.845	0.842	0.893	0.915	0.847
34	0.752	0.910	0.899	0.890	0.882	0.855	0.848	0.894	0.924	0.862
40	0.825	0.925	0.919	0.906	0.903	0.912	0.883	0.909	0.961	0.920

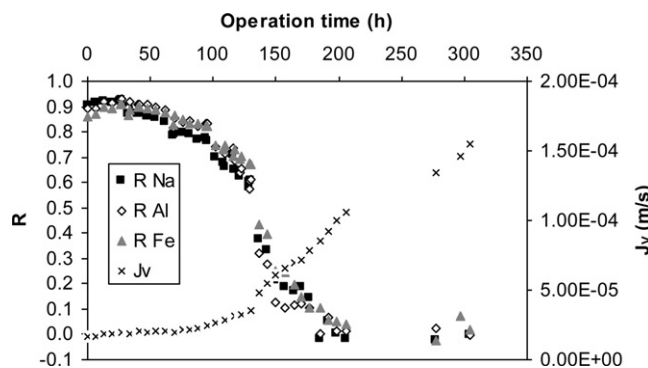


Fig. 4. Evolution of the rejection coefficients of the metals (R) and the permeate flux (J_V) in hydrogen peroxide solution medium.

up in two equations when the osmotic pressure related term is negligible (Abejón et al., 2010; Soltanieh & Gill, 1981):

$$J_V = L_P \Delta P \quad (1)$$

$$R = \frac{\sigma J_V}{J_V + \omega} \quad (2)$$

The estimation of the Kedem-Katchalsky parameters according to the experimentally obtained values of permeate flux and rejection coefficients was carried out and a great agreement of the modeled values with the experimental ones was achieved (the percentage of variation explained for the overall system was higher than 94%). The assessed model parameters are shown in Table 3.

Experiments oriented to evaluate membrane resistance when working in concentrated hydrogen peroxide medium have also been carried out. The evolution of the permeate rate and rejection coefficients was studied along a 300 h lasting trial. The permeate flux was constant for the first 70 h but after this initial period an initially small increase on the permeate production was found. Evidences of faster flux increase appeared after 120 h and, as shown in Fig. 4, an exponential growth graph can be sensed when the complete evolution of the membrane performance is observed. As the applied pressure was maintained constant at 40 bar, the permeate variation is explained as consequence of changes in the hydraulic permeability coefficient of the membrane (L_P) due to membrane degradation in such as an oxidant medium. Additionally, the observed retention coefficients during the experiment follow a decreasing logistic behavior: after the initial phase where values were maintained constant for around 70 h, the rejection coefficients fell down initially slowly and then drastically until reaching the zero level after 170 h of contact between the membrane and the hydrogen peroxide (Fig. 4). This decline with respect to rejection performance also confirms the hypothesis of severe membrane degradation after short contact period, so it can be concluded that the effective lifetime for the BE membrane in 35% hydrogen peroxide medium working under applied pressure of 40 bar should not be extended for more than 75 h (72 h, corresponding to 3 full days, would be an adequate limit).

3. Design of integrated countercurrent membrane cascades

3.1. Reverse osmosis cascades modeling

The proposed simulation model is based on the Kedem-Katchalsky equations (Eqs. (1) and (2)) for solvent and solute transport through reverse osmosis membranes and overall and component material balances. To demonstrate the modeling procedure, the representation for a general n -stages cascade is detailed.

Firstly, the overall and component (metal) material balances for each stage are composed:

Initial stage (1)

$$F + R_2 = F_1 \quad (3)$$

$$F C_F^{\text{metal}} + R_2 C_{R2}^{\text{metal}} = F_1 C_{F1}^{\text{metal}} \quad (4)$$

$$F_1 = P_1 + R_1 \quad (5)$$

$$F_1 C_{F1}^{\text{metal}} = P_1 C_{P1}^{\text{metal}} + R_1 C_{R1}^{\text{metal}} \quad (6)$$

Intermediate stages (i)

$$P(i-1) + R(i+1) = F(i) \quad (7)$$

$$P(i-1) C_{P(i-1)}^{\text{metal}} + R(i+1) C_{R(i+1)}^{\text{metal}} = F(i) C_{F(i)}^{\text{metal}} \quad (8)$$

$$F(i) = P(i) + R(i) \quad (9)$$

$$F(i) C_{F(i)}^{\text{metal}} = P(i) C_{P(i)}^{\text{metal}} + R(i) C_{R(i)}^{\text{metal}} \quad (10)$$

Final stage (n)

$$P(n-1) = F(n) \quad (11)$$

$$P(n-1) C_{P(n-1)}^{\text{metal}} = F(n) C_{F(n)}^{\text{metal}} \quad (12)$$

$$F(n) = P + R(n) \quad (13)$$

$$F(n) C_{F(n)}^{\text{metal}} = P C_{P(n)}^{\text{metal}} + R(n) C_{R(n)}^{\text{metal}} \quad (14)$$

The feed, permeate and retentate volume flows of the corresponding i membrane stage are represented by $F(i)$, $P(i)$ and $R(i)$ respectively; $C_{F(i)}^{\text{metal}}$, $C_{P(i)}^{\text{metal}}$ and $C_{R(i)}^{\text{metal}}$ are the metal concentrations of the corresponding feed, permeate and retentate streams and F and P relate to the initial feed and final permeate streams. The material balances can be formulated in terms of mass or volume base taking into account that there is no change in the density of the aqueous hydrogen peroxide during the process operation. There is no dilution or concentration of the solution as it was checked experimentally in a previous study (Abejón et al., 2010).

Secondly, the characteristic variables that describe the performance of the i reverse osmosis stage, namely membranes specific permeate flux ($J_{V(i)}$) and retention coefficient of each metal ($R_{(i)}^{\text{metal}}$), can be defined by direct application of the Kedem-Katchalsky equations:

$$J_{V(i)} = L'_P \Delta P_{(i)} \quad (15)$$

$$R_{(i)}^{\text{metal}} = \frac{\sigma^{\text{metal}} J_{V(i)}}{J_{V(i)} + \omega_{\text{metal}}} \quad (16)$$

The applied pressure in the i stage is symbolized by $\Delta P_{(i)}$. Once the membrane transport is defined, the characteristics of the

Table 3

Kedem-Katchalsky model parameters for BE membrane in hydrogen peroxide solution medium.

	B	Na	Al	Ti	Cr	Mn	Fe	Ni	Cu	Zn
ω' (m/s)	5.58×10^{-6}	2.60×10^{-7}	3.38×10^{-7}	5.11×10^{-7}	7.19×10^{-7}	2.50×10^{-6}	1.40×10^{-6}	4.03×10^{-7}	1.17×10^{-6}	1.53×10^{-6}
σ	1.000	0.926	0.920	0.917	0.925	1.000	0.928	0.920	1.000	0.964
L_P (m/s bar)						4.92×10^{-7}				

Table 4

Economic model parameters.

Parameter	Unit	Value
Y_{memb}	(\$/m ²)	50
LT_{memb}	(d)	3
LT_{inst}	(d)	1825
K_{memb}		0.12
Y_{raw}	(\$/m ³)	790
Y_{EG1}	(\$/m ³)	2592
Y_{EG2}	(\$/m ³)	3537
Y_{EG3}	(\$/m ³)	3780
Y_{EG4}	(\$/m ³)	8721
Y_{EG5}	(\$/m ³)	11,826
Y_{by}	(\$/m ³)	600
Y_{lab}	(\$/h)	7
Y_{elec}	(\$/kWh)	0.08
η		0.70
CC_{clean}	(\$/d)	2590

permeate streams (flow and metal concentrations) can be calculated as function of the membrane area of the corresponding i stage ($A_{(i)}$):

$$P(i) = A_{(i)} J_{V(i)} \quad (17)$$

$$C_{P(i)}^{\text{metal}} = (1 - R_{(i)}^{\text{metal}}) C_{F(i)}^{\text{metal}} \quad (18)$$

Finally, the recovery ratio of each module ($\text{Rec}_{(i)}$) is defined:

$$\text{Rec}_{(i)} = \frac{P(i)}{F(i)} \quad (19)$$

3.2. Economic considerations

A straightforward economic model based on revenues and costs is proposed to evaluate the profitability of the simulated membranes cascades. Information about the values for all the parameters appearing in the economic model can be observed in **Table 4**. The commercial prices of the different SEMI Grades of hydrogen peroxide and the employed membrane are taken from references (Freedonia Group, 2004 and Maskan, Wiley, Johnston, & Clements, 2000 respectively).

The daily profit of the process (Z), defined as the difference between total daily revenues (Rev) and costs (TC), was the selected evaluable variable:

$$Z = \text{Rev} - \text{TC} \quad (20)$$

The electronic grade hydrogen peroxide obtained as the final stage permeate (P) is the main product of the membrane cascade, but the other output stream of the process, the retentate of the first stage ($R1$), can also be considered valuable as it could be commercialized as a by-product useful for hydrogen peroxide applications where metallic content is not a limiting factor. According to this approach, two different terms have to be incorporated to assess the total daily revenues:

$$\text{Rev} = PY_{\text{EG}} + R1Y_{\text{by}} \quad (21)$$

The total daily costs of the system were calculated by the addition of the capital costs (CC) and the operation costs (OC). The capital costs attributable to membranes or to the rest of the installation were differentiated, while the operation costs were itemized into raw materials, labor, energy and maintenance costs:

$$\text{TC} = \text{CC} + \text{OC} \quad (22)$$

$$\text{CC} = CC_{\text{memb}} + CC_{\text{ins}} \quad (23)$$

$$\text{OC} = OC_{\text{raw}} + OC_{\text{lab}} + OC_{\text{en}} + OC_m \quad (24)$$

The capital costs of the membranes modules considering straight-line depreciation were expressed as function of the total membrane area of the installation:

$$CC_{\text{memb}} = \frac{Y_{\text{memb}} \sum A_i}{LT_{\text{memb}}} \quad (25)$$

Once the membranes costs were defined, the capital costs corresponding to the rest of the installation were related to them by mean of a coefficient (K_{memb}) that expressed the contribution of the investment in membranes to the total capital costs. The percentage of the total investment attributable to the membranes typically range between 12% and 30% (Fariñas, 1999; Medina SanJuan, 2000), so the value of K_{memb} was fixed to 0.12 with the intention of representing the most disadvantageous scenario:

$$CC_{\text{ins}} = CC_{\text{memb}} \frac{(1 - K_{\text{memb}})}{K_{\text{memb}}} \frac{LT_{\text{memb}}}{LT_{\text{inst}}} + CC_{\text{clean}} \quad (26)$$

Ultrapurification processes require contamination control, so the installation needed to be included in a cleanroom to provide the necessary controlled atmosphere. The capital costs attributable to the cleanroom (CC_{clean}) were calculated according to the model proposed by Yang and Eng Gan (2007) for a Class 100 space of 200 m² (200 air changes per hour) with raised floor and FFU type air ventilation:

$$CC_{\text{clean}} = -1645051 + 5156.6CA + 68.8MAV + 34EAV + 2996627AFC + AN \quad (27)$$

The term AN, that did not appear in the originally formulated model (Yang & Eng Gan, 2007), was added to include the costs related to analysis and quality control. Its value was assessed according to the research group experience in analytical equipment management, mainly inductively coupled plasma mass spectrometry (ICP-MS) and ion chromatography (IC).

The operation costs are essentially based on the consumption of the corresponding resource, except for the case of maintenance costs, which are function of the total capital costs (Shaalaa, Sorour, & Tewfik, 2000). The only required raw material was the technical grade hydrogen peroxide employed as feed and the installation was designed to be totally managed by a single worker:

$$OC_{\text{raw}} = FY_{\text{raw}} \quad (28)$$

$$OC_{\text{lab}} = 24Y_{\text{lab}} \quad (29)$$

$$OC_{\text{en}} = \frac{\sum (F(i)\Delta P_i)}{36\eta} Y_{\text{elec}} \quad (30)$$

$$OC_m = 0.05CC \quad (31)$$

3.3. Simulation and optimization

By implementation of the aforementioned proposed models in the Aspen Custom Modeler software, simulations of diverse membrane cascades can be executed and their economic trends can be investigated. But optimum design parameters and operation condition that would maximize profit can easily be obtained by applying an optimization routine (Guria et al., 2005; Sassi & Mujtaba, 2010; Voros et al., 1996). GAMS software was selected as optimization tool to manage the posed nonlinear programming (NLP) model using CONOPT3 solver. The General Algebraic Modeling System (GAMS) is a high-level modeling system for mathematical programming and optimization. It consists of a language compiler and a stable of integrated high-performance solvers (Brooke, Kendrick, & Raman, 1998).

The daily profit (Z), defined by Eq. (20), was chosen as the formulated objective function to maximize. All the model variables have

Table 5
Optimization problem formulation.

Objective function	Z (Eq. (20))
Optimization target	Maximization
Independent variables	$Rec_{(i)}, \Delta P_{(i)}$
Constraints to independent variables	$0.5 < Rec_{(i)} < 0.9$ $10 < \Delta P_{(i)} < 40$
Other constraints	Conc Prod < Conc SEMI

been expressed in terms of the independent design and operation variables, that is to say, recovery rates (Rec_i) and applied pressures (ΔP_i). Constraints for the independent variables have been set as gathered in Table 5. The valid interval of the recovery rate was defined from 0.5 to 0.9 taking into account the values referenced when membrane processes are applied to industrial installations (Noronha, Mavrov, & Chmiel, 2002; Shaalan et al., 2000; Zhu et al., 2010). Recovery rates close to 1 may cause problems of polarization, and recovery rate values close to 0 imply very low production rates. Related to the pressure range, it has been chosen to operate under safe conditions taking into account the maximum pressure recommended by the manufacturer of the BE membranes.

In mathematical terms (general form with all the terms of the equations or inequalities in the left side) the optimization model can be expressed as follows:

$$\begin{aligned} \max Z &= f(x) \\ \text{s.t. } h(x) &= 0 \\ w(x) &\leq 0 \\ x \in \mathbb{R}^n & \\ x_L < x &< x_U \end{aligned}$$

being Z the daily profit, x the vector of continuous variables ($\Delta P_{(i)}$ and $Rec_{(i)}$), h the vector of equality constraint functions (material balance equations (Eqs. (3)–(14)) and transport equations (Eqs. (15)–(19))) and w the vector of inequality constraint functions defining the product requirements based on the concentration limit for each metallic cation:

$$C_P^{\text{metal}} \leq C_{\text{SEMI}}^{\text{metal}} \quad (32)$$

4. Results of RO cascades and discussion

4.1. Evaluation of two-stage cascade

Simulation was undertaken assuming the coupling of the ultra-purification installation to a manufacturing plant with a target annual production aimed to electronic grade purposes of 9000 tons of hydrogen peroxide. When 330 operating days per year are considered, the corresponding feed flow is $24.2 \text{ m}^3/\text{d}$. The characterization of the feed stream is based on typical impurities content of technical grade hydrogen peroxide and the concentrations of the

main metallic impurities are showed in Table 6. The recovery ratios of the modules were chosen as design variables and a value of 0.7 was selected. The applied pressure was the only remaining operation variable and it was decided to simulate the process under 25 bar pressure.

The main results of the simulated two-stage integrated reverse osmosis cascade for hydrogen peroxide ultrapurification are presented in Table 6, where the flows and metallic contents of each stream can be observed. The checking of the material balances, total and component, resulted in acceptable relative errors, being calculated that the maximum relative error in the balances for all the metal ions was 0.6%. The permeate flow of the second stage was $15.0 \text{ m}^3/\text{d}$, so 62% of the feed stream was recovered as ultrapurified product. The final product achieved impurities concentrations that satisfied the SEMI Grade 1 requirements. On the one hand, the most efficiently retained metal was Cu, which concentration reduced by 99.4% from feed conditions. On the other hand, B rejection is the lowest among the analyzed metals (90.7% of reduction). In relation to the dimensions of the modules, 20.2 and 14.1 m^2 of membrane area were required for stages 1 and 2 respectively.

4.2. Influence of design and operation variables in two-stage cascade

A sensibility analysis to study the influence of the main design and operation variables (recovery rates and applied pressures) over the principal variables of a two-stage integrated simulated installation was previously performed by this research group (Abejón et al., 2012).

High applied pressures in both stages are beneficial for the process in both equipment dimensions and product quality terms: the total membrane area required for a constant recovery rate is smaller when high pressures are applied and the final product stream is obtained with lower metallic content. This is a direct effect of the greater permeate flux and rejection coefficients resulting from higher applied pressures. Upper energy consumption is the counterbalance to these advantages.

The analysis of the effects produced by design decisions about the recovery rates is not as simple as that corresponding to the applied pressures. Obviously, high recovery rates (especially in the first stage) imply high product stream flow as less material is able to leave the system by the first stage retentate stream. The counterpoint to the greater production is the higher demanded membrane area required to permit the increased permeate flow. The maximum membrane area corresponds to the case where the maximum recovery rate is wanted for the first stage while the second stage works at its minimum value. This situation implies the highest flow for the recirculation stream and, as a consequence, the flow entering the first stage reaches its maximum after feed and recirculation

Table 6
Material flow for the two-stage integrated reverse osmosis cascade.

	Streams					SEMI Grade 1 limits
	F	R1	P1	R2	P	
Flow (m^3/d)	24.19	9.19	21.43	6.43	15.01	
Concentration (ppb)						
B	8	20	2.4	6.2	0.7	100
Na	25,000	65,535	1960	6105	183	1000
Al	1300	3404	115	356	12	1000
Ti	80	209	8.2	25	1.0	300
Cr	55	144	6.0	18	0.8	50
Mn	5	13	0.7	2.2	0.1	50
Fe	200	519	29	87	4.9	100
Ni	30	79	2.8	8.6	0.3	50
Cu	3	7.9	0.2	0.7	0.0	50
Zn	15	39	1.9	5.6	0.3	100

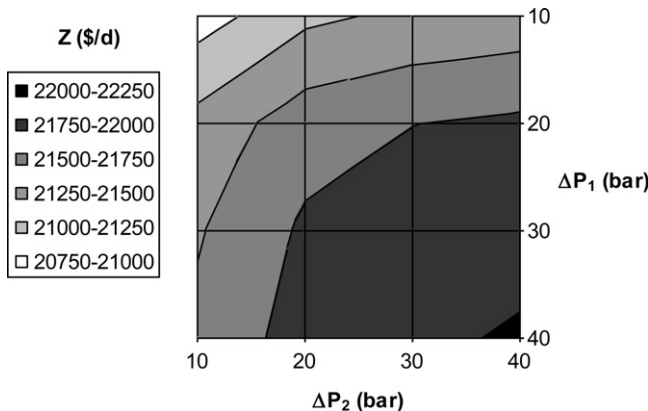


Fig. 5. Dependence relation of the applied pressures (ΔP_1 and ΔP_2) over the two reverse osmosis stages upon the daily profit of the process (Z).

mixing. On the other hand, when the recovery in the first stage is low, the system becomes very little sensitive in terms of membrane area variation to changes in the second stage recovery design. The maximum membrane area case is also characterized because it is the situation where the highest final product quality is achieved. The high recovery rate implies the dilution of the stream entering the first stage with retentate from the second stage.

To condense all the information relative to the changes in the system performance caused by variation in the design and operation variables, a new sensibility analysis was carried out. In this case, the daily economic profit of the process Z (Eq. (20)) was selected as studied variable since it included all the impacts of the different system changes.

The applied pressures were changed in the bracket from 10 to 40 bar to study the evolution of the installation performance while the recovery rates of both stages were fixed at 0.7. Trends depicted in Fig. 5 indicate that the extra energy costs attributable to higher applied pressures are compensated only too well for the reduction of the total membrane area of the installation. On the other hand, the recovery rates were changed between 0.5 and 0.9 for a constant applied pressure of 25 bar in both stages. Again in this case, as showed in Fig. 6, the maximum profit is achieved when the recovery rates equal the upper limit of the range. Despite the larger total membrane area required for elevated recovery rates, this situation implies very scarce by-product stream from first stage retentate so most of the feed leaves the system as second stage permeated product. It is worth making such an inversion in membranes because of the high economic yield of electronic grade hydrogen peroxide (due

to its profitable price). When results relative to applied pressures and recovery rates are compared, it is obvious that the decision about the recovery rates of the system is a factor much more crucial for the profitability of the installation than the resolution of the main operational variable, as modification of the applied pressures causes impacts on the economy of the process an order of magnitude smaller than the ones corresponding to recovery rates (about 2000 \$/d range versus higher than 20,000 \$/d). Specifically, the recovery rate of the first stage is the most controlling variable of the process in economic terms, as it is the most important factor in defining the flow of obtained by-product.

4.3. Optimization of two-stage cascade

After examination of the general trends depicted by the sensibility analysis of the independent variables (applied pressures and recovery rates), their optimum values that would maximize the daily profit of the ultrapurification process were identified by run of the corresponding NLP problem within GAMS software. The results of the simulated and optimized installations are compiled in Table 7.

It was found that the optimum applied pressures for both stages were 40 bar, which is the upper boundary restriction for these variables. In a similar way, both optimum recovery rates were limited by the upper limit of the defined range. Under these conditions, the daily profit could attain 34,928 \$/d (equivalent to an annual profit of 11.5 mill\$). This amount is 60% higher than the profit of the simulated process, so demonstration of the significance of proper design and operation conditions was clear. The extra profit of the simulated case was obtained by both increase in the process revenues and decrease in the total costs. The higher revenues corresponded to higher second stage permeate production (added-value stream) as consequence of the raised recovery rates, while the reduced total costs were attributable to the shorter membrane area of the system when maximum pressures were applied. The optimization results are in total agreement with the tendencies pointed out by the sensibility analysis, so the module recovery and applied pressure should be as high as practically possible in both stages.

4.4. Optimum reverse osmosis cascade for each SEMI Grade hydrogen peroxide ultrapurification

Once the membrane cascade integrated by two stages was optimized for production of SEMI Grade 1 hydrogen peroxide, simulations were run to assess the number of required stages for achievement of each of the other SEMI Grades (from Grade 2 to 5). The optimum values for the independent variables (applied pressures and recovery rates) obtained in the two-stage case were taken as basis for the simulated systems. Subsequently, optimization of the cascades consisted of the number of stages calculated by the simulation process was resolved.

The Table 7 illustrates the size of the cascades required for each SEMI Grade. The number of integrated stages rose to 7 when the most exigent Grade 5 was the target product. Optimization solutions for all the cascades are also showed in Table 7. The optimum values for the design and operation variables were maintained at their upper boundary limit for all the cases: 0.9 recoveries and 40 bar for all the stages in every cascade. The maximum profit of the process grew exponentially for the two strictest grades (SEMI Grade 4 and 5) mainly as a consequence of their high market prices. The costs of the installations, as showed in Fig. 7, are much more stable (hardly increased) than the related revenues.

The main cost of the process was the acquisition the raw material that represented more than 80% of the total costs for all the cascades (Table 8). The rest of the operational costs became insignificant when compared to the cost corresponding to feed hydrogen

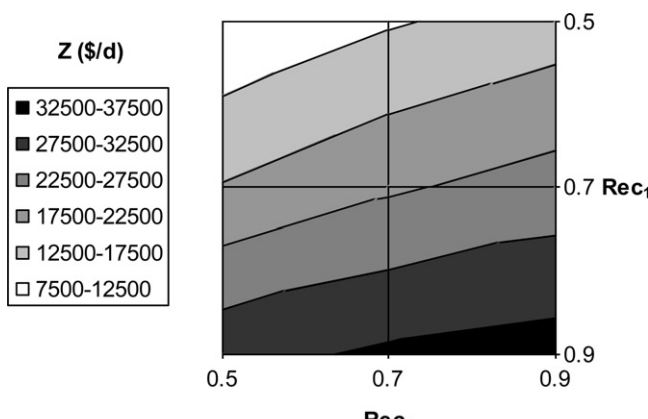


Fig. 6. Dependence relation of the recovery rates (Rec_1 and Rec_2) of the two reverse osmosis stages upon the daily profit of the process (Z).

Table 7
Optimization results.

H_2O_2 Grade	Grade 1		Grade 2		Grade 3		Grade 4		Grade 5	
	Simulation case (2 stages)	Optimized case (2 stages)	Optimized case (4 stages)	Optimized case (5 stages)	Optimized case (6 stages)	Optimized case (7 stages)				
$\Delta P_{(i)}$ (bar)	25	40	40	40	40	40				
$Rec_{(i)}$	0.7	0.9	0.9	0.9	0.9	0.9				
P (m^3/d)	15.0	21.5	21.5	21.5	21.5	21.5				
$C_p^{(N)}$ (ppb)	183	182	1.3	0.1	0.01	0.001				
ΣA (m^2)	34.3	26.8	54.2	68.2	82.2	96.2				
Economic terms (\$/d)										
Z	21,793	34,928	54,696	59,668	165,657	232,170				
Rev	44,402	57,405	77,677	82,891	189,132	255,896				
TC	22,609	22,477	22,972	23,223	23,474	23,726				
CC	3169	3041	3505	3741	3977	4213				
CC_{memb}	572	446	904	1137	1371	1604				
CC_{inst}	2597	2595	2601	2604	2607	2609				
OC	19,441	19,436	19,467	19,482	19,497	19,512				
OC_{raw}	19,110	19,110	19,110	19,110	19,110	19,110				
OC_{lab}	168	168	168	168	168	168				
OC_{en}	4	6	13	17	20	23				
OC_m	159	152	175	187	199	211				

Table 8
Breakdown of the total costs of the optimized installations.

H_2O_2 Grade	Contributions to total costs (%)					
	Grade 1		Grade 2		Grade 3	
	Simulation case (2 stages)	Optimized case (2 stages)	Optimized case (4 stages)	Optimized case (5 stages)	Optimized case (6 stages)	Optimized case (7 stages)
CC	14.0	13.5	15.3	16.1	16.9	17.8
CC_{memb}	2.5	2.0	4.0	4.9	5.8	6.8
CC_{inst}	11.5	11.5	11.3	11.2	11.1	11.0
OC	86.0	86.5	84.7	83.9	83.1	82.2
OC_{raw}	84.5	85.0	83.2	82.3	81.4	80.5
OC_{lab}	0.7	0.8	0.7	0.7	0.7	0.7
OC_{en}	<0.1	<0.1	0.1	0.1	0.1	0.1
OC_m	0.7	0.7	0.7	0.8	0.9	0.9

peroxide as none of them attained the 1%. On the other hand, when focusing on the capital costs, the investment on membranes contributes by no more than 7% to the total costs (even for the seven-stage cascade that required close to 100 m^2 of total membrane area) despite the high replacement rate consequence of the short membrane lifetime in such an oxidant medium.

The manufacturer of the BE membranes provides also the spiral wound modules for large scale applications, so the arrangement of several modules in parallel would be an option to get the required total membrane area (it was considered to summarize as total membrane area of each installation, taking into account that the areas of every stages were in the same order of magnitude and none of them tend to zero).

The process economy invited to promote the production of the higher quality hydrogen peroxide but market restrictions (in the

case of limited demand for the most exigent SEMI Grades) may represent the counterpoint to this situation. Further work is focused to the multi-objective optimization problem, in order to include the quality grade objective besides the economic profit.

5. Conclusions

This work is focused to the application of integrated reverse osmosis cascades as configurations of membrane process to be introduced for the ultrapurification of wet chemicals to electronic grade. For the particular case of hydrogen peroxide as one of the most consumed wet electronic chemicals, five different electronic grades are demanded by the semiconductor industry, as SEMI has recently updated the applicable specifications through SEMI Document C30-1110.

It was determined the size of the integrated stages in the reverse osmosis cascade required for achieving each SEMI Grade hydrogen peroxide from the technical grade peroxide, given by the comparison of the metal ion concentrations, calculated from the solution of the material balances and the transport model (Kedem-Katchalsky equations), related to their limiting impurities content (SEMI). The number of integrated stages rose to 7 when the most exigent Grade 5 was the target product.

The optimization results showed the benefits of the reverse osmosis process, with profit values of 20–85 million\$/year, for a target annual production of 9000 tons of electronic hydrogen peroxide. The maximum profit of the process grew exponentially for the two strictest grades (SEMI Grade 4 and 5) mainly as a consequence of their high market prices. The main cost of the process

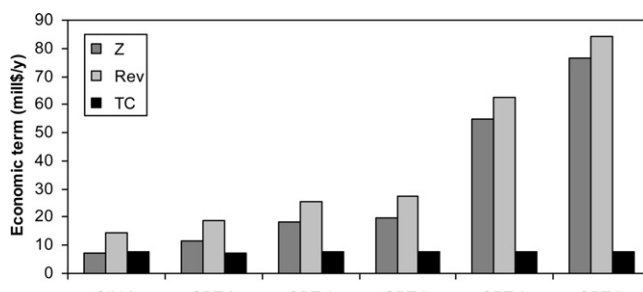


Fig. 7. Optimum profits (Z) and the corresponding revenues (Rev) and total costs (TC) of each electronic grade.

was the acquisition the raw material that represented more than 80% of the total costs for all the cascades. Focusing on the capital costs, the investment on membranes contributed by no more than 7% to the total costs (even for the seven-stage cascade that required close to 100 m² of total membrane area) despite the high replacement rate consequence of the short membrane lifetime in such an oxidant medium.

The optimum values for the design and operation variables were maintained at their upper boundary limit for all the cases, 0.9 recovery rate and 40 bar pressure, for all the stages in every cascade. A sensitivity analysis was used to study the influence of these variables in the profit of the reverse osmosis process, concluding with the recovery rate as the most crucial factor for decision.

Acknowledgments

This research has been financially supported by the Ministry of Science and Innovation of Spain (MICINN) through CTM2006-00317 and CTQ2010-16608 Projects. R. Abejón acknowledges also the assistance of MICINN for the award of a FPI grant (BES-2008-003622).

References

- Abatemarco, T., Stickel, J., Belfort, J., Frank, B. P., Ajayan, P. M., & Belfort, G. (1999). Fractionation of multiwalled carbon nanotubes by cascade membrane microfiltration. *Journal of Physical Chemistry B*, 103, 3534–3538.
- Abejón, R., Garea, A., & Irabien, A. (2010). Ultrapurification of hydrogen peroxide solution from ionic metals impurities to semiconductor grade by reverse osmosis. *Separation and Purification Technology*, 76, 44–51.
- Abejón, R., Garea, A., & Irabien, A. (2012). Analysis, modelling and simulation of hydrogen peroxide ultrapurification by multistage reverse osmosis. *Chemical Engineering Research & Design*, 90, 442–452.
- Ahmetović, E., & Grossmann, I. E. (2010). Strategies for the global optimization of integrated process water networks. *Computer Aided Chemical Engineering*, 28, 901–906.
- Ahmetović, E., & Grossmann, I. E. (2011). Global superstructure optimization for the design of integrated process water networks. *AIChE Journal*, 57, 434–457.
- Atsumi, J., Ohtsuka, S., Munehira, S., & Kajiyama, K. (1990). Metallic contamination on Si wafers from cleaning solutions. *Proceedings – The Electrochemical Society*, 90, 59–66.
- Baker, R. W. (2010). Research needs in the membrane separation industry: Looking back, looking forward. *Journal of Membrane Science*, 362, 134–136.
- Baker, R. W., Cussler, E. L., Eykamp, W., Koros, W. J., Riley, R. L., & Strathmann, H. (1991). *Membrane separation systems: Recent developments and future directions*. Park Ridge: Noyes Data Corporation.
- Benito, Y., & Ruiz, M. L. (2002). Reverse osmosis applied to metal finishing wastewater. *Desalination*, 142, 229–234.
- Bianchi, U. P., Leone, U., & Lucci, M. (2001). Process for the industrial production of high purity hydrogen peroxide. U.S. Patent 6333018.
- Brooke, A., Kendrick, D., & Raman, R. (1998). *GAMS: A user's guide, release 2.50*. Washington, DC: GAMS Development Corporation.
- Caus, A., Braeken, L., Boussu, K., & van der Bruggen, B. (2009). The use of integrated countercurrent nanofiltration cascades for advanced separations. *Journal of Chemical Technology and Biotechnology*, 84, 391–398.
- Caus, A., Vanderhaegen, S., Braeken, L., & van der Bruggen, B. (2009). Integrated nanofiltration cascades with low salt rejection for complete removal of pesticides in drinking water production. *Desalination*, 241, 111–117.
- Daigle, S., Vogelsberg, E., Lim, B., & Butcher, I. (2007). Electronic chemicals. In *Ullmann's encyclopedia of industrial chemistry*. Electronic Release, Weinheim: Wiley-VCH.
- Das, C., DasGupta, S., & De, S. (2010). Treatment of dyeing effluent from tannery using membrane separation processes. *International Journal of Environment and Waste Management*, 5, 354–367.
- Duffalo, J. M., & Monkowski, J. R. (1984). Particulate contamination and device performance. *Solid State Technology*, 27, 109–114.
- Faigon, M., & Hefer, D. (2008). Boron rejection in SWRO at high pH conditions versus cascade design. *Desalination*, 223, 10–16.
- Fariñas, M. (1999). *Osmosis inversa: fundamentos, tecnología y aplicaciones*. Madrid: McGraw-Hill.
- Freedonia Group. (2004). Electronic chemicals to 2008. Industry Study n° 1852.
- Gassner, M., & Maréchal, F. (2010). Combined mass and energy integration in process design at the example of membrane-based gas separation systems. *Computers & Chemical Engineering*, 34, 2033–2042.
- Glueckstern, P., & Priel, M. (2003). Optimization of boron removal in old and new SWRO systems. *Desalination*, 156, 219–228.
- Gorenflo, A., Brusilovsky, M., Faigon, M., & Liberman, B. (2007). High pH operation in seawater reverse osmosis permeate: First results from the world's largest SWRO plant in Ashkelon. *Desalination*, 203, 82–90.
- Gosh, R. (2003). Novel cascade ultrafiltration configuration for continuous high-resolution protein-protein fractionation: A simulation study. *Journal of Membrane Science*, 226, 85–99.
- Gurak, P. D., Cabral, L. M. C., Rocha-Leao, M. H. M., Matta, V. M., & Freitas, S. P. (2010). Quality evaluation of grape juice concentrated by reverse osmosis. *Journal of Food Engineering*, 96, 421–426.
- Guria, C., Bhattacharya, P. K., & Gupta, S. K. (2005). Multi-objective optimization of reverse osmosis desalination units using different adaptations of the non-dominated sorting genetic algorithm (NSGA). *Computers & Chemical Engineering*, 29, 1977–1995.
- Ibáñez Mengual, J. A. (2009). *Desalación de aguas: aspectos tecnológicos, medioambientales, jurídicos y económicos*. Espinardo: Instituto Euromediterráneo del Agua.
- Isa, M. H. M., Coraglia, D. E., Frazier, R. A., & Jauregui, P. (2007). Recovery and purification of surfactin from fermentation broth by a two-step ultrafiltration process. *Journal of Membrane Science*, 296, 51–57.
- Karuppiah, R., & Grossmann, I. E. (2006). Global optimization for the synthesis of integrated water systems in chemical processes. *Computers & Chemical Engineering*, 30, 650–673.
- Lin, J. C. T., & Livingston, A. G. (2007). Nanofiltration membrane cascade for continuous solvent exchange. *Chemical Engineering Science*, 62, 2728–2736.
- Maskan, F., Wiley, D. E., Johnston, L. P. M., & Clements, D. J. (2000). Optimal design of reverse osmosis module networks. *AIChE Journal*, 46, 946–954.
- Mayani, M., Mohanty, K., Filipe, C., & Gosh, R. (2009). Continuous fractionation of plasma proteins HSA and IgG using cascade ultrafiltration systems. *Separation and Purification Technology*, 70, 231–241.
- Medina San Juan, J. A. (2000). *Desalación de aguas salobres y de mar. Osmosis inversa*. Madrid: Mundipress.
- Mellal, M., Ding, L. H., Jaffrin, M. Y., Delattre, C., Michaud, P., & Courtois, J. (2007). Separation and fractionation of oligouridines by shear-enhanced filtration. *Separation Science and Technology*, 42, 349–361.
- Morisaki, A., Sawaguri, Y., & Matsuda, Y. (1999). Apparatus and method for removing impurities from aqueous hydrogen peroxide. US Patent 5906738.
- Noronha, M., Mavrov, V., & Chmiel, H. (2002). Efficient design and optimisation of two-stage NF processes by simplified process simulation. *Desalination*, 145, 207–215.
- Overdevest, P. E. M., Hoenders, M. H. J., van't Riet, K., van der Padt, A., & Keurentjes, J. T. F. (2002). Enantiomer separation in a cascaded micellar-enhanced ultrafiltration system. *AIChE Journal*, 48, 1917–1926.
- Pérez, G., Fernández-Alba, A. R., Urtiaga, A. M., & Ortiz, I. (2010). Electro-oxidation of reverse osmosis concentrates generated in tertiary water treatment. *Water Research*, 44, 2763–2772.
- Redondo, J., Busch, M., & De Witte, J. P. (2003). Boron removal from seawater using FILMTEC™ high rejection SWRO membranes. *Desalination*, 156, 229–238.
- Restolho, J. A., Prates, A., de Pinho, M. N., & Afonso, M. D. (2009). Sugars and lignosulphonates recovery from eucalyptus spent sulphite liquor by membrane processes. *Biomass and Bioenergy*, 33, 1558–1566.
- Saehan Industries Corporation. (2007). RE8040-BE Product Specification Sheet Rev. 241112.
- Sassi, K. M., & Mujitaba, I. M. (2010). Simulation and optimization of full scale reverse osmosis desalination plant. *Computer Aided Chemical Engineering*, 28, 895–900.
- Scholz, W., & Lucas, M. (2003). Techno-economic evaluation of membrane filtration for the recovery and re-use of tanning chemicals. *Water Research*, 37, 1859–1867.
- Schweitzer, P. A. (1988). *Handbook of separation techniques for chemical engineers*. New York: McGraw-Hill.
- Semiconductor Equipment and Material International Association (SEMI®). (2010). Specifications for Hydrogen Peroxide. SEMI Document C30-1110.
- Shaalaa, H. F., Sorour, M. H., & Tewfik, S. R. (2000). Simulation and optimization of a membrane system for chromium recovery from tanning wastes. *Desalination*, 141, 315–324.
- Soltanieh, M., & Gill, W. N. (1981). Review of reverse osmosis membranes and transport models. *Chemical Engineering Communications*, 12, 279–363.
- Taniguchi, M., Fusaoka, Y., Nishikawa, T., & Kurihara, M. (2004). Boron removal in RO seawater desalination. *Desalination*, 167, 419–426.
- Tanuwidjaja, D., & Hoek, E. M. V. (2006). High-efficiency seawater desalination via NF/RO multi-pass arrays. In: AIChE Annual Meeting Conference Proceedings, San Francisco, CA, November 12–17.
- Voros, N., Maroulis, Z. B., & Marinou-Kouris, D. (1996). Optimization of reverse osmosis networks for seawater desalination. *Computers & Chemical Engineering*, 20(Suppl. 1), S345–S350.
- Voros, N. G., Maroulis, Z. B., & Marinou-Kouris, D. (1997). Short-cut structural design of reverse osmosis desalination plants. *Journal of Membrane Science*, 127, 47–68.
- Yang, L., & Eng Gan, C. (2007). Costing small cleanrooms. *Building and Environment*, 42, 743–751.
- Zhu, A., Christofides, P. D., & Cohen, Y. (2009). Minimization of energy consumption for a two-pass membrane desalination: Effect of energy recovery, membrane rejection and retentate recycling. *Journal of Membrane Science*, 339, 126–137.
- Zhu, A., Rahardianto, A., Christofides, P. D., & Cohen, Y. (2010). Reverse osmosis desalination with high permeability membranes – cost optimization and research needs. *Desalination and Water Treatment*, 15, 256–266.

4.4. Abejón, R.; Garea, A.; Irabien, A. *Optimum design of reverse osmosis systems for hydrogen peroxide ultrapurification*. AIChE Journal, 58:3718-3730 (2012).

Resumen

Este trabajo está orientado a la optimización de redes de ósmosis inversa propuestas para la ultrapurificación de reactivos desde grado técnico a los grados semiconductores demandados para aplicaciones electrónicas que requieren el empleo de reactivos líquidos de gran pureza para la producción de semiconductores, como en el caso del peróxido de hidrógeno que es habitualmente utilizado en los procesos de limpieza de obleas y acondicionamiento de sus superficies. Una instalación industrial capaz de producir de forma simultánea los diferentes cinco Grados Semiconductor Equipment and Materials International de peróxido de hidrógeno es representada por una configuración de superestructura simplificada formulada como un problema de programación no lineal. La red integra módulos de membranas de ósmosis inversa, mezcladores y distribuidores, definidos por las ecuaciones de los balances de materia y el modelo Kedem-Katchalsky de transporte para la descripción del flujo de permeado y los coeficientes de rechazos de los metales en cada etapa de membranas. El objetivo del diseño es maximizar el beneficio diario obtenido de la venta de los grados electrónicos de peróxido de hidrógeno producidos por el sistema de ultrapurificación.

Original abstract

This work is focused on the optimization of a reverse osmosis network proposed for the ultrapurification of chemicals, from technical grade to semiconductor grades demanded in electronic applications that require the use of high-purity wet chemicals in the semiconductor manufacturing, as it is the case of hydrogen peroxide that is commonly used in the wafer cleaning and surface conditioning processes. An industrial installation able to produce simultaneously the five different Semiconductor Equipment and Materials International Grades of hydrogen peroxide is represented by a simplified superstructure configuration formulated as a nonlinear programming problem. The network integrates reverse osmosis membrane modules, mixers, and split functions, defined by the equations of mass balances and the Kedem–Katchalsky transport model for the description of the permeate flux and the metal rejection coefficients at each membrane stage. The objective of the design is to maximize the daily profit obtained from the sale of the electronic grades of hydrogen peroxide produced by the ultrapurification system.

Optimum Design of Reverse Osmosis Systems for Hydrogen Peroxide Ultrapurification

Ricardo Abejón, Aurora Garea, Angel Irabien

Dept. de Ingeniería Química y Química Inorgánica, Universidad de Cantabria, Santander 39005, Cantabria, Spain

DOI 10.1002/aic.13763

Published online February 15, 2012 in Wiley Online Library (wileyonlinelibrary.com).

This work is focused on the optimization of a reverse osmosis network proposed for the ultrapurification of chemicals, from technical grade to semiconductor grades demanded in electronic applications that require the use of high-purity wet chemicals in the semiconductor manufacturing, as it is the case of hydrogen peroxide that is commonly used in the wafer cleaning and surface conditioning processes. An industrial installation able to produce simultaneously the five different Semiconductor Equipment and Materials International Grades of hydrogen peroxide is represented by a simplified superstructure configuration formulated as a nonlinear programming problem. The network integrates reverse osmosis membrane modules, mixers, and split functions, defined by the equations of mass balances and the Kedem-Katchalsky transport model for the description of the permeate flux and the metal rejection coefficients at each membrane stage. The objective of the design is to maximize the daily profit obtained from the sale of the electronic grades of hydrogen peroxide produced by the ultrapurification system. © 2012 American Institute of Chemical Engineers AICHE J, 58: 3718–3730, 2012

Keywords: reverse osmosis, membrane cascades, hydrogen peroxide, ultrapurification

Introduction

Semiconductor manufacturing involves a highly complex and delicate process, and a great variety of high-purity chemicals are required. As a typical silicon wafer might spend the equivalent of 2 days immersed in various liquids (specifically called wet chemicals) during the manufacturing process, the importance of extremely low levels of impurities in these wet chemicals becomes critical.¹ Ionic impurities in the wet chemicals cause problems resulting in the device failures.²

Aqueous hydrogen peroxide is among the most commonly used wet chemicals in semiconductor manufacturing.³ The traditional approach of wafer cleaning and surface conditioning is based on aqueous chemical processes that typically use hydrogen peroxide mixtures.⁴ The hydrogen peroxide demand in electronic applications along the last two decades and near-future forecast are depicted in Figure 1.⁵ The same graph also shows the percentage of total wet chemicals demand corresponding to hydrogen peroxide. The demand of hydrogen peroxide continues growing despite the static importance of this chemical among the wet chemicals. The likely decrease of relative contribution of hydrogen peroxide is due to alternatives technologies.⁶ Environmental health and safety issues are promoting the substitution of the strong chemicals used by this industrial sector, including hydrogen peroxide.^{7,8} However, hydrogen peroxide has also found new chances in this green revolution of the semiconductor industry.^{9–13}

Semiconductor Equipment and Materials International (SEMI) is the global industry association serving the manufacturing supply chains for the microelectronic, display, and photovoltaic industries. This association develops the worldwide most respected technical standards in this field. Among all the topics regulated, SEMI Document C30-1110 standardizes requirements for hydrogen peroxide used in the semiconductor industry.¹⁴ The requirements for hydrogen peroxide listed in Table 1 define five different electronic grades (Grades 1–5). Although typically commercialized grades of hydrogen peroxide have been treated by traditional purification techniques (L-L extraction, adsorption, membrane technologies, distillation, etc.) for reducing impurity levels, the very low content of contaminants demanded by the semiconductor industry requires of further ultrapurification treatment.¹⁵ While the least strict electronic grade (Grade 1) can be achieved by expert selection from technical grade and little additional treatment (filtration), the more stringent electronic grades require employment of further ultrapurification technologies.¹⁶

When the patents published over the last 20 years about ultrapurification of hydrogen peroxide for electronic purposes are reviewed,¹⁷ ion exchange emerges as the most frequently mentioned technology; but distillation is also widely used, especially for organic contamination reduction. Despite the wide number of different adsorbents that have been tested for hydrogen peroxide ultrapurification, this technology has become obsolete because of its low maximum efficiency when compared to other alternative options. All these referenced separation techniques could be replaced by membranes with lower operating expenses due to energy and chemicals.¹⁸ Some patents based on reverse osmosis can be found, but reverse osmosis is still not a dominant

Correspondence concerning this article should be addressed to R. Abejón at abejonr@unican.es.

© 2012 American Institute of Chemical Engineers

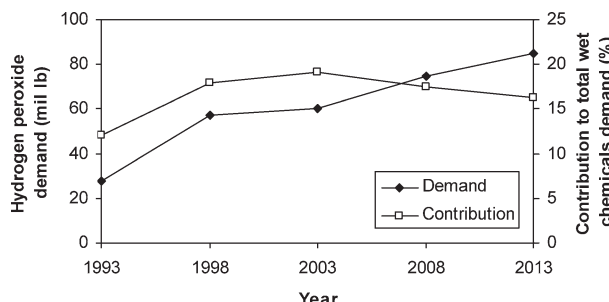


Figure 1. Evolution of hydrogen peroxide demand in electronic applications and contribution to total wet chemicals demand (based on Ref. 5).

ultrapurification technology, as membranes are used in combination with other separation techniques (mainly ion exchange) in hybrid processes. However, this research group has demonstrated recently the technical and economic viability of a reverse osmosis process without auxiliary techniques for production of electronic grade hydrogen peroxide.^{17,19}

Reverse osmosis membrane systems are mainly used for seawater and brackish water desalination, as this application has become the main source for supplying fresh water in the regions suffering from scarcity of natural fresh water resources.²⁰ The typical installation consists of a network of modules designed to fulfill technical, economic, and environmental requirements.^{21–24} The complete optimization of a reverse osmosis network has to include the optimal design of both individual modules and the network configuration. The performance of individual reverse osmosis modules in terms of particular module geometry and design and operational conditions has been widely analyzed,^{25–30} so suitable transport equations to describe the behavior of membrane modules are available to be applied to module optimization. The optimal configuration of reverse osmosis networks themselves had been less investigated,³¹ but recently, several research groups have focused their efforts on the research of optimum design of reverse osmosis systems based on the previous pioneer works.^{32–44} The configuration of reverse osmosis networks can be described by the use of stream distribution and matching boxes, designed to represent all possible combinations of stream splitting, mixing, bypass, and recycle.⁴⁵ By this formulation, all possible structure arrangements are considered, and the resulting mathematical optimization model can be solved as a mixed integer nonlinear programming (MINLP) problem. However, this network model can be simplified if the splitting boxes are considered as junctions.⁴⁶ In this case, the model can be formulated as a NLP problem by consideration of variable split ratios.

Table 1. Requirements for Electronic Grade Hydrogen Peroxide According to SEMI Standard

SEMI Electronic Grade	Assay (H_2O_2 , %)	Total Oxidizable Carbon (TOC) Limit (ppm)	Anion Limit Range	Cation Limit Range
1	30–32	20	2–5 ppm	10–1000 ppb
2	30–32	20	200–400 ppb	5–10 ppb
3	30–32	20	200–400 ppb	1 ppb
4	30–32	10	30 ppb	100 ppt
5	30–32	10	30 ppb	10 ppt

This study investigates the optimization of a reverse osmosis network used for ultrapurification of hydrogen peroxide from technical grade to semiconductor grades. An industrial installation able to produce the five different SEMI Grades is represented by a simplified superstructure formulated as a NLP problem. A membrane transport model adequate to describe the permeation of aqueous hydrogen peroxide solutions through reverse osmosis membranes is presented. The model is useful for the optimum selection of design (recovery rates) and operation (applied pressures) conditions and the configuration of the entire network.

Transport Model for Reverse Osmosis

The ion exclusion model has been used to describe the permeation of hydrogen peroxide through reverse osmosis membranes. This model had been previously applied for estimation of the permeation of weakly dissociated compounds in purification and ultrapurification processes by membranes technologies.^{47,48}

The derivation of the ion exclusion model is based on the following assumptions (Figure 2):

- All ions are excluded by the membrane (double layer effect).
- All species in molecular form permeate the membrane completely.
- Perfect mixing conditions prevail on the retentate and permeate sides of the membrane.
- Concentration polarization is ignored.

The final equation for estimating the permeate concentration (x_P) from the feed concentration (x_F) is presented as Eq. 1 (the complete derivation of the ion exclusion model equation was published by Kulkarni et al.⁴⁸). The only required parameter in Eq. 1 is the dissociation constant of the molecule to permeate.

$$x_P = x_F - \sqrt{K_A \cdot x_F} - \sqrt{K_A(x_F - \sqrt{K_A \cdot x_F})} \quad (1)$$

For the particular case of hydrogen peroxide, it can be considered as weakly acidic in aqueous solution, having a pK_A

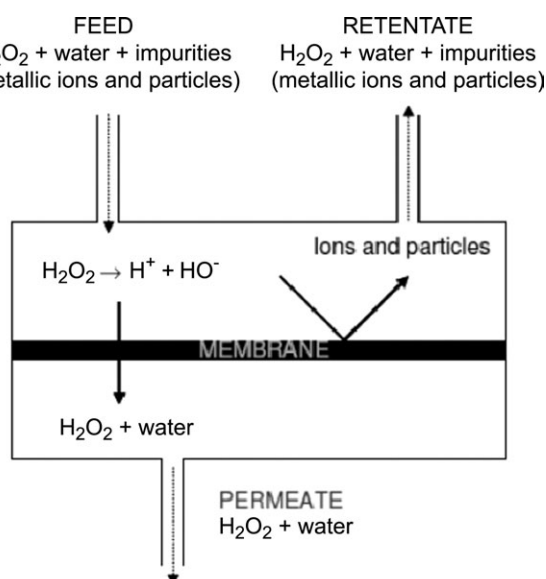


Figure 2. Schematic diagram of mass transfer through a reverse osmosis membrane for hydrogen peroxide aqueous solutions.

Table 2. Kedem–Katchalsky Model Parameters for Reverse Osmosis Membrane in Hydrogen Peroxide Solution Medium

	B	Na	Al	Ti	Cr	Mn	Fe	Ni	Cu	Zn
ω'_{metal} (m/d)	0.482	0.023	0.029	0.044	0.062	0.216	0.121	0.035	0.101	0.132
σ_{metal}	1.000	0.926	0.920	0.917	0.925	1.000	0.928	0.920	1.000	0.964
L_P (m/s bar)	4.92×10^{-7}									

of 11.75 ($K_A = 1.78 \times 10^{-12}$ M) at 20°C.¹⁵ The dissociation of the second proton is insignificant.⁴⁹ When the model was applied to feed concentrations limited by the minimum and maximum values of allowed SEMI Standard, namely, 30–32% (equivalent to x_F values in the range 8.8–9.4 M), the resultant permeate concentrations (x_P) predicted by the model reached values upper than 99.999% of their corresponding feed concentrations. These results imply no theoretical dilution of aqueous hydrogen peroxide solutions when forced to permeate through reverse osmosis membranes. Experimental determination of hydrogen peroxide concentration in both feed and permeated streams of a lab-scale reverse osmosis installation confirmed the performance predicted by the ion exclusion model.¹⁷

Once the validity of reverse osmosis for aqueous hydrogen peroxide solutions without practical dilution or concentration effects was asserted, the technical grade hydrogen peroxide could be considered as a unique solvent matrix (aqueous hydrogen peroxide solution) with several solutes (metallic impurities). Numerous transport models for reverse osmosis membrane separations can be found in bibliographic sources.⁵⁰ Some of the most common models were tested for the representation of the performance of the technical grade hydrogen peroxide ultrapurification process by means of a lab-scale experimental installation working with a polyamide flat-sheet reverse osmosis membrane.¹⁷ The Kedem–Katchalsky model was considered the most suitable for representing the performance of the reverse osmosis process, when used in the ultrapurification of aqueous hydrogen peroxide solutions.⁵¹ The Kedem–Katchalsky model has been widely used for predicting the behavior and performance of reverse osmosis systems^{52–54} and other membrane separations as nanofiltration and ultrafiltration.^{55–57}

The Kedem–Katchalsky model is based on three parameters: the solvent permeability of the membrane (L_P), the coefficient of solute mobility (ω), and the reflection coefficient (σ). According to the model, the solvent and solute fluxes (J_V and J_S respectively) are given as follows

$$J_V = L_P (\Delta P - \sigma \Delta \Pi) \quad (2)$$

$$J_S = \omega \Delta \Pi + (1 - \sigma) J_V (C_S)_{\ln} \quad (3)$$

where ΔP is the applied pressure, $\Delta \Pi$ is the osmotic pressure difference across the membrane, and $(C_S)_{\ln}$ logarithmic average solute concentration across the membrane. For the particular case of ultrapurification applications, the osmotic pressure difference can be neglected ($\Delta \Pi \approx 0$), as confirmed by the agreement between the values of the solvent fluxes for ultrapure water and water doped with metallic ions in the low ppm level.¹⁷ Hence, Eq. 2 can be simplified by elimination of the osmotic pressure term

$$J_V = L_P \Delta P \quad (4)$$

showing a proportional relationship between solvent flux and applied pressure (the solvent permeability L_P behaves as

proportionality coefficient between both variables). The solute flux J_S is not a practical variable, when tackling the management of reverse osmosis systems and the solute rejection coefficient appears as a more practical variable. The rejection coefficient (R) is defined as

$$R = \frac{C_F - C_P}{C_F} \quad (5)$$

where C_F and C_P represent the solute concentration on the feed and permeate streams, respectively. The rejection coefficient R can be expressed in terms of the Kedem–Katchalsky parameters by Pusch's approach^{58,59}

$$R = \frac{\sigma J_V}{J_V + \omega'} \quad (6)$$

where ω' is the modified coefficient of solute mobility obtained by application of the Morse equation (Eq. 7) for conversion of the osmotic pressure difference to concentration difference

$$\Pi = m i \mathfrak{R} T \quad (7)$$

$$\omega' = \omega v \mathfrak{R} T \quad (8)$$

where \mathfrak{R} is the gas constant, T the temperature, i the van't Hoff factor, m the solute molar concentration, and v a stoichiometric coefficient based on van't Hoff factor.

The equations of the reverse osmosis model have been incorporated to the optimization programming with the corresponding parameters derived from experimental results. The estimation of the Kedem–Katchalsky parameters for hydrogen peroxide ultrapurification by reverse osmosis membrane had been previously carried out by this research group according to experimentally obtained values of permeate flux and rejection coefficients for varying applied pressures.¹⁷ The obtained parameters are listed in Table 2.

Superstructure Configuration

The typical module arrangements for reverse osmosis networks can be categorized as straight-through, tapered, or cascade designs.³¹ The straight-through and tapered arrangements are multistage systems with several modules in parallel in each stage. In the straight-through scheme, the number and size of the modules are identical for every stage, whereas in the tapered scheme, the number or the size of the modules decreases over successive stages. Both arrangements can be modified by addition of recycle and bypass streams or inclusion of retentate or permeate reprocessing. On the other hand, cascade design of reverse osmosis systems follows the principles for multistage fractionation columns: multipass permeate configuration is applied to purify the permeate, when the target solute rejection cannot be accomplished in a single stage, and reflux is reproduced by stream recycling for each stage.

As a previous work of this research group,⁶⁰ the applicability of reverse osmosis membrane cascade configuration

Table 3. Feeding Conditions (Concentrations of Metals and Flow of the Feed Stream F)

Concentration (ppb)	
B	8
Na	25000
Al	1300
Ti	80
Cr	55
Mn	5
Fe	200
Ni	30
Cu	3
Zn	15
Flow (m ³ /d)	24.19

to hydrogen peroxide ultrapurification was investigated. The number of stages required for obtaining each electronic grade was determined by means of simulation, based on the cation limit range (Table 3), and the results show viable installations from two to seven stages (corresponding to SEMI Grade 1 and 5, respectively). Based on these results, the superstructure shown in Figure 3 was designed. It represents a seven-stage countercurrent cascade system able to produce simultaneously all the different SEMI Grades. The network integrates reverse osmosis membrane modules, mixers, and split junctions. The complete mathematical model that describes the superstructure was formulated as follows by the appropriate equations based on mass balances and the Kedem–Katchalsky transport model.

Mixers:

$$Q(i)_{\text{mixin}1} + Q(i)_{\text{mixin}2} = Q(i)_{\text{mixout}} \quad (9)$$

$$Q(i)_{\text{mixin}1} C(i)_{\text{mixin}1}^{\text{metal}} + Q(i)_{\text{mixin}2} C(i)_{\text{mixin}2}^{\text{metal}} = Q(i)_{\text{mixout}} C(i)_{\text{mixout}}^{\text{metal}} \quad (10)$$

where $Q(i)_{\text{mixin}1}$, $Q(i)_{\text{mixin}2}$ and $C(i)_{\text{mixin}1}^{\text{metal}}$, $C(i)_{\text{mixin}2}^{\text{metal}}$ denote, respectively, the flows of the streams entering the i mixer and the corresponding concentrations of each metal in the same streams, and $Q(i)_{\text{mixout}}$ and $C(i)_{\text{mixout}}^{\text{metal}}$ denote the flow of the stream leaving the i mixer and the respective metal concentration, respectively.

Split junctions:

$$Q(j)_{\text{splitin}} = Q(j)_{\text{splitout}1} + Q(j)_{\text{splitout}2} \quad (11)$$

$$Q(j)_{\text{splitin}} X(j)_{\text{split}} = Q(j)_{\text{splitout}1} \quad (12)$$

$$C(j)_{\text{splitin}}^{\text{metal}} = C(j)_{\text{splitout}1}^{\text{metal}} = C(j)_{\text{splitout}2}^{\text{metal}} \quad (13)$$

where $Q(j)_{\text{splitin}}$ and $C(j)_{\text{splitin}}^{\text{metal}}$ denote the flow of the stream entering the j split junction and the corresponding concentration of each metal in the same stream and $Q(j)_{\text{splitout}1}$, $Q(j)_{\text{splitout}2}$ and $C(j)_{\text{splitout}1}^{\text{metal}}$, $C(j)_{\text{splitout}2}^{\text{metal}}$ denote the flows of the streams leaving the j split junction and their respective metal concentrations, respectively. The performance of each split junction is defined by a variable, $X(j)_{\text{split}}$, defined as continuous in the $[0,1]$ interval.

Reverse osmosis membrane modules:

$$Q(k)_{\text{memb}} = Q(k)_{\text{perm}} + Q(k)_{\text{ret}} \quad (14)$$

$$Q(k)_{\text{memb}} C(k)_{\text{memb}}^{\text{metal}} = Q(k)_{\text{perm}} C(k)_{\text{perm}}^{\text{metal}} + Q(k)_{\text{ret}} C(k)_{\text{ret}}^{\text{metal}} \quad (15)$$

where $Q(k)_{\text{memb}}$ and $C(k)_{\text{memb}}^{\text{metal}}$ denote the flow of the stream entering the k reverse osmosis membrane module and the corresponding concentration of each metal in the same stream, respectively, $Q(k)_{\text{perm}}$ and $C(k)_{\text{perm}}^{\text{metal}}$ denote the flow of the permeate stream leaving the k membrane module and its respective metal concentrations, respectively, and $Q(k)_{\text{ret}}$ and $C(k)_{\text{ret}}^{\text{metal}}$ denote the flow of the retentate stream leaving the same membrane module and its respective metal concentrations, respectively.

The characteristic variables that describe the performance of each k reverse osmosis stage, namely, the specific permeate flux $J(k)$ and the rejection coefficient of each metal $R(k)_{\text{metal}}$, can be formulated by direct application of the Kedem–Katchalsky equations

$$J(k) = L_P \Delta P(k) \quad (16)$$

$$R(k)_{\text{metal}} = \frac{\sigma_{\text{metal}} J(k)}{J(k) + \omega'_{\text{metal}}} \quad (17)$$

where the applied pressure in the k stage is symbolized by $\Delta P(k)$.

Once the membrane transport is defined, the characteristics of the permeate streams (flow and metal concentrations) can be calculated taking into account the membrane area of the corresponding k stage, $A(k)$

$$Q(k)_{\text{perm}} = 86,400 A(k) J(k) \quad (18)$$

$$C(k)_{\text{perm}}^{\text{metal}} = (1 - R(k)_{\text{metal}}) C(k)_{\text{memb}}^{\text{metal}} \quad (19)$$

Finally, the recovery ratio of each module, $\text{Rec}(k)$ can be defined

$$\text{Rec}(k) = \frac{Q(k)_{\text{perm}}}{Q(k)_{\text{memb}}} \quad (20)$$

Optimization Procedure

The main objective of the design was to maximize the daily economic profit of the process obtained from the sale of electronic grade hydrogen peroxide produced by the

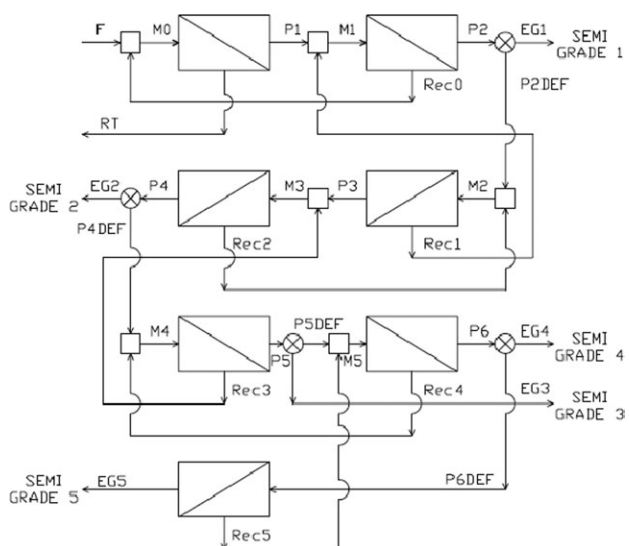


Figure 3. Superstructure configuration.

Table 4. Model Parameters for Calculation

Parameter	Unit	Value
LT _{memb}	d	3
LT _{inst}	d	1825
K _{memb}		0.12
Y _{raw}	\$/m ³	790
Y _{EG1}	\$/m ³	2592
Y _{EG2}	\$/m ³	3537
Y _{EG3}	\$/m ³	3780
Y _{EG4}	\$/m ³	8721
Y _{EG5}	\$/m ³	11826
Y _{memb}	\$/m ²	50
Y _{by}	\$/m ³	600
Y _{lab}	\$/h	7
Y _{elec}	\$/kWh	0.08
η		0.70
CC _{clean}	\$/d	2590

ultrapurification system. A straightforward economic model based on revenues and costs was proposed. The main optimization parameters required are listed in Table 4.

The daily profit (Z) can be expressed as the difference between the total daily revenues of the process (Rev) and the total costs (TC)

$$Z = \text{Rev} - \text{TC} \quad (21)$$

On the one hand, the five different electronic grades of hydrogen peroxide obtainable through the reverse osmosis network contribute to the total revenues of the process, but other output stream of the system, the retentate of the first stage, can also be considered valuable, as it could be commercialized as a by-product useful for hydrogen peroxide applications where metallic content is not a limiting factor. According to this approach, six different terms have to be incorporated to take into account all the contributions implied to assess the total daily revenues

$$\text{Rev} = \text{RT}Y_{\text{by}} + \sum_{n=1}^5 \text{EG}(n)Y_{\text{EG}(n)} \quad (22)$$

where RT denotes the flow of the first stage retentate stream and Y_{by} , the corresponding price assigned to this by-product stream, EG(n) denotes the flow of the corresponding n SEMI Grade product stream, and $Y_{\text{EG}(n)}$, the price of each SEMI Grade hydrogen peroxide.

On the other hand, the total daily costs of the system were calculated by the addition of the capital costs (CC) and the operation costs (OC). The CC attributable to membranes (CC_{memb}) or to the rest of the installation (CC_{inst}) were differentiated, while the OC were itemized into raw materials (OC_{raw}), energy (OC_{en}), labor (OC_{lab}), and maintenance costs (OC_m)

$$\text{TC} = \text{CC} + \text{OC} \quad (23)$$

$$\text{CC} = \text{CC}_{\text{memb}} + \text{CC}_{\text{inst}} \quad (24)$$

$$\text{OC} = \text{OC}_{\text{raw}} + \text{OC}_{\text{en}} + \text{OC}_{\text{lab}} + \text{OC}_{\text{m}} \quad (25)$$

The CC of the membranes modules considering straight-line depreciation along their lifetime (LT_{memb}) were expressed as function of the total membrane area of the installation

$$\text{CC}_{\text{memb}} = \frac{Y_{\text{memb}}}{\text{LT}_{\text{memb}}} \sum_k A(k) \quad (26)$$

where the price of the reverse osmosis membrane elements is symbolized by Y_{memb} .

Once the membranes costs were defined, the CC corresponding to the rest of the installation were related to them by mean of an empirical coefficient (K_{memb}) that expressed the contribution of the investment in membranes to the total CC. The percentage of the total investment attributable to the membranes typically range between 12 and 30%,^{61,62} so a value of K_{memb} equal to 0.12 was chosen with the intention of representing the most exigent scenario (an ultrapurification system requires very high-quality and -purity materials)

$$\text{CC}_{\text{ins}} = \text{CC}_{\text{memb}} \frac{(1 - K_{\text{memb}})}{K_{\text{memb}}} \frac{\text{LT}_{\text{memb}}}{\text{LT}_{\text{inst}}} + \text{CC}_{\text{clean}} \quad (27)$$

where LT_{inst} denotes the installation lifetime and CC_{clean}, the CC attributable to the cleanroom. As ultrapurification processes require contamination control, the entire installation need to be included in a cleanroom to provide the necessary controlled atmosphere. The CC attributable to the cleanroom were calculated according to a formula based on the model proposed by Yang and Eng Gan⁶³

$$\begin{aligned} \text{CC}_{\text{clean}} = & -1645051 + 5156.6\text{CA} + 68.8\text{MAV} \\ & + 34\text{EAV} + 2996627\text{AFC} + \text{AN} \end{aligned} \quad (28)$$

where CA refers to the cleanroom area, MAV refers to the make-up air volume, EAV refers to the exhaust air volume, and AFC refers to the average filter coverage ratio. The parameters required by the formulated model for the cost of the cleanroom (Eq. 28) were chosen according to the design of a Class 100 (200 air changes per hour) space of 200 m² with raised floor and fan filter unit (FFU) type air ventilation.⁶⁴ The term AN, that did not appear in the originally formulated model, was added to include the costs related to analysis and quality control. Its value was assessed according to the research group experience in analytical equipment management, mainly inductively coupled plasma mass spectrometry and ion chromatography.

The OC are essentially based on the consumption of the corresponding resource, except for the case of maintenance costs, which are function of the total CC.⁶⁵ The only required raw material was the technical grade hydrogen peroxide used as feed, and the installation was designed to be totally managed by a single worker

$$\text{OC}_{\text{raw}} = F Y_{\text{raw}} \quad (29)$$

$$\text{OC}_{\text{lab}} = 24 Y_{\text{lab}} \quad (30)$$

$$\text{OC}_{\text{en}} = \frac{Y_{\text{elec}}}{36 \eta} \sum_k (\mathcal{Q}(k)_{\text{memb}} \Delta P(k)) \quad (31)$$

$$\text{OC}_{\text{m}} = 0.05\text{CC} \quad (32)$$

where F denotes the flow of the feed stream, Y_{raw} , the price of the technical grade hydrogen peroxide used as feed raw material, Y_{lab} , the salary assigned to the employee, Y_{elec} , the electricity price, and η , the pump efficiency.

The objective function depends on a large number of quantities that can be separated into variables with respect to

Table 5. Optimization Results

K	Membrane Stages		Split Junctions		Product Streams		
	$\Delta P(k)$ (bar)	Rec(k)	$A(k)$ (m 2)	j	$X(j)_{\text{split}}$	n	$Q_{\text{EG}(n)}$ (m 3 /d)
1	40	0.9	14.0	1	1	1	0
2	40	0.9	14.0	2	1	2	0
3	40	0.9	14.0	3	1	3	0
4	40	0.9	14.0	4	1	4	0
5	40	0.9	14.0			5	
6	40	0.9	13.8				
7	40	0.9	12.4				
							21.5

which the function is maximized and parameters that can be considered as constants during the optimization procedure.

For each reverse osmosis stage, the applied pressure and the recovery ratio were chosen as variables. The investigated ranges of each variable were

$$\Delta P_{\min} = 10 \text{ bar} \leq \Delta P(k) \leq 40 \text{ bar} = \Delta P_{\max} \quad (33)$$

$$\text{Rec}_{\min} = 0.3 \leq \text{Rec}(k) \leq 0.9 = \text{Rec}_{\max} \quad (34)$$

The configuration of the network is characterized by the split decision variables of each split junctions. The split decision variables are defined in the continuous [0,1] interval (the variable equals to 0, when all the entering flow is derived to the stream leaving the system, and it equals to 1, when the flow is derived to the stream feeding the next stage, whereas intermediate values of the variable imply division of the flow between both streams)

$$X_{\text{split min}} = 0 \leq X(j)_{\text{split}} \leq 1 = X_{\text{split max}} \quad (35)$$

Quality constraints concerning the maximum allowable metallic content in each of the different electronic grade hydrogen peroxide product streams must be taken into account

$$C_{\text{EG}(n)}^{\text{metal}} \leq C_{\text{SEMI}(n)}^{\text{metal}} \quad (36)$$

where $C_{\text{EG}(n)}^{\text{metal}}$ denotes the concentration of each metal in the n SEMI Grade product stream and $C_{\text{SEMI}(n)}^{\text{metal}}$ denotes the maximum allowed concentration for each metal in the corresponding n SEMI Grade.

In mathematical terms the optimization model can be expressed as follows

$$\begin{aligned} \max Z &= f(x) \\ \text{s.t. } & h(x) = 0 \\ & w(x) \leq 0 \\ & x \in \mathbb{R}^n \\ & x_L < x < x_U \end{aligned}$$

being Z the daily profit, x the vector of continuous variables ($\Delta P(k)$, $\text{Rec}(k)$, and $X(j)_{\text{split}}$), h the vector of equality constraint functions (mass balance and membrane transport equations), and w the vector of inequality constraint functions (product requirements based on the concentration limit for each metallic cation).

Results and Discussion

The installation scale was defined assuming the coupling of the ultrapurification installation to a manufacturing plant with a target annual production aimed to electronic grade

purposes of 9000 tons of technical grade hydrogen peroxide. When 330 operating days per year are considered, the corresponding feed flow is above 24 m 3 /d. The characterization of the feed stream is based on typical metallic impurities content of technical grade hydrogen peroxide. The feeding conditions (flow and metals concentrations of the feed stream F) are shown in Table 3.

The lifetime of the reverse osmosis membrane in hydrogen peroxide medium (based on the experimental results with BE polyamide membrane from Woongjin Chemical) is notoriously shorter (few days)¹⁹ than the relative one to the most classical applications with seawater or brackish water (some years),^{66,67} and the cost of replacement was taken into account in the costs function.

The resulting NLP problem was solved using CONOPT3 solver within the software GAMS. Several starting points were proved to demonstrate the robustness of the solution. In general, a typical run to solve the mathematic programming problem has taken 0.17 central processing unit (CPU) time (s), equivalent to 77 iterations to finish.

Generalized findings

The optimum values that maximize the target function (daily profit Z) of the ultrapurification process were identified by run of the corresponding NLP problem within GAMS software. The results of the optimized configuration are compiled in Table 5.

It was found that the optimum applied pressures for all the stages were 40 bar, which is the upper boundary restriction for these variables. In a similar way, the optimum recovery rates were limited by the upper limit of the defined range (0.9). The optimum system configuration (Figure 4) corresponded to the one that only produce SEMI Grade 5 product stream (all the split junction variables equal to 1 which implies no output of intermediate Grades). Under these conditions, the daily profit could attain 232,170 \$/d, equivalent to an annual profit of 76.6 mill\$.

The main cost of the system was the acquisition the raw material that represented more than 80% of the TC (Figure 5). The rest of the operational costs became insignificant

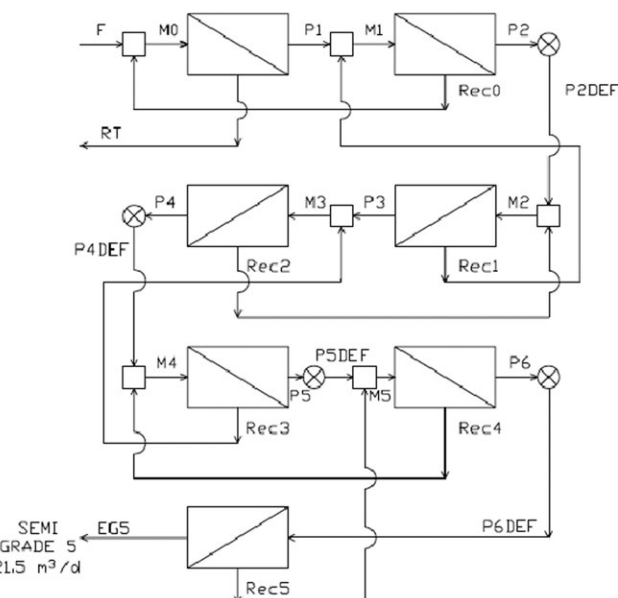


Figure 4. Optimal process configuration.

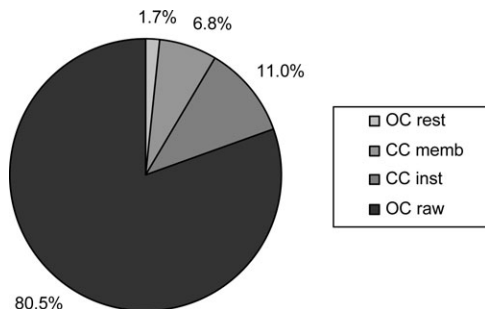


Figure 5. Costs breakdown for the optimum configuration.

when compared to the cost corresponding to feed hydrogen peroxide as none of them attained individually the 1% (they contribute jointly only by 1.7%). On the other hand, when focusing on the CC, the investment on membranes contributes by no more than 7% to the TC despite the high replacement rate consequence of the short membrane lifetime in such an oxidant medium.

Previous results, corresponding to optimization of ultrapurification cascade systems with increasing number of stages (from two to seven stages), had demonstrated that production of the most stringent electronic grades was more profitable despite the higher number of stages than the least strict grades.⁶⁰ This fact can be explained by the great influence of the market prices of the different Grades: SEMI Grade 5 is much more valuable than SEMI Grade 1 (four times more expensive as seen in Table 4), but the TC of the installation required to produce Grade 5 (seven stages) is only less than 6% higher than the corresponding to Grade 1 manufacturing (two stages). So the optimum results of the superstructure configuration confirm the trend to promote the production of higher quality hydrogen peroxide.

The characteristics of the product stream (impurities content) for the optimally configured system are listed in Table 6. As expected, all the metallic concentrations fell below the limit of 10 ppt. The limiting solute is the Na, because its concentration (0.747 ppt) is the highest among all the impurities but still quite lower than the bound fixed by SEMI. To quantify in an easier way the product quality when compared to the requirements, a safety factor (SF) was defined according to Eq. 37

$$SF_n = \frac{C_{SEMI(n)}^{\text{metal}}}{C_{EG(n)}^{\text{metal}}} = \frac{\text{Failure concentration}}{\text{Design concentration}} \quad (37)$$

where the SF is represented as the ratio between the failure and design concentrations (in this case the maximum allowed concentration divided by the product concentration). Now, it can be said that Na is the limiting impurity in terms of SFs, as it has the lowest value. Anyway, a value equal to 13 for the SF is a common figure when compared to commercially available electronic grade hydrogen peroxides.

Effect of market restrictions

As aforementioned, the process economy invited to stimulate the production of the strictest grade hydrogen peroxide, but market restrictions may represent the counterpoint to this situation. It seems more reasonable to expect that the demand of the most stringent Grade 5 would be limited, not allowing the commercialization of all the output obtained

under a “produce the highest quality Grade as much as possible” strategy. This proposed realistic framework would include also some commitments acquired with the corresponding clients to serve them with products others than the strictest Grade 5 (only required for very exigent tasks during the manufacturing of semiconductor materials and microelectronic devices and replaceable by lower quality product for the rest of productive steps).

Therefore, three different scenarios (Scenarios 1–3) were initially projected to represent more realistic commercial situations to investigate the influence of market restrictions over the configuration of the ultrapurification process. The scenarios were defined by a minimum and a maximum flow for each of the grades (Table 7).

The Scenario 1 represents the market baseline: production limitations are just imposed by both low and upper bounds. On the one hand, at least a minimum production of each grade has to be obtained to fulfill obligations acquired with consumers. On the other hand, there is a maximum production for each grade that can be absorbed by the demand. The Scenarios 2 and 3 consider the high- and low-demand circumstances respectively. In each situation, both minimum and maximum restrictions are increased or decreased if compared with the baseline Scenario 1.

The optimization results of the different basic scenarios are given in Table 8. Again, all the optimum values of the design and operation variables coincided with the defined upper bounds (0.9 for the recovery rates and 40 bar for the applied pressures, respectively) whichever scenario is observed. The profits of the three proposed scenarios were severely reduced when compared with the ideal situation without market restrictions: the highest drop corresponded to the low-demand Scenario 3 (61%) and the lowest discount to the baseline Scenario 1 (40%), remaining the high-demand Scenario 2 in an intermediate situation with 54% reduction. The main reason of the reduced profit was the lower revenues of the system related with commercialization of less valuable products, because the TC of the restricted scenarios were also reduced (but not in a relevant way, as the highest decrease corresponding to Scenario 3 is only 2%, not comparable with the 55% cut in the revenues of the same scenario).

When paying attention to the system configuration, Scenario 1 was characterized by just achievement of the minimum demands for the least stringent Grades 1–3; Grade 5 stream equal to its maximum allowed bound; and the rest of the production leaving the system as Grade 4 hydrogen peroxide. The high-demand Scenario 2 could be expected to be more profitable than the baseline demand scenario (higher total demand). But the results showed that the Scenario 1

Table 6. Impurities Content of the Product Stream for the Optimum Configuration

	C_{EG5} (ppt)	SF_5
B	0.353	28
Na	0.747	13
Al	0.085	118
Ti	0.012	864
Cr	0.009	1152
Mn	0.001	9566
Fe	0.164	61
Ni	0.002	4088
Cu	<0.001	>10000
Zn	0.002	5085

Table 7. Flow Restrictions of Each Product Stream Under the Different Marketing Scenarios

Scenario	Flow Restrictions to Product Streams (m^3/d)									
	SEMI Grade 1		SEMI Grade 2		SEMI Grade 3		SEMI Grade 4		SEMI Grade 5	
	Q_{EG1min}	Q_{EG1max}	Q_{EG2min}	Q_{EG2max}	Q_{EG3min}	Q_{EG3max}	Q_{EG4min}	Q_{EG4max}	Q_{EG5min}	Q_{EG5max}
1	2	30	1	3	5	30	2	10	1	5
2	4	40	2.5	9	7	38	3.7	18	1.9	8
3	1	14	0.6	1.3	2	12	0.8	3.6	0.6	2.1
4	4	40	2.5	9	7	38	0.8	3.6	0.6	2.1
5	1	14	0.6	1.3	2	12	3.7	18	1.9	8

was more satisfactory in economic terms. The Scenario 2 was defined by minimum productions of every Grades but Grade 5. Under these conditions, the main part of the raw material had to be used to fulfill the requirements of the least profitable grades, remaining few resources to be assigned to the most valuable grades. The Scenario 3 is just the opposite case: the low-demand restrictions implied that all the grades except Grade 1 were produced in their maximum amounts. Anyway, as these limits are quite lower than the ones corresponding to the baseline situation, the profit of the system fell down (in this case because the low demand of the high-valuable Grades forced to spend most of the raw material in the least profitable Grade 1).

In light of the results obtained for the basic market restrictions, two new scenarios were proposed for consideration: the Scenarios 4 and 5 corresponded to mixed demand situations. The Scenario 4 included the high-demand conditions for Grades 1–3 (as in Scenario 2) and the low-demand conditions for Grades 4 and 5 (as in Scenario 3). In a reverse way, the Scenario 5 covered the low-demand limits for Grades 1–3 (corresponding to Scenario 3) and the high-demand values for Grades 4 and 5 (as in Scenario 2).

The optimization results of the different mixed demand scenarios are shown in Table 9. Once again, all the optimum

values of the design and operation variables coincided with the defined upper bound for both scenarios. The economic aspects of the different scenarios are compiled in Table 10. As expected, the Scenario 4 was the least profitable one, because it joined two undesirable factors: high demand of less valuable grades and low demand of the preferred high-quality grades. This combination implied an unbalanced distribution of the resources between both types of grades, converting the low-quality ones into the predominant products. On the other hand, Scenario 5 represented also out of balance market conditions, but in this case as the more valuable Grades became dominant, the economic profit of the corresponding system configuration reached a value better than the baseline Scenario 1 (23% of extra profit). The main results of the optimization of the different scenarios restricted by market conditions are depicted in Figure 6.

By way of guidance, the quality characteristics of the different grades obtained under the Scenario 1 conditions are listed in Table 11. It can be observed that Na is the limiting impurity whichever considered grade as the corresponding SFs are the lowest ones. However, all the SFs are higher than 5, so no problems could be expected, even under some uncertainty conditions about the metallic content of the raw material or the performance of the membrane modules. After comparison of the dated included in Table 11 with those of the Table 6 (corresponding to the ideal situation without market restriction), it can be concluded that the ideal situation obtained a higher quality SEMI Grade 5 hydrogen peroxide. This result can be explained by the assignment of material out of the system to the production of intermediate

Table 8. Optimization Results for the Basic Marketing Scenarios

k	Membrane Stages		Split Junctions		Product Streams		
	$\Delta P(k)$ (bar)	$Rec(k)$	$A(k)$ (m^2)	j	$X(j)_{split}$	n	$Q_{EG(n)}$ (m^3/d)
<i>Scenario 1</i>							
1	40	0.9	14.0	1	0.916	1	2.0
2	40	0.9	13.9	2	0.954	2	1.0
3	40	0.9	12.7	3	0.751	3	5.0
4	40	0.9	12.6	4	0.395	4	8.5
5	40	0.9	11.6			5	5.0
6	40	0.9	8.1				
7	40	0.9	2.9				
<i>Scenario 2</i>							
1	40	0.9	14.0	1	0.831	1	4.0
2	40	0.9	13.7	2	0.870	2	2.5
3	40	0.9	11.4	3	0.561	3	7.0
4	40	0.9	11.1	4	0.564	4	3.7
5	40	0.9	9.2			5	4.3
6	40	0.9	4.9				
7	40	0.9	2.5				
<i>Scenario 3</i>							
1	40	0.9	14.0	1	0.895	1	2.5
2	40	0.9	13.8	2	0.938	2	1.3
3	40	0.9	12.3	3	0.346	3	12.0
4	40	0.9	12.2	4	0.393	4	3.6
5	40	0.9	10.6			5	2.1
6	40	0.9	3.4				
7	40	0.9	1.2				

Table 9. Optimization Results for the Mixed Demand Marketing Scenarios

k	Membrane stages		Split junctions		Product streams		
	$\Delta P(k)$ (bar)	$Rec(k)$	$A(k)$ (m^2)	j	$X(j)_{split}$	n	$Q_{EG(n)}$ (m^3/d)
<i>Scenario 4</i>							
1	40	0.9	14.0	1	0.831	1	4.0
2	40	0.9	13.7	2	0.870	2	2.5
3	40	0.9	11.4	3	0.406	3	9.3
4	40	0.9	11.1	4	0.393	4	3.6
5	40	0.9	9.1			5	2.1
6	40	0.9	3.4				
7	40	0.9	1.2				
<i>Scenario 5</i>							
1	40	0.9	14.0	1	0.958	1	1.0
2	40	0.9	13.9	2	0.974	2	0.6
3	40	0.9	13.3	3	0.909	3	2.0
4	40	0.9	13.3	4	0.473	4	9.9
5	40	0.9	12.7			5	8.0
6	40	0.9	10.9				
7	40	0.9	4.6				

Table 10. Economic Breakdown of the Different Scenarios

Economic Terms (mill\$/y)	No Market Restrictions	Market Scenario 1	Market Scenario 2	Market Scenario 3	Market Scenario 4	Market Scenario 5
Z	76.616	45.928	35.407	30.057	29.399	56.555
Rev	84.445	53.636	43.062	37.717	37.037	64.305
TC	7.829	7.708	7.655	7.660	7.638	7.750
CC	1.390	1.276	1.227	1.231	1.210	1.315
CC _{memb}	0.529	0.417	0.368	0.372	0.351	0.455
CC _{inst}	0.861	0.860	0.859	0.859	0.859	0.860
OC	6.439	6.432	6.428	6.429	6.427	6.434
OC _{raw}	6.306	6.306	6.306	6.306	6.306	6.306
OC _{lab}	0.055	0.055	0.055	0.055	0.055	0.055
OC _{en}	0.008	0.006	0.005	0.005	0.005	0.007
OC _m	0.070	0.064	0.061	0.062	0.061	0.066

grades instead of allowing it to be recirculated to previous stages, improving the quality of the streams leaving the mixers because of the input of higher fluxes of recirculated streams with lower metallic content.

A second optimization problem was also formulated and solved to investigate the effects of the different market restrictions. In this case, the objective was the minimization of the TC of the system corresponding with the situations where all the demand of each scenario can be satisfied (Scenarios 1–3 Full). In order to be able to assure the total demand, the feed stream of the system was not previously fixed, and it was set as another variable of the system.

In mathematical terms this new optimization problem can be expressed as follows

$$\begin{aligned} \min \text{TC} &= f(x) \\ \text{s.t. } h(x) &= 0 \\ w(x) &\leq 0 \\ x &\in \Re^n \\ x_L < x &< x_U \end{aligned}$$

being x the vector of continuous variables (F , $\Delta P(k)$, Rec(k), and $X(j)_{\text{split}}$), h the vector of equality constraint functions (mass balance and membrane transport equations), and w the vector of inequality constraint functions (product requirements).

Once again, the optimum applied pressures resulted 40 bar for all the stages (upper boundary restriction). In a similar

way, the optimum recovery rates were limited by the upper limit of the defined range (0.9). These results showed that minimization of TC and maximization of economic profit led to the same optimum solutions.

The optimization results of the different fully satisfied scenarios are listed in Table 12, and the corresponding economic breakdown can be observed in Table 13. Under these conditions, the raw material required by the system is much greater than the original baseline: the high-demand Scenario 2 Full consumed more than five times the baseline feed flow (127.1 m³/d vs. 24.2 m³/d). On the other hand, the higher consumption of technical grade hydrogen peroxide was compensated with greater profits. As an example, the Scenario 1 Full is approximately twice more profitable than the Scenario 1. Another result worth mentioning is the comparison of the three fully satisfied Scenarios. The Scenario 2 Full, related with high-demand patterns, is more profitable than the Scenario 1 Full (corresponding with baseline demand). When the feed stream flow was limited, the Scenario 1 was more favorable than the Scenario 2 as the high demand of low-price grades limited the production of Grades 4 and 5. Without feed restrictions, the limitations disappeared, and the Scenario 2 Full became the most lucrative. Anyway, the Scenario 3 Full appeared again as the least beneficial one because of its low-demand framework.

Effect of unit costs

All the previous optimization results demonstrated a very robust performance of the system, as the variables had acquired the maximum allowed value in the corresponding range in every case. A simple sensitivity analysis was carried out to advance in the investigation of the influence of the parameters governing the costs associated with the main design and operation variables: the electricity unit price influences the energy costs attributable to the pressurization of the

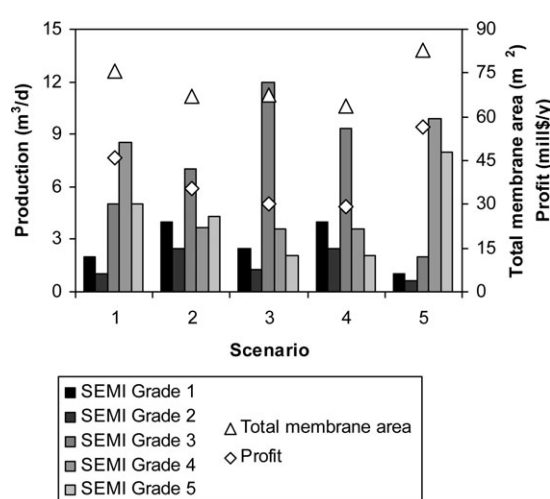


Figure 6. Main results of the optimization of the different scenarios under market restrictions.

Table 11. Impurities Contents of the Product Streams for the Optimum Configuration Under Scenario 1 Conditions

	SF ₁	SF ₂	SF ₃	SF ₄	SF ₅
B	213	370	167	100	32
Na	6	8	10	11	13
Al	87	99	100	111	116
Ti	338	1000	1000	910	859
Cr	80	1429	1314	1228	1147
Mn	806	>10000	>10000	>10000	9566
Fe	27	149	111	100	62
Ni	177	3333	3870	3957	4031
Cu	6250	>10000	>10000	>10000	>10000
Zn	617	5000	5504	5276	5049

Table 12. Optimization Results (Minimum TC) for the Full Satisfied Marketing Scenarios

Membrane Stages <i>K</i>	Split Junctions		Product Streams		Feed Stream <i>F</i> (m ³ /d)
	<i>A(k)</i> (m ²)	<i>j</i>	<i>X(j)split</i>	<i>N</i>	
<i>Scenario 1 Full</i>					
1	50.5	1	0.643	1	30.0
2	48.6	2	0.944	2	3.0
3	31.2	3	0.358	3	30.0
4	30.8	4	0.357	4	10.0
5	27.0			5	5.0
6	9.0				
7	2.9				
<i>Scenario 2 Full</i>					
1	73.2	1	0.672	1	40.0
2	70.7	2	0.888	2	9.0
3	47.4	3	0.433	3	38.0
4	46.6	4	0.331	4	18.0
5	38.8			5	8.0
6	15.6				
7	4.6				
<i>Scenario 3 Full</i>					
1	21.4	1	0.604	1	14.0
2	20.5	2	0.938	2	1.3
3	12.3	3	0.346	3	12.0
4	12.2	4	0.393	4	3.6
5	10.6			5	2.1
6	3.4				
7	1.2				

streams entering the reverse osmosis modules, and the membrane unit price controls the membrane costs related to the total membrane area of each stage. In each case, the available membrane area defines the quantity of permeate obtained by each stage and, consequently, the recovery ratio of them. Besides, the membrane costs are used as the basis

Table 13. Economic Breakdown of the Different Full Satisfied Scenarios

Economic Terms (mill\$/y)	Market Scenario 1 Full	Market Scenario 2 Full	Market Scenario 3 Full
TC	25.003	35.837	11.109
CC	1.968	2.507	1.309
CC _{memb}	1.100	1.633	0.449
CC _{inst}	0.868	0.874	0.860
OC	23.034	33.330	9.800
OC _{raw}	22.864	33.125	9.673
OC _{lab}	0.055	0.055	0.055
OC _{en}	0.016	0.024	0.007
OC _m	0.098	0.125	0.065
Rev	116.798	177.928	47.830
Z	91.795	142.091	36.720

to calculate the rest of the CC and even the maintenance costs are related with the total CC.

The sensitivity analysis results (Table 14) showed that the total profit of the system under Scenario 1 conditions is very insensitive to changes in electricity, membrane, and raw material unit prices. The optimum values of the variables resulted again at the upper bounds (0.9 and 40 bar). The variations in the profit were located in the range $\pm 1\%$ even for changes in an order of magnitude in the price of the electricity or when the membrane price was doubled. As the raw material is the main cost of the system, the influence of its unitary cost is higher than those of the other costs, but the revenues are so dominant that a decrease or increase of 20% in the price of the feed only affect in the range $\pm 3\%$ to the economic profit of the process.

To confirm the robustness of the optimum values for the design and operation variables, a search of such conditions that would modify the optimal solution was planned out. For the case of applied pressures, the electricity unit price of 6 \$/kW h would move the optimum value for the applied pressures from the upper bound to 39.4 bar for every stages under Scenario 1 conditions. Such a high-expensive electricity situation seems very improbable, because it would require a nearly 100-fold increase in the price of the energy. A quite similar result was obtained after exploration of conditions for different optimal recovery rates: very expensive reverse osmosis membranes (6000 \$/m²) would move the optimal recovery rate of the first stage to 0.647 (but none of the rest of stages). Again, an approximately 100-fold raise in membranes prices cannot be considered as a logic panorama; and in the case it could happen, the process would not be longer economically viable.

Conclusions

The proposed superstructure represents a seven-stage countercurrent cascade system able to produce simultaneously all the different SEMI grades, from two stages corresponding to SEMI Grade 1, to seven stages that are required for SEMI Grade 5, the strictest grade related to the metal impurities.

The objective of the design was to maximize the daily profit obtained from the sale of the electronic grades of hydrogen peroxide produced by the ultrapurification system, calculated as the difference between the total daily revenues and the TC (capital and operation).

The obtained results allow to conclude with the viability of the ultrapurification process based on the reverse osmosis modules, with the optimum system configuration that only produce SEMI Grade 5 hydrogen peroxide (the strictest grade, high-value product) as the best option in economic terms when there are no market restrictions: 232,170 \$/day, equivalent to an

Table 14. Sensitivity Analysis for Electricity, Membrane, and Technical Grade Hydrogen Peroxide Unit Prices

Economic terms (mill\$/y)	Electricity price (\$/(kW h))			Membrane price (\$/m ²)			Technical grade hydrogen peroxide price (\$/m ³)		
	0.02	0.08	0.80	10	50	100	632	790	948
CC _{memb}				0.083	0.417	0.833			
CC _{inst}				0.856	0.860	0.865			
OC _m				0.047	0.064	0.085			
OC _{en}	0.002	0.006	0.061				5.045	6.306	7.568
OC _{raw}	45.933	45.928	45.873	46.282	45.928	45.486	47.189	45.928	44.667
Z	+0.01			-0.12	0.77	-0.96	+2.75		-2.75

annual profit of 76.6 mill\$ (for a plant capacity of 9000 tons/year of technical grade hydrogen peroxide).

The main cost of the system was the raw material that represents more than 80% of the TC. The investment on membranes contributes by no more than 7% to the CC, despite the high replacement rate due to the membrane lifetime in such an oxidant medium.

The influence of market restrictions was studied under different scenarios, given in terms of production of each SEMI Grade hydrogen peroxide, taking into account that the strictest Grade 5 may be only required for very exigent tasks during the manufacturing of semiconductor materials. The economic profit of the system configuration reached a value better than the baseline scenario in the scenario that represents the dominance of the more valuable Grades 4 and 5, with 23% of extra profit mainly given by the high market price of these demanded electronic grades.

The effect of unit costs was analyzed in terms of electricity, membrane, and raw material unit prices showing that the total profit of the system is very insensitive to changes, being remarked the key factor of the market prices of the electronic grades of hydrogen peroxide.

Acknowledgments

This research has been financially supported by the Ministry of Science and Innovation of Spain (MICINN) through CTM2006-00317 and CTQ2010-16608 Projects. R. Abejón acknowledges also the assistance of MICINN for the award of a FPI grant (BES-2008-003622).

Notation

- $A(k)$ = membrane area of the k stage, m^2
- AFC = average filter coverage ratio
- AN = capital costs attributable to analysis and quality control, \$
- CA = cleanroom area, m^2
- CC = capital costs, \$/d
- CC_{clean} = capital costs attributable to cleanroom, \$/d
- CC_{inst} = capital costs attributable to installation, \$/d
- CC_{memb} = capital costs attributable to membranes, \$/d
- C_F = solute feed concentration, mol/m^3
- $C(i)_{\text{mixin1}}$ = metal concentration of the first stream entering the i mixer, ppb
- $C(i)_{\text{mixin2}}$ = metal concentration of the second stream entering the i mixer, ppb
- $C(i)_{\text{mixout}}$ = metal concentration of the output stream leaving the i mixer, ppb
- $C(j)_{\text{splitin}}$ = metal concentration of the stream entering the j split junction, ppb
- $C(j)_{\text{splitout1}}$ = metal concentration of the stream leaving the j split junction to the next stage, ppb
- $C(j)_{\text{splitout2}}$ = metal concentration of the stream leaving the j split junction out of the system, ppb
- $C(k)_{\text{memb}}$ = metal concentration of the stream entering the k membrane stage, ppb
- $C(k)_{\text{perm}}$ = metal concentration of the permeate stream leaving the k membrane stage, ppb
- $C(k)_{\text{ret}}$ = metal concentration of the retentate stream leaving the k membrane stage, ppb
- C_P = solute permeate concentration, mol/m^3
- $(C_S)_{\text{ln}}$ = logarithmic average solute concentration across the membrane, mol/m^3
- EAV = exhaust air volume, m^3/h
- $\text{EG}(n)$ = flow of the corresponding n SEMI Grade product stream, m^3/d
- i = van 't Hoff factor
- $J(k)$ = permeate flux of the k membrane stage, m/s
- J_S = solute flux, $\text{mol}/(\text{m}^2 \cdot \text{s})$
- J_V = solvent flux, m/s
- K_A = dissociation constant, M
- K_{memb} = ratio membrane capital costs to total capital costs
- L_P = solvent permeability coefficient, $\text{m}/\text{s bar}$

- LT_{memb} = membrane lifetime, d
- LT_{inst} = installation lifetime, d
- m = solute molar concentration, (mol/m^3)
- MAV = make-up air volume, m^3/h
- OC = operation costs, \$/d
- OC_{en} = energy costs, \$/d
- OC_{lab} = labor costs, \$/d
- OC_{m} = maintenance costs, \$/d
- OC_{raw} = raw material costs, \$/d
- $Q(i)_{\text{mixin1}}$ = flow of the first stream entering the i mixer, m^3/d
- $Q(i)_{\text{mixin2}}$ = flow of the second stream entering the i mixer, m^3/d
- $Q(i)_{\text{mixout}}$ = flow of the output stream leaving the i mixer, m^3/d
- $Q(j)_{\text{splitin}}$ = flow of the stream entering the j split junction, m^3/d
- $Q(j)_{\text{splitout1}}$ = flow of the stream leaving the j split junction to the next stage, m^3/d
- $Q(j)_{\text{splitout2}}$ = flow of the stream leaving the j split junction out of the system, m^3/d
- $Q(k)_{\text{memb}}$ = flow of the stream entering the k membrane stage, m^3/d
- $Q(k)_{\text{perm}}$ = flow of the permeate stream leaving the k membrane stage, m^3/d
- $Q(k)_{\text{ret}}$ = flow of the retentate stream leaving the k membrane stage, m^3/d
- R = rejection coefficient
- \mathfrak{R} = gas constant, $\text{bar} \cdot \text{m}^3/\text{K mol}$
- $R(k)_{\text{metal}}$ = rejection coefficient of the corresponding metal in the k stage
- $\text{Rec}(k)$ = recovery rate of the k stage
- Rev = daily revenues, \$/d
- RT = flow of the first stage retentate stream, m^3/d
- T = temperature, K
- TC = total costs, \$/d
- x_F = feed hydrogen peroxide concentration, M
- x_P = permeate hydrogen peroxide concentration, M
- $X(j)_{\text{split}}$ = decision variable of the j split junction
- Y_{by} = price of by-product hydrogen peroxide from first stage retentate, $$/\text{m}^3$
- $Y_{\text{EG}(n)}$ = price of n SEMI Grade hydrogen peroxide, $$/\text{m}^3$
- Y_{elec} = electricity price, $$/(\text{kW} \cdot \text{h})$
- Y_{lab} = salary, \$/h
- Y_{memb} = price of reverse osmosis membranes, $$/\text{m}^2$
- Y_{raw} = price of technical grade hydrogen peroxide, $$/\text{m}^3$
- Z = daily profit, \$/d

Greek letters

- ΔP = pressure difference across the membrane, bar
- $\Delta P(k)$ = applied pressure difference in the k membrane stage, bar
- $\Delta \Pi$ = osmotic pressure difference across the membrane, bar
- η = pump efficiency
- v = stoichiometric coefficient based on van 't Hoff factor
- Π = osmotic pressure, bar
- σ = reflection coefficient
- σ_{metal} = reflection coefficient of the corresponding metal
- ω = coefficient of solute mobility, $\text{mol}/(\text{m}^2 \cdot \text{s bar})$
- ω' = modified coefficient of solute mobility, m/s
- ω'_{metal} = modified coefficient of solute mobility of the corresponding metal, m/d

Indexes

- i = number of mixers
- j = number of split junctions
- k = number of membrane stages
- n = number of SEMI Grades

Literature Cited

- Davison JB, Hoffman JG, Yuan WI. *Ultrapurification of semiconductor process liquids*. In: 9th ICCCS Proceedings, Los Angeles, CA, Sept. 26-30, 1988.
- Reinhardt K, Kern W. *Handbook of Silicon Wafers Cleaning Technology*. Norwich: William Andrew, Inc., 2008.
- Sievert WJ. A European perspective on electronic chemicals. *Semicond Fabtech*. 2000;10:199–204.
- Kern W, Puotinen D. Cleaning solutions based on hydrogen for use in silicon semiconductor technology. *RCA Rev*. 1970;31:187–206.
- Freedonia Group. Electronic chemicals to 2008. Industry Study No. 1852, 2004.

6. Olson ED, Reaux CA, Ma WC, Butterbaugh JW. Alternatives to standard wet cleans. *Semicond Int.* 2000;23:70–75.
7. The Engineer. Electrolysed acid strips for semiconductors, March 2007 (Online version).
8. Jeon JS, Ogle B, Baeyens M, Mertens P. Evaluation of cleaning recipes based on ozonated water for pre-gate oxide cleaning. *Solid State Phenom.* 1999;65–66:119–122.
9. Sohn HS, Butterbaugh JW, Olson ED, Diedrick J, Lee NP. Using cost-effective dilute acid chemicals to perform postetch interconnect cleans. *MICRO*. 2005;23:67–76.
10. Rath DL, Ravikumar R, Delehaney DJ, Filippi RG, Kiewra EW, Stojakovic G, McCullough KJ, Miura DD, Rhoads BN. New aqueous clean for aluminum interconnects: Part I. Fundamentals. *Solid State Phenom.* 2001;76–77:31–34.
11. Ravikumar R, Rath DL, Delehaney DJ, Filippi RG, Kiewra EW, Stojakovic G, McCullough KJ, Miura DD, Gambino J, Schnabel F, Rhoads BN. New aqueous clean for aluminum interconnects: Part II. Applications. *Solid State Phenom.* 2001;76–77:51–54.
12. Archer L, Henry SA, Nachreiner D. Removing postash polymer residue from BEOL structures using inorganic chemicals. *MICRO*. 2001;6:95–103.
13. Couteau T, Dawson G, Halladay J, Archer L. Comparing single-wafer and batch polymer cleans using inorganic chemicals in BEOL applications. *MICRO*. 2006;24:45–49.
14. Semiconductor Equipment and Materials International (SEMI). Specifications for hydrogen peroxide. SEMI Document C30-1110, 2010.
15. Goor G, Glenneberg J, Jacobi S. *Hydrogen peroxide*. In: *Ullmann's Encyclopedia of Industrial Chemistry*. Weinheim: Wiley-VCH, 2007 (Electronic release).
16. Sievert WJ. Setting standards—The developments of standards in the field of electronic chemicals. *Semicond Fabtech*. 2001;13:175–179.
17. Abejón R, Garea A, Irabien A. Ultrapurification of hydrogen peroxide solution from ionic metals impurities to semiconductor grade by reverse osmosis. *Sep Purif Technol.* 2010;76:44–51.
18. Caus A, Braeken L, Boussu K, Van der Bruggen B. The use of integrated countercurrent nanofiltration cascades for advanced separations. *J Chem Technol Biotechnol*. 2009;84:391–398.
19. Abejón R, Garea A, Irabien A. Analysis, modelling and simulation of hydrogen peroxide ultrapurification by multistage reverse osmosis. *Chem Eng Res Des*. 2012;90 (doi:10.1016/j.cherd.2011.07.025).
20. Fritzmann C, Löwenberg J, Wintgens T, Melin T. State-of-the-art of reverse osmosis desalination. *Desalination*. 2007;216:1–76.
21. Aboabdou M, Elmasallati S. Potable water production from seawater by the reverse osmosis technique in Libya. *Desalination*. 2007;203:119–133.
22. Park C, Park PK, Mane PP, Hyung H, Gandhi V, Kim SH, Kim JH. Stochastic cost estimation approach for full-scale reverse osmosis desalination plants. *J Membr Sci*. 2010;364:52–64.
23. Peñate B, García-Rodríguez L. Retrofitting assessment of the Lanzarote IV seawater reverse osmosis desalination plant. *Desalination*. 2011;266:244–255.
24. Voutchkov N. Overview of seawater concentrate disposal alternatives. *Desalination*. 2011;273:205–219.
25. Geraldes V, Semiãoa V, de Pinho N. Optimization of ladder-type spacers for nanofiltration and reverse osmosis spiral-wound modules by computational fluid dynamics. *Comput Aided Chem Eng*. 2004;18:187–192.
26. Senthilmurugan S, Gupta SK. Modeling of a radial flow hollow fiber module and estimation of model parameters for aqueous multi-component mixture using numerical techniques. *J Membr Sci*. 2006;279:466–478.
27. Fujiwara N, Matsuyama H. The analysis and design of a both open ended hollow fiber type RO module. *J Appl Polym Sci*. 2008;110: 2267–2278.
28. Johnson J, Busch M. Engineering aspects of reverse osmosis module design. *Desalination Water Treat*. 2010;15:236–248.
29. Mo H, Ng HY. An experimental study on the effect of spacer on concentration polarization in a long channel reverse osmosis membrane cell. *Water Sci Technol*. 2010;61:2035–2041.
30. Kostoglou M, Karabelas AJ. Mathematical analysis of the meso-scale flow field in spiral-wound membrane modules. *Ind Eng Chem Res*. 2011;50:4653–4666.
31. Maskan F, Wiley DE, Johnston LPM, Clements DJ. Optimal design of reverse osmosis module networks. *AICHE J*. 2000;46:946–954.
32. Wilf W, Klinko K. Optimization of seawater RO systems design. *Desalination*. 2001;138:299–306.
33. Villafafila A, Mujtaba IM. Fresh water by reverse osmosis based desalination: simulation and optimisation. *Desalination*. 2003;155: 1–13.
34. Glueckstren P, Priel M. Optimization of boron removal in old and new SWRO systems. *Desalination*. 2003;156:219–228.
35. Wilt M, Bartels C. Optimization of seawater RO systems design. *Desalination*. 2005;173:1–12.
36. Avlonitis SA. Optimization of the design and operation of seawater RO desalination plants. *Sep Sci Technol*. 2005;40:2663–2678.
37. Guria C, Bhattacharya PK, Gupta SK. Multi-objective optimization of reverse osmosis desalination units using different adaptations of the non-dominated sorting genetic algorithm (NSGA). *Comput Chem Eng*. 2005;29:1977–1995.
38. Lu YY, Hu YD, Zhang XL, Wu LY, Liu QZ. Optimum design or reverse osmosis system under different feed concentration and product specification. *J Membr Sci*. 2007;287:219–229.
39. Gilat AM, Small MJ. Designing cost-effective seawater reverse osmosis system under optimal energy options. *Renew Energy*. 2008;33:617–630.
40. Vince F, Marechal F, Aoustin E, Bréant P. Multi-objective optimization of RO desalination plants. *Desalination*. 2008;222:96–118.
41. Zhu A, Christofides PD, Cohen Y. Minimization of energy consumption for a two-pass membrane desalination: effect of energy recovery, membrane rejection and retentate recycling. *J Membr Sci*. 2009;339:126–137.
42. Zhu A, Rhardianto A, Christofides PD, Cohen Y. Reverse osmosis desalination with high permeability membranes—cost optimization and research needs. *Desalination Water Treat*. 2010;15:256–266.
43. Li M. Minimization of energy in reverse osmosis water desalination using constrained nonlinear optimization. *Ind Eng Chem Res*. 2010;49:1822–1831.
44. Sassi KM, Mujtaba IM. Optimal design and operation of reverse osmosis desalination process with membrane fouling. *Chem Eng J*. 2011;171:582–593.
45. El-Halwagi MM, Mahmoud M. Synthesis of reverse osmosis networks for waste reduction. *AICHE J*. 1992;38:1185–1198.
46. Voros NG, Maroulis ZB, Marinos-Kouris D. Optimization of reverse osmosis networks for seawater desalination. *Comput Chem Eng*. 1996;20:345–350.
47. González MP, Navarro R, Saucedo I, Avila M, Revilla J, Bouchard C. Purification of phosphoric acid solutions by reverse osmosis and nanofiltration. *Desalination*. 2002;147:315–320.
48. Kulkarni A, Mukherjee D, Mukherjee D, Gill WN. Reprocessing hydrofluoric acid etching solutions by reverse osmosis. *Chem Eng Commun*. 1994;129:53–68.
49. Eul W, Moeller A, Steiner N. *Hydrogen peroxide*. In: *Kirk-Othmer Encyclopedia of Chemical Technology*. New York: Wiley-VCH, 2001 (Electronic release).
50. Soltanieh M, Gill WN. Review of reverse osmosis membranes and transport models. *Chem Eng Commun*. 1981;12:279–363.
51. Kedem O, Katchalsky A. Thermodynamic analysis of the permeability of biological membranes to non-electrolytes. *Biochim Biophys Acta*. 1958;27:229–246.
52. Gupta SK. Design and analysis of reverse osmosis systems using three parameter models for transport across the membrane. *Desalination*. 1992;85:283–296.
53. Van Gauwbergen D, Baeyens J. Modelling reverse osmosis by irreversible thermodynamics. *Sep Purif Technol*. 1998;13:117–128.
54. Tu KL, Nghiem LD, Chivas AR. Boron removal by reverse osmosis membranes in seawater desalination applications. *Sep Purif Technol*. 2010;75:87–101.
55. Bhattacharjee C, Sarkar P, Datta S, Gupta BB, Bhattacharya PK. Parameter estimation and performance study during ultrafiltration of Kraft black liquor. *Sep Purif Technol*. 2006;51:247–257.
56. Kovács Z, Discacciati M, Samhaber W. Modeling of amino acid nanofiltration by irreversible thermodynamics. *J Membr Sci*. 2009;332:38–49.
57. Prabhavathy C, De S. Estimation of transport parameters during ultrafiltration of pickling effluent from a tannery. *Sep Sci Technol*. 2010;45:11–20.
58. Pusch W. Determination of transport parameters of synthetic membranes by hyperfiltration experiments, Part I: Derivation of transport relationship from linear relations of thermodynamics of irreversible processes. *Ber Bunsen Phys Chem*. 1977;81:269–276.
59. Pusch W. Determination of transport parameters of synthetic membranes by hyperfiltration experiments, Part II: Membrane transport parameters independent of pressure and/or pressure difference. *Ber Bunsen Phys Chem*. 1977;81:854–864.

60. Abejón R, Garea A, Irabien A. Membrane process optimization for hydrogen peroxide ultrapurification. *Comput Aided Chem Eng*. 2011;29:678–682.
61. Fariñas M. *Osmosis inversa: fundamentos, tecnología y aplicaciones*. Madrid: McGraw-Hill, 1999.
62. Medina San Juan JA. *Desalación de aguas salobres y de mar: osmosis inversa*. Madrid: Mundi-Prensa, 2000.
63. Yang L, Eng Gan C. Costing small cleanrooms. *Build Environ*. 2007;42:743–751.
64. Rumsey Engineers, Inc. *Energy efficiency baselines for cleanrooms*. Non-Residential New Construction and Retrofit Incentive Programs of PG&E, Oakland, 2009.
65. Shaalan HF, Sorour MH, Tewfik SR. Simulation and optimization of a membrane system for chromium recovery from tanning wastes. *Desalination*. 2000;141:315–324.
66. Goosen MFA, Sablani SS, Al-Hinai H, Al-Obeidani S, Al-Belushi R, Jackson D. Fouling of reverse osmosis and ultrafiltration membranes: a critical review. *Sep Sci Technol*. 2004;39:2261–2297.
67. Avlonitis SA, Kouroumbas K, Vlachakis N. Energy consumption and membrane replacement cost for seawater RO desalination plants. *Desalination*. 2003;157:151–158.

Manuscript received Oct. 31, 2011, and revision received Jan. 19, 2012.

Anexo: Difusión de resultados

Anexo: Difusión de resultados

A continuación se listan otras publicaciones, así como congresos internacionales a través de los cuales se ha realizado la difusión de los resultados de la presente Tesis.

Otras publicaciones:

1. Abejón R.; Garea, A.; Irabien A. *Membrane process optimization for hydrogen peroxide ultrapurification*. Computer Aided Chemical Engineering, 29:678-682 (2011).
2. Abejón R.; Garea, A.; Irabien A. *Multiobjective optimization of membrane processes for chemicals ultrapurification*. Computer Aided Chemical Engineering, 30:542-546 (2012).
3. Abejón R.; Garea, A.; Irabien A. *Minimization of energy consumption for chemicals ultrapurification processes*. Chemical Engineering Transactions, 29:1549-1554 (2012).
4. Abejón R.; Garea, A.; Irabien A. *Time evolution of reverse osmosis membranes in a highly oxidant environment: ultrapurification of hydrogen peroxide*. Journal of Membrane Science, enviado.
5. Abejón R.; Garea, A.; Irabien A. *Multiobjective optimization of membrane processes for chemicals ultrapurification*. Computers & Chemical Engineering, enviado.

Congresos Internacionales:

1. Abejón R.; Garea, A.; Irabien A. *Membrane processes in the purification of hydrogen peroxide to electronic grade*. 11th Mediterranean Congress of Chemical Engineering, Barcelona (2008). Póster.
2. Abejón R.; Garea, A.; Irabien A. *Use of reverse osmosis for ultrapurification of hydrogen peroxide to semiconductor grade*. 2nd International Congress on Green Process Engineering and 2nd European Process Intensification Conference, Venecia (2009). Póster.

3. Abejón R.; Garea, A.; Irabien A. *Reverse osmosis for the ultrapurification of aqueous hydrogen peroxide to electronic grade*. EUROMEMBRANE 2009, Montpellier (**2009**). Póster.
4. Abejón, R.; Garea, A.; Luis, P.; Irabien, A. *Ultrapurification of aqueous hydrogen peroxide by membranes technology*. 7th Ibero-American Conference on Membrane Science and Technology CITEM 2010, Sintra (**2010**). Póster.
5. Abejón R.; Garea, A.; Irabien A. *Ultrapurification of aqueous hydrogen peroxide by multistage reverse osmosis*. 19th International Congress of Chemical and Process Engineering CHISA 2010, Praga (**2010**). Póster.
6. Abejón R.; Garea, A.; Irabien A. *Optimum design of a zero-effluent membrane process for hydrogen peroxide ultrapurification*. 8th European Congress of Chemical Engineering ECCE 8, Berlin (**2011**). Oral.
7. Abejón R.; Garea, A.; Irabien A. *Membrane process optimization for hydrogen peroxide ultrapurification*. 21st European Symposium on Computer-Aided Process Engineering ESCAPE 21, Tesalónica (**2011**). Póster.
8. Abejón R.; Garea, A.; Irabien A. *Modeling and simulation of multi-pass reverse osmosis for hydrogen peroxide ultrapurification*. 13th Network Young Membranes NYM13, Enschede (**2011**). Oral.
9. Abejón R.; Garea, A.; Irabien A. *Technical and economic viability of multi-pass reverse osmosis for hydrogen peroxide ultrapurification*. International Congress on Membranes and Membrane Processes ICOM 2011, Amsterdam (**2011**). Póster.
10. Abejón R.; Garea, A.; Irabien A. *Chemicals ultrapurification by cellulose acetate reverse osmosis membranes*. 12th Mediterranean Congress of Chemical Engineering, Barcelona (**2011**). Oral.
11. Abejón R.; Garea, A.; Irabien A. *Multiobjective decision tool in hydrogen peroxide ultrapurification by reverse osmosis*. 1st ANQUE's International Congress of Chemical Engineering ANQUE-ICCE 2012, Sevilla (**2012**). Póster.

12. Abejón R.; Garea, A.; Irabien A. *Multiobjective optimization of membrane processes for chemicals ultrapurification*. 22st European Symposium on Computer-Aided Process Engineering ESCAPE 22, Londres (**2012**). Oral.
13. Abejón R.; Garea, A.; Irabien A. *Minimization of energy consumption for chemicals ultrapurification processes*. 15th Conference on Process Integration, Modelling and Optimisation for Energy Saving and Pollution Reduction PRES 2012, Praga (**2012**). Póster.
14. Abejón R.; Garea, A.; Irabien A. *Analysis of hybrid reverse osmosis cascades for ultrapurification of chemicals*. EUROMEMBRANE 2012, Londres (**2012**). Póster.
15. Abejón R.; Garea, A.; Irabien A. *Optimum integrated reverse osmosis cascades with polyamide and cellulose acetate membranes for chemicals ultrapurification*. 14th Aachener Membran Kolloquium, Aquisgrán (**2012**). Póster.